UNIVERSITI TEKNOLOGI MARA

CHARACTERIZATION OF CARBOXYPEPTIDASE A1, BILE–SALT ACTIVATED LIPASE, TRIACYLGLYCEROL LIPASE, AND ALPHA–AMYLASE FROM BOVINE (*BOS TAURUS*) AND SHEEP (*OVIS ARIES*) PANCREAS AS POTENTIAL HALAL REPLACEMENTS FOR PORCINE ENZYMES

NUR HIDAYAH BINTI RESHIDAN

PhD

August 2026

UNIVERSITI TEKNOLOGI MARA

CHARACTERIZATION OF CARBOXYPEPTIDASE A1, BILE–SALT ACTIVATED LIPASE, TRIACYLGLYCEROL LIPASE, AND ALPHA–AMYLASE FROM BOVINE (*BOS TAURUS*) AND SHEEP (*OVIS ARIES*) PANCREAS AS POTENTIAL HALAL REPLACEMENTS FOR PORCINE ENZYMES

NUR HIDAYAH BINTI RESHIDAN

Thesis submitted in fulfilment
of the requirements for the degree of
Doctor of Philosophy
(Science)

Faculty of Applied Sciences

August 2026

CONFIRMATION BY PANEL OF EXAMINERS

I certify that a Panel of Examiners has met on 21st January 2026 to conduct the final examination of Nur Hidayah binti Reshidan on her Doctor of Philosophy thesis entitled "Characterization of Carboxypeptidase A1, Bile–Salt Activated Lipase, Triacylglycerol Lipase, and Alpha–Amylase from Bovine (*Bos taurus*) and Sheep (*Ovis aries*) Pancreas as Potential Halal Replacements for Porcine Enzymes" in accordance with Universiti Teknologi MARA Act 1976 (Akta 173). The Panel of Examiners recommends that the student be awarded the relevant degree. The Panel of Examiners was as follows:

Khalilah Abdul Khalil, PhD
Associate Professor
Faculty of Applied Sciences
Universiti Teknologi MARA
(Chairperson)

Mohd Fakharul Zaman Raja Yahya, PhD
Associate Professor
Faculty of Applied Sciences
Universiti Teknologi MARA
(Internal Examiner)

Mohd Shukuri Mohamad Ali, PhD
Professor
Faculty of Biotechnology and
Biomolecular Sciences
Universiti Putra Malaysia
(External Examiner)

PROF DR HJH ZURAEDA IBRAHIM
Dean
Institute of Postgraduate Studies
Universiti Teknologi MARA

Date: 26 August 2026

AUTHOR'S DECLARATION

I declare that the work in this thesis was carried out in accordance with the regulations of Universiti Teknologi MARA. It is original and is the results of my own work, unless otherwise indicated or acknowledged as referenced work. This thesis has not been submitted to any other academic institution or non-academic institution for any degree or qualification.

I, hereby, acknowledge that I have been supplied with the Academic Rules and Regulations for Postgraduate, Universiti Teknologi MARA, regulating the conduct of my study and research.

Name of Student	:	Nur Hidayah binti Reshidan
Student ID. No.	:	2020187567
Programme	:	Doctor of Philosophy (Science) – AS950
Faculty	:	Applied Sciences
Thesis Title	:	Characterization of Carboxypeptidase A1, Bile–Salt Activated Lipase, Triacylglycerol Lipase, and Alpha–Amylase from Bovine (*Bos taurus*) and Sheep (*Ovis aries*) Pancreas as Potential Halal Replacements for Porcine Enzymes
Signature of Student	:	
Date	:	August 2026

ABSTRACT

Pancreatic enzymes are essential biocatalysts widely applied in the pharmaceutical and food industries, particularly for Pancreatic Enzyme Replacement Therapy (PERT). Currently, the enzyme market is dominated by porcine–derived enzymes, which pose significant religious and cultural barriers for Muslim and Kosher populations. This study aimed to utilise animal biological waste by extracting, purifying, and characterizing specific pancreatic enzymes such as Protease (Carboxypeptidase A1 – CBPA1), Lipase (Bile–Salt Activated Lipase – BSAL and Triacylglycerol Lipase – TL), and Amylase (Alpha–Amylase – AMYP) from fresh bovine (*Bos taurus*) and sheep (*Ovis aries*) pancreas tissues to determine their viability as high–value alternatives to porcine enzymes. Fresh pancreas collected from the Department of Veterinary Services, Shah Alam were treated for fat removal and crude extraction was performed using organic solvents. The pancreatic enzyme was further purified by anion exchange and gel filtration chromatography. Proteins were profiled using one–dimensional sodium dodecyl sulfate polyacrylamide gel electrophoresis (1D–SDS PAGE) and validated through liquid chromatography–mass spectrometry (LC–MS/MS). To ensure functional viability, the enzymatic activities of the purified Halal enzymes were benchmarked against commercialized porcine pancreatic enzymes. Glycosylation profiling was conducted *in–silico* focusing on prediction of glycosylation sites on bovine and sheep pancreatic enzymes against porcine and human followed by experimental enrichment using Con A lectin. The results confirmed the successful extraction and purification of CBPA1 (bovine and sheep), BSAL (bovine), and TL (sheep). However, AMYP purification was undetected, although the crude extracts from both species showed amylolytic activity comparable to the porcine standard. The most significant finding was the superior potency of the Halal proteases; sheep CBPA1 demonstrated a 55–fold increase in specific proteolytic activity, and bovine CBPA1 showed a 32–fold increase compared to the porcine positive control. Additionally, bovine BSAL was identified as an ideal direct substitute, exhibiting specific lipolytic activity (0.222 U/mg) statistically equivalent to the porcine standard (0.223 U/mg). In terms of PTMs, *in–silico* models indicated predominant N–linked glycosylation for all the purified pancreatic enzymes. However, experimental enrichment only confirmed glycosylation for CBPA1, verifying its biological relevance. In conclusion, these finding suggests that sheep CBPA1 and bovine BSAL are the most promising candidate for Halal PERT as alternative to porcine enzymes. The current study provides comprehensive evidence on the successful extraction and purification of bovine and sheep pancreatic enzymes, confirming that their enzymatic activities are comparable to established porcine standards with preliminary insights on their glycosylation state. Future work should focus on detail elucidation of glycan structure using Ultra Performance Liquid Chromatography (UPLC) to verify glycosylation patterns relative to porcine enzymes. Furthermore, detailed enzymatic activity profiling and feasibility studies are needed to evaluate the suitability of bovine and sheep pancreatic enzymes as functional and Halal–compliant industrial alternatives.

ACKNOWLEDGEMENT

"But perhaps you hate a thing, and it is good for you, and perhaps you love a thing, and it is bad for you. And Allah knows, while you know not." (Quran, 2:216)

First and foremost, I would like to express my sincere gratitude to my main supervisor, Dr Umi Marshida Abdul Hamid, for her continuous guidance and patience throughout my PhD. I am equally thankful to my co-supervisors, Associate Professor Dr Zaidah Zainal Ariffin and Associate Professor Dr Dhilia Uddie binti Lamasuddin, as well as my industrial co-supervisor, Dr Anuar bin Jonet, for their invaluable mentorship and support. My heartfelt thanks also go to Pn. Mazatulikhma Mat Zain and Dr Siti Mazleena Mohamed for their continuous encouragement and motivation during this journey.

I extend my appreciation to Dr Julaina binti Abdul Jalil, Dr Salina binti Abdul Rahman and En Affandi bin Omar from the Institute of Medical Research (IMR), alongside Cik Norliza Bahtiar Affendy and Cik Farahayu binti Khairuddin from the Malaysia Genome and Vaccine Institute (MGVI). Their generous technical assistance and shared resources were vital during the purification studies. I would also like to thank my PhD examiners, Professor Mohd Shukuri bin Mohamad Ali and Associate Professor Mohd Fakharul Zaman Raja Yahya, whose constructive feedback significantly improved the clarity and quality of this thesis.

A special note of thanks goes to my Director, Dr Noraini binti Samat, and my superiors, Dr Habsah binti Bidin and Dr Wan Somarny binti Wan Md Zain, at the Livestock Research Centre, Malaysian Agricultural Research and Development Institute (MARDI). Their understanding and the flexibility they granted allowed me the essential time preparing for my viva and focus on completing this thesis.

Finally, my deepest gratitude belongs to my family. To my late father, Hj Reshidan bin Hj Hasanudin, your values and life lessons continue to guide me. To my mother, , my stepfather, En Othman Jailani bin Embong, and my brother, Muhammad Muizz bin Hj Reshidan, thank you for your boundless love, prayers, and constant belief in me. To my best friend, Nur Nabilah binti Usman, thank you for standing by me since we were eighteen and for your endless patience in listening to my rants. I also deeply appreciate my 'extended' family in Shah Alam — Biha, Adzleen, Hidayah, Sharifah and Aida for always being present during my toughest times. To my lab mates — Naomi, Haifa, Intan, Iqbal, Aqilah, and Aireen, thank you for your friendship, shared laughter, and mutual support during the journey.

This journey has taught me that persistence and hard work eventually yield profound rewards. As the saying goes, *"Perseverance is not a long race; it is many short races, one after another."* May this achievement mark the beginning of more impactful contributions in the field of research.

TABLE OF CONTENTS

		Page
CONFIRMATION BY PANEL OF EXAMINERS		**ii**
AUTHOR'S DECLARATION		**iii**
ABSTRACT		**iv**
ACKNOWLEDGEMENT		**v**
TABLE OF CONTENTS		**vi**
LIST OF TABLES		**xiii**
LIST OF FIGURES		**xv**
LIST OF SYMBOLS		**xviii**
LIST OF ABBREVIATIONS		**xix**
CHAPTER 1: INTRODUCTION		**1**
1.1	Research Background	1
1.2	Problem Statement	6
1.3	Rationale of Study	6
1.4	Significance of Study	7
1.5	Research Questions	8
1.6	Hypotheses	8
1.7	Objectives	9
1.8	Scope and Limitation of Study	9
1.9	Conclusion	10
CHAPTER 2: LITERATURE REVIEW		**11**
2.1	Pancreas	11
	2.1.1 Endocrine and Exocrine Systems	12
	2.1.1.1 Endocrine System	13
	2.1.1.2 Exocrine System	14
	2.1.2 Exocrine Pancreatic Insufficiency	16
	2.1.2.1 Causes of Exocrine Pancreatic Insufficiency	17

2.2 Pancreatic Diseases 18
2.2.1 Chronic Pancreatitis 18
2.2.2 Pancreatic Cancer 20
2.2.3 Cystic Fibrosis 21
2.3 Pancreatic Enzyme 22
2.3.1 Enzyme Release Phase 23
2.4 Pancreatic Enzyme Therapy 23
2.4.1 Origin and Discovery of Pancreatic Enzyme Therapy 23
2.4.2 Pancreatic Enzyme Replacement Therapy 24
2.4.3 Challenges in Pancreatic Enzyme Replacement Therapy 25
2.4.4 Pancreatic Enzyme Drugs Available on the Market 26
2.4.5 Enzymes Used in Pancreatic Enzyme Replacement Therapy 28
2.4.5.1 Protease 29
2.4.5.2 Classes of Proteases 30
2.4.5.3 Amylase 33
2.4.5.4 Classes of Amylase 34
2.4.5.5 Lipase 36
2.4.5.6 Examples of Pancreatic Lipase 37
2.5 Major Industrial Application of Porcine Enzymes 39
2.5.1 Clinical and Pharmaceutical Industries 40
2.5.2 Cosmetic Industry 41
2.5.3 Food Industry 42
2.6 Halal 43
2.6.1 Halal Concerns About Porcine–Based Enzymes 43
2.6.2 Halal Market Demand 44
2.7 Potential Halal Enzyme Alternatives 45
2.7.1 Microbial Origin Enzyme 46
2.7.2 Plant-Origin Enzyme 48
2.7.3 Animal Origin Enzyme 48
2.7.4 Recombinant DNA–derived Enzyme 49
2.8 Protein Modification 50
2.8.1 Glycosylation 50
2.8.2 Types of Glycosylation 52
2.8.3 Biological Roles of Glycosylation and Glycans 53

2.9 Proteomic Approaches in Halal Enzymes Identification 55
2.10 Conclusion 57

CHAPTER 3: EXTRACTION AND PURIFICATION OF BOVINE (*BOS TAURUS)* CARBOXYPEPTIDASE A1 58

3.1 Introduction 58
3.2 Materials and Methods 60
3.2.1 Enzyme Extraction 60
3.2.2 Sequential Purification of Bovine Carboxypeptidase A1 61
3.2.2.1 Anion Exchange Chromatography (IEX) 61
3.2.2.2 Gel Filtration Chromatography (GFC) 63
3.2.3 Protein Identification and Confirmation of Bovine Carboxypeptidase A1 63
3.2.3.1 Determination of Protein Concentration 63
3.2.3.2 One–Dimensional Sodium Dodecyl Sulfate Polyacrylamide Gel Electrophoresis (1D–SDS PAGE) 64
3.2.3.3 Liquid Chromatography–Mass Spectrometry (LC–MS/MS) 65
3.2.4 Proteolytic Enzyme Assay 65
3.3 Results 67
3.3.1 Extraction and Purification of Bovine CBPA1 67
3.3.2 Protein Identification and Confirmation of Bovine Carboxypeptidase A1 69
3.3.3 Proteolytic Enzyme Assay 74
3.4 Discussion 75
3.5 Conclusion 77

CHAPTER 4: EXTRACTION AND PURIFICATION OF SHEEP (*OVIS ARIES*) CARBOXYPEPTIDASE A1 78

4.1 Introduction 78
4.2 Materials and Methods 80
4.2.1 Enzyme Extraction 80
4.2.2 Sequential Purification of Sheep Carboxypeptidase A1 81
4.2.2.1 Anion Exchange Chromatography (IEX) 81
4.2.2.2 Gel Filtration Chromatography (GFC) 83

4.2.3 Protein Identification and Confirmation of Sheep Carboxypeptidase A1 83
4.2.3.1 Determination of Protein Concentration 83
4.2.3.2 One–Dimensional Sodium Dodecyl Sulfate Polyacrylamide Gel Electrophoresis (1D–SDS PAGE) 84
4.2.3.3 Liquid Chromatography–Mass Spectrometry (LC–MS/MS) 85
4.2.4 Proteolytic Enzyme Assay 85
4.3 Results 87
4.3.1 Extraction and Purification of Sheep Carboxypeptidase A1 87
4.3.2 Protein Identification and Confirmation of Sheep Carboxypeptidase A1 89
4.3.3 Proteolytic Enzyme Assay 93
4.4 Discussion 94
4.5 Conclusion 96

CHAPTER 5: PURIFICATION AND CHARACTERISATION OF BILE–SALT ACTIVATED LIPASE ENZYME FROM BOVINE (*BOS TAURUS*) PANCREAS 97
5.1 Introduction 97
5.2 Materials and Methods 101
5.2.1 Extraction and Purification of Bovine Bile Salt Activated Lipase 101
5.2.2 Purification of Bovine Bile–Salt Activated Lipase 102
5.2.3 Protein and Peptide Identification of Bovine Bile–Salt Activated Lipase 103
5.2.3.1 Determination of Protein Concentration 103
5.2.3.2 One–Dimensional Sodium Dodecyl Sulfate Polyacrylamide Gel Electrophoresis (1D–SDS PAGE) 104
5.2.3.3 Liquid Chromatography–Mass Spectrometry (LC–MS/MS) 105
5.2.4 Lipolytic Enzyme Assay 106
5.3 Results 107
5.3.1 Extraction and Purification of Bovine Bile–Salt Activated Lipase 107

5.3.2 Protein and Peptide Identification of Bovine Bile–Salt Activated Lipase 108
5.3.3 Lipolytic Enzyme Assay 111
5.4 Discussion 112
5.5 Conclusion 115

CHAPTER 6: PURIFICATION AND CHARACTERIZATION OF SHEEP (*OVIS ARIES*) PANCREATIC TRIACYLGLYCEROL LIPASES 116
6.1 Introduction 116
6.2 Materials and Methods 119
6.2.1 Extraction and Purification of Sheep Triacylglycerol Lipase 119
6.2.2 Purification of Sheep Triacylglycerol Lipase 120
6.2.3 Protein and Peptide Identification of Sheep Triacylglycerol Lipase 122
6.2.3.1 Determination of Protein Concentration 122
6.2.3.2 One–Dimensional Sodium Dodecyl Sulfate Polyacrylamide Gel Electrophoresis (1D–SDS PAGE) 122
6.2.3.3 Liquid Chromatography–Mass Spectrometry (LC–MS/MS) 123
6.2.4 Lipolytic Enzyme Assay 124
6.3 Results 126
6.3.1 Extraction and Purification of Sheep Triacylglycerol Lipase 126
6.3.2 Protein and Peptide Identification of Sheep Triacylglycerol Lipase 127
6.3.3 Lipolytic Enzyme Assay 130
6.4 Discussion 131
6.5 Conclusion 134

CHAPTER 7: BOVINE (*BOS TAURUS)* AND SHEEP *(OVIS ARIES)* PANCREATIC ALPHA–AMYLASE EXTRACTION AND PURIFICATION 135
7.1 Introduction 135
7.2 Materials and Methods 137
7.2.1 Extraction and Purification of Bovine and Sheep Alpha–Amylase 137
7.2.2 Purification of Bovine and Sheep Alpha–Amylase 138

7.2.3 Bovine and Sheep Alpha–Amylase Protein and Peptide Identification 140
7.2.3.1 Determination of Protein Concentration 140
7.2.3.2 One–Dimensional Sodium Dodecyl Sulfate Polyacrylamide Gel Electrophoresis (1D–SDS PAGE) 140
7.2.3.3 Liquid Chromatography–Mass Spectrometry (LC–MS/MS) 141
7.2.4 Amylolytic Enzyme Assay 142
7.3 Results 143
7.3.1 Extraction and Purification of Bovine Alpha–Amylase 143
7.3.2 Extraction and Purification of Sheep Alpha–Amylase 145
7.3.3 Amylolytic Enzyme Assay 147
7.4 Discussion 149
7.5 Conclusion 152

CHAPTER 8: PANCREATIC ENZYMES BIOINFORMATICS *IN–SILICO* ANALYSIS AND EXPERIMENTAL GLYCOSYLATION PROFILING 153
8.1 Introduction 153
8.2 Materials and Methods 155
8.2.1 *In–Silico* Glycosylation Assessment 155
8.2.1.1 Gathering Selected Protein Information 155
8.2.1.2 Sequence and Structure Analysis of Homology Modeling 156
8.2.2 Experimental Glycosylation Profiling and Visualization 159
8.2.2.1 Glycosylation Profiling via 1D–SDS PAGE 159
8.2.2.2 Glycoprotein Enrichment via Glycosylation Isolation Kit 160
8.2.2.3 Glycoprotein Acetone Precipitation 161
8.2.2.4 Glycosylation Staining 162
8.3 Results 163
8.3.1 *In–silico* Characterization and Glycosylation Prediction. 163
8.3.2 Sequence Analysis 167
8.3.2.1 Multiple and Pairwise Sequence Alignment 167
8.3.3 Structure Analysis 172
8.3.3.1 Protein Modelling 172
8.3.3.2 Template Protein Structure Validation 177

8.3.4 Glycosylation Bioinformatics Assessment 181
8.3.4.1 Potential Glycosylation Sites Prediction 181
8.3.4.2 Potential Glycosylation Sites Location 187
8.3.5 Glycosylation Experimental Assessment 192
8.3.5.1 Protease Glycosylation Assessment for Bovine and Sheep Pancreatic Enzyme Sequential Purification 192
8.3.5.2 Lipase Glycosylation Assessment for Bovine and Sheep Pancreatic Enzyme Sequential Purification 194
8.3.5.3 Glycoprotein Enrichment for Bovine and Sheep Pancreatic Crude Extract 196
8.4 Discussion 197
8.5 Conclusion 201

CHAPTER 9: CONCLUSION AND RECOMMENDATION 202
9.1 Introduction 202
9.2 Conclusion and Recommendation 203

REFERENCES 204

APPENDICES 248

AUTHOR'S PROFILE 259

LIST OF TABLES

Tables	Title	Page
Table 2.1	Five Endocrine Secretion Cells in each Islet of Langerhans	13
Table 2.2	Aetiology of Exocrine Pancreatic Insufficiency	18
Table 2.3	List of Enzymes for Macronutrient Digestion	22
Table 2.4	Pancreatic Enzyme Drugs Available on the Market	27
Table 2.5	Differences between N–link and O–link Glycosylations	53
Table 3.1	Sample Preparation for SDS–PAGE	64
Table 3.2	Protein Identification from the LC–MS/MS	71
Table 3.3	Peptide Sequence Prediction of Bovine Pancreatic CBPA1 via LC–MS/MS	72
Table 3.4	Sequential Purification Bovine Pancreatic CBPA1	74
Table 4.1	Sample Preparation for SDS–PAGE	84
Table 4.2	Protein Identification from the LC–MS/MS	91
Table 4.3	Peptide Sequence Prediction of Sheep Pancreatic CBPA1 via LC–MS/MS	92
Table 4.4	Sequential Purification of Sheep Pancreatic CBPA1	93
Table 5.1	Sample Preparation for SDS–PAGE	104
Table 5.2	Protein Identification from the LC–MS/MS	109
Table 5.3	Peptide Sequence Prediction of Bovine Pancreatic BSAL via LC–MS/MS.	110
Table 5.4	Purification of Bovine Pancreatic BSAL	111
Table 6.1	Sample Preparation for SDS–PAGE	123
Table 6.2	Protein Identification from the LC–MS/MS	128
Table 6.3	Peptide Sequence Prediction of Sheep Pancreatic TL via LC–MS/MS	129
Table 6.4	Purification of Sheep Pancreatic TL	130
Table 7.1	Sample Preparation for SDS–PAGE	141
Table 7.2	Starch Hydrolysis of Bovine Samples on MHA	148
Table 7.3	Starch Hydrolysis of Sheep Samples on MHA	148
Table 8.1	Sample Preparation for SDS–PAGE	160

Table 8.2	Protein Information of Pancreatic Enzymes of Interest	165
Table 8.3	CBPA1 Protein Templates	168
Table 8.4	BSAL Protein Templates	169
Table 8.5	TL Protein Templates	170
Table 8.6	AMYP Protein Templates	171
Table 8.7	Protein Structure Validation	178
Table 8.8	Prediction of Potential Glycosylation Sites for CBPA1	182
Table 8.9	Prediction of Potential Glycosylation Sites for BSAL	183
Table 8.10	Prediction of Potential Glycosylation Sites for TL	184
Table 8.11	Prediction of Potential Glycosylation Sites for AMYP	185

LIST OF FIGURES

Figures	Title	Page
Figure 2.1	Anatomic View Structure of the Pancreas (Longnecker, 2014).	12
Figure 2.2	Exocrine and Endocrine Pancreas System (Pandol, 2015).	13
Figure 2.3	Exocrine Pancreatic Secretion (Berry, 2014).	15
Figure 2.4	Normal Human Pancreas (Longnecker, 2014).	15
Figure 2.5	Stages of Pancreatic Enzyme Release.	23
Figure 2.6	Overview of Pancreatic Enzymes and Their Role in Pancreatic Enzyme Replacement Therapy (PERT). Note: Image Generated using the Prompt "A Graphical Image Summarize the Pancreatic Enzymes in Pancreatic Enzyme Replacement Therapy" by NotebookLM, 2026 (https://notebooklm.google).	28
Figure 2.7	Comparative Host–Specific Glycan Structure Across Mammalian Species. Modified and gathered from Gallego *et al*. (2001), Miyagawa *et al*. (2014) and Nakano *et al*. (2004).	55
Figure 3.1	Bovine Carboxypeptidase A1 (CBPA1) Purification Scheme.	60
Figure 3.2	Anion–exchange Chromatography of Aqueous Crude Bovine Pancreatic Extract. The Partially Purified Bovine CBPA1 was eluted at Peak D (30% NaCl concentration).	67
Figure 3.3	Gel Filtration Chromatography of Pure Bovine CBPA1.	68
Figure 3.4	1D–SDS PAGE (Bis–Tris 12%) of Pure Bovine CBPA1. Pure Bovine CBPA1 was approximately estimated to be 47 kDa (Lane 4).	69
Figure 4.1	Sheep Carboxypeptidase A1 (CBPA1) Purification Scheme.	80
Figure 4.2	Anion–exchange Chromatography of Aqueous Crude Sheep Pancreatic Extract. The Partially Purified Sheep CBPA1 was eluted at Peak D (30% NaCl concentration).	87
Figure 4.3	Gel Filtration Chromatography of Purified Sheep CBPA1.	88
Figure 4.4	1D–SDS PAGE (Bis–Tris 12%) of Pure Sheep CBPA1. Pure Sheep CBPA1 was approximately estimated to be 46 kDa (Lane 4).	89

Figure 5.1	Bovine Bile–Salt Activated Lipase (BSAL) Purification Scheme.	101
Figure 5.2	Anion–exchange Chromatography of Aqueous Crude Bovine Pancreatic Extract. The Purified Bovine BSAL was eluted at Peak B (10% NaCl concentration).	107
Figure 5.3	1D–SDS PAGE (Bis–Tris 12%) of Pure Bovine BSAL. Pure Bovine BSAL was approximately estimated to be 60 kDa (Lane 3).	108
Figure 6.1	Sheep Triacylglycerol Lipase (TL) Purification Scheme.	119
Figure 6.2	Anion–exchange Chromatography of Aqueous Crude Sheep Pancreatic Extract. The Purified Sheep TL was eluted at Peak C (20% NaCl concentration).	126
Figure 6.3	1D–SDS PAGE (Bis–Tris 12%) of Pure Sheep TL. Pure Sheep TL was approximately estimated to be 53 kDa (Lane 3).	127
Figure 7.1	Bovine and Sheep Alpha–Amylase (AMYP) Purification Scheme.	137
Figure 7.2	Anion–exchange Chromatography of Aqueous Crude Bovine Pancreatic Extract. There was no Bovine AMYP identified across NaCl gradient.	143
Figure 7.3	1D–SDS PAGE (Bis–Tris 12%) of Bovine Crude Extract. There was no Bovine AMYP identified across at the targeted molecular weight (57 kDa).	144
Figure 7.4	Anion–exchange Chromatography Of Aqueous Crude Sheep Pancreatic Extract. The predicted Sheep AMYP was eluted at Peak C (20% NaCl concentration) and at Peak D (30% NaCl concentration).	145
Figure 7.5	1D–SDS PAGE (Bis–Tris 12%) of Sheep Crude Extract. The Sheep AMYP was predicted to be approximately 57 kDa (b: Lane 5,6, and 7).	146
Figure 7.6	Starch hydrolysis of a) Bovine and b) Sheep samples on MHA.	148
Figure 8.1	*In–silico* Characterization and Glycosylation Site Prediction of Pancreatic Enzymes.	158

Figure 8.2	Structure Alignment for CBPA1 a) Bovine, b) Sheep, c) Porcine and d) Human with Template Candidates.	173
Figure 8.3	Structure Alignment for BSAL a) Bovine and b) Human with Template Candidates.	174
Figure 8.4	Structure Alignment for TL a) Sheep, b) Human and c) Porcine with Template Candidates.	175
Figure 8.5	Structure Alignment for AMYP a) Sheep, b) Porcine and c) Human with Template Candidates.	176
Figure 8.6	3D Model of CBPA1.	179
Figure 8.7	3D Model of BSAL.	179
Figure 8.8	3D Model of TL.	180
Figure 8.9	3D Model of AMYP.	180
Figure 8.10	CBPA1 Potential Glycosylation Site Locations.	188
Figure 8.11	BSAL Potential Glycosylation Site Locations.	189
Figure 8.12	TL Potential Glycosylation Site Locations.	190
Figure 8.13	AMYP Potential Glycosylation Site Locations.	191
Figure 8.14	1D–SDS PAGE (Bis–Tris 12%) of Bovine and Sheep CBPA1 Sequential Purification. a) Coomassie Brilliant Blue staining, b) Pro–Q ® Emerald 300 Glycoprotein staining, and c) Sypro Ruby staining.	193
Figure 8.15	1D–SDS PAGE (Bis–Tris 12%) of Bovine BSAL and Sheep TL Sequential Purification. a) Coomassie Brilliant Blue staining, b) Pro–Q ® Emerald 300 Glycoprotein staining, and c) Sypro Ruby staining.	195
Figure 8.16	1D–SDS PAGE (Bis–Tris 12%) of Bovine and Sheep Pancreatic Crude Extract Glycoprotein Enrichment.	196

LIST OF SYMBOLS

Symbols

α	Alpha
β	Beta
γ	Gamma
g	Gram
kg	Kilogram
^{o}C	Degree Celsius
cm	Centimetre
µg	Microgram
µL	Microlitre
mU	Milliunit
m	Meter
min	Minute
mL	Millilitres

LIST OF ABBREVIATIONS

Abbreviations	
1D–SDS PAGE	One–Dimensional Sodium Dodecyl Sulfate Polyacrylamide Gel Electrophoresis
2D–SDS PAGE	Two–Dimensional Sodium Dodecyl Sulfate Polyacrylamide Gel Electrophoresis
AMYP	Alpha–Amylase
AP	Acute Pancreatitis
BSAL	Bile–Salt Activated Lipase
CAGR	Compound Annual Growth Rate
CBPA1	Carboxypeptidase A1
CCK	Cholecystokinin
CEL	Carboxyl Ester Lipase
CF	Cystic Fibrosis
CP	Chronic Pancreatitis
DVS	Department of Veterinary Services
ELISA	Enzyme–Linked Immunosorbent assays
EPI	Exocrine Pancreatic Insufficiency
FDA	Food and Drug Administration
FDR	False Discovery Rate
GFC	Gel Filtration Chromatography
GH13	Glycoside Hydrolase family 13

GH14	Glycoside Hydrolase family 14
GH15	Glycoside Hydrolase family 15
GlcNAc	N-acetylglucosamine
HL	Hepatic Lipase
HSL	Hormone-Sensitive Lipase
HPL	Human Pancreatic Lipase
IEX	Anion Exchange Chromatography
JAKIM	Jabatan Kemajuan Islam Malaysia
LPL	Lipoprotein Lipase lysosomal acid lipase (LAL)
LC–MS/MS	Liquid Chromatography–Mass Spectrometry
MALDI–TOF MS	Matrix-Assisted Laser Desorption/Ionization Time-of-Flight Mass Spectrometry
ML	Microbial Lipase
MS	Mass Spectrometry
MW	Molecular Weight
Neu5Ac	N-acetylneuraminic acid
Neu5Gc	N-glycolylneuraminic acid
NLG	N–linked Glycosylation
NICE	National Institute of Clinical Excellence
OIC	Organisation of Islamic Cooperation
OLG	O–linked Glycosylation
PC	Pancreatic Cancer

PERT	Pancreatic Enzyme Replacement Therapy
PET	Pancreatic Enzyme Therapy
pI	Isoelectric Point
PL	Pancreatic Lipase
PLA	Phospholipase A2
PLEM	Pancreatic–like Enzyme of Microbial
PTM/s	Post–Translational Modification/s
RCSB PDB	Research Collaboratory for Structural Bioinformatics Protein Data Bank
RMSD	Root Mean Square Deviation
TAG	Triglycerides
TL	Triacylglycerol Lipase
TPCK	Trypsin Tosyl phenylalanyl chloromethyl ketone
UPLC	Ultra–Performance Liquid Chromatography
USP	United State Pharmacopeia

CHAPTER 1
INTRODUCTION

1.1 Research Background

Enzymes comprise large biological macromolecules known as amino acids that catalyse thousands of metabolic processes (Choi *et al.,* 2015). It has been widely used since ancient times. After 1940, advancements in biochemistry allowed the isolation and characterisation of enzymes to be explored. As industrial biocatalysts, enzymes pose numerous advantages over traditional chemical processes regarding sustainability and process efficiency (Chapman *et al.,* 2018; Cheng *et al.,* 2020). They are considered essential as the catalyse processes are more efficient and can work under mild reaction conditions, resulting in a reduction of organic waste and pollutants production, which helps to cut production costs (Cheng *et al.,* 2020). In addition, enzymes show exceptional product selectivity with lower environmental and physiological toxicities that are very useful for large–scale industrial applications (Chapman *et al.,* 2018; Kumar *et al.,* 2014).

Enzymes are crucial in various applications, industries, and daily usage (Latip *et al.,* 2019). They are among the most promising technologies for long–term molecule synthesis for pharmaceutical, biotechnological, and industrial functions (Abdelraheem *et al.,* 2019). Numerous applications in biotechnological products and processes commonly employ enzymes to produce cleaning supplies, transportation fuels, clothing, food and beverages, paper products, clinicals, pharmaceuticals, and monitoring devices (Prasad & Roy, 2017). Intensive research has been conducted globally to produce the enzyme system more efficiently, cost–effectively, and sustainably (Tarafdar *et al.,* 2021). In 2021, the enzymes market was valued at approximately US$11.71 billion and is anticipated to exceed US$20.5 billion by 2030, growing at a 6.42% compound annual growth rate (CAGR) (Precedence Research, 2022a).

Porcine enzymes are one of the most significant segments of the global enzyme market used in various industries. The porcine enzymes extracted from their organs or tissues possess unique properties and characteristics that make them valuable in many industrial applications. Among mammals, the porcine is an animal that mimics humans the best in most aspects, as they share many genetic, physiological, and anatomical

similarities that make it relevant in various scientific investigations related to human study (Krupa *et al.,* 2020; Ogun *et al.,* 2022). Their organs are anatomically and histologically similar to humans (Dawson *et al.,* 2017). The same genes and proteins could be found in humans and porcine (Dawson *et al.,* 2013; Groenen *et al.,* 2012; Herdiana *et al.,* 2024). Furthermore, the similarities between humans and porcine can be validated by an *in–silico* approach. High returns in the sequence identity of the genes and protein sequence and structure result in over 80% similarity compared to other organisms (Marengo *et al.,* 2022).

The effective use of organ by–products, namely the lung, stomach, heart, liver, small intestine, and large intestine from the porcine production process, helps to reduce waste and improve the utilization efficiency of livestock products (Lee *et al.,* 2021). In addition, porcine is considered a cheap source of industrial enzymes as it is abundantly found in nature. Besides, porcine and bacterial–derived enzymes are more economical and accessible than human–derived enzymes. However, industries have been observed shifting from porcine towards Halal sources of enzymes since the Halal market demand is increasing. In addition, the use of porcine enzymes has also been observed to decline in recent years due to many concerns, including the Halal status and religious restrictions.

The pancreas, known as the largest gland within the digestive system, is a retroperitoneal organ located posterior to the lesser sac, resting on the floor of the supracolic compartment (Ellis, 2013; Mahadevan, 2019). The primary function of the pancreas can be subcategorized as exocrine and endocrine (Wilschanski & Shaoul, 2014) by coordinating and regulating digestion and nutrient metabolism (Cade & Hanison, 2017; Henry *et al.,* 2019). Normal pancreatic function is crucial for effective digestion and nutrient absorption (Fieker *et al.,* 2011). The pancreas secretes three necessary digestive pancreatic enzymes, namely amylase, lipase, and protease, that play an indispensable role in exocrine and endocrine functions (Imrie *et al.,* 2010). The proteolytic, amylolytic, and lipolytic enzymes play essential roles in the intraluminal hydrolysis to break down macronutrients into smaller, absorbable metabolites (Ianiro *et al.,* 2016). The highly sought–after enzymes are essential for digesting carbohydrates, lipids, and protein and are used for food production and medical purposes.

Pancreatic enzymes are broadly utilized in clinical practice, particularly in Pancreatic Enzyme Replacement Therapy (PERT), for the management of Exocrine Pancreatic Insufficiency (EPI) (Alexandre-Heymann *et al.,* 2024; Brennan & Saif, 2019). Meanwhile, EPI is a consequence of pancreatic failure and leads to pancreatic disorders. These include acute pancreatitis (AP), chronic pancreatitis (CP), pancreatic cancer (PC), and cystic fibrosis (CF).

CP is a progressive fibro–inflammatory condition characterized by the persistent destruction of acinar, ductal, and islet cells, resulting in the gradual replacement of exocrine and endocrine pancreatic cells with fibrotic tissues (Gardner *et al.,* 2020; Li *et al.,* 2022). Previously, CP ranges from 5 to 12 cases per 100,000 persons annually (Gagyi *et al.,* 2024). The CP prevalence has been estimated to have grown to 120–140 per 100,000 (Olesen, 2019). PC is a highly aggressive malignancy marked by invasive behaviour and rapid disease progression, with a prominent resistance to standard therapeutic interventions (Jelski & Mroczko, 2019; Rozengurt & Eibl, 2026). Ranking as the seventh leading cause of global cancer deaths in industrial countries (Pezzilli *et al.,* 2020). It is expected to become the second to lung cancer of cancer deaths in the US by 2030 (Miller *et al.,* 2020). CF is estimated to affect between 70,000 – 100,000 people worldwide (Kelsey *et al.,* 2019). It is a genetically inherited, progressive, and life–threatening condition that predominantly impairs the functionality of the respiratory and digestive systems (Sankari & Sharma, 2024).

In the context of PERT alone, the market values are estimated to reach billions of US dollars within the next five years. To date, due to promising Halal quality assurance, there is a high demand for Halal pancreatic enzymes from all over the world, including for Muslim and Kosher populations. The growing Muslim population and Kosher consumers have created a global demand for Halal enzymes. Among the reasons is that the global recognition of Halal products signifies quality and health with a higher degree of food safety management. Thus, there is a consideration of Halal sources as an alternative to porcine for the pancreatic enzymes to also cater to other groups, such as Jews, Seventh Day Adventists, and Hindus. Other than that, patients with porcine allergies could also benefit from the production of Halal enzymes.

The main enzymes produced by the pancreas, such as protease, lipase, and amylase, are highly sought after being secreted. The pancreatic enzymes are subjected to glycosylation, a post–translational protein modification (PTM) that affects 50% of all proteins (Johnson, 2012). Two most common type of glycosylation are being investigated are N–linked glycosylation and O–linked glycosylation. The N–glycosylation, an N–acetylglucosamine (GlcNAc) residue is attached by an amide bond to an asparagine residue belonging to a consensus sequence NX(S/T), where X can be any amino acid except proline (He *et al.,* 2024). In addition, O–glycosylation may occur at any serine or threonine residue with no single common core structure or consensus protein sequence (Ji *et al.,* 2026).

The analysis of PTM, particularly glycosylation, is integral to characterize the purified pancreatic enzymes to determine and confirm the efficacy, stability and suitability of bovine and sheep enzymes as functional alternatives to porcine–based products. Glycosylation, which affects approximately half of all proteins, plays a pivotal role in dictating the structural stability, biological function, and bioavailability of pancreatic enzymes (An *et al.,* 2009; Schjoldager *et al.,* 2020). This study integrates *in–silico* characterization to predict glycosylation sites and compares them against human and porcine to identify structural variations that could impact enzyme activity. This comparison is crucial because abnormal glycosylation patterns can lead to reduced enzymatic half–life or trigger unwanted immunogenicity that cause allergic reactions in patients, making the verification of these glycan structures essential for establishing the biological relevance and safety of Halal pancreatic enzyme replacement therapies.

Notably, most of the pancreatic enzymes used for PERT are harvested from porcine; the religious view has become a matter that should be addressed. To date, there is no equivalent replacement for pork sources for PERT. From the Muslim religious point of view, they strongly abstain from consuming any porcine–based products available in the industry (Konstan *et al.,* 2018). This situation has become a significant concern to find Halal animal sources as an alternative for PERT to meet the high demand for Halal animal–derived medication, with promising profit to Halal pharmaceutical industries. The Quranic ‘Halal’ term is originally from an Arabic word that means allowed or permitted by Islamic Law (Ermis, 2017). The most common Halal terms used in the industries are ‘Halal’, ‘Guaranteed Halal’, or ‘Muslim Food’ to indicate that it is permissible to be consumed by Muslims. According to Halal Malaysia Official (2020), Halal products must not contain any part from animals forbidden to

Muslims, contain no substances considered impure, and are not prepared, processed, or manufactured using equipment or utensils that are not free from impurities as defined by Islamic law (Othman *et al.,* 2026). Therefore, it is critical to search for avenues that can be manipulated to highlight possible candidates that can serve a broader population at a reasonable cost with good enzyme efficiency.

The extraction and purification of pancreatic enzymes demand a rigorous methodological approach to transition from raw biological tissue to a functional biocatalyst. Building on previous studies that utilized established sources, this research emphasizes the necessity of purifying enzymes from fresh bovine and sheep pancreas to serve as viable Halal alternatives. The purification workflow typically initiates with the removal of fats and crude extraction using organic solvents to isolate the total protein content from the fresh pancreatic tissue. To achieve high purity and specificity for protease, lipase, and amylase, the process advances to sequential chromatographic techniques, specifically utilizing anion exchange chromatography (IEX) and gel filtration chromatography (GFC). This multi–step purification is critical for isolating the enzyme of interest from the crude extract, allowing for precise molecular weight analysis via one–dimensional sodium dodecyl sulfate polyacrylamide gel electrophoresis (1D–SDS PAGE) and validation through liquid chromatography–mass spectrometry (LC–MS/MS).

Generally, this study aimed to utilise agricultural biological waste by extracting, purifying, and characterizing specific pancreatic enzymes such as Protease (Carboxypeptidase A1 – CBPA1), Lipase (Bile–Salt Activated Lipase – BSAL and Triacylglycerol Lipase – TL), and alpha–amylase (AMYP) from fresh bovine (*Bos taurus*) and sheep (*Ovis aries*) pancreas tissues to determine their viability as high–value alternatives. The purified enzyme profiling was also identified and validated through LC–MS/MS analysis after the molecular weight analysis using 1D–SDS PAGE. To ensure functional viability, the enzymatic activities of the purified Halal enzymes were compared against an established commercialized porcine pancreatic enzyme. Furthermore, glycosylation profiling was conducted using *in–silico* prediction focusing on the glycosylation prediction site of bovine and sheep pancreatic enzymes against porcine and human and experimental enrichment using Con A lectin to assess PTMs. The overall methodology sections and findings on the enzymes' purification, identification, and confirmation, as well as on the enzymatic activity, were already published in the journal (Reshidan *et al.,* 2024, 2025).

1.2 Problem Statement

Porcine–derived PERT remains the global standard due to their availability, activity, and low production cost for EPI treatment. It is a condition intimately linked to malnutrition and maldigestion that leads to pancreatic disorders. These populations are subjected to a condition where the pancreas loses the ability to stimulate, produce, and deliver pancreatic enzymes, which causes pancreatic failure. However, the reliance on porcine sources presents a critical barrier for Muslim patients due to religious prohibitions, while also posing clinical risks such as zoonotic viral transmission and allergic reactions to porcine proteins. While the Fatwa Council permits these medications in the absence of alternatives, this exemption highlights the urgent unmet need for Halal–compliant sources, specifically from permissible animals like bovine (*Bos taurus*) and sheep (*Ovis aries*), which are currently discarded as agricultural biological waste.

Although, the agricultural by–products of bovine and sheep pancreases are available, there is a lack on critical scientific evidence regarding their biochemical viability as therapeutic substitute. Existing literature lacks a comprehensive, comparative analysis of the specific enzymatic efficiency of these ruminant enzymes against the established porcine standard. In addition, the structural integrity of these Halal candidates remains uncharacterized, particularly concerning on the glycosylation PTM. As glycosylation governs protein stability, solubility, and immunogenicity, the absence of detailed glycan profiling constitutes a major barrier to establishing these enzymes as safe, bioequivalent candidates for PERT.

1.3 Rationale of Study

PERT has been strongly associated with human EPI management, and porcine is still the only established option for PERT resources. There is limited research on Halal sources of pancreatic enzymes. It is, therefore, uncertain if animals such as bovine and sheep have the same pancreatic enzyme characteristics, behaviour, and activities as porcine. Therefore, it is unclear whether the pancreatic enzyme activities of Halal pancreatic enzymes have the same effects in treating EPI compared to porcine–based PERT. It must be ascertained that having Halal sources of PERT is an alternative to treating EPI in individuals.

1.4 Significance of Study

Porcine is commonly sourced for PERT. To date, limited studies have been conducted on bovine and sheep pancreatic enzymes as Halal PERT sources and their role in human EPI management. This study suggests a novel, an updated method for bovine and sheep pancreatic enzyme purification utilizing fresh pancreatic tissue as the starting material and adapting a simplified purification techniques employed by an automated purification system (AKTA Avant™) with pre–packed columns to purify the enzymes of interest. This approach demonstrates that Halal enzymes can be efficiently produced from agricultural by–products (fresh pancreas) without laborious and time–consuming steps such as relying on manual column packing, depending on gravity–flow or using older pump system for purification as mentioned in the previous study.

Furthermore, this study reports on the enzyme activity and compares it with the established commercial porcine enzymes. In addition, the *in–silico* analysis helps to determine glycosylation site prediction that gives unique characteristics to the enzyme of interest, namely Protease (Carboxypeptidase A1 – CBPA1), Lipase (Bile–Salt Activated Lipase – BSAL and Triacylglycerol Lipase – TL), and Alpha–amylase (AMYP) from fresh bovine (*Bos taurus*) and sheep (*Ovis aries*) pancreas. The *in–silico* findings allow direct comparison between different sources to help determine the alternative enzyme candidate. Gathering data from *in–silico* analysis and experimental findings help to comprehensively assess whether Halal enzymes can perform similarly to porcine enzymes. The major areas of comparison include sequence and structural similarity, and enzyme activity performance.

The novelty of this study lies in the successful modernization of decades–old protocol of pancreatic enzyme purification with minimum and simplified purification strategies that is sufficient to yield active Halal enzymes comparable to porcine enzymes. Thus, combining all outcomes will provide substantial information on the potential of using Halal sources for PERT that may perform similarly to the non–Halal porcine enzymes. In the future study, it is also important that Halal enzymes can demonstrate comparable functional and safety profiles to porcine enzymes and serve as a viable alternative for Halal–compliant PERT treatments without compromising efficacy.

1.5 Research Questions

Are Halal pancreatic enzymes from bovine and sheep enzyme activities comparable to or better than non–Halal porcine pancreatic enzymes relative to the glycosylation state?

a) What are the suitable methods to purify pancreatic enzymes such as protease (CBPA1), lipase (BSAL and TL), and amylase (AMYP)?
b) What are the differences between pancreatic enzyme activities for protease (CBPA1), lipase (BSAL and TL), and amylase (AMYP) from bovine and sheep compared with commercialized porcine as a positive control?
c) What are the differences in the glycosylation site prediction of pancreatic enzymes from bovine and sheep compared with porcine and human?

1.6 Hypotheses

a) Pancreatic enzymes, specifically protease (CBPA1), lipase (BSAL and TL), and amylase (AMYP), can be successfully extracted and purified from the fresh pancreas tissues of bovine (*Bos taurus*) and sheep (*Ovis aries*) using chromatographic separation techniques.
b) The purified pancreatic enzymes from bovine and sheep exhibit specific enzymatic activities that are comparable to the commercialized porcine pancreatic enzymes used as a positive control, thereby demonstrating their suitability as functional Halal–compliant alternatives.
c) The purified bovine and sheep pancreatic enzymes possess detectable PTM glycosylation patterns, predominantly N–linked glycosylation, which can be predicted through *in–silico* structural homology modelling and confirmed via experimental glycoprotein enrichment.

1.7 Objectives

The general objective of this research is to purify and characterise pancreatic enzymes from bovine (*Bos taurus*) and sheep (*Ovis aries*). The specific objectives of this study are as follow:

a) To identify and characterize pancreatic enzymes such as protease (CBPA1), lipase (BSAL and TL), and amylase (AMYP) from bovine (*Bos taurus*) and sheep (*Ovis aries*) pancreas.
b) To evaluate and compare the specific enzymatic activities of the purified bovine and sheep enzymes against commercial porcine enzyme as a positive control by evaluating their suitability as Halal–compliant alternatives.
c) To characterize the PTM glycosylation patterns of the purified enzymes using *in–silico* prediction through sequence and structural homology modelling and experimental profiling to confirm the glycosylation state.

1.8 Scope and Limitation of Study

This study aims to investigate Halal alternative sources of PERT, specifically protease (CBPA1), lipase (BSAL and TL), and amylase (AMYP) by utilisation of animal biological waste, the pancreas derived from bovine (*Bos taurus*) and sheep (*Ovis aries*). The first scope is enzyme identification which employs sequential purification techniques. The purification techniques employed in this study is limited to two steps purification which are IEX for all enzymes (CBPA1, BSAL, TL and AMYP) and GFC only for CBPA1.

The second scope involves on the comparison of the purified bovine and sheep pancreatic enzymes with established commercial porcine standard as positive control for their proteolytic, lipolytic and amylolytic activities. The aim is to identify whether these Halal pancreatic enzymes candidates from bovine and sheep process bioequivalence or superior potency when compared to the porcine standard. For CBPA1, BSAL, and TL, this comparison was conducted using purified enzymes. In contrast, due to the purification challenges, the comparative analysis for AMYP is limited to the amylolytic activity observed in the pancreatic crude extract only.

The final scope of this study, addressing the critical gap regarding the structural integrity and PTM glycosylation profiling of the purified enzymes to be compared with human and porcine. This scope only limited to *in–silico* analysis to predict N–linked and O–linked glycosylation sites using bioinformatic homology modelling and experimental validation utilizing Con A lectin enrichment with specific glycoprotein staining to confirm the biological presence of glycans. This study does not encompass detailed glycan structural elucidation or the identification of specific sugar moieties via high–resolution techniques such as Ultra–Performance Liquid Chromatography (UPLC) or mass spectrometry–based glycomics. This analysis is pivotal for providing preliminary data on the enzymes' sequence and structural stability relative to human and porcine standards.

1.9 Conclusion

In conclusion, this study successfully purified and verified bovine CBPA1, sheep CBPA1, bovine BSAL and sheep TL. Notably, the extraction and purification of AMYP from both bovine and sheep pancreas were unsuccessful using the designated purification protocols; while crude extracts demonstrated amylolytic activity comparable to the positive control, the enzyme could not be isolated as a pure fraction or identified via LC–MS/MS, excluding it from final purified recommendations. Among the purified pancreatic enzymes, sheep CBPA1 and bovine BSAL are strongly suggested for the PERT replacements as it shows potent enzymatic activities when compared to the positive porcine standards. Although, the structural characterisation via *in–silico* analysis predicted a predominance of N–linked glycosylation across all enzymes, the experimental validation utilising glycoprotein enrichment confirmed that only CBPA1 possesses detectable glycosylation, thereby substantiating its structural stability and biological relevance as a prime candidate for Halal therapeutic applications in PERT.

CHAPTER 2
LITERATURE REVIEW

2.1 Pancreas

The word **pancreas** is derived from the Greek words ‘pan’ and ‘creas’, meaning ‘all’ and ‘flesh’, respectively (Cruickshank, 1986; Tsuchiya & Fujisawa, 1997). The Greeks first recognized it as a distinct organ without conceptualizing its function. The first description of the pancreas was made by Herophilus of Chalcedon (circa 300 B.C.) (Busnardo *et al.,* 1983). The pancreas is located close to the duodenum's beginning point. Its primary function is to secrete pancreatic juice, which flows into the duodenum, where it contains pancreatic enzymes that have different functions in the human body.

The pancreas is the largest gland in the digestive system, a retroperitoneal organ situated immediately behind the posterior wall of the lesser sac on the floor of the supracolic (Ellis, 2013; Mahadevan, 2019). It is an elongated, soft, flat, lobulated, and yellowish gland that lies on the posterior abdominal wall transversely (Mahadevan, 2019). Figure 2.1 shows the anatomic view and structure of the pancreas with surrounding organs partitioned into three parts, namely, head, neck, and tail (Roder *et al.,* 2016). It is surrounded by the adrenal gland, the left and right kidneys, the duodenum, and the spleen.

The head of the pancreas lies in the loop of the duodenum as it exits the stomach. The head part consists of the minor and major papilla, the right kidney, and the second part of the duodenum. The minor papilla is where the accessory pancreatic duct drains into the duodenum; meanwhile, the major papilla is where the main pancreatic duct enters the duodenum. The neck consists of major blood vessels such as the superior mesenteric arteries, the superior mesenteric–portal vein, the inferior vena cava, and the aorta. The tail part lies near the hilum of the spleen with the splenic artery (Splenic a). Below the splenic artery is a splenic vein running to form a vena port (Sup. Mesenteric v and a), as in Figure 2.1.

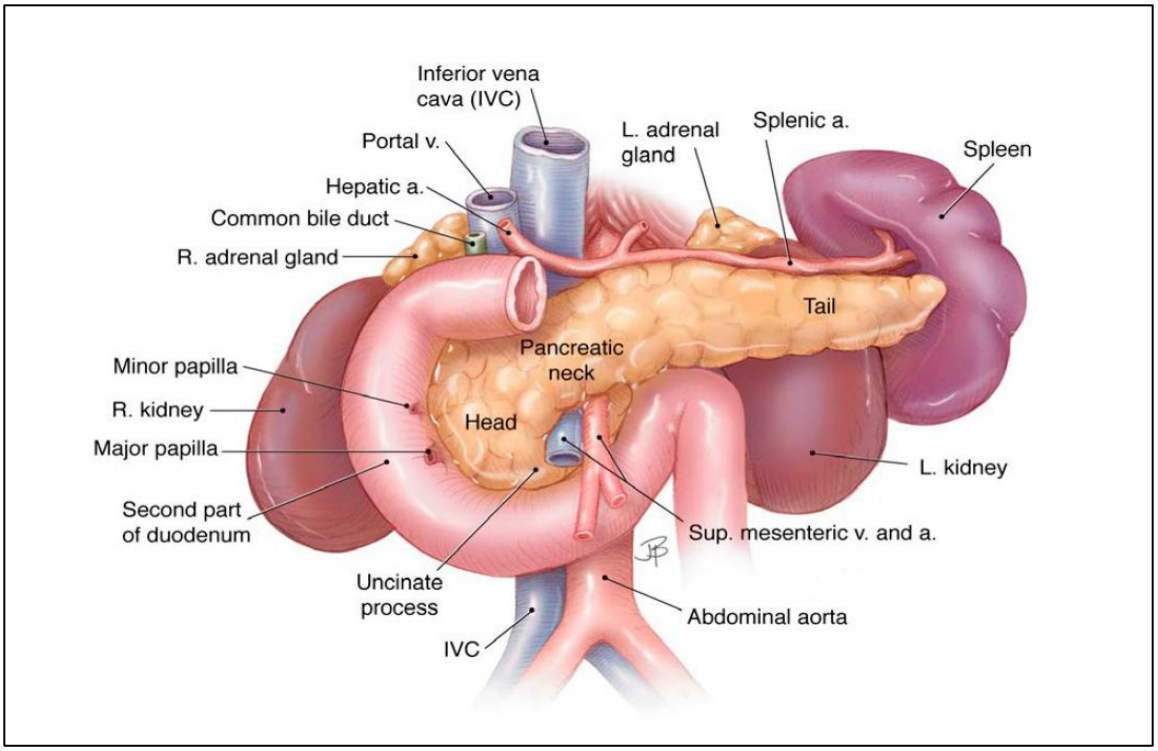


Figure 2.1 Anatomic View Structure of the Pancreas (Longnecker, 2014).

2.1.1 Endocrine and Exocrine Systems

The primary function of the pancreas can be subcategorized as **exocrine** and **endocrine** (Wilschanski & Shaoul, 2014). Figure 2.2, shows the exocrine and endocrine components of the pancreas. The exocrine portion is made up of acinar and duct tissues, while the endocrine portion is made up of islets of Langerhans (Pandol, 2015).

Notably, the pancreas is a vital organ that plays a critical role in nutrient metabolism and the regulation of digestion via endocrine and exocrine processes (Cade & Hanison, 2017; Henry *et al.,* 2019). The pancreas has very important endocrine and exocrine components (Imrie *et al.,* 2010; Pandol, 2015). Both the exocrine and endocrine pancreas are anatomically and physiologically closely linked together (Zsóri *et al.,* 2018). Any diseases affecting one of these parts will inevitably affect the other (Zsóri *et al.,* 2018). The pancreas is a complex organ that encompasses both endocrine and exocrine glands that secrete hormones directly into the bloodstream and secrete digestive enzymes into the intestinal lumen, respectively (Henry *et al.,* 2019).

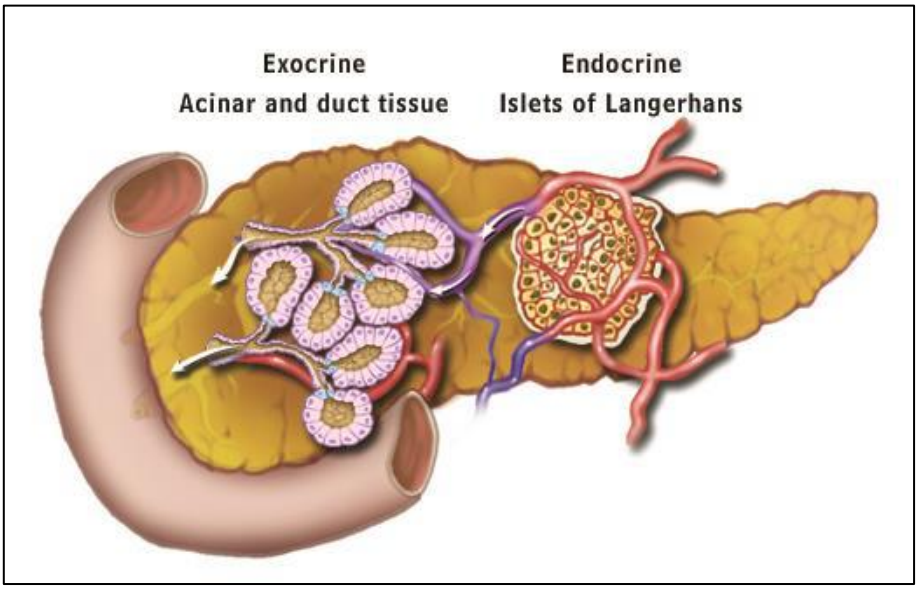


Figure 2.2 Exocrine and Endocrine Pancreas System (Pandol, 2015).

2.1.1.1 Endocrine System

In the **endocrine system**, the primary function of the pancreas is as an endocrine gland that produces many important hormones. The hormone will be secreted into the bloodstream once the gland produces it. The endocrine glands are known to secrete glucagon from alpha cells, insulin from beta cells, somatostatin from delta cells, a pancreatic polypeptide from gamma cells, and ghrelin from epsilon cells (Aziz, 2018; Cade & Hanison, 2017; Henry *et al.,* 2019). The endocrine cells are organized into compact clusters known as the islets of Langerhans, which are small, island–like structures dispersed throughout the pancreatic tissue (Roder *et al.,* 2016). Table 2.1 explains the five major types of hormones secreted by the secretory cells in each islet of Langerhans in the endocrine gland.

Table 2.1
Five Endocrine Secretion Cells in each Islet of Langerhans

Type of Cells	The proportion of Islet Cells	Hormone Secreted
Alpha	35%	Glucagon
Beta	55%	Insulin
Delta	<10%	Somatostatin
Gamma	<5%	Pancreatic Polypeptide
Epsilon	<1%	Ghrelin

Note: The data gathered from Cade & Hanison (2017).

These hormones, secreted by all the cell types, are important and carry different essential functions in the human body. In other words, a hormone is a chemical substance that affects the activity of another part of the body known as a target site. Principally, the hormones serve as messengers, controlling and coordinating the body's activities (Morley, 2019). The hormones control the entire organ function, which impacts various processes such as growth and development, reproduction, and sexual characteristics (Morley, 2019). However, certain organs and tissues will also be influenced by specific hormones.

Insulin and glucagon are regulators of glucose metabolism (Roder *et al.,* 2016). The findings of these hormones have revolutionized the understanding of diabetes, as the role of insulin and the impact of glucagon have been recognized in diabetic patients (Ojha *et al.,* 2019). Somatostatin is a regulator for the anterior pituitary gland that exerts potent inhibitory action on hormone secretion, to some extent, pituitary tumour cell growth, and neuronal excitability (Eigler & Ben-Shlomo, 2014; Günther *et al.,* 2018).

2.1.1.2 Exocrine System

The **exocrine** glands secrete pancreatic juices approximately 1200 – 1500 mL daily, containing water, bicarbonate ions, and numerous enzymes such as carboxypeptidases, lipase, phospholipase A, amylase, trypsinogen, chymotrypsinogen, elastase, DNAse, and RNAse (Berry, 2014; Henry *et al.,* 2019). Then, these pancreatic juices will pass through the small intestine to further their functions and break down carbohydrates, proteins, and fats. The exocrine gland is a lobulated, branched, acinar gland rich in mitochondria that helps to secrete non–enzymatic components of the pancreatic juice. Figure 2.3 explains the exocrine pancreas secretion controlled by hormonal and neuronal stimulation (Brennan & Saif, 2019; Cade & Hanison, 2017).

Notably, the hormone secretin acts on the pancreas for bicarbonate release, and cholecystokinin (CCK) acts on the gallbladder and the pancreas to stimulate the release of bile and pancreatic secretions (Berry, 2014). CCK is released by neuroendocrine cells within the small bowel in response to food availability (Cade & Hanison, 2017). It will stimulate cell activity and secretion of the acinar cell by binding to the receptor cell surface present on the basolateral membrane of the acinar cell (Cade & Hanison, 2017).

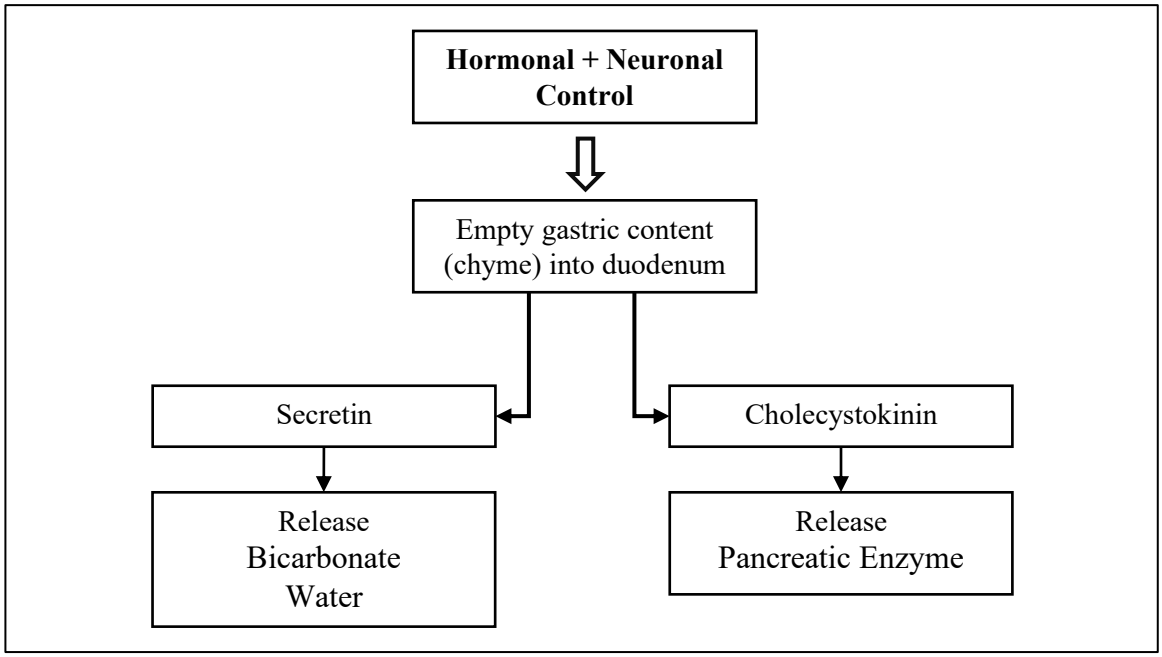


Figure 2.3 Exocrine Pancreatic Secretion (Berry, 2014).

Normal exocrine pancreatic function is crucial for effective digestion and nutrient absorption (Fieker *et al.,* 2011). Figure 2.4 shows the healthy human pancreas after an autopsy without fat and adjacent organs. The exocrine pancreas plays a critical role in the digestive system by secreting pancreatic juice consisting of numerous enzymes and an aqueous solution rich in sodium bicarbonate (Antonini *et al.,* 2017).

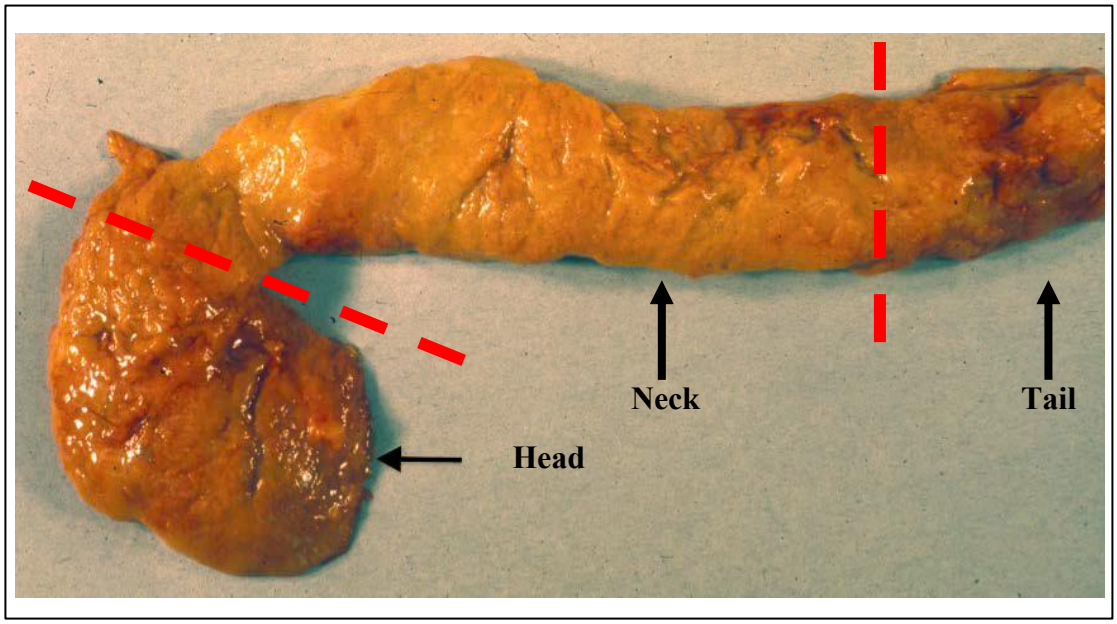


Figure 2.4 Normal Human Pancreas (Longnecker, 2014).

Sodium bicarbonate is essential to neutralize the acidic pH of gastric content delivered to the intestine from the stomach, where neutral pH is necessary for healthy digestion and absorption (Pandol, 2015). Naturally, the pancreas secreted active forms of amylase, lipase, enterokinase, trypsin, and bicarbonate. It also secretes inactive forms of proteolytic enzymes, including trypsinogens, chymotrypsinogen A, chymotrypsinogen B, procarboxypeptidase A, and procarboxypeptidase B (Berry, 2014).

Besides, pancreatic secretion is a complex process regulated by both neural and endocrine controls. When the pancreas secretion fails to maintain healthy digestive function, it leads to clinical exocrine pancreatic insufficiency (EPI), resulting in nutrient malabsorption and diarrhoea (Fieker *et al.,* 2011). Clearly, due to proper digestion and absorption processes, any alteration that causes impaired pancreatic secretion could vastly affect absorption capacity (Berry, 2014). Malnutrition will affect life quality. For instance, EPI distracts healthy growth, life expectancy, and immune system response.

2.1.2 Exocrine Pancreatic Insufficiency

Exocrine Pancreatic Insufficiency (EPI) is defined as a reduction, absence of stimulation and production, inadequate activity or deficiency of the pancreatic digestive enzymes to digest food within the intestinal lumen, resulting in maldigestion, malabsorption, and ultimately, malnutrition (Antonini *et al.,* 2017; Brennan & Saif, 2019; Jawaid & Forsmark, 2019). The general EPI prevalence is unknown (Capurso *et al.,* 2019). EPI and maldigestion were reported to occur in up to 80% of patients following gastric, duodenal, or pancreatic surgery (Tang *et al.,* 2025). EPI is reported to be prevalent in children with severe acute malnutrition, especially in children with edema (Bartels *et al.,* 2016).

It is clinically evident that EPI happens when 90% of the pancreas's function is impaired, with 10% less of pancreatic enzyme secretion, leading to malabsorption (Landers *et al.,* 2019). It is a chronic condition resulting from pancreatic diseases and or surgery, which disturbs normal exocrine pancreatic function and lowers the production and secretion of both digestive enzymes and bicarbonate (Pierzynowska *et al.,* 2018). Loss of exocrine function is preceded by and clinically visible by poor fat absorption following carbohydrate and protein malabsorption (Imrie *et al.,* 2010;

Sikkens *et al.,* 2010). EPI is classified as a deficiency of three major pancreatic digestive enzyme groups: protease, amylase, and lipase (Wilschanski & Shaoul, 2014).

Two types of EPIs are primary and secondary. Primary EPI happens due to low exocrine pancreatic tissue or innervation disturbances, and secondary EPI occurs when the release of pancreatic enzymes does not function well due to anatomical changes and impropriated activation or inactivation (Oliver *et al.,* 2013). The symptoms of EPI include diarrhoea, steatorrhea, weight loss, fatigue, flatulence, abdominal distention or discomfort, bloating, edema, and, in some cases, anaemia (Aziz, 2018; Bellomo, 2020). Other conditions, such as bone loss, compromised immunity, and deficiency of fat–soluble vitamins (A, D, E, K), can be associated with EPI (Antonini *et al.,* 2017; González-Sánchez *et al.,* 2017). The nonspecific EPI symptoms frequently overlap with other gastrointestinal conditions, with maldigestion or malabsorption, resulting in diagnostic difficulties (Bellomo, 2020; Sankararaman *et al.,* 2019).

These substantially impair the quality of life, where EPI and diabetes mellitus contribute to the low median survival of 15–20 years from diagnosis (Iglesia-García *et al.,* 2017). The impact of EPI and malnutrition cannot be underestimated (Pezzilli *et al.,* 2020). Therefore, early diagnosis with subsequent treatment of EPI is significant to improve life quality and to increase the survival rate (Powell-Brett *et al.,* 2020). EPI diagnosis can be made in two ways: via invasive and non–invasive methods. The invasive method is a measurement of pancreatic juice collected from the duodenum, while the non–invasive method is a measurement of digestion products either passed through or absorbed and detected in blood (Sikkens *et al.,* 2010). Moreover, pancreatic function tests should be ideally valuable to monitor adequate Pancreatic Enzyme Replacement Therapy (PERT) (González-Sánchez *et al.,* 2017).

2.1.2.1 Causes of Exocrine Pancreatic Insufficiency

EPI is a predominantly clinical diagnosis (Fieker *et al.,* 2011; Pierzynowska *et al.,* 2018). It is the consequence of several different diseases, which all share the typical pathophysiologic result of inadequate enzyme production (Brennan & Saif, 2019). It is a common and severe complication of different pancreatic as well as extra–pancreatic diseases. Several genetic, molecular, and clinical factors can impair pancreatic function (Imrie *et al.,* 2010).

There are multiple causes of EPI, including chronic pancreatitis (CP), cystic fibrosis (CF), and pancreatic cancer (PC) (Brennan & Saif, 2019; Dominguez-Muñoz *et al.,* 2025). The leading cause of EPI in adults is CP, while in children, it is CF (Stockley, 2014). Gastrointestinal and pancreatic surgical resections, obstruction of the ventral pancreatic duct, decreased pancreatic stimulation, or acid–mediated pancreatic enzyme inactivation do contribute to EPI (Zsóri *et al.,* 2018). Life–threatening EPI aetiology includes both pancreatic and extra–pancreatic causes, as listed in Table 2.2 (Bellomo, 2020; Ianiro *et al.,* 2016).

Table 2.2
Aetiology of Exocrine Pancreatic Insufficiency

Primary Pancreatic Diseases	Extra–Pancreatic Diseases
Pancreatitis (Acute and Chronic)	Diabetes Mellitus
Pancreatic Cancer	Coeliac disease
Pancreatic Surgery	Gastric Surgery
Pancreatic Agenesia	Bariatric Surgery
Cystic Fibrosis	Peri–ampullary tumors
Congenital Disorders Pancreatic hypoplasia Isolated lipase–colipase deficiency Shwachman–Diamond syndrome Johanson–Blizzard Syndrome	Extrapancreatic neuroendocrine tumors Gastrinoma Somatostanimo
Pancreatic Lipomatosis or Atrophy	Inflammatory Bowel Disease Ulcerative Colitis Crohn's Disease

Note: The data was adopted from Antonini *et al*. (2018).

2.2 Pancreatic Diseases

2.2.1 Chronic Pancreatitis

Chronic pancreatitis (CP) is a progressive fibro–inflammatory disorder with sustained destruction of acinar, ductal, and islet cells and gradual replacement of the exocrine and endocrine cells with fibrotic tissues (Gardner *et al.,* 2020; Olesen, 2019). It is characterized by an inflammatory reaction of the pancreas, progressively destroying the gland and leading to pancreatic exocrine and endocrine dysfunction (Frulloni *et al.,* 2010). The combination of chronic inflammation, calcification, and atrophy of the pancreas leads to CP development (Pirahanchi & Sharma, 2019).

CP is reported to have an annual incidence of 5–12 per 100,000 population in 2013, and the number keeps increasing worldwide (Zhang *et al.,* 2026). However, the CP prevalence is estimated to have grown to 120–140 per 100,000 recently (Olesen, 2019). At the same time, CP is increasingly recognized in the pediatric population, with incidence rates approaching those seen in adults (Gagyi *et al.,* 2025). EPI is one of the influential independent risk factors for mortality in CP, and the EPI prevalence in CP is at 30–40% (Fieker *et al.,* 2011; Jawaid & Forsmark, 2019). The mortality rate increased 5–fold in patients with CP regardless of the background population (Olesen, 2019).

The early stage is characterized by pain or recurrent episodes of pancreatitis and complications, whereas in the advanced phase, symptoms related to the onset of exocrine and endocrine insufficiency (Frulloni *et al.,* 2010). Painful CP is a very vexing problem for patients and clinicians, where 0.4–5% of the adult population is affected (Winstead & Wilcox, 2009). During the disease progression, 80–90% complained of feeling the pain, yet the remaining 10–20% experienced painless pancreatitis (Frulloni *et al.,* 2010). The most dominant symptom of CP is upper abdominal pain, presented with weight loss and bowel habit changes caused by EPI (Gardner *et al.,* 2020; Olesen *et al.,* 2019).

There are various etiologies of CP, including toxic metabolic, idiopathic, single, or multiple gene mutations, genetic predisposition, hyperglycemia, hypertriglyceridemia, autoimmune, recurrent severe acute pancreatitis–related, and obstructive (Wilschanski & Shaoul, 2014). The environment's toxic metabolic inclusive of prolonged excessive massive alcohol exposure, cigarette smoking, prescription, and illicit drugs (Iglesia-García *et al.,* 2017; Olesen *et al.,* 2019). Smoking limits the pancreas's ability to secrete bicarbonate, and water leads to premature digestive enzymes before they can enter the intestine (Wilschanski & Shaoul, 2014). Whereas the genetic mutations can occur in any of the genes, such as *PRSS1, SPINK1, CTRC, CASR, CFTR, CLDN2,* and *CPA1* (Iglesia-García *et al.,* 2017).

EPI from CP reduces the absorption of fat, including essential fatty acids, fat–soluble vitamins A, D, E, and K, calcium, magnesium, zinc, thiamine, and folic acid (Iglesia-García *et al.,* 2017). Pancreatic enzyme supplementation helps to improve fat absorption in patients with CP and EPI (Frulloni *et al.,* 2010). PERT is reported as the standard of care in patients with EPI in the setting of CP (Bartel *et al.,* 2015).

2.2.2 Pancreatic Cancer

The relation of CP to **pancreatic cancer (PC)** was addressed in several epidemiologic case–control and cohort studies (Frulloni *et al.,* 2010). The patients with CP reported increased mortality and a higher risk of developing PC (Olesen *et al.,* 2019). PC is an aggressive malignancy and devastating disease characterized by invasiveness, rapid progression, and profound resistance to treatment (Jelski & Mroczko, 2019). The mortality and incidence are nearly equal, as one of the deadliest of all malignancies (Chabot *et al.,* 2010). It is the seventh leading cause of global cancer deaths in industrialized countries (Pezzilli *et al.,* 2020). It is expected to become second only to lung cancer as the leading cause of cancer–related deaths in the United States (US) by 2030 (Miller *et al.,* 2020). It is listed as the deadliest cancer, with an exceptionally high mortality rate (Jelski & Mroczko, 2019).

The most common form of PC is pancreatic ductal adenocarcinoma (PDAC) (Dindyal & Spalding, 2019; Miller *et al.,* 2020). EPI has become one of the standard hallmark features in PC patients (Landers *et al.,* 2019). There are several mechanisms of EPI that have been described in the context of PC. EPI is a common and progressive condition in unresectable PC, with a prevalence between 50–100% (Bartel *et al.,* 2015). However, the treatment is often restricted only to the oncological aspect, although EPI is ubiquitous in PC (Bartel *et al.,* 2015).

There are multiple risk factors for developing PC, including genetic syndromes such as Lynch syndrome and Peutz–Jeghers syndrome (Lombardo *et al.,* 2018). The most established risk factor identified for PC is being a cigarette smoker, which may account for approximately 25–30% of cases (Dindyal & Spalding, 2019). Other well–recognized risk factors include obesity and type II diabetes (Miller *et al.,* 2020). In PC, 68–92% of patients present malabsorption symptoms during diagnosis. These symptoms may include diarrhoea, excessive flatulence, cramping, steatorrhea, abdominal bloating, and weight loss (Landers *et al.,* 2019).

PC is usually diagnosed late and has a biological phenotype characterized by resistance to all cancer treatment modalities and early metastasis (Dindyal & Spalding, 2019). The main focus of PC research can be achieved by improving the early diagnosis of PC and strengthening the comprehensive standardized treatment (Jelski & Mroczko, 2019). The previous study reported that PERT is a safe therapy for malabsorption symptoms in PC patients (Landers *et al.,* 2019).

2.2.3 Cystic Fibrosis

Cystic Fibrosis (CF) is an autosomal recessive inherited disorder with a broad spectrum of multi–organ manifestations associated with defective epithelial ion transport and pancreatic exocrine secretion (Johns & Rowe, 2019; Mennitt, 2012). Mutations in the CF transmembrane regulator (*CFTR*) gene modulate other properties of epithelial ion channels that affect the intestinal milieu (Hayee *et al.,* 2019). A mutated *CFTR* gene leads to dehydrated epithelial surfaces and a build–up of mucus in a variety of tissues, including the lungs and pancreas (Kelsey *et al.,* 2019). It is considered a chronic, life–threatening disease that primarily affects the respiratory and digestive systems' function (American Lung Asscociation, 2020).

CF is estimated to affect between 70,000–100,000 people worldwide (Kelsey *et al.,* 2019). Approximately 85–90% of CF patients suffer from pancreatic duct obstruction associated with EPI, where lack of pancreatic enzymes leads to maldigestion and malabsorption, contributing to poor nutritional status (Trapnell *et al.,* 2011, 2020). Positively, maldigestion in CF does affect 90% of patients' lives (Munck *et al.,* 2009). Correspondingly, EPI is conventional in children with CF, and the prevalence is between 80–90% (Fieker *et al.,* 2011; Sankararaman *et al.,* 2019).

CP in adults and CF in children are the primary indications for the use of PERT, and it is critical for EPI correction (Oliver *et al.,* 2013; Trapnell *et al.,* 2011). Both CP and CF are classified as irreversible EPI (American Medical Association, 2017). 85–90% of individuals with CF have pancreatic insufficiency and require PERT to manage maldigestion and malabsorption (Stapleton *et al.,* 2012). PERT is the treatment of choice for EPI in CF patients to prevent malabsorption and maintain an optimal nutritional status (Trapnell *et al.,* 2011). Digestive enzyme replacement is necessary, especially for children with CF, as a result of damaged pancreatic ducts and acinar cells (Mennitt, 2012). In addition to pulmonary medications, more than 80% of patients with CF younger than 40 years are prescribed PERT to treat EPI (Trapnell *et al.,* 2020).

2.3 Pancreatic Enzyme

Pancreatic enzymes are medications containing the active ingredient pancrelipase, a mixture of the digestive enzymes – protease, amylase, and lipase (Berry, 2014; Mennitt, 2012). Pancreatic enzymes play an essential role in the biological process, which is significant in the medical and pharmaceutical fields. The pancreatic digestive enzymes are divided based on their respective role, known as proteolytic, amylolytic, and lipolytic enzymes, that are essential for the hydrolytic intraluminal breakdown of macronutrients into smaller, absorbable metabolites (Ianiro *et al.,* 2016).

The digestive enzymes are in the zymogen form before they can be used as pancreatic enzymes. It is also known as a proenzyme with no catalytic activity (Brittanica, 2020). These enzymes need to be cleaved at a specific site before being used. The cleavage process will transform the enzymes into an active form, which can later be used in food digestion. The most common zymogens secreted by the pancreas are trypsinogen and chymotrypsinogen, which will be activated to trypsin and chymotrypsin in the intestinal tract (Brittanica, 2020).

According to the (Pancreatic Cancer Action Network (2020), different types of pancreatic enzymes will have different functions and impacts on shortage. The three types of enzymes secreted to digest the ingested macronutrients are proteins, starches foods, and lipids. Under normal physiological conditions, the three main types of digestive enzymes are responsible for digesting micronutrients present in chyme and nutrient absorption (Antonini *et al.,* 2017; Ianiro *et al.,* 2016). Table 2.3 lists the enzymes in the control to digest ingested macronutrients. Factors including age, gender, and diet determine the enzyme content of pancreatic fluid (Fieker *et al.,* 2011).

Table 2.3
List of Enzymes for Macronutrient Digestion

Protein	Starch	Lipid
Trypsinogen I, II, and III	α–Amylase	Pancreatic Lipase
Chymotrypsinogen		Pancreatic Lipase–Related Protein I and II
Proelastase I and II		Carboxyl Ester Lipase
Protease E		Phospholipase AII
Kallikreinogen		
Procarboxypeptidase AI, AII, BI and BII		

Source: (Fieker *et al.,* 2011).

2.3.1 Enzyme Release Phase

Pancreatic enzyme release involves three stages, known as the cephalic, gastric, and intestinal phases (Bartel *et al.,* 2015). The cephalic phase is initiated by vagal–mediated nutritional intake. Following gastric distension, the gastric phase increased pancreatic enzyme release via the gastropancreatic. Less commonly, excessive fluctuation and abdominal distension may be caused by bacterial fermentation of unabsorbed food substances (Wilschanski & Shaoul, 2014). Lastly, in the intestinal phase, mostly mediated by CCK in the chyme passage through the duodenum, the stimulation of exocrine pancreatic secretion takes place to hydrolyse TAG and free fatty acids. The pancreatic enzyme release physiology is explained in Figure 2.5.

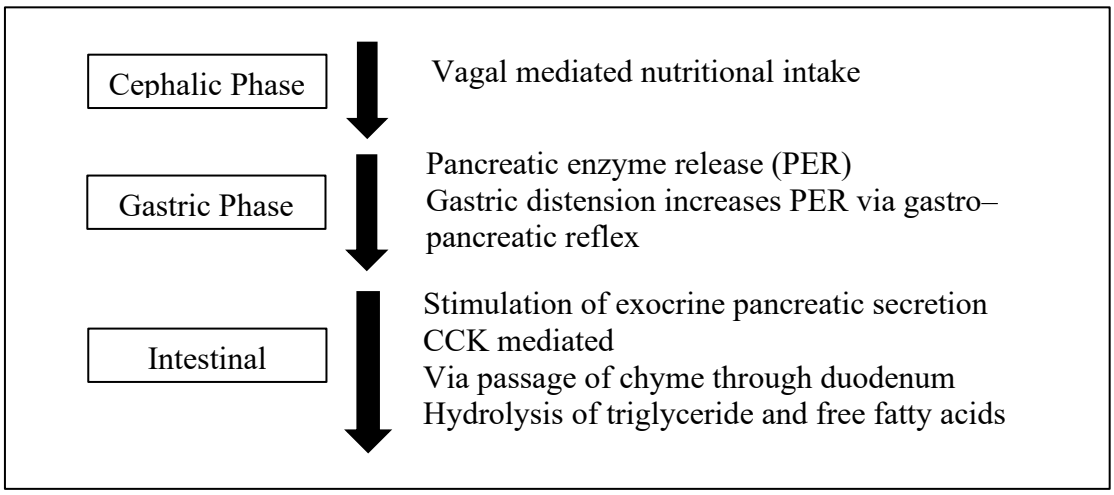


Figure 2.5 Stages of Pancreatic Enzyme Release.

2.4 Pancreatic Enzyme Therapy

2.4.1 Origin and Discovery of Pancreatic Enzyme Therapy

Pancreatic Enzyme Replacement Therapy (PERT) was initially known as **Pancreatic Enzyme Therapy (PET)**. There are controversy and debate on the PET discoveries (Gonzalez, 2014). PET was first discovered by the Scottish scientist John Beard in 1906 (Chabot *et al.,* 2010). He was honoured by the French Academy of Sciences in 1890 and nominated with the Nobel Prize for Medicine in 1906 (Rose, 2017). Through the trophoblast cancer model, he found that pancreatic enzyme, principally trypsin, helps convert cancer cells to normal trophoblasts (Rose, 2017). His

findings recommended the therapeutic use of pancreatic proteolytic enzymes in treating cancers and other diseases (Chabot *et al.,* 2010; Moss, 2008). He was the first scientist to propose anticancer activity for trypsin (Gonzalez, 2014).

The therapeutic use of enzymes has become a part of conventional medical practice. In 1978, the US Food and Drug Administration (FDA) approved asparagine and urokinase for acute lymphocytic leukemia, acute myocardial infarctions, and pulmonary embolism treatments. In 1988, the FDA granted orphan drug status enzyme combination for myeloma treatment. The FDA also granted a new drug application using PET to treat EPI associated with CF and CP. Thus, PERT has become the standard treatment for EPI (American Medical Association, 2017).

2.4.2 Pancreatic Enzyme Replacement Therapy

According to the OncoLink website, **Pancreatic Enzyme Replacement Therapy (PERT)** is the use of medication containing pancreatic enzymes, namely, proteases, amylases, and lipases, to replace the enzymes the pancreas no longer available to produce (Claghorn, 2019). It is set as a 'present standard' and central management strategy clinically relevant to treat confirmed symptomatic EPI (Ashkar *et al.,* 2025). It has been recommended by the National Institute of Clinical Excellence (NICE) for all patients in the United Kingdom (González-Sánchez *et al.,* 2017; Kovacheva-Slavova *et al.,* 2017; Pierzynowska *et al.,* 2018; Powell-Brett *et al.,* 2020).

Oral PERT is given as a standard treatment for EPI (Pezzilli *et al.,* 2020). Supplemental pancreatic enzyme preparations are commonly provided to patients with conditions of pancreatic exocrine deficiency to facilitate nutritional improvement (Dunleavy *et al.,* 2018). PERT requirements vary based on many factors, including the degree of pancreatic insufficiency, pharmaceutical action, and pharmacokinetic activities (Stapleton *et al.,* 2012).

In PERT alone, the market values are estimated to reach billions of US dollars within the next five years. Based on the Global Exocrine Pancreatic Insufficiency Market 2018 research report, the EPI market will grow significantly at a compound annual growth rate between 2019 and 2028 (Market Watch, 2019). The report included a meaningful analysis of market size, the latest trends, drivers, threats, opportunities, and key market segments. Advanced treatments are in demand, and increasing incidences of EPI worldwide drive critical factors for global EPI market growth (Market

Research, 2020). Meanwhile, the industrial enzymes' global revenue is estimated at US$7.2 billion annually in 2020 (Ranke *et al.,* 2020).

PERT treatment has been reported to improve life expectancy and confer significant survival advantages (Powell-Brett *et al.,* 2020). The orally administered pancreatic enzyme has been available since at least the 19th century, when many formulations were available as digestive aids (Trang *et al.,* 2014). Nutritional counselling and oral pancreatic enzyme replacement are the basic therapy for EPI (Domínguez-Muñoz, 2011). PERT is safe and effective at treating EPI based on clinical experience and well–controlled clinical trials (Brennan & Saif, 2019; Trapnell *et al.,* 2011). Most formulations are marketed in different strengths based on enzyme activity per capsule or tablet (Trang *et al.,* 2014).

2.4.3 Challenges in Pancreatic Enzyme Replacement Therapy

PERT aims to restore normal fat absorption by delivering sufficient active enzymes at the right place and at the right time in parallel with the gastric emptying of nutrients (Trang *et al.,* 2014). It is crucial to achieve the treatment goal of replicating the physiological process that allows an adequate amount of active pancreatic enzymes in the duodenum, simultaneously with the presence of meal nutrients (Antonini *et al.,* 2017). It is essential for optimal nutrient absorption (Peter *et al.,* 2001). Above all, the main focus of EPI management is to prevent weight loss, EPI–related symptoms, and vitamin deficiencies, as well as to improve the nutritional status (Domínguez-Muñoz, 2011; Sikkens *et al.,* 2010).

There are multifaceted challenges in PERTS that includes clinical management complexities, safety risk with escalating market demands for ethical compliance. Effective therapy is limited by the ability to replicate the physiologic process of enzyme delivery to the appropriate site, in general, the duodenum, at the appropriate time (Fieker *et al.,* 2011). The challenges include enzyme destruction in the stomach, lack of adequate mixing with the chyme in the duodenum, and failure to deliver and activate at the appropriate time (Fieker *et al.,* 2011). In addition, it is difficult to find the ideal PERT dosing for a particular patient, as the response to treatment could varies from patient to patient (Brennan & Saif, 2019).

Since pancreatic function is challenging to quantify, the recommended dosage of pancreatic enzymes can be given based on symptom improvement or relevant nutritional targets set for patients (Dominguez-Muñoz *et al.,* 2025). PERT recommends doses are based on body weight or the amount of fat present in the food consumed (Sankararaman *et al.,* 2019). Therefore, appropriate delivery and dosing timing are vital for effective PERT treatment. Delivering sufficient concentrations of pancreatic enzymes into the duodenal lumen concurrently with meals significantly alleviates nutrient malabsorption (Ferrone *et al.,* 2007).

It was reported that the porcine pancreatic enzyme supplement is the first option for pancreatic failure (Mayberry, 2014). Porcine pancreatic enzymes are highly requested for both food production and medical purposes. However, there is a high demand for Halal pancreatic enzymes for Muslim and Kosher populations, as Halal serves as reasonable quality assurance. Moreover, for religious reasons, the believers abstain from consuming products made from pork (Konstan *et al.,* 2018).

Instead, the PERT formulations available in the market are enteric and non–enteric coated and originated from porcine (Brennan & Saif, 2019; Sankararaman *et al.,* 2019). According to American Medical Association (2017), available pancreatic enzyme replacement in the US market containing a mixture of porcine–derived proteases, lipases, and amylases. Enteric–coated enzymes are formulated to protect the enzymes until they enter a higher pH of the intestinal lumen and are orally taken (Berry, 2014).

2.4.4 Pancreatic Enzyme Drugs Available on the Market

Pancreatic enzyme replacement products have been used for years with the same goal of improving digestion in patients with EPI (American Medical Association, 2017). The current commercially Food and Drug Administration (FDA) approved PERTs in the US are Creon, Zenpep, Pancreze, Pertzye (all enteric–coated), and Viokase (only non–enteric coated) (Ianiro *et al.,* 2016). Recent study reported that the differences in prescription of PERT products that contained pancrelipase were given based on formulation–specific attributes with access/coverage consideration (Ashkar *et al.,* 2025). In EPI, most exogenous pancreatic enzyme products used for PERT are usually extracted from the swine pancreas. There are two types of FDA–approved PERT products for EPI: immediate and delayed release.

Admittedly, there is a necessity to find alternatives for porcine–based pancreatic enzymes to cater to vegetarians and vegans, Muslims, Jews, Seventh Day Adventists, and Hindus. Patients with porcine allergy have also become significantly concerned about consuming PERT extracted from porcine (Berry, 2014; Konstan *et al.,* 2018). Different brands from different companies developed PERT with the same objective to cure and reduce the effects of EPI in humans. Other examples of PERT available are Ultresa, Nutrizyme, and Pancrex. However, any PERT consumption needs to be advised by qualified medical teams such as doctors, pharmacists, and dietitians. Table 2.4 lists the available pancreatic enzyme drugs on the market.

Table 2.4
Pancreatic Enzyme Drugs Available on the Market

Product Name	Sources	Dosage	Company
Creon (Pancrelipase) Delay–release	Pancrelipase contains multiple enzyme classes, including porcine–derived lipases, proteases, and amylases.	3000 USP (Lipase) 9500 USP (Protease) 15000 USP (Amylase)	RxList Inc.
Zenpep (Pancrelipase) Delay–release	A mixture of digestive enzymes (lipases, proteases, and amylases) from pig pancreas.	3000 USP 5000 USP 10000 USP 15000 USP 20000 USP 25000 USP 40000 USP	Nestle Health Science
Pertzye (Pancrelipase)	Contain porcine–derived protease, lipase amylase and bicarbonate buffer.	4000 USP 8000 USP 16000 USP 24000 USP	Chiesi Inc.
Viokase (Pancrelipase) Immediate–release	Contain porcine–derived protease, lipase, amylase as well as other pancreatic enzymes.	8000 USP (Lipase) 30000 USP (Protease) 30000 USP (Amylase)	RxList Inc.
Ultresea (Pancrelipase)	Contains porcine–derived protease, lipase, and amylase.	4000 USP (Lipase) 8000 USP (Protease) 8000 USP (Amylase)	RxList Inc.
Nutrizyme	The combination 335 mg proprietary blend includes proteolytic enzymes Pepsin, Bromelain, Papain, Pancreatin, Trypsin and Chymotrypsin.	8 USP (Pancreatin) 16000 FCC (Papain) 1200 DU/GM (Bromelain) 10M X (Pepsin) 1000 USP/mg (Chymotrypsin) Rutin Trypsin	DR Vitamin Solutions
Pancrex	Contains pancreatin as an active ingredient.	160 BP (Protease) 2950 BP (Lipase) 3300 BP (Amylase)	Essential Pharmaceuticals

Note: USP (United States Pharmacopeia)

2.4.5 Enzymes Used in Pancreatic Enzyme Replacement Therapy

The therapeutic formulations of the PERT primarily consist of three main classes of essential digestive enzymes, namely as protease, lipase and amylase. These enzymes were classified based on their respective biological functions as proteolytic, lipolytic and amylolytic, respectively. The combination of these digestive pancreatic enzymes is crucial to facilitate the hydrolysis of macronutrient, specifically for protein, carbohydrates and lipid into smaller and absorbable metabolites. Figure 2.6 shows the overview of the main classes of pancreatic enzymes that consist of proteases, lipases and amylases for PERT applications.

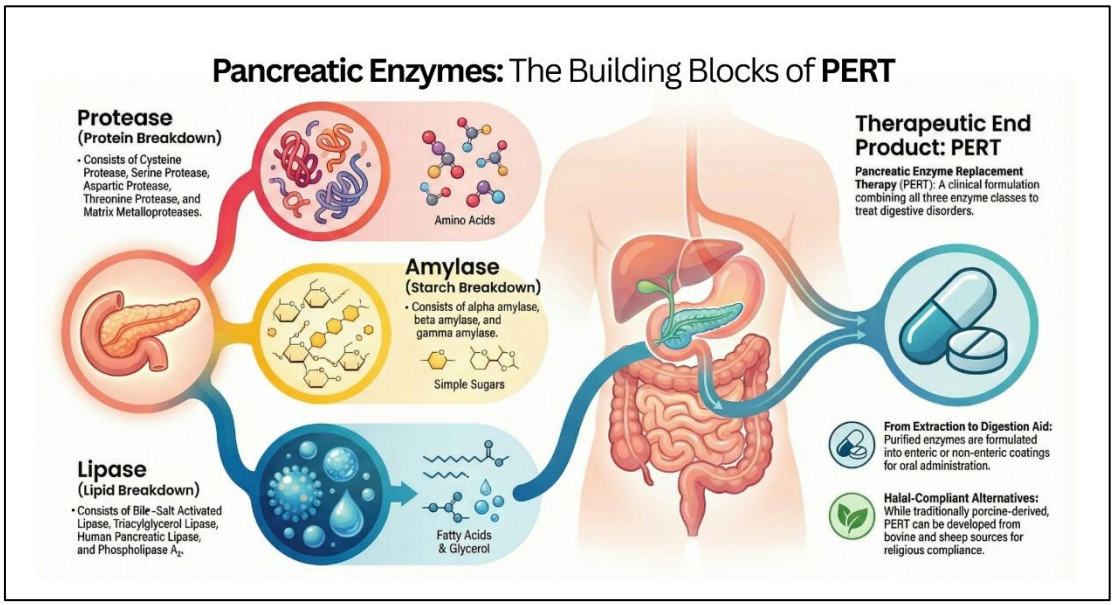


Figure 2.6 Overview of Pancreatic Enzymes and Their Role in Pancreatic Enzyme Replacement Therapy (PERT). Note: Image Generated using the Prompt "A Graphical Image Summarize the Pancreatic Enzymes in Pancreatic Enzyme Replacement Therapy" by NotebookLM, 2026 (https://notebooklm.google).

2.4.5.1 Protease

Protease is responsible for protein catabolism and amino acid generation in the primitive organism (López-Otín & Bond, 2008; Poreba, 2020). Protease is also known as proteinase or peptidase. With ubiquitous characteristics, it is responsible for the hydrolyse of peptide bonds between amino acid residues in a protein (Gupta & Gupta, 2020). Protein digestion begins in the stomach with hydrochloric acid and pepsin concomitant actions, continues with pancreatic proteases in the duodenum, and finishes with numerous brush border peptidases in the small intestine (Fieker *et al.,* 2011).

The irreversible catalytic reaction is known as proteolysis, by hydrolysing peptide bonds (CO–NH) by attacking the carbonyl moiety involved in the peptide bond formation (Ganeshpurkar *et al.,* 2020; Shukla *et al.,* 2020; Trezza *et al.,* 2020). Protease is an enzyme with a powerful strength, where it can break the peptide bonds in less than a few microseconds faster than in hostile conditions, such as in a boiling concentrated acid environment (Trezza *et al.,* 2020). Proteases play significant roles in many signalling pathways, combating parasites and viruses, and represent potential drug targets ranging from cardiovascular to cancer (Drag & Salvesen, 2010).

The involvement of proteases in various cellular pathways and biological processes has made proteases a promising target in drug development (Ganeshpurkar *et al.,* 2020). In a normal cell, it is essential to carry out biological processes and regulate cellular processes such as gene expression, differentiation, proliferation, migration, protein turn over and cell death (Poreba, 2020). Mainly, proteases are very important since protease gene mutations cause more than one hundred diverse hereditary diseases (Pérez-Silva *et al.,* 2016). In humans, about 990 known protease genes and about 1605 known protease inhibitor genes have been reported (Eatemadi *et al.,* 2017; Ganeshpurkar *et al.,* 2020; Rai & Poddar, 2020).

According to Gupta & Gupta (2020), there are five classes of proteases: cysteine, serine, aspartic, threonine, and matrix metalloproteases. However, there is another addition to protease classes, which is glutamic acid, as discussed in the review by Eatemadi *et al*.,(2017) and Ganeshpurkar *et al*. (2020). Proteases usually use water to break the peptide bond in aspartate, metalloproteases, and glutamic proteases (Rai & Poddar, 2020). Examples of proteases are pepsin, trypsin, chymotrypsin, papain, cathepsins, calpains, thermolysin, carboxypeptidase A and B, proteasomes, peptidases, and caspases (Bond, 2019).

2.4.5.2 Classes of Proteases

Cysteine Proteases

Cysteine proteases, also known as thiol proteases, are a class of nucleophilic proteolytic enzymes containing cysteine residues in the enzymatic domain (Yang *et al.,* 2023). It is characterized by highly reactive cysteine residue within their catalytic active site containing a Cys-His-Asn triad (Eatemadi *et al.,* 2017; Verma *et al.,* 2016). The precise catalytic action of this specific amino acid is fundamental in regulating a wide array of physiological functions within host cells and tissues (Eatemadi *et al.,* 2017). These cysteine proteases predominantly localized in two distinct cellular compartments, which are cytosol and lysosome (Eatemadi *et al.,* 2017). The examples of cysteine proteases are papain, cathepsin, calpains and caspases are very common and can be found in a series of living organisms (Elsässer *et al.,* 2017). They have an indispensable control for executing broad cellular processes, primarily acting in general intracellular protein catabolism and protein processing (Verma *et al.,* 2016). It also serves in selective activation that involves with vital signalling molecules such as interleukins, enkephalins, and protein kinase C (Gupta & Gupta, 2020).

Serine Proteases

Serine proteases constitute a major class of proteolytic enzymes characterized by the presence of a highly reactive serine residue utilizing a Ser-His-Asp triad within their catalytic active site (Eatemadi *et al.,* 2017; Krem & Cera, 2001; Schulten, 2025). It is the most abundant protease and widely distributed across biological sources (Harish & Uppuluri, 2020). Trypsin, chymotrypsin, and elastase are the example of serine proteases synthesised and secreted as inactive zymogens by the exocrine pancreas (Berry, 2014). Trypsin remains one of the most prominent and well-characterized serine proteases , which has been found to play crucial roles in pathological and physiological processes (Rai & Poddar, 2020). It carries diverse physiological and cellular functions, ranging from digestive and degradative processes to blood clotting, cellular and humoral immunity, fibrinolysis, fertilization, embryonic development, protein processing and tissue remodelling (Krem & Cera, 2001). The normal regulation of their activities is essential for the physiological activities of the cell, whereas any dysregulation can lead to severe pathological conditions (Gupta & Gupta, 2020).

Aspartic Protease

Aspartic proteases constitute a significant class of proteolytic enzymes characterized by the presence of two highly conserved aspartic acid residues within their catalytic active site. The aspartic acid is also known as acid proteases, aspartyl proteinases, aspartic proteases, aspartic proteinases, aspartic–type endopeptidases, and carboxyl proteases (Ganeshpurkar *et al.,* 2020). It is widely distributed among vertebrates, plants, yeast, nematodes, parasites, fungi and viruses (Simões & Faro, 2004). Aspartic protease is optimally active in acidic environment, which is typically below pH 6 and specifically inhibited by pepstatin (Simões & Faro, 2004). During proteolysis, they uniquely utilize an activated water molecule bound to one or more of these aspartate residues to successfully catalyze the cleavage of their peptide substrate (Gupta & Gupta, 2020). Eukaryotic aspartic proteases include pepsins, cathepsins, and renin. Cathepsin–D is universally found in lysosomes and is one of the aspartic proteases that play significant roles as biological activation precursors for active proteins in prelysosomal compartments and as a major protein–degrading enzyme in lysosomes and phagosomes (Eatemadi *et al.,* 2017).

Threonine Protease

Threonine proteases constitute a highly specific family of proteolytic enzymes that are biochemically characterized by the presence of a reactive threonine residue within their catalytic active site (Gupta & Gupta, 2020). The prototype members of this class of enzymes are the catalytic subunits of the proteasome, the multi subunit complex responsible for most non lysosomal protein degradation (Fung *et al.,* 2025; Ward *et al.,* 2009). Threonine protease is relatively recent addition to the proteases classification that have been recognized in the 1990s (Fung *et al.,* 2025). Functionally, threonine proteases execute a fundamentally critical role in regulating normal cellular health by driving the continuous turnover and degradation of unnecessary or damaged intracellular proteins. Specifically, this highly controlled degradation process is rigorously executed only after the target proteins have been chemically tagged for removal through a complex PTM known as poly-ubiquitination. Thus, it is essential to remove cellular protein through the PTM poly–ubiquitination before degradation can takes place (Eatemadi *et al.,* 2017).

Matrix Metalloproteases

Matrix metalloproteases (MMPs), which are also commonly referred to as matrixins, constitute a significant class of calcium-dependent, zinc-containing endopeptidases (Dimesa *et al.,* 2026; Verma & Tonk, 2020). These MMPs enzymes are characterised by a conserved catalytic domain containing a Zn^{2+} ion coordinated by histidine residues, which is essential for peptide bond cleavage and belong to a more prominent family of proteases known as the metzincin superfamily (Yang & Candelario-Jalil, 2017). In humans, the MMP family includes 23 endopeptidases that have important roles in cancer progression (Shukla *et al.,* 2020; Sorsa *et al.,* 2026). The primary function of MMPs is to degrade all kinds of extracellular matrix (ECM) proteins (Dimesa *et al.,* 2026). They have significant roles in cell behaviours such as cell proliferation, migration (adhesion/dispersion), differentiation, remodelling of ECM, and tissue invasion and vascularization (Cui *et al.,* 2017). Tissue degradation caused by the overactivation of these enzymes leads to the progression of many diseases, such as rheumatoid arthritis, osteoarthritis, tumour metastasis, multiple sclerosis, and congestive heart failure (Gupta & Gupta, 2020). One of the examples of MMPs is Carboxypeptidase A1 (CBPA1), a prominent proteolytic enzyme highly function as zinc-dependent metalloprotease (Sándor *et al.,* 2022).

2.4.5.3 Amylase

Amylases are a class of enzymes that catalyze the hydrolysis of carbohydrate into sugars such as glucose and maltose (Liu & Kokare, 2017). They are broadly classified into three groups which are alpha amylase , beta amylase and gamma amylase based on their mode of action and with distinct glycosydic linkages they can cleave (Akinfemiwa *et al.,* 2023; Kumar & Chakravarty, 2018; Tesfaye *et al.,* 2025). Alternatively, these amylases can be subcategorized into exoamylase and endoamylase based on the catalytic mode. These enzymes are ubiquitously distributed and can be obtained from animals, plants, and microorganisms (Gopinath *et al.,* 2017; Kumar & Chakravarty, 2018; Zhang *et al.,* 2017). Amylolytic enzymes are responsible helping to hydrolyse glycosidic bonds present in the chain of amylose and amylopectin in the starch structure, the most common carbohydrate in nature (Ranke *et al.,* 2020; Zhang *et al.,* 2017).

Amylase plays a central role in digestive physiology because starch represents one of the most abundant carbohydrates in the human diet and a major source of metabolic energy. At the same time, it is also the most abundance enzymes that are being synthesis and secreted by pancreatic acinar cells and salivary glands (Hou *et al.,* 2013; Ismail & Bhayana, 2017). Although there are three prime group of amylases, only one isoenzyme of alpha–amylase is present in human with different isoforms specific to the pancreatic or salivary gland (Ismail & Bhayana, 2017). It is a vital starch hydrolase, that is essential for energy acquisition and is secreted into the duodenum as a significant component of pancreatic fluid (Date *et al.,* 2015). The starch digestion is initiated in the oral cavity by salivary alpha amylase, continues in the duodenum through the action of pancreatic alpha amylase and ends with several intestinal brush border oligosaccharides (Fieker *et al.,* 2011). Insufficient of these amylases causes starch indigestion, leading to diarrhoea.

Amylase is one of the most extensively utilised industrial enzymes applied in many industrial processes, such as the saccharification of starchy materials, food, pharmaceutical, detergent, and textile industries (Gopinath *et al.,* 2017; Simair *et al.,* 2017). It also stands out in the manufacturing industrial sector with various applications for detergent, food, textile, brewing, chemistry, paper, bakery, pharmaceutical, and clinical analysis (Al-Bedak *et al.,* 2025; Ranke *et al.,* 2020). Meanwhile in the clinical and pharmaceutical industries, the involvement of amylases is exceptional and hold a

significant responsibility for therapeutic management of EPI gastrointestinal disorders. A deficiency or impaired secretion of these amylases lead to starch indigestion, severe diarrhoea, and profound nutrient malabsorption. Thus, amylase is one of the cores active ingredients together with protease and lipase are the formulation of the PERT for the EPI disorders management, which help to compromise the enzymes that the pancreas can no longer produce by the body. These industrial amylases contribute substantially to the global enzyme market, historically accounting for a major proportion of commercial enzyme production (Elmansy *et al.,* 2018). In addition, the annual industrial demand for amylases continues to grow, currently constituting up to 25% of the global enzyme market (Alhazmi & Alshehri, 2025).

2.4.5.4 Classes of Amylase

Alpha Amylase

Alpha–amylase α–(1–4 glucan 4–glucanohydrolase, EC 3.2.1.1) is a ubiquitous endo–acting glycoside hydrolase that is crucial for carbohydrate metabolism across animals, plants, and microorganisms (Böswald *et al.,* 2023). Biologically, it catalyzes the cleavage of internal α–(1–4) glycosidic linkages within complex polysaccharides like glycogen and starch, effectively breaking down linear amylose and branched amylopectin into smaller, absorbable oligosaccharides such as maltose and dextrins (Gómez-villegas *et al.,* 2021). It can be found widely in microbes, plants and animals (Basso *et al.,* 2025). In mammals, this highly abundant enzyme is primarily secreted by the salivary glands and pancreatic acinar cells, facilitating starch digestion sequentially from the oral cavity to the small intestine (Ismail & Bhayana, 2017) . Most of the alpha amylase is structurally classified under glycoside hydrolase family 13 (GH13) (Zinck *et al.,* 2026). Alpha amylase is a calcium–dependent enzyme characterized by a conserved $(\beta/\alpha)_8$–barrel fold catalytic domain and an aspartate–glutamate–aspartate catalytic triad, which together ensure its remarkable catalytic efficiency and structural stability (Janeček *et al.,* 2014; Samanta, 2022; Tesfaye *et al.,* 2025). Because of its broad substrate specificity and indispensable physiological role in energy acquisition, alpha amylase is highly valued as a diagnostic marker for pancreatic diseases and serves as a fundamental therapeutic component in enzymatic therapy for EPI treatment.

Beta Amylase

Beta–amylase is another distinct mechanistic class of the ubiquitous amylase enzymes, that is widely distributed across plants and microbes (Akinfemiwa *et al.,* 2023). Functioning specifically as an exoamylase (EC 3.2.1.2), it catalyses the stepwise hydrolysis of α–(1,4) glycosidic bonds from the non–reducing ends of complex polysaccharides like amylose and amylopectin, consistently releasing maltose as its primary end product (Nascimento *et al.,* 2006; Obe & Fatoki, 2021). While it plays a critical role in microbial carbohydrate metabolism and in mobilising stored starch for energy during the germination of seeds, cereal grains, and sweet potatoes, beta amylase is notably absent in humans (Akinfemiwa *et al.,* 2023). Instead, mammalian digestion relies exclusively on alpha amylase isoenzymes (Böswald *et al.,* 2023). It is structurally classified under the glycoside hydrolase family 14 (GH14), this enzyme operates optimally under mildly acidic to neutral conditions (Obe & Fatoki, 2021). Because of its capacity to yield high amounts of maltose, beta amylase is highly valued in the commercial sector for the saccharification of starchy materials, proving particularly indispensable for fermentation, malting, and brewing within the food manufacturing industry.

Gamma Amylase

Gamma–amylase (EC 3.2.1.3) is also known as glucoamylase, is an exo–acting glycoside hydrolase uniquely capable of cleaving both α–(1,4) and α–(1,6)–glycosidic linkages within complex polysaccharides like glycogen, amylose, and amylopectin (Norouzian *et al.,* 2006). Operating sequentially from the non–reducing ends of these chains, this enzyme achieves the complete saccharification of starch by directly releasing free glucose as its primary end product, rather than intermediate oligosaccharides like maltose. While mammalian starch digestion relies predominantly on alpha amylase, gamma amylase is synthesized abundantly by bacteria and fungi such as *Aspergillus* and *Rhizopus* species, and certain plant tissues. It is structurally classified within the glycoside hydrolase family 15 (GH15) and optimally functions in acidic environments (Tesfaye *et al.,* 2025). With exceptional stability, high yield, and efficiency in generating pure glucose, microbial gamma amylase is an indispensable biocatalyst in industrial biotechnology, particularly extensive for applications in food manufacturing, bioethanol production, fermentation, and commercial starch processing.

2.4.5.5 Lipase

Lipases are an important hydrolytic enzyme, known as a lipolytic enzyme, that is central for triacylglycerol hydrolysis, with numerous applications and industrial potential (Bharathi *et al.,* 2019). It is responsible for the breakdown of triglycerides (TAG), commonly referred to as fats, into free acids and glycerol (Pirahanchi & Sharma, 2019, 2023). The process of triglyceride catabolism stored in cellular lipid droplets into fatty acids and glycerol is known as lipolysis (Zechner *et al.,* 2012). Intracellular lipolysis is an essential step in the cellular process in fundamental metabolic tissues since unhydrolyzed TAG cannot enter the cells (Mottillo *et al.,* 2014).

The lipases enzymes have been found in wide applications across various industries due to their remarkable ability to function under diverse environmental conditions, such as extreme pH and temperature (Sharma *et al.,* 2025). In addition to its physiological role, lipases have extensive industrial applications due to its catalytic efficiency and substrate specificity. It is widely utilised in the food, pharmaceutical, detergent, biodiesel, and chemical industries for lipid modification, flavour development, and biocatalysis, making it one of the most commercially important enzyme groups after proteases and carbohydrases (Phukon *et al.,* 2020).

Lipase is also crucial in the mechanism of some medications that are used to lower cholesterol levels (Pirahanchi & Sharma, 2019). With the ability to hydrolyze lipid substrates and catalyze esterification reactions under mild conditions makes the lipases relevance in medical and significant industries (Abdelaziz *et al.,* 2025). Lipases have become the third largest group of enzymes after proteases and carbohydrases in the industrial sector (Phukon *et al.,* 2020).

These lipase enzymes are widely distributed across biological systems and can be obtained from animal tissues, plants, and microorganisms, highlighting their ubiquitous metabolic importance (Liu *et al.,* 2020). There are several classes of lipases have been identified in mammals based on their physiological roles and tissue localisation, namely pancreatic lipase (PL), lipoprotein lipase (LPL), hepatic lipase (HL), hormone-sensitive lipase (HSL), lysosomal acid lipase (LAL), and microbial lipases (ML). These wide range of lipases can be found in pancreatic acinar cells, the gastrointestinal tract–oesophagus, duodenum, stomach, and colon, liver, heart, lungs, and leukocytes (Hameed *et al.,* 2015). Among the lipases, PL is the most important enzymes responsible for dietary fat digestion and absorption.

2.4.5.6 Examples of Pancreatic Lipase

There are various types of lipases are present in the digestive system, namely tongue lipase, gastric lipase, and PL. However, the PL secreted from the pancreas is the most important type of digestive enzymes, which is directly responsible for fatty acid absorption in the intestine (Liu *et al.,* 2020). The digestion of dietary lipids starts with gastric lipase action in the stomach at 5–30% of TAG hydrolysis, followed by synergic action of biliary and pancreatic secretions in the duodenum at 30–75% of TAG hydrolysis (Berton *et al.,* 2012).

These PL are important to hydrolyse dietary lipids in the digestive system by converting triacylglycerol to monoglycerides and free fatty acids before absorption. Clinically, these PLs are essential component of PERT, which is used to treat EPI by restoring fat digestion and improving nutrient absorption. There is broad example of PL such as Bile–Salt Activated Lipase (BSAL), Triacylglycerol Lipase (TL), Human Pancreatic Lipase (HPL), and Phospholipase A_2 (PLA). These PLs are mainly produced by acinar cells of the pancreas (Ismail & Bhayana, 2017).

Bile–Salt Activate Lipase

BSAL is a lipolytic enzyme that hydrolyses various species of lipids in the gut (Qiu *et al.,* 2020). It is also known as bile–salt–stimulated lipase, carboxyl ester lipase, cholesterol esterase, and lysophospholipase (Cui *et al.,* 2019; Johansson *et al.,* 2018; Qiu *et al.,* 2020). It is highly expressed in pancreatic acinar cells (Johansson *et al.,* 2018) and also secreted by mammary gland cells to hydrolyse TAG, diglycerides, phospholipids, and esters of lipid–soluble vitamins and cholesterol (Qiu *et al.,* 2020). It is also one of four major pancreatic lipases secreted into the digestive tract (Fjeld *et al.,* 2020). It has an important role in milk fat digestion and absorption in suckling newborns (Lombardo *et al.,* 2018). This is essential, as the human pancreas starts to lose the ability to secrete sufficient lipolytic enzymes for lipid digestion during birth. BSAL has been present in all vertebrates to date (Johansson *et al.,* 2018). It has two major structural domains, which are a globular N–terminal catalytic domain of 535 amino acid residues and a C–terminal, intrinsically disordered and extended arm of repeated 11 amino acid segments (Terzyan *et al.,* 2000).

Triacylglycerol Lipase

Triacylglycerol lipase (TL, EC 3.1.1.3) is a fundamental hydrolytic enzyme classified as hydrolase that plays a central role in lipid digestion and overall fat metabolism (Palmer & Bonner, 2011). This ubiquitous biocatalyst is commonly referred to by several other names, including pancreatic lipase, triacylglycerol ester hydrolases, triacylglycerol hydrolases, and triglyceride lipase (Jawed *et al.,* 2019). Its primary biological function is to catalyze the hydrolytic breakdown of dietary TAG into simpler, absorbable molecules such as glycerol, unesterified free fatty acids, and monoglycerides (Pirahanchi & Sharma, 2023). TL facilitates the absorption of the body's highest dietary source of calories by a critical reaction with the oil-water interface during the interfacial activation (Kim *et al.,* 1997). Furthermore, this enzyme acts synergistically with gastric lipase to ensure the complete digestion and optimal absorption of dietary fats within the intestinal lumen (Li *et al.,* 2007). In nature, this versatile enzyme is widely distributed and can be produced by various sources, including plants, microorganisms such as bacteria and fungi, and animals (Ezema *et al.,* 2023). Within mammalian biological systems, TL is predominantly synthesized and secreted directly into the digestive tract by the exocrine pancreas (Chen *et al.,* 2012).

Human Pancreatic Lipase

Human Pancreatic Lipase (HPL) is the first mammalian lipase to be identified with a single polypeptide structure and 50 kDa in size (Sharath *et al.,* 2020). It is the main lipolytic enzyme involved in dietary fat digestion and represents 3% of the total protein secreted by the exocrine pancreas (Kawaguchi *et al.,* 2018). The primary function of the HPL is to break down dietary fats in the small intestine and act as the key digestive enzyme produced by the human pancreas (Fan *et al.,* 2025). The presence of HPL is pivotal to regulate lipid metabolism by hydrolyzing 50 to 70% of the dietary fats which is essential for lipid absorption (Upadhyaya *et al.,* 2025).

The primary structure of HPL was established by cDNA clone analysis isolated from a human pancreas cDNA library (Winkler *et al.,* 1990). The HPL specifically cleaves the outer sn–1 and sn–3 esters on the TAG molecules and generates two free fatty acids and a 2–monoglyceride (Berton *et al.,* 2012; Fieker *et al.,* 2011). It is responsible for the hydrolysis of 40% to 70% of TAG (Fieker *et al.,* 2011).

Phospholipase A_2

Among phospholipases, the family of Phospholipase A2s (PLA) is extensively studied by reflecting their biological relevance (Shayman & Tesmer, 2019). PLA_2 is one of the enzymes involved in cardiovascular diseases, vascular inflammation, heart attacks, and stroke development (Sharifpour *et al.,* 2020). PLA_2 hydrolyses phospholipids to lysophospholipids, which are essential for the optimal absorption of lipid nutrients (Fieker *et al.,* 2011). This enzyme is essential in catalysing the hydrolytic cleavage of phospholipid ester bonds in the inflammatory biological pathway (Sharifpour *et al.,* 2020). PLA_2 catalyses the ester bond hydrolysis at the sn–2 position of the glycerophospholipids membrane to liberate the free fatty acids and lysophospholipids (Hou *et al.,* 2020; Shridas & Webb, 2014).

The enzymes were first purified and characterized from cobra venom and later from rattlesnake venom (Dennis *et al.,* 2011). The PLA_2 has many family members, such as Group IB, IIA, IIC, IIE, IIF, V, X, III, and XII (XIIA and XIIB), which have been identified in mammals (Shayman & Tesmer, 2019). The PLA_2 enzyme family is mostly small proteins, ranging between 14 kDa of molecular weight, and usually have 6–8 disulfide bonds, highly conserved with a catalytic dyad His/Asp (Dennis *et al.,* 2011). PLA_2 exhibits a variety of cellular functions, such as antibacterial, antiviral, inflammation, atherosclerosis, and anticoagulant, where the specific functions depend on the PLA2 group or subgroups.

2.5 Major Industrial Application of Porcine Enzymes

Porcine enzymes comprise a significant portion of the global enzymes market and are employed in various industries. Due to their broad spectrum of enzymatic activities and remarkable stability, the enzymes derived from *Sus scrofa* domesticus (domestic pig) have been extensively utilised across multiple industries. These porcine enzymes are pivotal in numerous clinical, pharmaceutical, cosmetic, and food sectors.

2.5.1 Clinical and Pharmaceutical Industries

Efficient and selective biochemical catalyst systems have made enzymes predominant in the clinical and pharmaceutical industries. Thus, enzyme deficiency in its activity gives rise to several medical conditions (Tandon *et al.,* 2021). For instance, inadequate activity, reduction, loss of stimulation, and production of pancreatic enzymes to digest food within the intestinal lumen have caused EPI, which leads to maldigestion, malabsorption, and consequently, malnutrition (Antonini *et al.,* 2017; Brennan & Saif, 2019; Jawaid & Forsmark, 2019). It is clinically evident that EPI happens when 90% of the pancreas's function is impaired, whereby the pancreatic enzyme secretion is less than 10% of normal, and leads to malabsorption (Landers *et al.,* 2019; Sikkens *et al.,* 2010; Stockley, 2014).

PERT is considered as clinical therapeutics regimen widely used for the EPI treatment. It is extracted from porcine pancreas, inclusive of three different pancreatic enzymes classes known as amylases, proteases, and lipases as enzymes substitution that the pancreas is no longer able to produce (Claghorn, 2019). It involves supplementing porcine pancreatic enzymes, such as pancreatin and pancrelipase to produce enough digestive enzymes to improve symptoms and nutritional status (Chaudhary *et al.,* 2020). The pancreatic enzymes are categorized based on their respective role, known as amylolytic, proteolytic, and lipolytic enzymes.

Different pancreatic enzymes will carry different functions that impact their shortage (Pancreatic Cancer Action Network, 2020). Protease is vital for protein catabolism and amino acid generation in the primitive organism (López-Otín & Bond, 2008). Lipase is essential for breaking down TAG (Hameed *et al.,* 2015). Amylase is crucial for starch hydrolase, essential for energy acquisition, and secreted into the duodenum as a significant component of pancreatic fluid (Date *et al.,* 2015). The combination of these enzymes carries proteolytic, lipolytic, and amylolytic functions, made up the PERT ingredients.

The porcine enzyme has also shown some potential effects in other clinical applications, such as Angiotensin I–Converting enzyme for blood pressure regulation (Yu *et al.,* 2006), Serine Protease Factor 1 for xenotransplantation (Nakahata *et al.,* 2008), and Matrix metalloproteinases for myocardial remodelling in cardiovascular disease (Kiczak *et al.,* 2013).

Apart from that, porcine gelatine is the most popular biopolymer for hard and soft capsules manufacturing in the pharmaceutical industry (Hediana & Rusdiana, 2021). It is a colourless protein purified from a connective tissue called collagen, available in the skins/hides and bones of the animals (Uddin *et al.,* 2021). It is reported that commercialized gelatine is primarily extracted from pig skins, cattle hide, and demineralised cattle bone (Gomez-Guillen *et al.,* 2011; Lin *et al.,* 2015). With approximately 326,000 tons per year in global gelatine production, pig skin is reported to be the highest single contributor to this production (Pradini *et al.,* 2018). The gelatine is used as an emulsifier, stabilizer, thickener, gelling agent, and film former (Uddin *et al.,* 2021). It is found in tablets, serum substitutes, sugar–coated pills, and vitamin encapsulation that helps to protect medicine against harmful influences, such as light and oxygen (Sahilah *et al.,* 2016). More importantly, gelatine has also been developed as a matrix for injection drug delivery microspheres, intravenous infusions, and implants (Alipal *et al.,* 2021). Furthermore, gelatine is also crucial in the medical industry as nano microsphere containers, hydrogel, pharmaceutical additives, nanofibers, and cell transplantation carriers (Kumosa *et al.,* 2018; Ma *et al.,* 2017).

2.5.2 Cosmetic Industry

Wrinkles and atypical pigmentation are the most common skin ageing problems that are common in the cosmetic industry. This is caused by intracellular and extracellular oxidative stress initiated by reactive oxygen species (Masaki, 2010). Many substances derived from animals are used as ingredients in the cosmetic industry, and one of the most common sources is porcine. The ability of the porcine enzymes to enhance skin health and appearance makes them a prominent ingredient to overcome cosmetic problems.

Collagen, fatty acids, and glycerine originating from pigs are the most common ingredients in mask packs, body lotions, and face creams (Zabidi *et al.,* 2020). Various formulations containing high amounts of pig traces can be found in cosmetic products, such as anti–ageing creams, serums, lotions, moisturisers, sunscreens, and make–up products available on the market. The pig ingredients, such as glycerine and hyaluronic acid, act as humectants that attract water to the skin surface and prevent moisture loss; collagen promotes cellular turnover and regenerations, strengthens the skin's natural barrier by reducing trans–epidermal water loss, protecting against environmental

aggression and improving skin elasticity; and the anti–inflammatory agent that helps in redness reduction and irritation (Nagae *et al.,* 2020). The porcine enzyme is one of the most abundant ingredients in the cosmetic industry.

Porcine collagen hydrolysate by–products originating from porcine placenta and skin have been utilized for their antioxidative and anti–ageing formulations in cosmetic products (Hong *et al.,* 2019). Another example of a porcine enzyme is Superoxide dismutase, a common ingredient found in cosmetic products, as it is a powerful antioxidant that eliminates free radicals, thus promoting cellular health (Ahasan *et al.,* 2018; Salin & Wilson, 1981). Other than that, porcine amniotic fluid has also been reported to have the potential to be an anti–wrinkle agent in cosmetic products (Kim *et al.,* 2011). Collagenase extracted from bovine, porcine, and marine sources is also used in cosmetic applications for its natural properties as natural humectants and skin moisturisers (Adhikari *et al.,* 2020).

2.5.3 Food Industry

The manufacturing of food and beverages represents the most extensive application of industrial enzymes, led by the increasing economic availability of consumers and the growing demand for highly nutritional diets (Trono, 2019). The application of enzymes, including food processing (cereal, fruit and vegetables, meats, and dairy products) and food preservation (lysozyme and glucose oxidase) in the field of the food industry is mainly based on their high efficiency and specificity (Wang *et al.,* 2024).

Porcine plasma transglutaminase activities were found in surimi products (Alina *et al.,* 2012). It is used to improve gelling properties in surimi production. Pork gelatinase is commonly used in food production for various applications, including food ingredients as a thickener, gel foaming agent, emulsifier, plasticizer, moisture agent, foaming agent, and binding agent (Sahilah *et al.,* 2016). Trypsin, extracted from porcine, is used for whey protein hydrolysis and employed as an ingredient in infant formulae, follow–on formulae, and food for particular medical purposes (Lambre *et al.,* 2021).

2.6 Halal

The '**Halal**' term is originally from an Arabic word that means allowed or permitted by Islamic Law (Arham *et al.,* 2026) .The global Halal industry is the fastest–growing consumer segment worldwide, with over one trillion dollars in estimation (Lubis *et al.,* 2016). The philosophies of life and religious beliefs have a restrictive effect on the food consumption of their devotees (Karahalil, 2020). Muslim life revolves around two main concepts: Halal and haram (Ahmad *et al.,* 2018). The Quranic 'Halal' term means lawful or permissible. It has been getting significant interest due to the escalating demand for Halal products (Ermis, 2017). In contrast, haram refers to prohibited items (Ahmad *et al.,* 2018). These include the consumption of pork, dead carrion, blood, all blood derivatives, alcohol, and all harmful materials to human health, which are prohibited and identified as haram (non–permissible) in Islamic terminology (Karahalil, 2020).

The industrial enzyme application Halal status is ambiguous to consumers since they may not be adequately traced back to their source of origin or production method (Ermis, 2017). Enzymes are extensively and increasingly used in research and food processing as important processing aids or biocatalysts (Ermis, 2017). Pancreatic enzyme research has become of significant interest in medical usage.

2.6.1 Halal Concerns About Porcine–Based Enzymes

Although it is safe to consume porcine–based products, the porcine enzymes usage remains controversial, as some people believe it is not Halal to use products containing porcine as their ingredients. Halal means 'permissible' or 'lawful'; traditionally, it signifies 'pure food' regarding meat (Anish, 2022). Proper Islamic practices, including pork avoidance and ritual slaughter, not only for food but also for biotechnology and care products, must be taken care of to gain purity. Several Muslim requirements have been met, such as an injunction to avoid any substances contaminated with porcine residues or gelatine, alcohol, enzymes, emulsifiers, glycerine, and flavours (Fischer, 2016). Muslims is strongly forbidden to consume porcine products and their byproducts. Both Islam and Judaism follow strict guidelines regarding meat consumption; one of them is the prohibition of pork meat (*Sus scrofa*) consumption (Yuswan *et al.,* 2018).

Halal is for all humankind and has become a general issue due to global consumers shifting towards Halal products and/or services (Karia *et al.,* 2015). The kosher (kashrus) dietary laws determine which foods are "fit or proper" for consumption by Jewish consumers who observe these laws (Regenstein, 2019). Followers of Islam and Judaism have religious concerns about pork consumption; any deviation might result in lower consumption and violation of religious sentiments (Karabasanavar *et al.,* 2014). Other users include Seventh–Day Adventists, vegetarians, vegans, people with various types of allergies, and general consumers who, for one reason or another, prefer Halal products (Regenstein, 2019). Although Halal concepts are typical for Muslim consumers, due to health concerns, a Halal food business today has enormous potential to capture non–Muslims as a target market (Omar *et al.,* 2022). Henceforth, Halal enzymes should be considered in the food, cosmetic, clinical, and pharmaceutical industries. Thus, it is essential to find Halal alternatives to address the issue of using porcine–based ingredients in these demanding industries.

2.6.2 Halal Market Demand

The increasing demand for Halal products has challenged the use of porcine in many industrial applications, particularly in the food and pharmaceutical sectors. One of the primary reasons is the substantial expansion of the Muslim population worldwide. The global Muslim population is projected to reach approximately 2.8 billion by 2050 (Pew Research Center Religion & Public Life, 2015). The rise of transparency and sustainability, food safety concerns, an upsurge of Muslim–friendly tourism, and growing awareness of health and wellness in consuming Halal–certified products accelerate the demand for Halal products (Islamic Services of America, 2023).

The global Halal ingredients market was valued at US$325.7 billion in 2021 and is projected to be worth around US$435.2 billion by 2030, with a 3.27% CAGR (Precedence Research, 2022c). In addition, the global Halal industry is a trillion–dollar, fast–growing market segment (Rejeb *et al.,* 2021). During the forecast period 2021–2026, the Halal market is estimated to reach US$341 billion by 2026 with a 9.3% CAGR (Industry ARC, 2021). Regions with large Muslim populations, such as the Middle East, have shown high consumption of Halal ingredients in food products and have provided the largest market for Halal ingredients in recent years.

The global Halal food and beverages market is envisioned to grow from US$2.09 trillion in 2021 to US$3.27 trillion by 2028, with a 6.56% CAGR during the forecast years (Fortune Business Insight, 2022). Grand View Research (2022), lists some of the key companies operating in Halal food and beverage markets, which are Cargill Inc, Prima Agri–Products, Al–Falah Halal Foods, Midamar Corporation, QL Foods, Unilever, American Halal Company Inc, Nestlé S.A, One World Foods Inc, and Rosen's Diversified Inc (Grand View Research, 2022).

The shift in consuming Halal pharmaceutical products has been observed due to the rising awareness of Halal interest and the globalisation of Halal products. Market Research reported that the Halal pharmaceutical market is predicted to register a 13.2% CAGR in revenue, with the global market size expected to reach US$558.2 million by 2026 (Market Research, 2021b). Halal medicines strictly adhere to Islamic Shariah standards. From the Muslim consumer's point of view, the demands come in the form of whether a drug is Halal or allowed in Islam (Norazmi & Lim, 2015). Among the global key players in the Halal pharmaceutical market are NOOR VITAMINS, Simpor Pharma, Bosch Pharmaceuticals, Pharmaniaga, Rosemont Pharmaceuticals, and CCM Pharmaceuticals (Market.us, 2022).

During 2021–2025, the Halal cosmetics and personal care market is poised to grow by US$27.43 billion with a 7.48% CAGR monitored by Technavio during the forecast period (Market Research, 2021a). The Halal cosmetics market is escalating in regions dominated by Muslim countries like Saudi Arabia, UAE, Indonesia, Turkey, and Malaysia (Precedence Research, 2022b).

2.7 Potential Halal Enzyme Alternatives

Exogenous pancreatic enzymes are primarily extracted from porcine sources (Ianiro *et al.,* 2016). Porcine–derived PERT has been available and used to treat EPI for many years. It has been reported to be used in over 80% of patients with CF (Konstan *et al.,* 2018). Porcine–derived medicines have shown effective solutions for a broad range of human diseases. The use of porcine as a source for PERT brings several risks associated with its use, such as zoonotic infection, allergic reaction to porcine proteins, and hyperuricemia due to high purine content (Konstan *et al.,* 2018).

However, using porcine enzymes in the future will become uncertain in industrial applications since the demand for Halal is increasing steadily. In recent years, there has been a growing concern about using porcine enzymes in industrial applications. The issue of Halal has become a global concern, where conscientious Muslims are careful to consume a wide range of products, including food, beverages, insurance, leather goods, pharmaceuticals, and cosmetics (Herdiana *et al.,* 2024). Consumers can choose to avoid products containing porcine enzymes. For instance, patients need to know the origin of their medicines and the detailed ingredients, especially animal–derived medications (Laher, 2020). Halal drugs should contain Halal ingredients and must be produced, obligated with Islamic law (Hediana & Rusdiana, 2021). Previously, pancreatic enzymes have been extracted from various animal hosts, including rats (Clauser *et al.,* 1988), chickens (Srisantisaeng *et al.,* 2013), felines (Steiner *et al.,* 2003), dogs (Steiner & Williams, 2002), ostriches (Bradley *et al.,* 1994), dromedary (Bacha *et al.,* 2006), bovine (Julien *et al.,* 1972) and porcine (Iijima *et al.,* 1998). The crucial question for the Islamic community is the Halal status of the enzymes and whether they comply with Islamic laws.

Protease, amylase, and lipase are widely distributed in many sources, such as animals, plants, and microorganisms. The different sources of pancreatic enzymes bring different kinds of advantages and disadvantages in many factors, such as enzyme extraction, stability, survivability, and delivery to the target site (Ianiro *et al.,* 2016).

2.7.1 Microbial Origin Enzyme

Microbial enzymes are superior enzymes obtained from different microorganisms for industrial and commercial applications (Nigam, 2013). Microbial enzymes from bacteria, fungi, and yeast are the current primary source and are pivotal in various industries, including pharmaceuticals (Vardar-Yel *et al.,* 2024). Alternatively, PERT pharmaceutical applications can be replaced with pancreatic–like enzymes of microbial origin known as PLEM that improve fat and protein digestion, development, and reversed growth retardation, and normalized postprandial blood lipid profile, as shown in the EPI pig (Pierzynowska *et al.,* 2018). The PLEM was proven to have high activity and a wide pH range, purity, and compacted activity per gram of product, the relatively fastest production of the enzymes, and the cheapest compared to the PERT (Szwiec *et al.,* 2015).

Pancreatic–like enzymes of microbial origin (PLEM) are actively being investigated (Goncharova *et al.,* 2015; Pierzynowska *et al.,* 2018). The extracted PERT bacteria are stable against proteolysis hydrolysis and have high catalytic activity, where it is not affected by the presence of bile salt. Bacterial enzymes are highly resistant to both alkaline and acidic environments. One of the formulations, ALTU–135, containing bacterial lipase, fungal protease, and amylase, is a novel microbial enzyme that has been investigated as a PERT for CF patients (Borowitz *et al.,* 2006). Microbial pancreatic enzymes of fungal or bacterial origin are of potential interest due to their acid and protease stability and their activity at pHs 3 to 10 (Fieker *et al.,* 2011).

Fungal enzyme is the most stable enzyme as it is acid resistant and can survive in highly acidic conditions. However, the fungal enzymes are rapidly inactive in low–concentration environments where proteases can swiftly eliminate them. An example of a fungal enzyme used for PERT is *Rhizopus arrhizus* (Moreau *et al.,* 1988), *Candida cylindacea*, *Aspergillus niger* (Griffin *et al.,* 1989; Zentler-Munro *et al.,* 1992), and *Yarrowia lipolytica* (Aloulou *et al.,* 2007; Turki *et al.,* 2010). Among these, the *Aspergillus* and *Yarrowia* have been reported to have high survivability in the duodenal environment (Fieker *et al.,* 2011). In addition, *Aspergillus oryzae* (Zentler-Munro *et al.,* 1992) and *Yarrowia lipolytica* (Aloulou *et al.,* 2007) have been studied as alternatives to pancreatic enzymes derived from porcine. *Yarrowia lipolytica* lipase 2 (YLLIP2) was characterised for function at low pH, stability, and resistance to pepsin digestion with a high–fat absorption coefficient in the EPI mini–pig model (Aloulou *et al.,* 2007). Meanwhile, laccase is among the enzyme biocatalysts commercially used in food production. The laccase enzyme has been extracted from various microorganisms such as *Pleurotus ostreatus*, *Coriolopsis gallica*, *Trametes* sp., *Trametes versicolor*, and *Polyporus versicolor* (Minussi *et al.,* 2002). It has been used in the bioremediation of food industry wastewater, fruit juice processing, wine and beer stabilisation, baking, and improvement of sensory food parameters (Minussi *et al.,* 2002).

Other examples of biocatalytic syntheses for the cosmetic industry include immobilised lipase B from *Candida antartica*, *Rhizomucor miehei* (Lipozyme IM–77) n–Hexane, Lipozyme IM, Lipase *Candida* sp. 99–125, and Lipozyme TL IM (Abdelraheem *et al.,* 2019). Other examples of recombinant enzymes in food applications are aspartic protease, chymosin, protease, lipase, phospholipase A1, lactase, α–amylase, xylanase, phospholipase, glucose oxidase, asparaginase, subtilisin,

transglutaminase, pectin lyase, endopolygalacturonase, pectin methylesterase, β–glucanase, and glucoamylase (Trono, 2019).

Although many microbial enzymes are currently available, they are still inadequate for fulfilling the requirements of most industries, specifically in medicine and pharmaceuticals, due to the possible variation in behaviour and functionality compared to established animal enzymes.

2.7.2 Plant-Origin Enzyme

Cosmetic enzyme products like facial cleansers, scrubs, masks, and creams can be extracted from plant sources. Pineapple proteolytic bromelain enzyme is an active ingredient in skincare products for its exfoliating properties. It is effective in preventing and treating cellulite, soothing injuries caused by shaving, reducing skin–intensity blemishes, and promoting skin renewal (Lourenço *et al.,* 2016). Proteolytic papain enzymes extracted from papaya fruit have been studied for their ability to improve collagen content, hydrating agent, good skin hydration, skin rejuvenation, exfoliant, and antiaging properties in cosmetic applications (Banchhor & Saraf, 2008). Plant proteases such as papain, bromelain, and ficin have high antioxidant and antimicrobial properties, used for meat tenderization due to lower cost, improved sensory attributes of meat, and good meat tenderization (Azmi *et al.,* 2023; Wei *et al.,* 2014).

2.7.3 Animal Origin Enzyme

Various established studies have compared porcine enzymes with other animal regarding pancreatic enzyme applications. Besides porcine, the pancreatic enzyme has been extracted and purified bovine and sheep, as Halal alternatives. Furthermore, these Bovidae family pancreases are not being consumed and are discarded as waste (Li *et al.,* 2012). Thus, the Bovidae pancreas, a by–product of the meat industry, can be utilised as an alternative low–cost source of Halal pancreatic enzymes.

As for the gelatine, other non–porcine sources, such as bovine and fish, are also available for Halal consumers (Uddin *et al.,* 2021). However, fish gelatine is more favourable since it has no religious issues and is not associated with bovine spongiform encephalopathy outbreaks (Duan *et al.,* 2018). On the contrary, plant–based gelatine can be an option for vegetarians. Hydrocolloids in the Konjac and Yam plants become

primary sources of plant gelatin (Lestari *et al.,* 2019). Hitherto, changing to plant–based gelatine from mammalian–based gelatine production remains difficult, as the cost is high (Lestari *et al.,* 2019; Uddin *et al.,* 2021).

2.7.4 Recombinant DNA–derived Enzyme

Recombinant DNA technology involves altering genetic material outside the organism to obtain enhanced and desired characteristics in living organisms or as their products (Khan *et al.,* 2016). These enzymes act as important agents in many industrial applications, replacing porcine–based enzyme products. Therapeutic recombinant enzymes have been used widely to treat various diseases and conditions (Xu *et al.,* 2020). Human recombinant enzymes such as HPL and BSAL have been vigorously studied for the PERT application. It is expected to offer superior safety by reducing the risk of allergic reactions (Fieker *et al.,* 2011). The use of recombinant enzymes is inevitable as an effective supplement for patients with pig allergies (Kawaguchi *et al.,* 2018). It is naturally acid–resistant and helps to break down TAG and phospholipids.

One common application of recombinant DNA is in the pharmaceutical and clinical industries to treat diseases and improve health conditions. The enzyme derived from recombinant DNA has been widely used for gene therapy to treat genetic diseases (Hacein-Bey-Abina *et al.,* 2002), the production of antibodies and their derivatives (Adams *et al.,* 2006), and the development of vaccines and recombinant hormones (Assidi *et al.,* 2008).

Recombinant DNA enzymes also play a significant role in the food industry. Recombinant DNA technology has improved the production of microbial strains for the food industry. The enhancement of protease production, modification of fungi to reduce toxic release, and lysozyme to inhibit bacteria formation have been done through specific DNA recombinant engineering (Khan *et al.,* 2016).

Since animal–derived enzymes are costly, recombinant DNA technology is a cheaper option for producing enzymes for the cosmetic industry (Chen *et al.,* 2024). Furthermore, recombinant DNA enzymes, such as collagen, have been reported successfully in drug delivery (Olsen *et al.,* 2003). In addition, different types and forms of recombinant collagen, their effectiveness towards skin properties, and the effect of cosmetics containing collagen or its derivatives have been reviewed before (Jadach *et al.,* 2024).

2.8 Protein Modification

The most common protein modification is known as **Post–translational Modification (PTM)**. It refers to biochemical modification of specific amino acid residues in targeted proteins, which immensely increases the functional diversity of the proteome (Wu *et al.,* 2023). PTMs of proteins involves the attachment of small proteins, carbohydrates/lipids, or chemical groups to the proteins which are crucial for proper protein functions (Kumar *et al.,* 2020). It is an enzyme-mediated additions or removals of chemical groups regulating proteins stability and functions, vital in a variety of biological processes and cellular functions (Zhang *et al.,* 2025). Thus, abnormal PTMs may cause changes in protein properties and loss of protein functions, which are associated with the occurrence and progression of various diseases (He *et al.,* 2024; Zhong *et al.,* 2023).

One of the important areas of proteomic research is to identify those proteins that are post–translationally modified and their modification sites, and to characterize the function of the modifications and the interaction of the modified protein within a functional cellular network (Johnson, 2012). It is essential to identify, characterize, and map these modifications to specific amino acid residues on proteins to understand the functional significance in biological concepts, where the knowledge can be applied in drug discovery and development (Karve & Cheema, 2011). There are many types of PTM can be identified, such as phosphorylation, glycosylation, acetylation, ubiquitination, ubiquitylation, methylation, hydroxylation, amidation, nitration, oxidation and sulfation (He *et al.,* 2024; Mittal & Saluja, 2015; Scheuerer *et al.,* 2025; Zhang *et al.,* 2025).

2.8.1 Glycosylation

As with most proteins, pancreatic enzymes are subjected to glycosylation PTM that impacts their structure, function, and bioavailability. **Glycosylation** is a well–studied and most abundant form of PTM where a saccharide moiety is added to the protein, lipids, or other organic molecules inside or outside of the cell (He *et al.,* 2024; Munkley, 2019; Schjoldager *et al.,* 2020). This common PTM glycosylation occurs with the aid of glycosyltransferases (Chen *et al.,* 2022). It is a complex, multistep process that employs around 200 glycosyltransferase enzymes that determine which proteins

are to become glycoproteins, the positions of glycans on those proteins, and the glycan structures assembled (Schjoldager *et al.,* 2020).

The glycosylation is predominantly taking place in Endoplasmic reticulum and Golgi apparatus (Zhang *et al.,* 2025). The native glycosyltransferases and glycosidases attach different glycans to proteins using active nucleotide sugars as substrates, then transport from endoplasmic reticulum to Golgi apparatus to yield functional glycoproteins (Tian *et al.,* 2025). It is one of the most prevalent PTM proteins, and evidence indicates that the vast majority of proteins, estimated to be 85% in eukaryotes are glycosylated (Chen *et al.,* 2022; Tian *et al.,* 2025).

Glycosylation is the process of single sugar or a large number of glycans (polysaccharide chains) are covalent bound to protein residues, and is an important PTM that occurs during or after protein synthesis (Zhang *et al.,* 2025). Glycosylation is an enzyme–directed reaction at the site, as well as substrate–specific, tightly regulated, and reversible. Glycan chain assembly is catalysed by glycosyltransferases and glycosidases, which are encoded by 1–2% of the human genome (Lumibao *et al.,* 2022). The glycosylation has been highlighted among other PTMs because it is abundant and affecting 50 – 70% of human proteins that is fundamental in enzyme regulation (An *et al.,* 2017; Schjoldager *et al.,* 2020). Furthermore, protein glycosylation regulates key biological processes including cell signalling, cell adhesion or endocytosis (Potel *et al.,* 2025). Since glycosylation is one of the most prevalence and biologically significant, it plays an important role in the development of the Halal enzymes as it enables the production of functional enzymes. The glycosylation PTM influences the enzymes' structure, stability, function and activity (Arey, 2012).

Glycosylation is profoundly influences protein folding, solubility, and resistance to proteolysis, which are essential attributes for pancreatic enzymes to maintain enzymatic activity within the harsh environment of the digestive tract (Pienkowski *et al.,* 2025; Schjoldager *et al.,* 2020). Conversely, disruptions to this tightly regulated process resulting in aberrant glycosylation can severely impair the protein, causing diminished enzymatic activity, a shortened circulatory half-life, and undesirable immunogenic responses (Bangarh *et al.,* 2023; He *et al.,* 2024).

Thus, it is also critical to study the discrepancy in the glycosylation patterns across species as it can affect the enzyme function, immunogenicity and performance. Furthermore, by studying these glycosylation patterns it allows to determine other animal host such as bovine and sheep pancreases as Halal alternative sources that are

comparable to current established porcine–based sources enzymes available in the market. Moreover, enzymes from difference mammalian may undergo host–specific modification resulted in significant molecular weight, structural stability and enzymatic behavioural alterations (Kumar & Sharma, 2020; Scheuerer *et al.,* 2025).

2.8.2 Types of Glycosylation

Five known classes of glycans, namely N–linked glycan, O–linked glycan, C–linked glycan, phosphoglycans and glypiation (GPI–anchored) (He *et al.,* 2024; Karve & Cheema, 2011; Wu & Gao, 2023). The most common types of glycosylation are N–glycosylation and O–glycosylation (Jankowski *et al.,* 2025). Protein glycosylation is a complex PTM involving attachments of glycans at specific sites on a protein, commonly asparagine for N–glycosylation and serine or threonine for O–glycosylation residues (Chen *et al.,* 2022; Scheuerer *et al.,* 2025; Zhang *et al.,* 2016).

The N–linked glycosylation occurs at the consensus sequence of asparagine–X–serine (NXS/T) or threonine, where X is any amino acid except proline (Zhong *et al.,* 2025). The covalent attachment of oligosaccharides to asparagine side chains on protein surfaces is a ubiquitous modification that is critical to protein stability and function (Gazaway *et al.,* 2025). It is initiated in the endoplasmic reticulum, where lipid-linked oligosaccharide precursors are assembled and subsequently transferred to asparagine residues of nascent polypeptides (Yu *et al.,* 2025).

The O–linked glycans are usually attached to serine or threonine residues via an a–O–glycosidic bond formed between N–acetylgalactosamine (Gal–NAc) and the hydroxyl group (–OH) of serine or threonine (murine a–Gal–Nac O–glycans) (Rajesh *et al.,* 2025; Zhang *et al.,* 2016). Two common types of O–glycosylations are O–acetylgalactosamine (O–GalNAc) and O–acetylglucosamine (O–GlcNAc), where O–GalNAc is attached to the hydroxyl group of the protein serine or threonine residues through an α–linkage, while O–GlcNAc is attached through a β–linkage (Roth *et al.,* 2012; Yu *et al.,* 2025). It mainly occurs in the Golgi apparatus, beginning with the attachment of Gal–NAc to serine or threonine residues, followed by sequential elongation and capping to generate structurally diverse glycans that regulate protein secretion and receptor activity (Yu *et al.,* 2025). Table 2.5 summarizes the differences between N–glycosylation and O–glycosylation.

Table 2.5
Differences between N–link and O–link Glycosylations

Characteristic	N–Glycosylation	O–Glycosylation
Functional Group attachments	N–linked oligosaccharide is attached to the amide group of an asparagine residue.	O–linked oligosaccharide is attached to the protein serine or threonine hydroxyl group.
Residues of Glycan attachments	Asparagine	Serine or Threonine
Linkages	None	Alpha for GalNAc Beta for O–GlcNAc
Consensus Sequence	Consensus peptide sequence NXS/T. X is any amino acid except proline.	There are no consensus sequences.

2.8.3 Biological Roles of Glycosylation and Glycans

Protein glycosylation is an important PTM that serves fundamentally essential roles in regulating the normal biological function of proteins. In the past few decades, the importance of protein glycosylation has captured the attention of many researchers, as aberrant glycosylation causes implications in diverse disease progression, together referred to as congenital disorder of glycosylation (Rakus & Mahal, 2011; Roth *et al.,* 2012). It is a tightly regulated biochemical mechanism and glycosylation intensely critical in protein attributes such as protein folding, interaction, stability, mobility, and signal transduction to regulate the normal function of the protein. Furthermore, the glycan attachment in PTM is pivotal in controlling the enzyme activity, protein turnover and localization, protein–protein interactions, modulation for various signalling cascades, DNA repair, and cell division (He *et al.,* 2024; Karve & Cheema, 2011).

The biological functions of the attached glycans are classified into three main categories: structural and modulatory properties, the provision of specific recognition sites for other cellular molecules and energy metabolism (Gagneux *et al.,* 2022). The attachment of the glycans is highly dynamic, whereby the specific roles are depending on the target tissues, development stages of the organism and the surrounding environmental context. A wide array of proteins changes has been observed significantly in the glycosylation process, shifting from normal physiological to diseases progression. However, the alterations in these glycosylation process in various systems are highly variable and unpredictable.

Therefore, the disruptions in this intricate glycosylation trigger unwanted severe pathological implications. An aberrant glycosylation will lead to dysfunction glycan

formation. This abnormal glycosylation is severely impacted the pathogenesis of congenital disorders such as cancer, liver cirrhosis, diabetes, and exacerbated HIV infection (Onigbinde *et al.,* 2025). These diseases could happen due to genetic mutations or alterations in N–linked glycosylation pathways that reduce glycosylation in a tissue (Rakus & Mahal, 2011). The glycosylation profiling is substantial as it shows strong correlation with disease progression and it can be served as a highly informative parameters offering a significant insight for disease prognosis and in the development of the targeted therapeutic assay.

The glycosylation modification is one of the important features in selecting Halal alternative sources of pancreatic enzymes in order to indicate safety and effectiveness before it can be used in PERT application. This glycosylation modification can be further categorized into high mannose type, complex type, and hybrid type based on the branching pattern of the glycan chain (Chen *et al.,* 2022). For example, Figure 2.7 shows the comparative differences on host–specific glycan structures from mammalian such as human, porcine, bovine, sheep and rat gathered from the previous studies (Gallego *et al.,* 2001; Miyagawa *et al.,* 2014; Nakano *et al.,* 2004). These findings indicated that, porcine, bovine and human share same glycan structures containing high amount of sialic acid at the terminal branch (Gallego *et al.,* 2001; Miyagawa *et al.,* 2014). On a different study, the terminal branch of the glycan structures of bovine, sheep, human and rat were reported to be highly galactosylated (Nakano *et al.,* 2004).

Regardless of the mammalian species, every N-glycan structure shares the identical basic core foundation which is a chain of two N-acetylglucosamine (GlcNAc) with three mannose residues attached to the chain. The first mannose attached to the top of GlcNAc chain and branches outward into two separate mannose arms, creating a distinctive "Y" shape. Finally, the additional sugars made up the branches and terminals of the glycan structures as an elongation to the GlcNAc.

In summary, different animal hosts may have the same basic foundation structure, however the extended glycan structure could have different types of sugar attach. The typical sugars include fucose, galactose and sialic acids (N-acetylneuraminic acid (Neu5Ac) and N-glycolylneuraminic acid (Neu5Gc)) (Scheuerer *et al.,* 2025) and significantly affect the structure of glycan (He *et al.,* 2024). The bound glycans serve diverse biological roles, including acting as specific recognition and binding sites for carbohydrate-binding proteins modulating intermolecular interactions

and influences protein turnover rate (Scheuerer *et al.,* 2025). The glycan modifications of sialylation and fucosylation have shown a significant impact on immune cell function, pathogen recognition, and inflammatory responses (Onigbinde *et al.,* 2025).

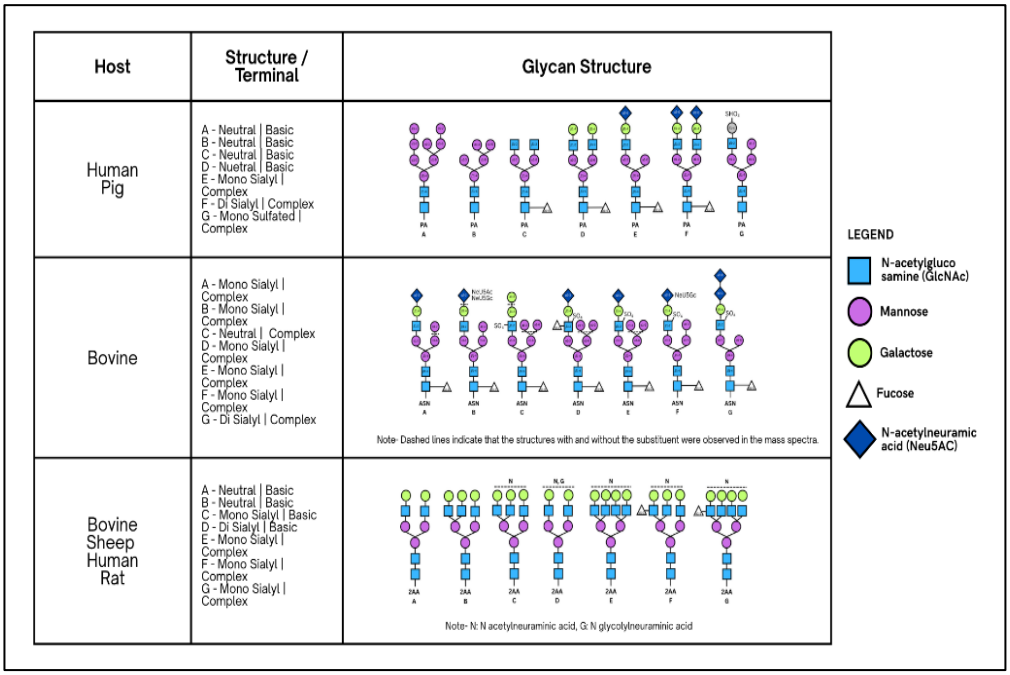


Figure 2.7 Comparative Host–Specific Glycan Structure Across Mammalian Species. Modified and gathered from Gallego *et al*. (2001), Miyagawa *et al*. (2014) and Nakano *et al*. (2004).

2.9 Proteomic Approaches in Halal Enzymes Identification

The development of therapeutic enzymes can be a highly complex and challenging endeavour, primarily due to the severe difficulties associated with isolating a single, functional enzyme from a complex mixture of tissue proteins and natural inhibitors (Tang *et al.,* 2024). Hence, the **proteomic approaches** are fundamental in Halal enzyme providing the necessary analytical framework for production from extraction, purification, classification and validation of these alternative pancreatic enzymes from halal animal, such as bovine and sheep in replacing the non-halal established porcine enzymes in the market. It is also crucial to verify their biological origin and molecular integrity of these alternative enzymes. Proteomic approaches have evolved significantly over time, encompassing a combination of traditional methodologies and advanced analytical techniques that have been widely applied in the development of therapeutic enzymes.

Historically, traditional proteomic methodologies mainly focused on a gel-based separation techniques such as one–dimensional sodium dodecyl sulfate polyacrylamide gel electrophoresis (1D–SDS PAGE) and two-dimensional sodium dodecyl sulfate-polyacrylamide gel electrophoresis (2D–SDS PAGE) providing the molecular weight alongside isoelectric focusing separation technique (Lim *et al.,* 2023). These approaches facilitated the protein isoforms detection that acquiring staining for visualization. Other than that, immunological assays, notably Western blotting and Enzyme-Linked Immunosorbent assays (ELISA), were frequently employed to identify species-specific markers via targeted antigen-antibody interactions (Alhajj *et al.,* 2023; Mishra *et al.,* 2017). The subsequent integration of early peptide mass fingerprinting via matrix-assisted laser desorption/ionization time-of-flight mass spectrometry (MALDI-TOF MS) marked a significant methodological progression, permitting protein identification derived from distinct peptide mass profiles (Henzel *et al.,* 2003). Nevertheless, these conventional techniques were frequently constrained by inadequate sensitivity, limited throughput, and low resolution, rendering them particularly disadvantageous when attempting to accurately differentiate highly homologous pancreatic enzymes derived from closely related mammalian sources, such as bovine, ovine, and porcine species.

Recent technological advancements in proteomics have greatly enhanced the accuracy and reliability on authentication of Halal enzyme classification. Contemporary mass spectrometry-based platforms, notably Liquid Chromatography–Mass spectrometry (LC-MS/MS) coupled with Ultra-Performance Liquid Chromatography (UPLC), facilitate highly sensitive and precise protein identification through rigorous peptide sequencing and database matching (Birhanu, 2023). Operationally, these techniques require systematic workflows encompassing protein extraction, trypsin-mediated enzymatic digestion, high-efficiency peptide separation, high-resolution mass spectrometric analysis, and bioinformatic interpretation using protein databases like UniProt and Mascot. Moreover, modern classification increasingly pairs the experimental data with advanced computational bioinformatic techniques such as molecular docking alongside with PTM profiling to provide deep molecular characterization (Kumar & Srivastava, 2024; Zhang *et al.,* 2025). This allows for the precise differentiation of enzymes based on their a high-resolution unique structural that is critical for authenticating highly homologous pancreatic enzymes.

In response to rigorous Halal certification requirements from global organizations like Jabatan Kemajuan Islam Malaysia (JAKIM) and the Organisation of Islamic Cooperation (OIC), proteomic analysis has become an indispensable tool in alternative enzyme research. Advanced techniques, particularly LC–MS/MS based profiling, provide the scientific foundation for Halal integrity by reliably verifying species origin, detecting trace contamination, and utilizing unique peptide biomarkers to differentiate porcine enzymes from other Halal sources such as bovine and sheep. Ultimately, these technological developments in proteomic are crucial for the comprehensive characterization of pancreatic enzymes and the successful commercialization of bovine and sheep pancreatic enzymes as viable Halal replacements for established porcine standards.

2.10 Conclusion

To date, porcine remains a primary and established source of industrial enzymes for clinical, pharmaceutical, cosmetics, and food production, as it is cheap and abundant in nature. However, the prospect of Halal sources of enzymes, such as from Halal animals, microbes, plants, and recombinant enzymes, must be considered since Halal demand has significantly increased in the 21st century to meet the demands of the rapidly growing global population. Key factors, including religious compliance, market demand, consumer confidence, and international reach, have contributed to the shift towards Halal enzyme products from non–Halal sources. Therefore, research geared towards producing novel Halal enzymes with industrial applications must be intensified to meet the demand for the Halal product market. Finding these valuable enzymes from alternative sources other than porcine would enhance the enzyme mark*et al*ongside the Halal industry markets in the future. Halal is not limited only to Muslims but to all humans worldwide.

CHAPTER 3
EXTRACTION AND PURIFICATION OF BOVINE (*BOS TAURUS)* CARBOXYPEPTIDASE A1

3.1 Introduction

Proteolytic enzymes are secreted by the exocrine pancreas with complementary activities to participate in the alimentary process, including exopeptidase and endopeptidase (Guasch *et al.,* 1992). One of which is Carboxypeptidase A1 (CBPA1, EC 3.4.17.1), which has been extensively studied since the late 1950s and is described as a zinc metalloprotease (Bradley *et al.,* 1994; Kemik *et al.,* 2012; Sándor *et al.,* 2022) produced abundantly in pancreatic acinar cells and is responsible for cleaving C–terminal branched chains and aromatic amino acids from dietary proteins (Uhlig *et al.,* 2022). CBPA1 is one of the significant proteolytic pancreatic enzymes, and the loss of its function is strongly associated with early–onset chronic pancreatitis disease (Witt *et al.,* 2013). Pancreatic and pancreatic–like carboxypeptidases are a family of zinc–containing exopeptidases released into the small intestine from the pancreas as a zymogen (Clauser *et al.,* 1988; Jitonnom & Sontag, 2012; Smith *et al.,* 1997).

Pancreatic enzymes such as trypsin, chymotrypsin B and C, carboxypeptidase A1 and A2, elastase IIA and IIB, lipase, and lipase–related proteins 1 and 2, carboxyl ester lipase, and phospholipase A2 are secreted as a proenzyme that has to be cleaved before it can become active (Kohlmeier, 2015). Trypsin is responsible for procarboxypeptidase zymogen activation to catalyze the cleavage of C–terminal amino acids from their substrates, which originate exclusively from pancreatic acinar cells. This reaction forms a CBPA1 complex, which is then released into the intestinal lumen for the digestion process to take place (Elamin *et al.,* 2014; Said *et al.,* 2020; Sándor *et al.,* 2022). The full activation of the procarboxypeptidase requires further peptide proteolysis activation by chymotrypsin (Sándor *et al.,* 2022). It exhibits peptidase and esterase activity with aliphatic C–terminal residues as a preference for catalytic and active sites (Sándor *et al.,* 2022).

CBPA1 has been isolated and characterized from humans (Goldstein *et al.,* 1989; Pascual *et al.,* 1989) and various animal hosts, including chicken (Zelikson *et al.,* 1971), bovine (Neurath *et al.,* 1970), porcine (Folk & Schirmer, 1963), sheep (Kerfelec *et al.,* 1985), dogfish (Lacko & Neurath, 1970), and ostrich (Bradley *et al.,* 1994), from the 1950s until the mid–1990s. Despite previously gaining much attention, there is no recent update on the methods related to the extraction and purification of CBPA1 from bovine. Based on the recent literature, the research interest of CBPA1 has shifted from purification efforts to applications as a new genetic marker for pancreatic acinar cell carcinoma (Ishimoto-Namiki *et al.,* 2023; Said *et al.,* 2020; Uhlig *et al.,* 2022), as its gene mutations have been reported to be associated with chronic pancreatitis (Reddy *et al.,* 2024; Sándor *et al.,* 2022; Sendler *et al.,* 2018).

Domestic cattle are members of the Bovidae family, widely distributed in Malaysia, particularly for Halal meat consumption. However, some animal organs, including the pancreas are not fully utilized and disposed of as waste. Mammalian pancreatic tissues are non–edible parts produced in significant quantities by the meat industry and represent waste disposal and potential pollution (Li *et al.,* 2012). Thus, the bovine pancreas, a by–product of the meat industry, could serve as an alternative source for Halal digestive enzymes, especially proteases. Furthermore, both Muslim and non–Muslim consumers are demanding the highest quality and Halal–certified products, including medicine and health supplements (Aziz *et al.,* 2014). Halal pharmaceutical products have gained the interest of non–Muslim consumers because these products are considered cleaner and healthier (Sudarsono & Nugrowati, 2020). The exocrine pancreas glands' alkaline secretions, including α–amylase, trypsin, chymotrypsin, and carboxypeptidase, are important for the small intestine's carbohydrates, proteins, and fat breakdown (Rafaqat *et al.,* 2023).

The study herein reports on the purification of CBPA1 from fresh bovine pancreas and simplified purification strategies compared to previous research, enabled by the latest purification system. This includes the selection of the column and buffer for purification of bovine CBPA1, as well as the two–step purification method: anion exchange chromatography (IEX) and gel filtration chromatography (GFC). In addition, there is an interest in the present work on the possible role of bovine CBPA1 as a functional substitute for porcine enzymes, especially in the Halal medical and pharmaceutical industries.

3.2 Materials and Methods

The bovine Carboxypeptidase A1 (CBPA1) purification scheme was summarised as in Figure 3.1.

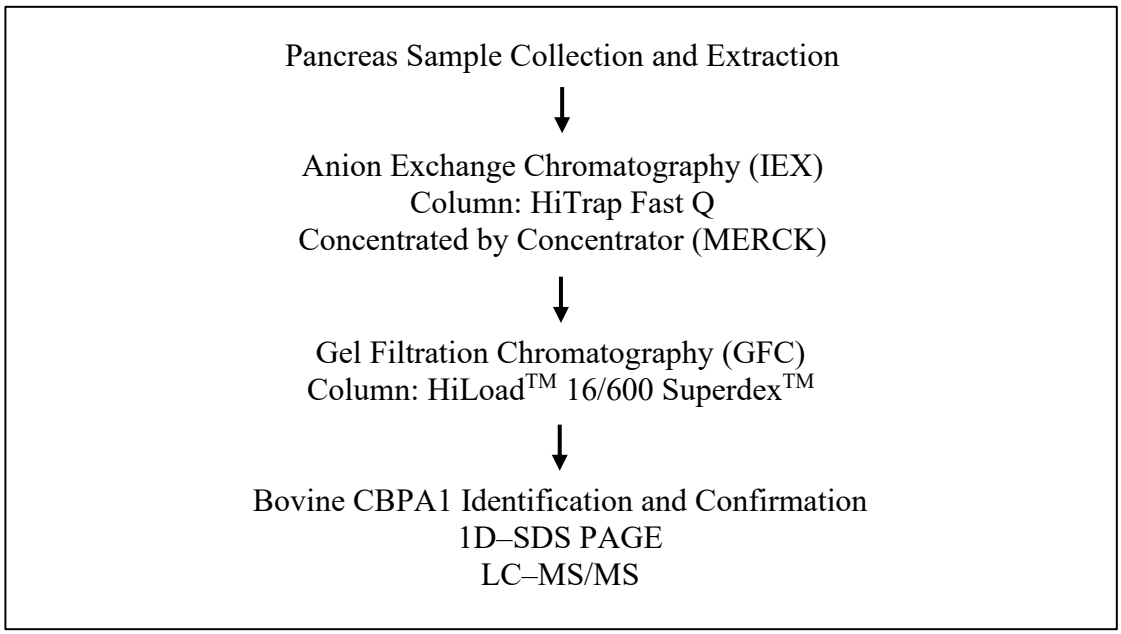


Figure 3.1 Bovine Carboxypeptidase A1 (CBPA1) Purification Scheme.

3.2.1 Enzyme Extraction

Bovine pancreas was collected freshly from slaughtered animals of Abattoir Complex, Department of Veterinary Services (DVS), Shah Alam, Malaysia (Coordinates: 3.05, 101.51), and stored on ice. There was no available information on the supplier or animal records from the abattoir. Nevertheless, it was determined that all the animals were male with an estimated age more than 2 years.

The pancreases were washed with tap water upon receiving. Then, the pancreas was dissected free from adherent fat and connective tissues with a scalpel blade (Elamin *et al.,* 2014). The pancreas was cut into smaller pieces on ice, and the tissue slices were washed with a 50 mM Tris pH 7.4 buffer containing 0.1 M sodium chloride (NaCl) to remove blood (Al-Ajlan & Bailey, 1999). The bovine pancreas collection and pancreatic crude extraction were done on the same day. Approximately 120 g – 160 g of pancreas samples were homogenized using a laboratory blender (Tefal – France), 1 min at low speed and 1 min at high speed (Bradley *et al.,* 1994).

Then, bovine pancreatic tissues were suspended in 20 mL of extraction buffer (50 mM Tris pH 7.4, 2 mM Ethylenediaminetetraacetic acid (EDTA) pH 8, 10 mM 4–(2–hydroxyethyl)–1–piperazineethanesulfonic acid (HEPES) pH 7.4, 1% Triton X–100, and 150 mM NaCl) and vortexed for 10 mins before centrifugation at 4000 rpm for 2 mins. The supernatants were collected and added with 70% (v/v) ethanol, bringing a total of 25 mL. The mixture was vortexed for 10 secs, and 2 mL of 5µg/mL of aprotinin as a protease inhibitor was added to the samples. Aprotinin is a serine protease inhibitor and essential in inhibiting endogenous serine proteolytic activity. The suppression of the non–targeted proteases preserved the enzymatic activities of the targeted proteins. This helps to mitigate the risk of proteolytic degradation of the targeted enzymes, whereby the recovery of intact soluble proteases was maximised in the collected supernatant during the extraction procedure. The samples were centrifuged at 14 000 rpm for 20 mins before collecting the supernatant to recover soluble proteins. The protein concentration was measured and stored at –20ºC until further use.

3.2.2 Sequential Purification of Bovine Carboxypeptidase A1

The purification is a critical step in this study to isolate the targeted enzymes. Following the preparation of the pancreatic tissue extraction, the bovine crude pancreatic extract was subjected to sequential purification. The crude extract underwent sequential purification beginning with anion exchange chromatography (IEX) to isolate the bovine CBPA1 based on surface net charge. Then, the enriched fraction was subsequently subjected to gel filtration chromatography (GFC). Ideally, the GFC was done to achieve higher homogeneity by utilizing the size–exclusion principles to further isolate the bovine CBPA1.

3.2.2.1 Anion Exchange Chromatography (IEX)

The purification step was performed at room temperature on the second day (within 24 hours) following the crude extraction. Bovine pancreatic CBPA1 was further purified by anion exchange chromatography (IEX) on a pre–packed HiTrap Q Fast Flow column containing a Sepharose–based resin (strong anion exchanger) (bed height 1.6 cm, column diameter 2.5 cm, column volume 5 mL) using an AKTA Avant™ chromatography system (Cytiva – USA). The column equilibration process began by

replacing the column's ethanol storage with distilled water to remove the preservative. Subsequently, the column was washed and equilibrated with the start buffer. The 20 mM Tris pH 8 was used as the start buffer, and 20 mM Tris 1 M NaCl pH 8 was used as the elution buffer. The sample was filtered using 0.45 µm and 0.25 µm cellulose acetate pore membrane filters (Merck – Germany). A total of 200 mL filtered sample was applied to the column in buffer A, and the column was washed until the absorbance monitored at 280 nm returned to baseline. The pancreatic enzymes were eluted using an elution buffer at a 2.4 mL/min flow rate, and 1.5 mL fractions were collected.

The IEX was chosen to separate the proteins depending on their ability to interact with a specific positive charge resin where negative charge proteins will bound to the resin. Generally, the proteins were eluted by increasing the ionic strength (salt concentration) of the elution buffer. In this study, the salt ions compete with the bound proteins for the positive charges on the surface of resin, which induced the elution of the bound proteins. As a result, the protein with lower net charge will elute first, following with higher net charge of protein that retained longer as it requires higher ionic strength of elution buffer to be eluted at the selected pH. Since bovine CBPA1 possesses an isoelectric point equal to 5.33, the IEX is performed using buffers with higher pH (pH 8).

Initially, a preliminary linear gradient IEX was conducted to determine the optimal ionic strength required to identify the best NaCl concentration for isolating each targeted enzyme. Subsequently, a NaCl step gradient was applied to purify and isolate the targeted enzymes within a single cycle of the IEX procedure. This allows distinct peak separation and efficient removal of contaminants at lower ionic strengths before eluting the targeted enzymes at their specific targeted salt concentrations. The IEX purification was repeated at least three times, and the chromatogram profiling was constructed based on the mean absorbance values.

The elution buffer composition was set up as a step gradient at 5%, 10%, 20%, 30%, 40%, 50%, and 100% sodium chloride (NaCl) to elute the targeted CBPA1. Each fraction representing different peaks was run on 1–dimensional sodium dodecyl sulphate–polyacrylamide gel electrophoresis (1D–SDS PAGE) for molecular weight determination. The bovine CBPA1 was eluted at 30% of salt concentration. Fractions containing protease activity based on the molecular weight were pooled and concentrated using a 30,000 MW and 50,000 MW Amicon® Ultra Centrifugal Filter (MERCK – Germany).

3.2.2.2 Gel Filtration Chromatography (GFC)

Final purification of bovine pancreatic CBPA1 was performed by GFC on a pre–packed HiLoad™ 16/600 Superdex™ 200 pg column (bed height 60.0 cm, column diameter 1.6 cm, column volume 120 mL) using the AKTA Avant™ chromatography system (Cytiva – USA). The column equilibration process began by replacing the column's ethanol storage with distilled water to remove the preservative. Subsequently, the column was washed and equilibrated with the mobile phase.

The mobile phase was 25 mM Tris Hydrochloride (Tris HCl), pH 8, 0.5 mM EDTA, 150 mM NaCl at a 1.0 mL/min flow rate. A total of 5 mL concentrated from the previously purified IEX sample was injected into the mobile phase, and the column was washed until the absorbance monitored at 280 nm returned to baseline. The bovine pancreatic CBPA1 was eluted at a 1.0 mL/min flow rate. Fractions of 1 mL each were collected and subjected to protein identification and proteolytic activity.

Principally, GFC is also known as a size exclusion chromatography where the molecules (proteins) are separated by their molecular weight passing through the cross–linked dextran with highly cross–linked agarose composite matrix. Generally, a larger protein size will be excluded from the resin and eluted first following with a smaller protein size that will penetrate the resin pores and eluted later.

3.2.3 Protein Identification and Confirmation of Bovine Carboxypeptidase A1

3.2.3.1 Determination of Protein Concentration

The total protein concentration of total crude pancreatic extract and purified fraction samples from IEX and GFC were measured. Absorbance was measured at 280 nm (A_{280}) using a NanoDrop® ND–1000 UV–Vis Spectrophotometer (Thermo Fisher Scientific – US). The obtained concentration values (mg/mL) were subsequently utilised to calculate the total protein content (mg) and were essential for determining the proteolytic enzymatic activity (U/mg) of the samples.

3.2.3.2 One–Dimensional Sodium Dodecyl Sulfate Polyacrylamide Gel Electrophoresis (1D–SDS PAGE)

The molecular weight of purified bovine pancreatic CBPA1 was estimated by 1D–SDS PAGE using NuPAGE 4–12% mini protein gel of Bis–Tris electrophoresis system in X Cell SureLock Mini–Cell (Invitrogen – US) stained with Coomassie Brilliant Blue stain (Invitrogen – US).

The sample was prepared as described in Table 3.1. The protein mixtures were prepared by adding protein sample (x µl), 4X NuPAGE LDS Sample Buffer (2.5 µl), 10X NuPAGE Reducing agent (1 µl), and Ultrapure water (y µl) in a 1.5 mL Eppendorf tube. The protein volume needed was calculated using the dilution formula (M1V1 = M2V2) based on the initial concentration of the protein. Then, Ultrapure water was added, bringing a 10 µl volume for sample preparation. The protein sample was heated at 70^{o}C for 10 mins before loading into the wells. The 1X NuPAGE MES SDS Running Buffer was prepared by adding 50 mL of 20X MES SDS Running Buffer to 950 mL of distilled water. The gel electrophoresis system was set up at 200 V (constant voltage) and 125 mA (current). The electrophoretic separation was conducted for approximately 35 to 45 minutes to ensure the complete resolution of the protein bands.

Table 3.1
Sample Preparation for SDS–PAGE

Chemicals	**Volume (µl)**
Protein Concentration	20 mg/mL
Protein Sample	*x*
NuPAGE LDS Sample Buffer (4X)	2.5
NuPAGE Reducing agent (10X)	1.0
Ultrapure water	*y*
Final Volume	**10.0**

The gel was transferred into a clean container and added with 50 mL of distilled water. Then, the gel was microwaved at high power for 1 min and shaken for 1 min. The steps were repeated twice. Then, the gel was added with Safely Blue Safe stain (Invitrogen – US) liquid. The gel was microwaved again at high for 45 secs and shaken for 5 mins. The gel was washed with distilled water and shaken for 10 mins before viewing with ChemiDoc^{TM} Imaging System (BioRad – US).

3.2.3.3 Liquid Chromatography–Mass Spectrometry (LC–MS/MS)

Protein bands were further identified using liquid chromatography–mass spectrometry (LC–MS/MS). Before the LC–MS/MS procedure, trypsin gel digestion was carried out. Then, a total of 5 µL sample was injected into Dionex Ultimate 3000 RSLCnano Orbitrap Fusion (Thermo Fisher Scientific – US) with EASY–Spray Acclaim PepMapTM C18 100 A0 (2 µm particle size, 50 µm id x 15 cm) separation column. The sample was eluted with LC–MS grade water, 0.1% formic acid (A), and ACN, 0.1% formic acid (B), at a 250 nL/min flow rate. The elution gradient was 5%–40% B for 91 min, 2 min to 85% B, 3 min at 85% B, 1 min at 5% B, and 4 min at 5% B. The full scan spectra were collected by Orbitrap MS (OTMS) scan mass ranging from 310 – 1800 m/z with 50 ms maximum injection. The spectra were analysed by ion trap MS (ITMS) with 250 ms maximum injection. The LC–MS/MS data was analysed using Thermo Scientific^{TM} Proteome Discoverer^{TM} Software Version 2.1. The results were matched with the database downloaded from UniProt. The variable modifications were oxidation and deamination, with fixed modification of carbamidomethyl. All peptides were validated using the percolator® algorithm, based on a q–value of less than 1% false discovery rate (FDR). The LC–MS/MS analysis was performed at the Proteomic Laboratory, Malaysian Genome and Vaccine Institute, Bangi, Malaysia.

3.2.4 Proteolytic Enzyme Assay

Proteolytic activity of crude extracts and purified fractions from IEX and GFC was determined using Pierce Protease Assay kit (Thermo Fisher Scientific – US) following the manufacturer's instructions alongside purified porcine Pancreatin (Sigma Aldrich – USA) as positive control. Protease activity was determined using a coupled enzyme reaction, which resulted in a colourimetric (450 nm) product proportional to the enzymatic activity present.

Trypsin Tosyl phenylalanyl chloromethyl ketone (TPCK) was used to construct a standard curve to determine the enzyme concentration tested, while succinylated casein was used as a substrate. The concentration of the substrate used was 2 mg/mL. The Trypsin TPCK standard curve was established by dissolving 50 mg of the lyophilized standard in 1 mL of ultrapure water or assay buffer to achieve a concentration of 50 mg/mL. Then, a fresh aliquot of this stock was diluted with assay

buffer to generate a working standard solution of 1.0 mg/mL. Subsequently, a series of 8 serial dilutions were prepared from the working standard; as recommended by the manufacturer, 5–fold dilutions were employed to ensure the standard curve spanned the full range of detectable protease activity. The Trypsin TPCK standard curve of logarithmic scale of absorbance at 450 nm against concentration (ng/mL) was constructed as recommended by the manufacturer.

For every standard concentration, corresponding blanks containing the specific standard dilution were prepared by adding 100 µL of assay buffer without succinylated casein. For the enzymatic reaction, total of 50 µL of each standard dilution and unknown sample to the reaction wells containing succinylated casein and the blank wells. The plate was incubated at room temperature for 20 mins. Then, 50 µL of the 2,4,6–trinitrobenzene sulfonic acid (TNBSA) was added to each well and incubated at room temperature for 20 mins. Finally, the absorbances at 450 nm were measured using microplate reader. The final absorbances was calculated based on the formula given. The experiments were conducted in duplicates.

$$A450 = A450\,(Casein\ well) - A450\,(Blank\ well) \quad 3.1$$

The enzyme concentration of the crude extract and purified sample were quantified by extrapolating the absorbance values of the samples against a Trypsin TPCK standard curve. The proteolytic activity was calculated based on the formula given.

$$Specific\ proteolytic\ activity\ \left(\frac{U}{mg}\right) = \frac{Total\ proteolytic\ activity\ (U)}{Total\ Protein\ content\ (mg)} \quad 3.2$$

One unit of protease is defined as the amount of enzyme that will generate 1.0 µmol of trypsin from the succinylated casein and trinitrobenzene sulfonic acid (TNBSA) reaction per minute at 37°C as measured at 450 nm using a Tecan M200 plate reader (GA, Switzerland).

3.3 Results

3.3.1 Extraction and Purification of Bovine CBPA1

Bovine pancreatic CBPA1 was successfully purified from the fresh pancreatic tissue by pancreatic tissue delipidation, protein extraction, IEX, and GFC. Total of 200 mL of filtered bovine crude extract was loaded onto the pre–packed HiTrap Q Fast Flow column. Figure 3.2 illustrates the elution pattern of IEX on the pre–packed HiTrap Q Fast Flow column. The IEX elution was performed with a step NaCl gradient (5 – 100%), whereby the enzymes were separated based on the ionic strength of the elution buffer. The elution profile shows eight distinct peaks after the IEX step. As shown in Figure 3.2, the bovine CBPA1 was present in fractions eluted at 30% NaCl concentration and labelled as **peak D**. These fractions were collected between the elution volumes of **235.0 mL** and **260.5 mL**. In total, 17 fractions (25.5 mL) were obtained from the IEX step, yielding a protein concentration of 6.99 mg/mL, corresponding to 178.5 mg of total protein.

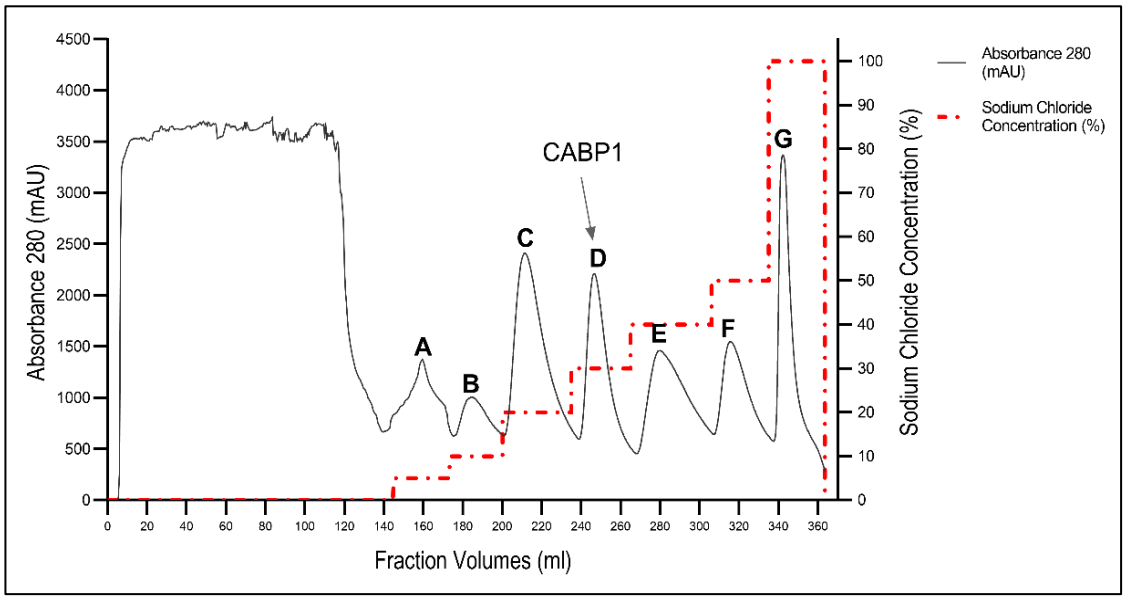


Figure 3.2 Anion–exchange Chromatography of Aqueous Crude Bovine Pancreatic Extract. The Partially Purified Bovine CBPA1 was eluted at Peak D (30% NaCl concentration).

Notes: The thin line shows the absorbance at a wavelength of 280nm during chromatography. The arrows marked peaks that showed the presence of bovine CBPA1 on the 1D–SDS PAGE with proteolytic activity. Tubes were pooled at 30% NaCl concentration, indicating the presence of active bovine CBPA1. Column: Hi Trap Q Fast Flow column (pre–packed); flow rate: 2.4mL/min; mobile phase: 20mM Tris pH8, 20mM Tris NaCl pH8.

Following IEX, all fractions containing bovine CBPA1 were pooled and loaded into GFC column – HiLoad™ 16/600 Superdex™ 200 pg. The pooled fractions from IEX were concentrated to 5 mL with Amicon® Ultra (30,000 MW and 50,000 MW) Centrifugal Filter (MERCK – Germany), then loaded onto GFC column. After the GFC, two distinct peaks were observed. The fractions corresponding to the two distinct peaks was individually subjected to 1D–SDS PAGE to determine the molecular weight of the eluted fractions (data not shown). Analysis of 1D–SDS PAGE revealed highly similar bands across the two fractions representing the peaks (similar bands as in Figure 3.4 – **Lane 4**). This indicates that the GFC is not effective in isolating a monomeric form of bovine CBPA1. From the Figure 3.3, the fractions eluted between **80.0 mL** and **106.0 mL** were pooled indicated as **red dashes** for enzyme activity determination. Thus, the GFC, resulted in 26 fractions (26.0 mL) of purified the bovine CBPA1 (Figure 3.3). The protein concentration is 1.69 mg/mL, corresponding to 43.94 mg of total protein.

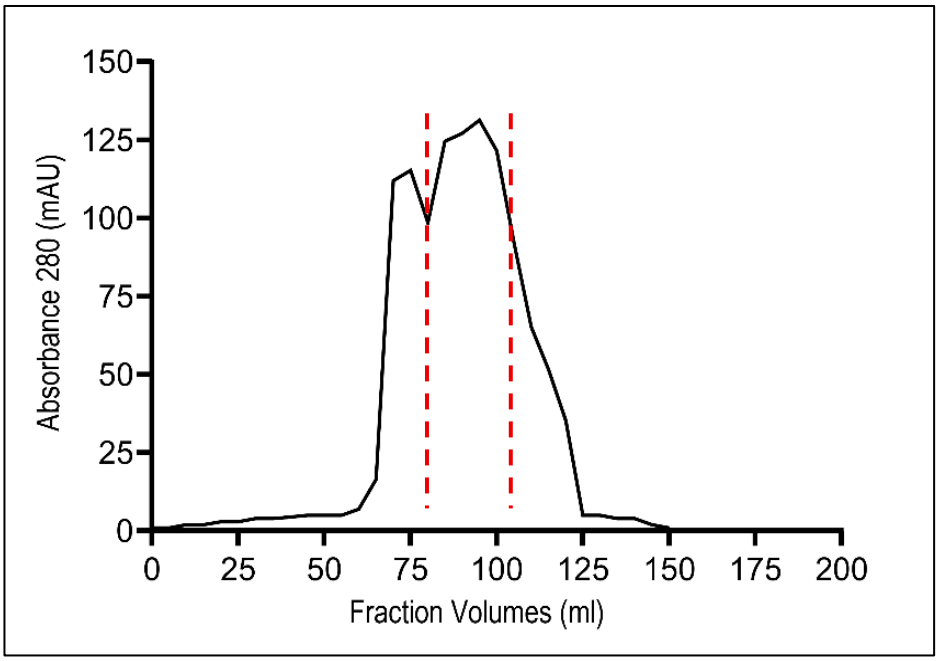


Figure 3.3 Gel Filtration Chromatography of Pure Bovine CBPA1.

Note: The thin line shows the absorbance at a wavelength of 280nm during chromatography. Tubes were pooled. Column: HiLoadTM 16/600 Superdex™ 200 pg (pre–packed); flow rate: 1.0mL/min; mobile phase: 25 mM Tris HCl pH 8 0.5 mM EDTA 150 mM NaCl.

3.3.2 Protein Identification and Confirmation of Bovine Carboxypeptidase A1

1D–SDS PAGE analysis of the bovine CBPA1 from crude extract, post–IEX and post–GFC are shown in Figure 3.4. From the 1D–SDS PAGE, the IEX revealed multiple bands – 45 kDa, 28 kDa, and 18 kDa in **Lane 3**. This postulated that the fractions still contained other proteins below the expected molecular weight. Further purification via GFC was objectively performed to isolate pure bovine CBPA1 to remove other protein with lower molecular weight. Unfortunately, the GFC purification step using HiLoad^{TM} 16/600 Superdex^{TM} 200 pg was unsuccessful because the fractions still contain lower molecular weight contaminants as seen in **Lane 4**. The low molecular weight contaminants were not adequately separated from the primary band of bovine CBPA1. However, the targeted bovine CBPA1 eluted at the expected molecular weight (47 kDa) of the enzyme in monomeric form. All bovine CBPA1 fractions from crude extract, IEX and GFC were pooled for proteolytic activity determination.

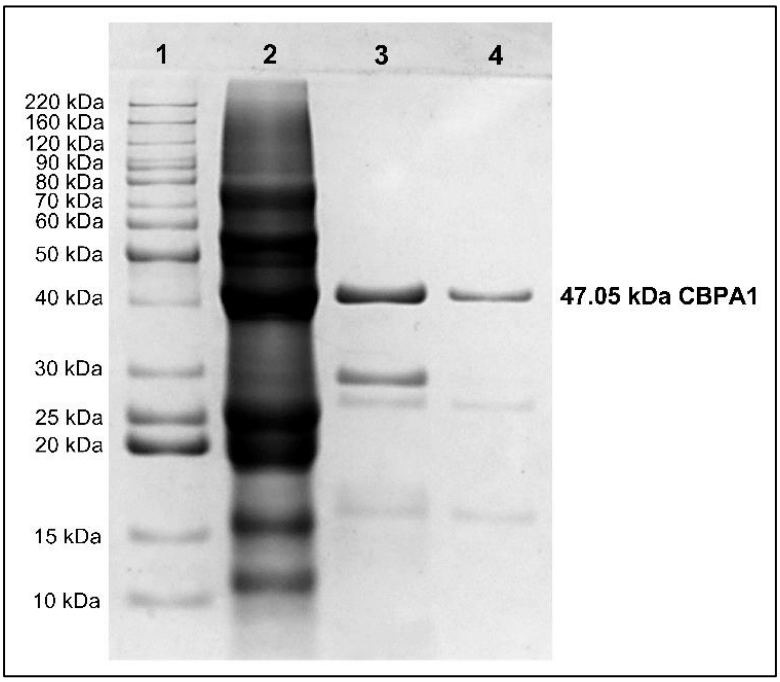


Figure 3.4 1D–SDS PAGE (Bis–Tris 12%) of Pure Bovine CBPA1. Pure Bovine CBPA1 was approximately estimated to be 47 kDa (Lane 4).

Note: Lane 1: Benchmark^{TM} Unstained Protein Ladder; Lane 2: Bovine crude extract; Lane 3: Bovine CBPA1 obtained after Hi Trap Q Fast Flow chromatography; and Lane 4: Bovine CBPA1 obtained after HiLoad^{TM} 16/600 Superdex^{TM} 200 pg chromatography. The gel was stained with Coomassie blue.

Following GFC, three protein bands were estimated to be 47 kDa, 28 kDa and 18 kDa were observed (Figure 3.4, **Lane 4**). The higher molecular weight bands at 47 kDa, expected to be bovine CBPA1, were excised and destained for LC–MS/MS protein identification. Table 3.3 lists the protein identified from the LC–MS/MS analysis. The LC–MS/MS revealed that bovine CBPA1 (Accession number – P00730) has protein coverage of 82.82% and recorded a mass of 47.05 kDa and 5.55 calc pI. The predictive peptide sequences related to bovine CBPA1 determined by the LC–MS/MS were selected as potential bovine pancreatic CBPA1 based on the percolator® algorithm with a q–value of less than 1% false discovery rate (FDR). The peptide identification results showed that 194 predictive peptides were obtained (data not shown). In the current study, thirty predictive peptides show similar characteristics to the same master protein of bovine pancreatic CBPA1. The result obtained was confirmed with low FDR with Qvality q–value (>0.01), XCorr Sequest HT (>2.0), and percolator q–value Sequest HT value (>0.01). In general, the reported peptides contained one or no missed cleavage events. The peptide sequence, position in the master protein, charge, and molecular weight are listed in Table 3.3. Most of the predictive peptides have a low molecular weight ranging from 902.49 – 4582.12 Da and a net charge of 2 to 4. Half of the predictive peptide sequences undergo modifications during the sample–handling process, as shown in Table 3.3, with frequent variable oxidation and deamination modifications, as well as with less frequent fixed carbamidomethyl modifications. Only three cysteine carbamidomethylation (CAM) modified sites were identified (Peptide amino acid 264–287 AGASSSP**C**SETYHGKYANSEVEVK, proposed CAM on C272; Peptide amino acid 239–255 TRSVTSSSL**C**VGVDANR, proposed CAM on C249; Peptide amino acid 241–263 SVTSSSL**C**VGVDANRNWDAGFGK, proposed CAM on C249).

Table 3.2
Protein Identification from the LC–MS/MS

No	Accession Number	Protein Identified	No of Peptides	Coverage (%)	Molecular Weight (kDa)	Calc PI
1	P00730	Carboxypeptidase A1 OS=Bos taurus OX=9913 GN=CPA1 PE=1 SV=3	30	82.82	47.05	5.55
2	Q0VCX2	Endoplasmic reticulum chaperone BiP OS=Bos taurus OX=9913 GN=HSPA5 PE=2 SV=1	28	42.90	72.36	5.16
3	P60712	Actin, cytoplasmic 1 OS=Bos taurus OX=9913 GN=ACTB PE=1 SV=1	17	60.80	41.71	5.48
4	P63258	Actin, cytoplasmic 2 OS=Bos taurus OX=9913 GN=ACTG1 PE=1 SV=1	17	60.80	41.77	5.48
5	P38657	Protein disulfide–isomerase A3 OS=Bos taurus OX=9913 GN=PDIA3 PE=2 SV=1	20	49.70	56.89	6.65

Table 3.3
Peptide Sequence Prediction of Bovine Pancreatic CBPA1 via LC–MS/MS

No	Annotated Sequence	Confidence	Modifications	Charge	Position in Master Protein	Theo. MH+ [Da]	Qvality q–value	XCorr Sequest HT	Percolator q–Value Sequest HT
1	[K].AFLSIHSYSQLLLYPYGYTTQSIPDK.[T]	High	–	3	301–326	3005.53	0	5.99	0
2	[K].AFLSIHSYSQLLLYPYGYTTQSIPDKTELNQVAK.[S]	High	1xDeamidated [N/Q]	4	301–334	3889.99	0	4.14	0
3	[K].AGASSSP**C**SETYHGK.[Y]	High	1xCarbamidomethyl [C8]	3	264–278	1538.65	0	4.08	0
4	[K].AGASSSP**C**SETYHGKYANSEVEVK.[S]	High	1xCarbamidomethyl [C8]	4	264–287	2558.15	0	4.10	0
5	[K].EDFVGHQVLR.[I]	High	–	2	18–27	1199.62	0	3.64	0
6	[K].ELEDLEHLQLDFWR.[G]	High	–	3	41–54	1842.90	0	5.02	0
7	[K].FSTGGSNRPAIWIDLGIHSR.[E]	High	–	3	162–181	2184.13	0	6.38	0
8	[K].FTEDYGQDPSFTAILDS**M**DIFLEIVTNPDGFAFTHSQNR.[L]	High	1xDeamidated [N/Q] 1xOxidation [M18]	3	196–234	4456.02	0	4.70	0
9	[K].KFTEDYGQDPSFTAILDS**M**DIFLEIVTNPDGFAFTHSQNR.[L]	High	1xDeamidated [Q/N] 1xOxidation [M19]	4	195–234	4584.12	0	8.24	0
10	[K].SIVDFVKDHGNFK.[A]	High	–	3	288–300	1505.77	0	4.69	0
11	[K].SLYGTSYK.[Y]	High	–	2	342–349	918.46	0	2.43	0
12	[K].TELNQVAK.[S]	High	–	2	327–334	902.49	0	3.09	0
13	[K].TRSVTSSSL**C**VGVDANR.[N]	High	1xCarbamidomethyl [C10]	3	239–255	1808.89	0	4.52	0
14	[K].VFLEAHGIR.[Y]	High	–	2	77–85	1041.58	0	3.46	0
15	[K].YA**N**SEVEVK.[S]	High	1xDeamidated [N3]	2	279–287	1039.49	0	3.80	0
16	[K].YGSIITTIYQASGGSIDWSYNQGIK.[Y]	High	1xDeamidated [Q/N]	2	350–374	2723.32	0	3.26	0
17	[K].YSFTFELR.[D]	High	–	2	375–382	1062.52	0	3.36	0
18	[R].EWITQATGVWFAK.[K]	High	–	2	182–194	1536.78	0	5.54	0
19	[R].GPGQPGSPIDVR.[V]	High	–	2	55–66	1179.61	0	4.19	0
20	[R].I**M**IEDVQSLLDEEQEQ**M**FASQSR.[A]	High	1xDeamidated [Q] 1xOxidation [M] 2xOxidation [M2; M17]	2	88–110	2726.26	0	8.02	0
21	[R].ITAADEAEVQTVK.[E]	High	–	2	28–40	1374.71	0	5.66	0
22	[R].ITAADEAEVQTVKELEDLEHLQLDFWR.[G]	High	1xDeamidated [Q]	4	28–54	3199.58	0	3.3	0
23	[R].**N**WDAGFGK.[A]	High	1xDeamidated [N1]	2	256–263	895.39	0	3.4	0
24	[R].STNTFNYATYHTLDEIYDFMDLLVAEHPQLVSK.[L]	High	1xOxidation [M20]	4	113–145	3891.84	0	7.0	0

25	[R].SVTSSSL**C**VGVDANR.[N]	High	1xCarbamidomethyl [C8]	2	241–255	1551.74	0	6.23	0
26	[R].SVTSSSL**C**VGVDANRNWDAGFGK.[A]	High	1xDeamidated [N]; 1xCarbamidomethyl [C8]	3	241–263	2428.12	0	6.44	0
27	[R].SYEGRPIYVLK.[F]	High	–	2	151–161	1324.73	0	3.11	0
28	[R].VPFPSLQAVK.[V]	High	–	2	67–76	1085.63	0	3.37	0
29	[R].YRI**M**IEDVQSLLDEEQEQ**M**FASQSR.[A]	High	1xOxidation [M4] 2xOxidation [M4; M19]	3	86–110	3077.42	0	7.52	0
30	[R].EWITQATGVWFAKK.[F]	High	–	3	182–195	1664.88	0	3.73	0

Note: Description of Bovine Pancreatic CBPA1 peptide sequence prediction. The bold symbol represents the possible site of fixed and variable modifications during the sample handling process. The confidence level for the identified protein was determined by the false discovery rate (FDR) and interpreted as high–confidence hits, which were 99% accurate. The charge is the sum of positive (basic) and negative (acidic) charge residues in neutral pH. Position in Master Protein is the location of the annotated predictive peptide sequence in the protein. Theo. MH+ [Da] is the protonated monoisotopic mass of the peptides in Daltons. Qvality q–value and Percolator q–Value Sequest HT are calculated from the number of target and decoy proteins and the minimum FDR is required for a hit to be considered correct (Qvality q–values and Percolator q–Value Sequest HT > 0.01 are considered high–confidence hits). XCorr Sequest HT indicates the number of fragment ions that are common to two different peptides with the same precursor mass and calculates the cross–correlation (XCorr) for all candidate peptides in search (XCorr value > 2 is considered favourable).

3.3.3 Proteolytic Enzyme Assay

The proteolytic activity was measured for all bovine crude extract, IEX, and GFC samples using the protease activity assay described. The Trypsin TPCK standard curve was constructed to determine the protease activity of bovine CBPA1 at different purification stages, with the R^2 value of 0.99 (Appendix 5). Table 3.4 summarizes the sequential purification and proteolytic enzyme activity measured for bovine CBPA1 in crude extract, IEX and GFC samples. The protein concentration of purified bovine CBPA1, as calculated from the $A_{280,}$ was 1.69 mg/mL.

Table 3.4
Sequential Purification Bovine Pancreatic CBPA1

Purification stage	Volume (mL)	A_{280}	Protein content (mg)	Specific proteolytic activity (U/mg)	Total proteolytic activity (U)	Yield (%)	Purification Fold
Crude extract	200.0	48.97	9794.0	503.93	4935490.42	100.00	1.00
IEX (*Peak D – 30% NaCl*)	25.5	6.996	178.5	64778.34	11562933.69	234.28	128.55
GFC	26.0	1.690	43.94	5819.37	255703.12	5.18	11.55

Note: Specific proteolytic activity of porcine Pancreatin (1 mg/mL) = 2030.08 U/mg

The bovine CBPA1 sequential purification demonstrates that IEX was the most effective step in enriching the proteolytic activity. The IEX samples marked increased in the specific proteolytic activity (64778.34 U/mg), correspond to 128.55–fold when compared to the crude extract samples. However, the subsequent GFC purification, resulted in a substantial reduction of purification fold to 11.55–fold with 5819.37 U/mg of the specific proteolytic activity, suggesting that there is potential loss in the enzyme activity due to degradation over time during the purification process.

Enzyme activity was also compared using commercially available porcine protease (Porcine Pancreatin) as a positive control. The concentration of the Pancreatin was standardized to 1 mg/mL and yielded 2030.08 U/mg of the specific proteolytic activity. This highlights that the protease of bovine is comparable to that of the porcine origin, particularly the purified bovine CBPA1 from IEX (32–fold, 64778.34 U/mg) and GFC (2.9–fold, 5819.37 U/mg) of specific proteolytic activity. Therefore, the bovine pancreas can be suggested as a potential alternative for pancreatic protease based on the prominent proteolytic activity.

3.4 Discussion

This is an updated report on the purification strategy of CBPA1 protease from the pancreatic tissues of bovine, following previous studies by Neurath and colleagues in 1970 (Neurath *et al.,* 1970) as well as Kerfelec and colleagues in 1985 (Kerfelec *et al.,* 1985). In particular, this study aims to evaluate the activity of CBPA1 in bovine, which could fulfil the Halal requirements compared to the commercially available animal protease from porcine, with a special interest in treating pancreatic diseases.

Pancreatic tissues from bovines were processed to obtain the crude extract, which was then subjected to a series of IEX and GFC. From the 1D–SDS PAGE result, the purified bovine CBPA1 was observed as three bands on the 1D–SDS PAGE (45 kDa, 28 kDa, and 18 kDa – Figure 3.4). This result was consistent with the previous study, where bovine CBPA1 was reported to have molecular weights in the range of 42–48 kDa (Kerfelec *et al.,* 1985; Reshidan *et al.,* 2024). The inability to isolate a single, homogeneous band of bovine CBPA1 following GFC, as evidenced by the persistence of a secondary band at approximately 28 kDa alongside the primary 47 kDa band, suggests that the enzyme does not exist solely as a monomeric species. This observation aligns with established biochemical characterizations of pancreatic CBPA1, which are known to present in two different forms; a monomer (45 kDa) and a stable binary complex, frequently associating with serine proteases such as pro–proteinase E (45 kDa + 26 kDa), or as ternary complexes containing inactive subunits (Vilanova *et al.,* 1985). In the past study, the bovine CBPA1 has also been found in more than one active molecular form which is similar to the porcine enzymes (Folk & Schirmer, 1963). In another study, most of the purified pancreatic CBPA1 were reported to be monomeric or can be associated with different functional proteins (Kerfelec *et al.,* 1985).

Consequently, the multiple bands observed under the denaturing conditions of 1D–SDS PAGE may represent dissociated subunit of these naturally occurring enzymatic CBPA1 complexes such as binary complexes with pro–proteinase E that co–eluted during GFC due to overlapping hydrodynamic volumes or strong non–covalent interactions. Furthermore, recent structural characterizations highlight that CBPA1 contains intrinsic regions prone to misfolding and instability, which may further contribute to the heterogeneity observed during isolation process (Sándor *et al.,* 2022). To resolve this heterogeneity and isolate a pure monomeric band of bovine CBPA1 in future investigations, it is recommended to incorporate high–specificity

affinity chromatography, utilizing ligands such as p–aminobenzyl succinic acid, which have successfully differentiated CBPA1 from their associated complexes in other species (Bradley *et al.,* 1994). By incorporating a high–selectivity purification step earlier may help to reduce enzymatic degradation associated with extended processing time required for the GFC step.

Alternatively, the utilization of native PAGE alongside 1D–SDS PAGE could provide valuable insight such as structural integrity confirmation and oligomeric state of bovine CBPA1. This is because, the native PAGE is a non–denaturing electrophoresis that preserve the natural quaternary structure and non–covalent interaction where the proteins migrations are influenced by the combination of molecular weight, shape and net charge. It is hypothesised that the active form of bovine CBPA1 would have migrated as a single stable complex in the native PAGE electrophoresis.

To the best of our knowledge, the literature on bovine CBPA1 purification is limited. The most recent finding on CBPA1 extraction and purification was a report on the CBPA1 extraction and purification from ostrich (*Struthio camelus),* whereby CBPA1 was observed as a single band of 34 kDa (Bradley *et al.,* 1994). An earlier study on ruminant species reported similar molecular weights of bovine CBPA1 with a mention of a ternary form of proxycarboxypeptidase A containing the inactive, non–activatable, and truncated subunit III (Kerfelec *et al.,* 1985).

Although the GFC demonstrate a successful bovine CBPA1 purification, the subsequent step resulted in a significance decline of the specific proteolytic activity to 5,819.37 U/mg with a drastic reduction in yield to 5.18%, suggesting potential enzyme instability or loss during this secondary process. Therefore, the IEX stage is suggested as a better purification step, as it produced the highest specific proteolytic activity. The purification enzymatic activity profile of bovine CBPA1 have demonstrated that the IEX was the most efficient and should be satisfactory in enriching the proteolytic activity (Table 3.4). A substantial increase in the specific proteolytic activity reaching 64,778.34 U/mg, which is approximately 32–fold higher than the commercial porcine pancreatin positive control (2,030.08 U/mg) was achieved after the IEX.

This study presents a simplified two–step purification of pancreatic CBPA1 from bovine using current readily available technology. Previously, bovine CBPA1 was extracted from acetone–dried pancreas powder, followed by ammonium precipitation and DE–tris acryl pH8 chromatography (Kerfelec *et al.,* 1985). The acetone–dried

pancreas powder has also been used with DAEA–cellulose and Sephadex G–50 or G–100 (Pharmacia) columns (Lacko & Neurath, 1970), as well as using a p–aminobenzyl succinic acid affinity column followed by a hydroxylapatite column and concentrated with PEG 2000 (Merck) (Bradley *et al.,* 1994). In addition, the purifications of the CBPA1 have also been conducted by desalting defatted acetone–dried powders of pig pancreas extracted with ammonium sulphate precipitation and separated on DEAE–Sepharose CL–6B (Pharmacia) column with linear NaCl gradient and varied pH settings (Vilanova *et al.,* 1985). In contrast to earlier reports, this study uses freshly extracted bovine pancreas to purify the enzyme based on its charge and size to obtain the final purified bovine CBPA1 product, which was confirmed by 1D–SDS PAGE, LC–MS/MS, and protease enzyme assay.

3.5 Conclusion

In conclusion, bovine CBPA1 was successfully extracted and characterized from bovine (*Bos taurus*) fresh pancreatic tissues, with its identity confirmed via LC–MS/MS. The purification profile indicates that the IEX stage represents the optimal purification stage with the highest specific proteolytic activity of 64778.34 U/mg, approximately 32–fold higher than the porcine pancreatin–positive control. Consequently, the IEX bovine CBPA1 is suggested as the most viable as an alternative to porcine enzyme. This warrants further investigation to validate the usefulness of bovine CBPA1 as a potential alternative to porcine, mainly to cater for Halal pharmaceutical and medical applications.

CHAPTER 4
EXTRACTION AND PURIFICATION OF SHEEP (*OVIS ARIES*) CARBOXYPEPTIDASE A1

4.1 Introduction

Proteolytic enzymes are secreted by the exocrine pancreas with complementary activities to participate in the alimentary process, including exopeptidase and endopeptidase (Guasch *et al.,* 1992). One of which is Carboxypeptidase A1 (CBPA1, EC 3.4.17.1), which has been extensively studied since the late 1950s and is described as a zinc metalloprotease (Bradley *et al.,* 1994; Kemik *et al.,* 2012; Sándor *et al.,* 2022) produced abundantly in pancreatic acinar cells and is responsible for cleaving C–terminal branched chains and aromatic amino acids from dietary proteins (Uhlig *et al.,* 2022). CBPA1 is one of the significant proteolytic pancreatic enzymes, and the loss of its function is strongly associated with early–onset chronic pancreatitis disease (Witt *et al.,* 2013).

Pancreatic and pancreatic–like carboxypeptidases are a family of zinc–containing exopeptidases released into the small intestine from the pancreas as a zymogen (Clauser *et al.,* 1988; Jitonnom & Sontag, 2012; Smith *et al.,* 1997). Pancreatic enzymes such as trypsin, chymotrypsin B and C, carboxypeptidase A1 and A2, elastase IIA and IIB, lipase, and lipase–related proteins 1 and 2, carboxyl ester lipase, and phospholipase A2 are secreted as a proenzyme that has to be cleaved before it can become active (Kohlmeier, 2015). Trypsin is responsible for procarboxypeptidase zymogen activation to catalyze the cleavage of C–terminal amino acids from their substrates, which originate exclusively from pancreatic acinar cells. This reaction forms a CBPA1 complex, which is then released into the intestinal lumen for the digestion process to take place (Elamin *et al.,* 2014; Jitonnom & Sontag, 2012; Said *et al.,* 2020; Sándor *et al.,* 2022). The full activation of the procarboxypeptidase requires further peptide activation proteolysis by chymotrypsin (Sándor *et al.,* 2022). It exhibits peptidase and esterase activity with aliphatic C–terminal residues as a preference for catalytic and active sites (Sándor *et al.,* 2022).

CBPA1 has been isolated and characterized from humans (Goldstein *et al.,* 1989; Pascual *et al.,* 1989) and various animal hosts, including chicken (Zelikson *et al.,* 1971), bovine (Neurath *et al.,* 1970), porcine (Folk & Schirmer, 1963), sheep (Kerfelec *et al.,* 1985), dogfish (Lacko & Neurath, 1970), and ostrich (Bradley *et al.,* 1994), from the 1950s until the mid–1990s. Despite previously gaining much attention, there is no recent update on the methods related to the extraction and purification of CBPA1 from sheep. Based on the recent literature, the research interest of CBPA1 has shifted from purification efforts to applications as a new genetic marker for pancreatic acinar cell carcinoma (Ishimoto-Namiki *et al.,* 2023; Said *et al.,* 2020; Uhlig *et al.,* 2022) , as its gene mutations have been reported to be associated with chronic pancreatitis (Reddy *et al.,* 2024; Sándor *et al.,* 2022; Sendler *et al.,* 2018).

Domestic sheep are members of the Bovidae family, widely distributed in Malaysia, particularly for Halal meat consumption. However, some animal organs, including the pancreas, are not fully utilized and are disposed of as waste. Mammalian pancreatic tissues are non–edible parts produced in significant quantities by the meat industry and represent waste disposal and potential pollution (Li *et al.,* 2012). Thus, the sheep pancreas, a by–product of the meat industry, could serve as an alternative source for Halal digestive enzymes, especially proteases. Furthermore, both Muslim and non–Muslim consumers are demanding the highest quality and Halal–certified products, including medicine and health supplements (Aziz *et al.,* 2014). Halal pharmaceutical products have gained the interest of non–Muslim consumers because these products are considered cleaner and healthier (Sudarsono & Nugrowati, 2020). The exocrine pancreas glands' alkaline secretions, including α–amylase, trypsin, chymotrypsin, and carboxypeptidase, are important for the small intestine's carbohydrates, proteins, and fat breakdown (Rafaqat *et al.,* 2023).

The study herein reports on the purification of CBPA1 from sheep from fresh sheep pancreas with simplified purification strategies compared to previous research, enabled by the latest purification system technology. This includes the selection of the column and buffer of sheep CBPA1 purification, as well as the two–step purification method: anion exchange chromatography (IEX) and gel filtration chromatography (GFC). In addition, there is an interest in the present work on the possible role of sheep CBPA1 as a functional substitute for porcine enzymes, especially in the Halal medical and pharmaceutical industries.

4.2 Materials and Methods

The sheep Carboxypeptidase A1 (CBPA1) purification scheme was summarised as in Figure 4.1.

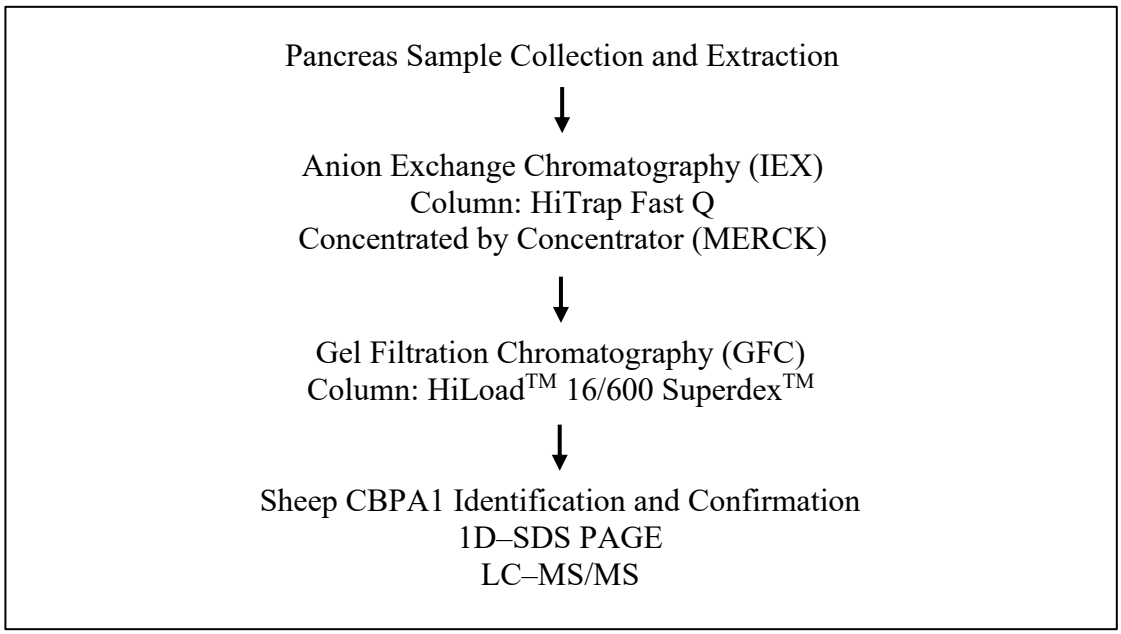


Figure 4.1 Sheep Carboxypeptidase A1 (CBPA1) Purification Scheme.

4.2.1 Enzyme Extraction

Sheep pancreas was collected freshly from slaughtered animals of Abattoir Complex, Department of Veterinary Services (DVS), Shah Alam, Malaysia (Coordinates: 3.05, 101.51), and stored on ice. There was no available information on the supplier or animal records from the abattoir. Nevertheless, it was determined that all the animals were male with an estimated age between 6 to 12 months.

The pancreases were washed with tap water upon receiving. Then, the pancreas was dissected free from adherent fat and connective tissues with a scalpel blade (Elamin *et al.,* 2014). The pancreas was cut into smaller pieces on ice, and the tissue slices were washed with a 50 mM Tris pH 7.4 buffer containing 0.1 M sodium chloride (NaCl) to remove blood (Al-Ajlan & Bailey, 1999). The bovine pancreas collection and pancreatic crude extraction were done on the same day. Approximately 120 g – 160 g of pancreas samples were homogenized using a laboratory blender (Tefal – France), 1 min at low speed and 1 min at high speed (Bradley *et al.,* 1994).

Then, sheep pancreatic tissues were suspended in 20 mL of extraction buffer (50 mM Tris pH 7.4, 2 mM Ethylenediaminetetraacetic acid (EDTA) pH 8, 10 mM 4–(2–hydroxyethyl)–1–piperazineethanesulfonic acid (HEPES) pH 7.4, 1% Triton X–100, and 150 mM NaCl) and vortexed for 10 mins before centrifugation at 4000 rpm for 2 mins. The supernatants were collected and added with 70% (v/v) ethanol, bringing a total of 25 mL. The mixture was vortexed for 10 secs, and 2 mL of 5µg/mL of aprotinin as a protease inhibitor was added to the samples. Aprotinin is a serine protease inhibitor and essential in inhibiting endogenous serine proteolytic activity. The suppression of the non–targeted proteases preserved the enzymatic activities of the targeted proteins. This helps to mitigate the risk of proteolytic degradation of the targeted enzymes, whereby the recovery of intact soluble proteases was maximised in the collected supernatant during the extraction procedure. The samples were centrifuged at 14 000 rpm for 20 mins before collecting the supernatant to recover soluble proteins. The protein concentration was measured and stored at –20^{o}C until further use.

4.2.2 Sequential Purification of Sheep Carboxypeptidase A1

The purification is a critical step in this study to isolate the targeted enzymes. Following the preparation of the pancreatic tissue extraction, the sheep crude pancreatic extract was subjected to sequential purification. The crude extract underwent sequential purification beginning with anion exchange chromatography (IEX) to isolate the sheep CBPA1 based on surface net charge. The enriched fraction was subsequently subjected to gel filtration chromatography (GFC). Ideally, the GFC was done to achieve higher homogeneity by utilizing size–exclusion principles to further isolate the sheep CBPA1.

4.2.2.1 Anion Exchange Chromatography (IEX)

The purification step was performed at room temperature on the second day (within 24 hours) following the crude extraction. Sheep pancreatic CBPA1 was further purified by anion exchange chromatography (IEX) on a pre–packed HiTrap Q Fast Flow column containing a Sepharose–based resin (strong anion exchanger) (bed height 1.6 cm, column diameter 2.5 cm, column volume 5 mL) using an AKTA Avant^{TM} chromatography system (Cytiva – USA). The column equilibration process began by

replacing the column's ethanol storage with distilled water to remove the preservative. Subsequently, the column was washed and equilibrated with the start buffer. The 20 mM Tris pH 8 was used as the start buffer, and 20 mM Tris 1 M NaCl pH 8 was used as the elution buffer. The sample was filtered using 0.45 μm and 0.25 μm cellulose acetate pore membrane filters (Merck – Germany). A total of 160 mL filtered sample was applied to the column in buffer A, and the column was washed until the absorbance monitored at 280 nm returned to baseline. The pancreatic enzymes were eluted using an elution buffer at a 2.4 mL/min flow rate, and 1.5 mL fractions were collected.

The IEX was chosen to separate the proteins depending on their ability to interact with a specific positive charge resin where negative charge proteins will bound to the resin. Generally, the proteins were eluted by increasing the ionic strength (salt concentration) of the elution buffer. In this study, the salt ions compete with the bound proteins for the positive charges on the surface of resin, which induced the elution of the bound proteins. As a result, the protein with lower net charge will elute first, following with higher net charge of protein that retained longer as it requires higher ionic strength of elution buffer to be eluted at the selected pH. Since bovine CBPA1 possesses an isoelectric point equal to 5.33, the IEX is performed using buffers with higher pH (pH 8).

Initially, a preliminary linear gradient IEX was conducted to determine the optimal ionic strength required to identify the best NaCl concentration for isolating each targeted enzyme. Subsequently, a NaCl step gradient was applied to purify and isolate the targeted enzymes within a single cycle of the IEX procedure. This allows distinct peak separation and efficient removal of contaminants at lower ionic strengths before eluting the targeted enzymes at their specific targeted salt concentrations. The IEX purification was repeated at least three times, and the chromatogram profiling was constructed based on the mean absorbance values.

The elution buffer composition was set up as a step gradient at 5%, 10%, 20%, 30%, 40%, 50%, and 100% sodium chloride (NaCl) to elute the targeted CBPA1. Each fraction representing different peaks was run on 1–dimensional sodium dodecyl sulphate–polyacrylamide gel electrophoresis (1D–SDS PAGE) for molecular weight determination. The sheep CBPA1 was eluted at 30% of salt concentration. Fractions containing protease activity based on the molecular weight were pooled and concentrated using a 30,000 MW and 50,000 MW Amicon® Ultra Centrifugal Filter (MERCK – Germany).

4.2.2.2 Gel Filtration Chromatography (GFC)

Final purification of sheep pancreatic CBPA1 was performed by GFC on a pre–packed HiLoad™ 16/600 Superdex™ 200 pg column (bed height 60.0 cm, column diameter 1.6 cm, column volume 120 mL) using the AKTA Avant™ chromatography system (Cytiva – USA). The column equilibration process began by replacing the column's ethanol storage with distilled water to remove the preservative. Subsequently, the column was washed and equilibrated with the mobile phase.

The mobile phase was 25 mM Tris Hydrochloride (Tris HCl), pH 8, 0.5 mM EDTA, 150 mM NaCl at a 1.0 mL/min flow rate. A total of 5 mL concentrated from the previously purified IEX sample was injected into the mobile phase, and the column was washed until the absorbance monitored at 280 nm returned to baseline. The sheep pancreatic CBPA1 was eluted at a 1.0 mL/min flow rate. Fractions of 1 mL each were collected and subjected to protein identification and proteolytic activity.

Principally, GFC is also known as a size exclusion chromatography where the molecules (proteins) are separated by their molecular weight passing through the cross–linked dextran with highly cross–linked agarose composite matrix. Generally, a larger protein size will be excluded from the resin and eluted first following with a smaller protein size that will penetrate the resin pores and eluted later.

4.2.3 Protein Identification and Confirmation of Sheep Carboxypeptidase A1

4.2.3.1 Determination of Protein Concentration

The total protein concentration of total crude pancreatic extract and purified fraction samples from IEX and GFC were measured. Absorbance was measured at 280 nm (A_{280}) using a NanoDrop® ND–1000 UV–Vis Spectrophotometer (Thermo Fisher Scientific – US). The obtained concentration values (mg/mL) were subsequently utilised to calculate the total protein content (mg) and were essential for determining the proteolytic enzymatic activity (U/mg) of the samples.

4.2.3.2 One–Dimensional Sodium Dodecyl Sulfate Polyacrylamide Gel Electrophoresis (1D–SDS PAGE)

The molecular weight of purified sheep pancreatic CBPA1 was estimated by 1D–SDS PAGE using NuPAGE 4–12% mini protein gel of Bis–Tris electrophoresis system in X Cell SureLock Mini–Cell (Invitrogen – US) stained with Coomassie Brilliant Blue stain (Invitrogen – US).

The sample was prepared as described in Table 4.1. The protein mixtures were prepared by adding protein sample (x µl), 4X NuPAGE LDS Sample Buffer (2.5 µl), 10X NuPAGE Reducing agent (1 µl), and Ultrapure water (y µl) in a 1.5 mL Eppendorf tube. The protein volume needed was calculated using the dilution formula (M1V1 = M2V2) based on the initial concentration of the protein. Then, Ultrapure water was added, bringing a 10 µl volume for sample preparation. The protein sample was heated at 70^{o}C for 10 mins before loading into the wells. The 1X NuPAGE MES SDS Running Buffer was prepared by adding 50 mL of 20X MES SDS Running Buffer to 950 mL of distilled water. The gel electrophoresis system was set up at 200 V (constant voltage) and 125 mA (current). The electrophoretic separation was conducted for approximately 35 to 45 minutes to ensure the complete resolution of the protein bands.

Table 4.1
Sample Preparation for SDS–PAGE

Chemicals	**Volume (µl)**
Protein Concentration	20 mg/mL
Protein Sample	*x*
NuPAGE LDS Sample Buffer (4X)	2.5
NuPAGE Reducing agent (10X)	1.0
Ultrapure water	*y*
Final Volume	**10.0**

The gel was transferred into a clean container and added with 50 mL of distilled water. Then, the gel was microwaved at high power for 1 min and shaken for 1 min. The steps were repeated twice. Then, the gel was added with Safely Blue Safe stain (Invitrogen – US) liquid. The gel was microwaved again at high for 45 secs and shaken for 5 mins. The gel was washed with distilled water and shaken for 10 mins before viewing with ChemiDoc^{TM} Imaging System (BioRad – US).

4.2.3.3 Liquid Chromatography–Mass Spectrometry (LC–MS/MS)

Protein bands were further identified using liquid chromatography–mass spectrometry (LC–MS/MS). Before the LC–MS/MS procedure, trypsin gel digestion was carried out. Then, a total of 5 µL sample was injected into Dionex Ultimate 3000 RSLCnano Orbitrap Fusion (Thermo Fisher Scientific – US) with EASY–Spray Acclaim PepMapTM C18 100 A0 (2 µm particle size, 50 µm id x 15 cm) separation column. The sample was eluted with LC–MS grade water, 0.1% formic acid (A), and ACN, 0.1% formic acid (B), at a 250 nL/min flow rate. The elution gradient was 5%–40% B for 91 min, 2 min to 85% B, 3 min at 85% B, 1 min at 5% B, and 4 min at 5% B. The full scan spectra were collected by Orbitrap MS (OTMS) scan mass ranging from 310 – 1800 m/z with 50 ms maximum injection. The spectra were analysed by ion trap MS (ITMS) with 250 ms maximum injection. The LC–MS/MS data was analysed using Thermo Scientific^{TM} Proteome Discoverer^{TM} Software Version 2.1. The results were matched with the database downloaded from UniProt. The variable modifications were oxidation and deamination, with fixed modification of carbamidomethyl. All peptides were validated using the percolator® algorithm, based on a q–value of less than 1% false discovery rate (FDR). The LC–MS/MS analysis was performed at the Proteomic Laboratory, Malaysian Genome and Vaccine Institute, Bangi, Malaysia.

4.2.4 Proteolytic Enzyme Assay

Proteolytic activity of crude extracts and purified fractions from IEX and GFC was determined using Pierce Protease Assay kit (Thermo Fisher Scientific – US) following the manufacturer's instructions alongside purified porcine Pancreatin (Sigma Aldrich – USA) as positive control. Protease activity was determined using a coupled enzyme reaction, which resulted in a colourimetric (450 nm) product proportional to the enzymatic activity present.

Trypsin Tosyl phenylalanyl chloromethyl ketone (TPCK) was used to construct a standard curve to determine the enzyme concentration tested, while succinylated casein was used as a substrate. The concentration of the substrate used was 2 mg/mL. The Trypsin TPCK standard curve was established by dissolving 50 mg of the lyophilized standard in 1 mL of ultrapure water or assay buffer to achieve a concentration of 50 mg/mL. Then, a fresh aliquot of this stock was diluted with assay

buffer to generate a working standard solution of 1.0 mg/mL. Subsequently, a series of 8 serial dilutions were prepared from the working standard; as recommended by the manufacturer, 5–fold dilutions were employed to ensure the standard curve spanned the full range of detectable protease activity. The Trypsin TPCK standard curve of logarithmic scale of absorbance at 450 nm against concentration (ng/mL) was constructed as recommended by the manufacturer.

For every standard concentration, corresponding blanks containing the specific standard dilution were prepared by adding 100 µL of assay buffer without succinylated casein. For the enzymatic reaction, total of 50 µL of each standard dilution and unknown sample to the reaction wells containing succinylated casein and the blank wells. The plate was incubated at room temperature for 20 mins. Then, 50 µL of the 2,4,6–trinitrobenzene sulfonic acid (TNBSA) was added to each well and incubated at room temperature for 20 mins. Finally, the absorbances at 450 nm were measured using microplate reader. The final absorbances was calculated based on the formula given. The experiments were conducted in duplicates.

$$A450 = A450\,(Casein\ well) - A450\,(Blank\ well) \quad 4.1$$

The enzyme concentration of the crude extract and purified sample were quantified by extrapolating the absorbance values of the samples against a Trypsin TPCK standard curve. The proteolytic activity was calculated based on the formula given.

$$Specific\ proteolytic\ activity\ \left(\frac{U}{mg}\right) = \frac{Total\ proteolytic\ activity\ (U)}{Total\ Protein\ content\ (mg)} \quad 4.2$$

One unit of protease is defined as the amount of enzyme that will generate 1.0 µmol of trypsin from the succinylated casein and trinitrobenzene sulfonic acid (TNBSA) reaction per minute at 37°C as measured at 450nm using a Tecan M200 plate reader (GA – Switzerland).

4.3 Results

4.3.1 Extraction and Purification of Sheep Carboxypeptidase A1

Sheep pancreatic CBPA1 was successfully purified from the fresh pancreatic tissue by pancreatic tissue delipidation, protein extraction, IEX and GFC. Total of 160 mL of filtered sheep crude extract was loaded onto the pre–packed HiTrap Q Fast Flow column. Figure 4.2 illustrates the elution pattern of IEX on the pre–packed HiTrap Q Fast Flow column. The IEX elution was performed with a step NaCl gradient (5 – 100%), whereby the enzymes were separated based on the ionic strength of the elution buffer. The elution profile shows eight distinct peaks after the IEX step. As shown in Figure 4.2, the sheep CBPA1 was present in fractions eluted at 30% NaCl concentration and labelled as **peak D**. These fractions were collected between the elution volumes of **200.0 mL** and **222.50 mL**. In total, 15 fractions (22.5 mL) were obtained from the IEX step, yielding a protein concentration of 5.08 mg/mL, corresponding to 114.25 mg of total protein.

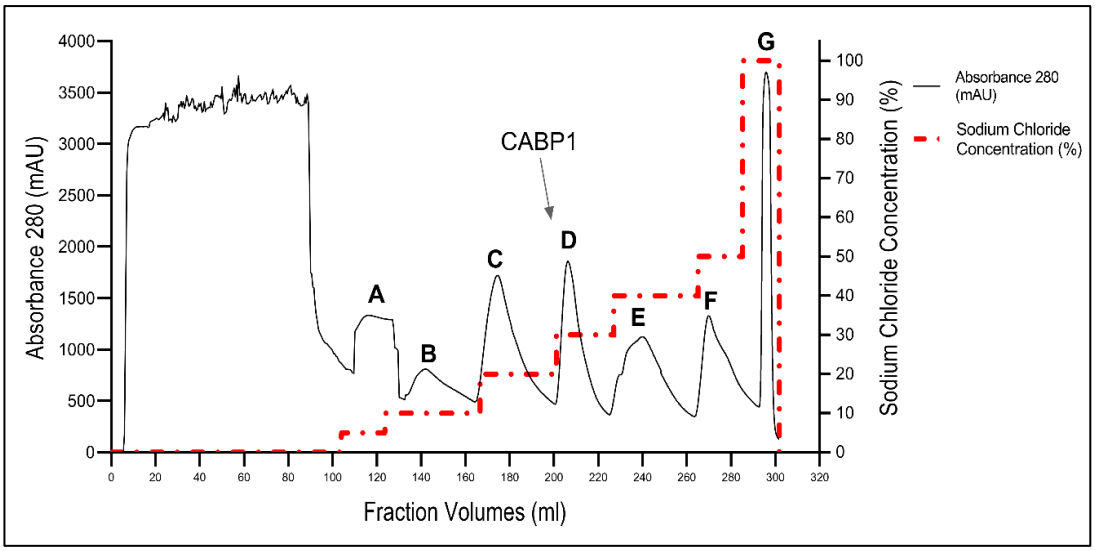


Figure 4.2 Anion–exchange Chromatography of Aqueous Crude Sheep Pancreatic Extract. The Partially Purified Sheep CBPA1 was eluted at Peak D (30% NaCl concentration).

Notes: The thin line shows the absorbance at a wavelength of 280nm during chromatography. The arrows marked peaks that showed the presence of sheep CBPA1 on the 1D–SDS PAGE with proteolytic activity. Tubes were pooled at 30% NaCl concentration, indicating the presence of active sheep CBPA1. Column: Hi Trap Q Fast Flow column (pre–packed); flow rate: 2.4mL/min; mobile phase: 20mM Tris pH8, 20mM Tris NaCl pH8.

After the IEX, all fractions containing sheep CBPA1 were pooled and loaded into GFC column – HiLoad™ 16/600 Superdex™ 200 pg. The pooled fractions from IEX were concentrated to 5 mL with Amicon® Ultra (30,000 MW and 50,000 MW) Centrifugal Filter (MERCK – Germany), then loaded onto GFC column. After the GFC, two distinct peaks were observed. The fractions corresponding to the two distinct peaks was individually subjected to 1D–SDS PAGE to determine the molecular weight of the eluted fractions (data not shown). Analysis of 1D–SDS PAGE revealed highly similar bands across the two fractions representing the peaks (similar bands as in Figure 4.4 – **Lane 4**). This indicates that the GFC is not effective in isolating a monomeric form of sheep CBPA1. From the Figure 4.3, the fractions eluted between **68.0 mL** and **95.0 mL** were pooled indicated as **red dashes** for enzyme activity determination. Thus, the GFC, resulted in 27 fractions (27.0 mL) of purified the sheep CBPA1 (Figure 4.3). The protein concentration is 0.99 mg/mL, corresponding to 26.73 mg of total protein.

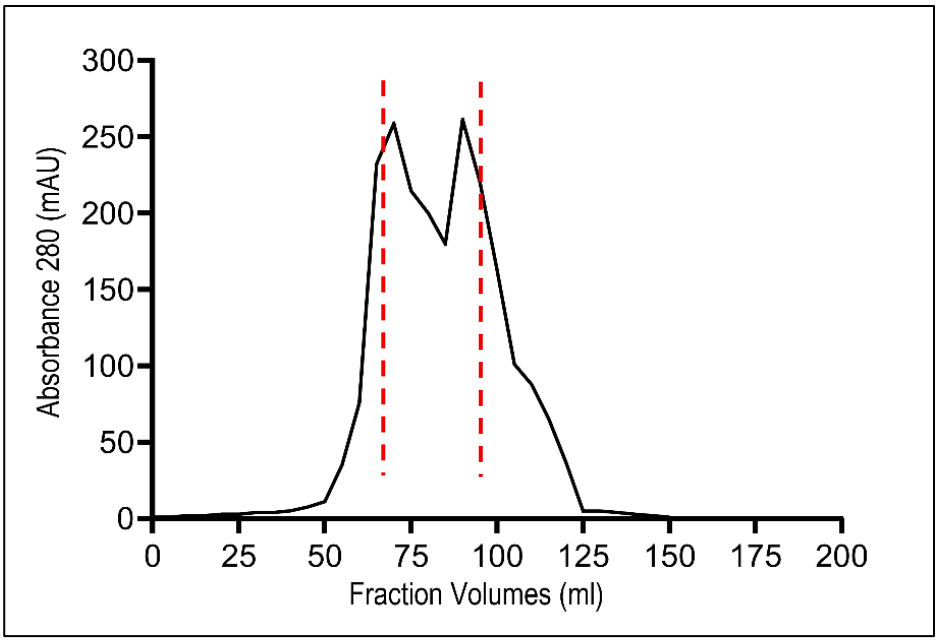


Figure 4.3 Gel Filtration Chromatography of Purified Sheep CBPA1.

Note: The thin line shows the absorbance at a wavelength of 280nm during chromatography. Tubes were pooled. Column: HiLoadTM 16/600 Superdex™ 200 pg (pre–packed); flow rate: 1.0mL/min; mobile phase: 25 mM Tris HCl pH 8 0.5 mM EDTA 150 mM NaCl.

4.3.2 Protein Identification and Confirmation of Sheep Carboxypeptidase A1

1D–SDS PAGE analysis of the sheep CBPA1 from crude extract, post–IEX and post–GFC are shown in Figure 4.4. From the 1D–SDS PAGE, the IEX revealed multiple bands – 45 kDa, 28 kDa, and 18 kDa in **Lane 3** postulated that the fractions still contained other proteins below the expected molecular weight. Further purification via GFC was objectively performed to isolate pure sheep CBPA1 to remove other protein with lower molecular weight. Unfortunately, the GFC purification step using HiLoad™ 16/600 Superdex™ 200 pg was unsuccessful because the fractions still contain lower molecular weight contaminants as seen in **Lane 4**. The low molecular weight contaminants were not adequately separated from the primary band of sheep CBPA1. However, the targeted sheep CBPA1 eluted at the expected molecular weight (47 kDa) of the enzyme in monomeric form. All sheep CBPA1 fractions from crude extract, IEX and GFC were pooled for proteolytic activity determination.

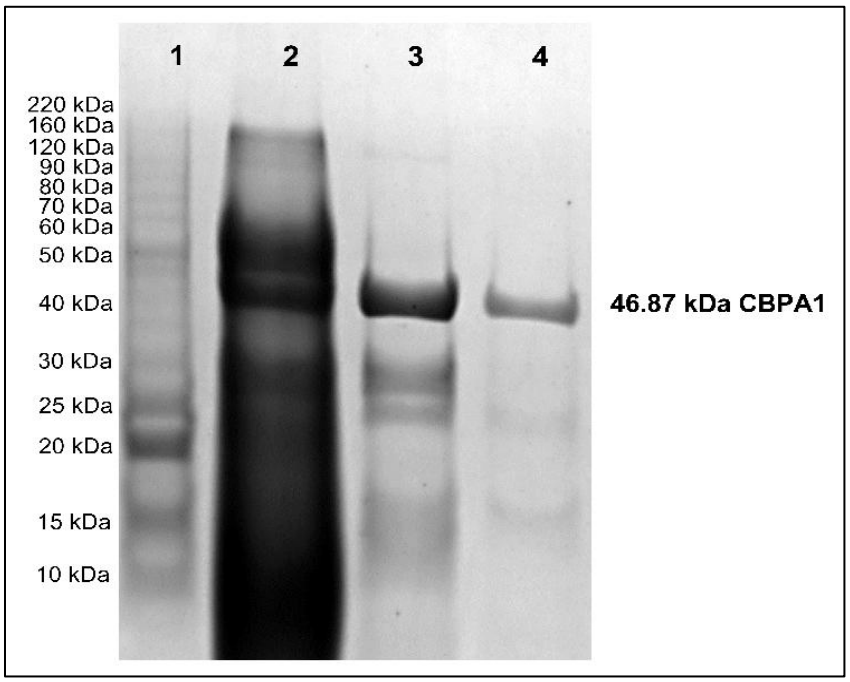


Figure 4.4 1D–SDS PAGE (Bis–Tris 12%) of Pure Sheep CBPA1. Pure Sheep CBPA1 was approximately estimated to be 46 kDa (Lane 4).

Note: Lane 1: Benchmark™ Unstained Protein Ladder; Lane 2: Crude extract; Lane 3: CBPA1 obtained after Hi Trap Q Fast Flow chromatography and Lane 4: CBPA1 obtained after HiLoad™ 16/600 Superdex™ 200 pg chromatography. The gel was stained with Coomassie blue.

Following GFC, three protein bands estimated to be 45 kDa, 25kDa and 18 kDa were observed (Figure 4.4, **Lane 4**). Next, the higher molecular weight band at 47 kDa, expected to be sheep CBPA1, was excised and destained for LC–MS/MS protein identification. Table 4.2 lists the protein identified from the LC–MS/MS analysis. LC–MS/MS revealed that sheep CBPA1 (Accession number—W5P5N4) has protein coverage of 82.53% and recorded a mass of 46.87 kDa and 5.29 calc pI. The predictive peptide sequences related to sheep CBPA1 determined by the LC–MS/MS were selected as potential sheep pancreatic CBPA1 based on the percolator® algorithm with a q–value of less than 1% false discovery rate (FDR). The peptide identification results showed that 75 predictive peptides were obtained (data not shown). In the current study, twenty predictive peptides show similar characteristics to the same master protein of sheep pancreatic CBPA1. The result obtained was confirmed with low FDR with Qvality q–value (>0.01), XCorr Sequest HT (>2.0), and percolator q–value Sequest HT value (>0.01). In general, the reported peptides contained one or no missed cleavage events. The peptide sequence, position in the master protein, charge, and molecular weight are listed in Table 4.3. Most of the predictive peptides have low molecular weight, ranging from 894.41 to 3878.8 Da and a net charge of 2 to 4. Only six of the predictive peptide sequences undergo modifications during the sample–handling process, as shown in Table 4.3, with frequent variable oxidation and deamination modifications, with only two fixed carbamidomethyl modifications. Two cysteine carbamidomethylation (CAM) modified sites were identified (Peptide amino acid 241–254 SVTSSL**C**VGVDANR, proposed CAM on C247; Peptide amino acid 263–277 AGASSNP**C**SETYHGK, proposed CAM on C270). Following this, all CBPA1 fractions were pooled for sheep before proteolytic activity determination.

Table 4.2
Protein Identification from the LC–MS/MS

No	Accession Number	Protein Identified	No of Peptides	Coverage (%)	Molecular Weight (kDa)	Calc PI
1	W5P5N4	Carboxypeptidase A1 OS=Ovis aries OX=9940 GN=LOC101117326 PE=3 SV=1	20	82.53	46.87	5.29
2	W5PTR5	78 kDa glucose–regulated protein OS=Ovis aries OX=9940 GN=HSPA5 PE=3 SV=1	18	32.62	72.51	5.20
3	W5Q687	Keratin 5 OS=Ovis aries OX=9940 GN=KRT5 PE=3 SV=1	13	24.28	62.66	7.81
4	A0A836A6R1	IF rod domain–containing protein OS=Ovis aries OX=9940 GN=JEQ12_002761 PE=3 SV=1	10	25.36	51.86	5.16
5	W5Q160	Keratin 10 OS=Ovis aries OX=9940 GN=KRT10 PE=3 SV=1	8	13.34	57.25	5.50

Table 4.3
Peptide Sequence Prediction of Sheep Pancreatic CBPA1 via LC–MS/MS

No	Annotated Sequence	Confidence	Modifications	Charge	Position in Master Protein	Theo. MH+ [Da]	Qvality q–value	XCorr Sequest HT	Percolator q–Value Sequest HT
1	[R].VPFPSLQAVK.[V]	High	–	2	67–76	1085.64	0	3.29	0
2	[R].SVTSSL**C**VGVDANR.[N]	High	1xCarbamidomethyl [C7]	2	241–254	1464.71	0	4.71	0
3	[R].STDSFNYATYHTLDEIYDF**M**DLLVAEHPQLVSK.[L]	High	1xOxidation [M20]	4	113–145	3878.81	0	5.45	0
4	[R].NWDAGFGK.[A]	High	–	2	255–262	894.41	0	2.68	0
5	[R].ISAADEAEVQTVK.[E]	High	–	2	28–40	1360.69	0	5.57	0
6	[R].I**M**IEDVQSLLDEEQE**QM**FASQSR.[A]	High	1xDeamidated [Q16]; 2xOxidation [M2; M17] 1xDeamidated [Q]; 1xOxidation [M]	2	88–100	2759.24	0	2.41	0
7	[R].GPAQPGSPIDVR.[V]	High	–	2	55–66	1193.62	0	3.76	0
8	[R].EWITQATGVWFAK.[K]	High	–	2	182–194	1536.784	0	5.53	0
9	[K].YSFTFELR.[D]	High	–	2	374–381	1062.52	0	3.20	0
10	[K].YGSIITTIY**Q**ASGGSIDWSY**NQ**GIK.[Y]	High	1xDeamidated [Q/N]	2	349–373	2723.32	0	4.06	0
11	[K].YANSEVEVK.[S]	High	–	2	278–286	1038.51	0	3.72	0
12	[K].VFLEAHGIR.[Y]	High	–	2	77–85	1041.58	0	3.44	0
13	[K].SIVDFVKDHGNFK.[A]	High	–	3	287–299	1505.77	0	3.14	0
14	[K].SAVEALSSLYGTSYK.[Y]	High	–	2	334–348	1575.79	0	5.86	0
15	[K].LQIGSSYEGRPIYVLK.[F]	High	–	2	146–161	1823.01	0	5.16	0
16	[K].FSTGGSNRPAIWIDLGIHSR.[E]	High	–	3	162–181	2184.13	0	5.78	0
17	[K].ELEDLEHLQLDFWR.[G]	High	–	3	41–54	1842.90	0	5.59	0
18	[K].EDFVGHQVLR.[I]	High	–	2	18–27	1199.61	0	3.13	0
19	[K].AGASSNP**C**SETYHGK.[Y]	High	1xCarbamidomethyl [C8]	2	263–277	1565.66	0	4.15	0
20	[K].AFLSIHSYS**Q**LLLYPYGYTT**Q**SVSDK[N]	High	1xDeamidated [Q]	3	300–325	2982.47	0	3.64	0

Note: Description of Sheep Pancreatic CBPA1 peptide sequence prediction. The bold symbol represents the possible site of fixed and variable modifications during the sample handling process. The confidence level for the identified protein was determined by the false discovery rate (FDR) and interpreted as high–confidence hits, which were 99% accurate. The charge is the sum of positive (basic) and negative (acidic) charge residues in neutral pH. Position in Master Protein is the location of the annotated predictive peptide sequence in the protein. Theo. MH+ [Da] is the protonated monoisotopic mass of the peptides in Daltons. Qvality q–value and Percolator q–Value Sequest HT are calculated from the number of target and decoy proteins and the minimum FDR is required for a hit to be considered correct (Qvality q–values and Percolator q–Value Sequest HT > 0.01 are considered high–confidence hits). XCorr Sequest HT indicates the number of fragment ions that are common to two different peptides with the same precursor mass and calculates the cross–correlation (XCorr) for all candidate peptides in search (XCorr value > 2 is considered favorable).

4.3.3 Proteolytic Enzyme Assay

The proteolytic activity was measured for all sheep crude extract, IEX, and GFC samples using the protease activity assay described. The Trypsin TPCK standard curve was constructed to determine the protease activity of sheep CBPA1 at different sequential purification stages, with the R^2 value of 0.99 (Appendix 5). Table 4.4 summarize the sequential purification and proteolytic enzyme activity measured for sheep CBPA1 in crude extract, IEX, and GFC samples. The protein concentration of purified sheep CBPA1, as calculated from the $A_{280,}$ was 0.99 mg/mL (Table 4.4).

Table 4.4
Sequential Purification of Sheep Pancreatic CBPA1

Purification stage	Volume (mL)	A_{280}	Protein content (mg)	Specific proteolytic activity (U/mg)	Total proteolytic activity (U)	Yield (%)	Purification Fold
Crude extract	160.0	47.247	7560.0	16179.05	122313618.00	100.00	1.00
IEX (*Peak D – 30% NaCl*)	22.5	5.088	114.25	111894.06	12814667.22	10.48	6.92
GFC	27.0	0.992	26.73	684.88	18306.84	0.01	0.04

Note: Specific proteolytic activity of porcine Pancreatin (1 mg/mL) = 2030.08 U/mg

The sheep CBPA1 sequential purification demonstrates that IEX was the most effective step in enriching the proteolytic activity. The IEX samples marked increased in the specific proteolytic activity (111894.06 U/mg), correspond to 6.92–fold when compared to the crude extract samples. However, the subsequent GFC purification, resulted in a substantial reduction of purification fold to 0.04–fold with 684.88 U/mg of the specific proteolytic activity, suggesting that there is potential loss in the enzyme activity due to degradation over time during the purification process.

Enzyme activity was also compared using commercially available porcine protease (Porcine Pancreatin) as a positive control. The concentration of the Pancreatin was standardized to 1 mg/mL and yielded 2030.08 U/mg of the specific proteolytic activity. This highlights that the protease of sheep is comparable to that of the porcine origin, particularly for the purified bovine CBPA1 from IEX with 6.92–fold, 111894.06 U/mg of specific proteolytic activity. Therefore, the sheep pancreas can be suggested as a potential alternative for pancreatic protease based on the prominent proteolytic activity.

4.4 Discussion

This is an updated report on the purification strategy of CBPA1 protease from the pancreatic tissues of sheep, following previous studies by Neurath and colleagues in 1970 (Neurath *et al.,* 1970) as well as Kerfelec and colleagues in 1985 (Kerfelec *et al.,* 1985). In particular, this study herein aims to evaluate the activity of CBPA1 in sheep that could fulfil the Halal requirements compared to the commercially available animal protease from porcine, with a special interest in the treatment of pancreatic diseases.

Pancreatic tissues from sheep were processed to obtain the crude extract, which was then subjected to a series of IEX and GFC. From the 1D–SDS PAGE result, the purified sheep CBPA1 was observed as three bands on the 1D–SDS PAGE (45 kDa, 28 kDa, and 18 kDa) (Figure 4.4). This result was consistent with the previous study, where sheep CBPA1 was reported to have molecular weights in the range of 42–48 kDa This result was consistent with the previous study (Kerfelec *et al.,* 1985). The persistence of secondary and tertiary bands on 1D–SDS PAGE after GFC, approximately 28 kDa and 18 kDa indicates that sheep CBPA1 was not isolated as a homogenous band and does not exist as monomeric form. This was consistent with previous study, where there is presence of three subunits of sheep CBPA1 with molecular weights in the range of 42–48 kDa (Kerfelec *et al.,* 1985) whilst CBPA1 of pig pancreas can be present in two different forms: a monomer (45 kDa) and a stable binary complex with pro–proteinase E (45 kDa + 26 kDa) (Vilanova *et al.,* 1985). This finding was similar to bovine CBPA1, which has also been found in more than one active molecular form (Folk & Schirmer, 1963; Reshidan *et al.,* 2024). In addition, most of the purified pancreatic CBPA1 were reported to be monomeric or can be associated with different functional proteins (Kerfelec *et al.,* 1985).

Hence, the presence of multiple bands was observed under the denaturing 1D–SDS PAGE condition suggesting that the purified fraction contained the dissociation of naturally occurring enzymatic complexes, such as the binary form with pro–proteinase E that were not fully isolated and may have been co–eluted during GFC due to overlapping hydrodynamic volumes or strong interactions. Additionally, recent structural insights suggest that CBPA1 possesses intrinsic regions susceptible to misfolding and instability, may contributed to the heterogeneity observed during the isolation process (Sándor *et al.,* 2022). To resolve this heterogeneity and isolate a pure

monomeric band of sheep CBPA1 in future investigations, it is recommended to incorporate high–specificity affinity chromatography, utilizing ligands such as p–aminobenzyl succinic acid. Previously, the CBPA1 was successfully isolated and differentiated from their associated complexes in other species adhering to this method (Bradley *et al.,* 1994). The incorporation of a high–selectivity purification step earlier may help to reduce enzymatic degradation associated with extended processing time required for the GFC step.

To further validate the sheep CBPA1, complimentary implementation of native PAGE in conjunction with 1D–SDS PAGE would provide critical insight on the sheep CBPA1 structural integrity confirmation and oligomeric state for future investigation. As a non–denaturing electrophoresis technique, the native PAGE will maintain the protein natural quaternary structure and non–covalent interaction, distinguishing proteins based on a combination of molecular weight, shape and net charge. It is hypothesised that the active form of sheep CBPA1 would have migrated as a single stable complex under this native PAGE conditions.

To the best of our knowledge, the literature on sheep CBPA1 purification is limited. The most recent finding on CBPA1 extraction and purification was a report on the CBPA1 extraction and purification from ostrich (*Struthio camelus),* whereby CBPA1 was observed as a single band of 34 kDa (Bradley *et al.,* 1994). An earlier study on ruminant species reported the similar molecular weights of bovine and sheep CBPA1 with a mention of a ternary form of proxycarboxypeptidase A containing the inactive, non–activatable, and truncated subunit III (Kerfelec *et al.,* 1985).

Although the GFC demonstrate a successful sheep CBPA1 purification, the subsequent step resulted in a significance decline of the specific proteolytic activity to 684.88 U/mg with a drastic reduction in yield to 0.01%, suggesting potential enzyme instability or loss during this secondary process. Therefore, the IEX stage is suggested as a better purification step, as it produced the highest specific proteolytic activity. The purification enzymatic activity profile of sheep CBPA1 have demonstrated that the IEX was the most efficient and should be satisfactory in enriching the proteolytic activity (Table 4.4). A substantial increase in the specific proteolytic activity reaching 111894.06 U/mg, which is approximately 55–fold higher than the commercial porcine pancreatin positive control (2,030.08 U/mg) was achieved with the IEX.

This study presents a simplified two–step purification of pancreatic CBPA1 from sheep using current readily available technology. Previously, pancreatic sheep CBPA1 was extracted from acetone–dried pancreas powder, followed by ammonium precipitation and DE–tris acryl pH8 chromatography (Kerfelec *et al.,* 1985). The acetone–dried pancreas powder has also been used with DAEA–cellulose and Sephadex G–50 or G–100 (Pharmacia) columns (Lacko & Neurath, 1970), as well as using a p–aminobenzyl succinic acid affinity column followed by a hydroxylapatite column and concentrated with PEG 2000 (Merck) (Bradley *et al.,* 1994). In addition, the purifications of the CBPA1 have also been conducted by desalting defatted acetone–dried powders of pig pancreas extracted with ammonium sulphate precipitation and separated on DEAE– Sepharose CL–6B (Pharmacia) column with linear NaCl gradient and varied pH settings (Vilanova *et al.,* 1985). In contrast to the earlier reports, this current study uses freshly extracted sheep pancreas to purify the enzyme based on its charge and size to obtain the final purified sheep CBPA1 product, which was confirmed by 1D–SDS PAGE, LC–MS/MS, and protease enzyme assay.

4.5 Conclusion

In conclusion, CBPA1 was successfully extracted and characterized from fresh sheep (*Ovis aries*) pancreatic tissues, with its identity confirmed via LC–MS/MS. The purification profile indicates that the IEX stage represents the optimal purification step, yielding the highest specific proteolytic activity of 111,894.06 U/mg, which is approximately 55–fold higher than the porcine pancreatin positive control. Consequently, the sheep CBPA1 purified via IEX is suggested as a highly viable alternative to the porcine enzyme. This warrants further investigation to validate the usefulness of sheep CBPA1 as a potential substitute for porcine–derived products, mainly to cater to Halal pharmaceutical and medical applications.

CHAPTER 5
PURIFICATION AND CHARACTERISATION OF BILE–SALT ACTIVATED LIPASE ENZYME FROM BOVINE (*BOS TAURUS*) PANCREAS

5.1 Introduction

There are three major classes of digestive enzymes, namely, protease, amylase, and lipase (Hou & Shimada, 2009), are produced in the pancreas to facilitate food digestion (Oliveira *et al.,* 2024). These enzymes can also be found in other sources, such as bacteria, fungi, and eukaryotes (Park & Park, 2022). Lipases are the third most utilised enzyme and biocatalysts in medicine, pharmaceutical, food, as well as detergent industries, after proteases and amylases (Vardar-Yel *et al.,* 2024; Yu *et al.,* 2016). This class of enzymes is responsible for catalysing the hydrolysis of triacylglycerols to glycerol and fatty acids essential (Hou & Shimada, 2009) to provide the highest dietary source of calories (Oliveira *et al.,* 2024).

Lipase has become of remarkable interest to many researchers, as most nutritional problems are secondary to the improper digestion of dietary fats (Szkopek *et al.,* 2024). Two major lipase clusters that work synergistically are gastric and pancreatic lipases. The exocrine pancreas synthesises and secretes several lipolytic enzymes, which work with gastric lipase to achieve complete dietary fat digestion and absorption (Li *et al.,* 2007). The gastric lipase contributes approximately 10–30% of lipolytic activities, which participate in the early stage of lipolysis to release fatty acids in the stomach alongside bile salt–dependent lipase and pancreatic colipase–dependent lipases (Oliveira *et al.,* 2024).

Bile salt–activated lipase (BSAL, EC 3.1.1.13) is one of the pancreatic lipases that plays a critical role in the digestion and absorption of dietary fats. It is also known as bile salt–stimulated lipase, carboxyl ester lipase, cholesterol esterase, pancreatic lysophospholipase, and bile salt–dependent lipase (Hui & Howles, 2002; Lindquist *et al.,* 2023; Lombardo, 2001). It is a lipase secreted from the vertebrate exocrine pancreas into the intestine and is essential for lipid digestion (Lombardo *et al.,* 2018). The presence of bile salt is crucial in activating BSAL mechanisms for digestion and absorption as a bio–surfactant in the gastrointestinal tract, particularly to address low

solubility and drug delivery transportation (Macierzanka *et al.,* 2019; Maldonado-Valderrama *et al.,* 2011).

BSAL has a comprehensive specificity and hydrolyses a variety of different substrates (Lindquist *et al.,* 2012, 2023), classified as significant lipids (dietary fat and triacylglycerol) and minor lipids (fat–soluble vitamin esters and cholesterol esters digestion) (Wang & Kloer, 1983; Wang *et al.,* 1999). A sound lipolytic system is needed for BSAL, along with other pancreatic lipolytic enzymes and gastric lipase, to act in concert for complete dietary lipid digestion (Bruneau *et al.,* 2000). Drastic reduction of BSAL leads to the development of many diseases, such as pancreatic cancer, necrotising pancreatitis, and chronic pancreatitis, affecting the gastrointestinal tract in the digestive system (Lombardo, 2001).

BSAL is mainly isolated from pancreatic tissues and has also been reported to be extracted from the liver and mammary gland (Gjellesvik *et al.,* 1992). BSAL was also reported to have considerable lipase activity in human milk, significantly contributing to milk lipid utilisation in newborns (Christie *et al.,* 1991). High BSAL content in breast milk significantly increases the fat digestion capacity of newborns during the first few months after birth due to immature pancreatic development and limited pancreatic lipase secretion (Koh *et al.,* 2020). The purification of pancreatic BSAL has been attempted from several sources, including humans (Abouakil *et al.,* 1988; Manson & Weaver, 1997; Wang & Kloer, 1983), porcine (Labow *et al.,* 1983; Momsen & Brockman, 1977; Rudd *et al.,* 1987), bovine (Chen *et al.,* 1998; Tanaka *et al.,* 1999), rats (Abouakil *et al.,* 1993; Mendes *et al.,* 2012), and fish (Gjellesvik *et al.,* 1992).

The isolation of BSAL from the pancreatic tissue is more complicated due to proteolytic digestion process (Wang & Hartsuck, 1993). However, pancreatic lipase from animal sources has been reported to have more excellent stability with high activity (Mendes *et al.,* 2012). In addition, pancreatic enzymes originating directly from the pancreas of mammals are naturally suitable for digestion and have been studied for their application in the medical and pharmaceutical fields, as the animal–origin enzyme is known to possess high therapeutic potential (Headon & Walsh, 1994). Although BSAL can be isolated from milk, pancreatic BSAL is also crucial as they have distinct physical and biochemical properties.

Both milk BSAL and pancreatic BSAL are vital digestive enzymes and carry different responsibilities for fat breakdown and the digestion of dietary fats within the

lumen of the intestine, respectively. As for the clinical implications, milk BSAL and pancreatic BSAL objectively depend on the specific requirement and application. Obtaining the pancreatic BSAL can be significant for developing pancreatic disorder treatment. On the other hand, milk BSAL may be used in dietary formulas and nutritional supplements to enhance fat digestion (Koh *et al.,* 2020). With biotechnological advancement, the extraction and purification of pancreatic enzymes from Halal sources can be achieved with lower production costs, thus fulfilling the demand for Halal products that is increasing globally.

Although the study on BSAL purification has previously received considerable attention, there has been no recent update on the methods related to the extraction and purification of BSAL, as well as the peptide sequence analysis by LC–MS/MS from the bovine pancreas. The research interest in BSAL has switched from purification to its application to induce smooth muscle cell proliferation (Augé *et al.,* 2003), as well as *in vitro* angiogenic effects suggesting potential implications in vascular pathophysiology (Rebaï *et al.,* 2005).

The Bovidae family, including domestic cattle, is widely distributed in Malaysia for the livestock agriculture sector, as beef is Malaysia's most popular source of red meat (Ariff *et al.,* 2015). Nevertheless, higher meat production contributes to large amounts of waste as some animal organs are not fully utilised and are finally disposed of. This includes the pancreas, a non–edible organ produced in significant quantities by the meat industry, which contributes towards waste disposal and potential pollution (Li *et al.,* 2012). Thus, the bovine pancreas, a by–product of the meat industry, can be utilised as an alternative low–cost source of Halal digestive enzymes, particularly for lipase applications. In addition, the premier quality and Halal–certified products, including medicine and health supplements, are gaining much attention from Muslim and non–Muslim consumers (Aziz *et al.,* 2014). Furthermore, Halal pharmaceutical products are considered healthier, more hygienic (Sudarsono & Nugrowati, 2020), and generally better in quality, with a projected market value of US$3.2 trillion by 2024 (American Halal Foundation, 2024). Combining Islamic principles with rigorous manufacturing standards and ethical considerations contributes to healthier and hygienic Halal pharmaceutical production. The ethical Halal guidelines not only prohibit harmful substances that can lead to adverse health effects but also emphasise quality sources of ingredients and stringent hygiene production protocol to adhere to the Halal manufacturing standards (Herdiana *et al.,* 2024).

In this study, the BSAL was successfully isolated and purified from fresh bovine pancreatic tissue, subsequently confirmed by ten predictive peptide sequences with the same protein accession number of P30122, representing the bovine BSAL characteristics with 30.9% of protein coverage identified through LC–MS/MS, and followed by determination of BSAL lipolytic activity. In the pharmaceutical industry, lipases have been utilised as modulators (activators and inhibitors) to treat lifestyle diseases such as obesity (Szkopek *et al.,* 2024) and show great promise in therapies (Chandra *et al.,* 2020). Microbial lipase from bacteria, fungi, and yeast is the current primary source and is pivotal in various industries, including pharmaceuticals (Vardar-Yel *et al.,* 2024; Vivek *et al.,* 2022). Although many microbial lipases are currently available, they are still inadequate for fulfilling the requirements of most industries, specifically in medicine and pharmaceuticals, due to the possible variation in behaviour and functionality compared to animal lipase. Therefore, successful purification of BSAL from bovine pancreas can be suggested as an alternative substitute for porcine lipase to cater to Halal medical and pharmaceutical demands.

5.2 Materials and Methods

The bovine Bile–Salt Activated Lipase (BSAL) purification scheme was summarised as in Figure 5.1.

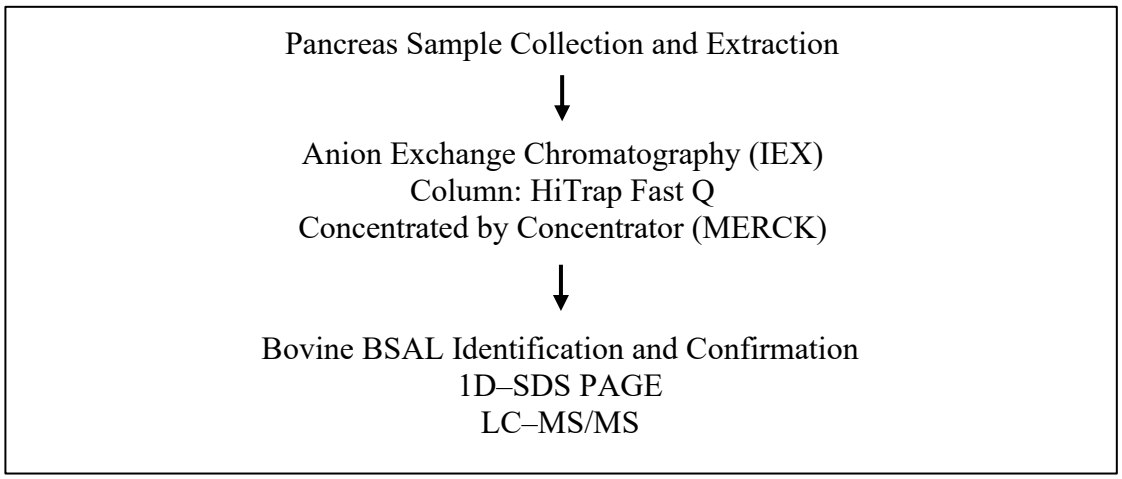


Figure 5.1 Bovine Bile–Salt Activated Lipase (BSAL) Purification Scheme.

5.2.1 Extraction and Purification of Bovine Bile Salt Activated Lipase

Bovine pancreas was collected freshly from slaughtered animals of Abattoir Complex, Department of Veterinary Services (DVS), Shah Alam, Malaysia (Coordinates: 3.05, 101.51), and stored on ice. There was no available information on the supplier or animal records from the abattoir. Nevertheless, it was determined that all the animals were male with an estimated age of more than 2 years.

The pancreases were washed with tap water upon receiving. Then, the pancreas was dissected free from adherent fat and connective tissues with a scalpel blade (Elamin *et al.,* 2014). The pancreas was cut into smaller pieces on ice, and the tissue slices were washed with a 50 mM Tris pH 7.4 buffer containing 0.1 M sodium chloride (NaCl) to remove blood (Al-Ajlan & Bailey, 1999). The bovine pancreas collection and pancreatic crude extraction were done on the same day. Approximately 120 g – 160 g of pancreas samples were homogenized using laboratory blender (Tefal – France), 1 min at low speed and 1 min at high speed (Bradley *et al.,* 1994).

Then, bovine pancreatic tissues were suspended in 20 mL of extraction buffer (50 mM Tris pH 7.4, 2 mM Ethylenediaminetetraacetic acid (EDTA) pH 8, 10 mM HEPES pH 7.4, 1% Triton X–100, and 150 mM NaCl) and vortexed for 10 mins before

centrifugation at 4000 rpm for 2 mins. The supernatants were collected and added with 70% (v/v) ethanol, bringing a total of 25 mL. The mixture was vortexed for 10 secs, and 2 mL of 5 µg/mL of aprotinin of aprotinin as a protease inhibitor was added to the samples. Aprotinin is a serine protease inhibitor and essential in inhibiting endogenous serine proteolytic activity. The suppression of the non–targeted proteases preserved the enzymatic activities of the targeted proteins. This helps to mitigate the risk of proteolytic degradation of the targeted enzymes, whereby the recovery of intact soluble proteases was maximised in the collected supernatant during the extraction procedure. The samples were centrifuged at 14,000 rpm for 20 mins before collecting the supernatant to recover soluble proteins. The protein concentration was measured and stored at –20^{o}C until further use.

5.2.2 Purification of Bovine Bile–Salt Activated Lipase

The purification is a critical step in this study to isolate the targeted enzymes. Following the preparation of the pancreatic tissue extraction, the bovine crude pancreatic extract was subjected to a one–step anion exchange chromatography (IEX) purification to isolate the bovine BSAL based on surface net charge. No further purification step was done after the IEX since the bovine BSAL was successfully purified at this stage.

The purification step was performed at room temperature on the second day (within 24 hours) following the crude extraction. Bovine pancreatic BSAL was purified by IEX on a pre–packed HiTrap Q Fast Flow column containing a Sepharose–based resin (strong anion exchanger) (bed height 1.6 cm, column diameter 2.5 cm, column volume 5 mL) using an AKTA Avant^{TM} chromatography system (Cytiva – USA). The column equilibration process began by replacing the column's ethanol storage with distilled water to remove the preservative. Subsequently, the column was washed and equilibrated with the start buffer. The 20 mM Tris pH 8 was used as the start buffer, and 20 mM Tris 1 M NaCl pH 8 was used as the elution buffer. The sample was filtered using 0.45 µm and 0.25 µm cellulose acetate pore membrane filters (Merck – Germany). A total of 160 mL filtered sample was applied to the column in buffer A, and the column was washed until the absorbance monitored at 280 nm returned to baseline. The pancreatic enzymes were eluted using an elution buffer at a 2.4 mL/min flow rate, and 1.5 mL fractions were collected.

The IEX was chosen to separate the proteins depending on their ability to interact with a specific positive charge resin where negative charge proteins will bound to the resin. Generally, the proteins were eluted by increasing the ionic strength (salt concentration) of the elution buffer. In this study, the salt ions compete with the bound proteins for the positive charges on the surface of resin, which induced the elution of the bound proteins. As a result, the protein with lower net charge will elute first, following with higher net charge of protein that retained longer as it requires higher ionic strength of elution buffer to be eluted at the selected pH. Since bovine BSAL possesses an isoelectric point equal to 5.32, the IEX is performed using buffers with higher pH (pH 8).

Initially, a preliminary linear gradient IEX was conducted to determine the optimal ionic strength required to identify the best NaCl concentration for isolating each targeted enzyme. Subsequently, a NaCl step gradient was applied to purify and isolate the targeted enzymes within a single cycle of the IEX procedure. This allows distinct peak separation and efficient removal of contaminants at lower ionic strengths before eluting the targeted enzymes at their specific targeted salt concentrations. The IEX purification was repeated at least three times, and the chromatogram profiling was constructed based on the mean absorbance values.

The elution buffer composition was set up as a step gradient at 5%, 10%, 20%, 30%, 40%, 50%, and 100% sodium chloride (NaCl) to elute the bovine BSAL. Each fraction representing different peaks was run on 1–dimensional sodium dodecyl sulphate–polyacrylamide gel electrophoresis (1D–SDS PAGE) for molecular weight determination. The bovine BSAL was eluted at 10% of salt concentration. Fractions containing protease activity based on the molecular weight were pooled and concentrated using a 30,000 MW and 50,000 MW Amicon® Ultra Centrifugal Filter (MERCK – Germany).

5.2.3 Protein and Peptide Identification of Bovine Bile–Salt Activated Lipase

5.2.3.1 Determination of Protein Concentration

The total protein concentration of total crude pancreatic extract and purified fraction samples from IEX were measured. Absorbance was measured at 280 nm (A_{280}) using a NanoDrop® ND–1000 UV–Vis Spectrophotometer (Thermo Fisher Scientific

– US). The obtained concentration values (mg/mL) were subsequently utilised to calculate the total protein content (mg) and were essential for determining the proteolytic enzymatic activity (U/mg) of the samples.

5.2.3.2 One–Dimensional Sodium Dodecyl Sulfate Polyacrylamide Gel Electrophoresis (1D–SDS PAGE)

The molecular mass of purified bovine pancreatic BSAL was estimated by 1D–SDS PAGE using NuPAGE 4–12% mini protein gel of Bis–Tris electrophoresis system in X Cell SureLock Mini–Cell (Invitrogen – US) stained with Coomassie Brilliant Blue stain (Invitrogen – US).

The sample was prepared as described in Table 5.1. The protein mixtures were prepared by adding protein sample (x µl), 4X NuPAGE LDS Sample Buffer (2.5 µl), 10X NuPAGE Reducing agent (1 µl), and Ultrapure water (y µl) in a 1.5 mL Eppendorf tube. The protein volume needed was calculated using the dilution formula (M1V1 = M2V2) based on the initial concentration of the protein. Then, Ultrapure water was added, bringing a 10 µl volume for sample preparation. The protein sample was heated at 70^{o}C for 10 mins before loading into the wells. The 1X NuPAGE MES SDS Running Buffer was prepared by adding 50 mL of 20X MES SDS Running Buffer to 950 mL of distilled water. The gel electrophoresis system was set up at 200 V (constant voltage) and 125 mA (current). The electrophoretic separation was conducted for approximately 35 to 45 minutes to ensure the complete resolution of the protein bands.

Table 5.1
Sample Preparation for SDS–PAGE

Chemicals	**Volume (µl)**
Protein Concentration	20 mg/mL
Protein Sample	*x*
NuPAGE LDS Sample Buffer (4X)	2.5
NuPAGE Reducing agent (10X)	1.0
Ultrapure water	*y*
Final Volume	**10.0**

The gel was transferred into a clean container and added with 50 mL of distilled water. Then, the gel was microwaved at high power for 1 min and shaken for 1 min. The steps were repeated twice. Then, the gel was added with Safely Blue Safe stain (Invitrogen – US) liquid. The gel was microwaved again at high for 45 secs and shaken for 5 mins. The gel was washed with distilled water and shaken for 10 mins before viewing with ChemiDoc^{TM} Imaging System (BioRad – US).

5.2.3.3 Liquid Chromatography–Mass Spectrometry (LC–MS/MS)

Protein bands were further identified using liquid chromatography–mass spectrometry (LC–MS/MS). Before the LC–MS/MS procedure, trypsin gel digestion was carried out. Then, a total of 5 µL sample was injected into Dionex Ultimate 3000 RSLCnano Orbitrap Fusion (Thermo Fisher Scientific – US) with EASY–Spray Acclaim PepMapTM C18 100 A^0 (2 µm particle size, 50 µm id x 15 cm) separation column. The sample was eluted with LC–MS grade water, 0.1% formic acid (A), and ACN, 0.1% formic acid (B), at a 250 nL/min flow rate. The elution gradient was 5%–40% B for 91 min, 2 min to 85% B, 3 min at 85% B, 1 min at 5% B, and 4 min at 5% B. The full scan spectra were collected by orbitrap MS (OTMS) scan mass ranging from 310 – 1800 m/z with 50 ms maximum injection. The spectra were analysed by ion trap MS (ITMS) with 250 ms maximum injection. The LC–MS/MS data was analysed using Thermo Scientific^{TM} Proteome Discoverer^{TM} Software Version 2.1. The results were matched with the database downloaded from UniProt. The variable modifications were oxidation and deamination with fixed modification of carbamidomethyl. All peptides were validated using the percolator® algorithm, based on a q–value of less than 1% false discovery rate (FDR). The LC–MS/MS analysis was performed at the Proteomic Laboratory, Malaysian Genome and Vaccine Institute, Bangi, Malaysia.

5.2.4 Lipolytic Enzyme Assay

The lipolytic activity of crude extracts and purified fractions from IEX were determined using the modified method from previous studies (Vardar Yel, 2021; Vo *et al.,* 2022) alongside the commercial porcine pancreatic lipase (Sigma Aldrich – Germany) as a positive control. Lipase activity was evaluated through the conversion of 4–nitrophenyl Palmitate (pNPP) into p–nitrophenol (pNP) product formation, which resulted in enzymatic reaction (Vo *et al.,* 2022).

The pNP calibration standard curve was construct to determine the enzyme concentration tested. The pNPP was used as substrate. The pNP standard curve was established by preparing 50 mM stock solution of pNPP in 1 mL acetonitrile (ACN). Subsequently, a series of 8 serial dilutions were prepared in 25 mM sodium phosphate ($NaPO_4$) pH 7 from the working standard, 5–fold dilutions were employed to ensure the standard curve spanned the full range of detectable lipase activity. The final volume for each dilution was adjusted to a final volume of 600 µL. The pNP standard curve of linear scale of absorbance at 405 nm against concentration (mM) was constructed as recommended by the previous study.

The standard assay contained 10 µL of lipase sample, 150 µL of substrates, and 40 µL of 25 mM $NaPO_4$ buffer pH 7. The 25 mM $NaPO_4$ buffer pH 7 and ACN mixture was used as a blank. The lipolytic assay was performed in a 96–well microplate with a 200 µL reaction volume, incubated at 25°C. Finally, the absorbances at 405 nm were measured periodically at 1, 5, 10, 15, 30, 45, 60, 90 and 120 mins using microplate reader. The experiments were conducted in triplicates.

The enzyme concentration of the crude extract and purified sample were quantified by extrapolating the absorbance values of the samples against a pNP standard curve. The lipolytic activity was calculated based on the formula given.

$$Specific\ lipolytic\ activity\ \left(\frac{U}{mg}\right) = \frac{Total\ lipolytic\ activity\ (U)}{Total\ Protein\ content\ (mg)} \qquad 5.1$$

One unit of lipase is defined as the amount of enzyme that will generate 1.0 µmole of pNP from the pNPP reaction per minute at 25°C as measured at 405 nm using a SpectraMax iD5 Multi–mode Microplate reader (Molecular Devices – USA).

5.3 Results

5.3.1 Extraction and Purification of Bovine Bile–Salt Activated Lipase

Bovine pancreatic BSAL was successfully purified from the fresh pancreatic tissue by pancreatic tissue delipidation, protein extraction, and IEX. Total of 200 mL of filtered bovine crude extract was loaded onto the pre–packed HiTrap Q Fast Flow column. Figure 5.2 illustrates the elution pattern of IEX on the pre–packed HiTrap Q Fast Flow column. The IEX elution was performed with a step NaCl gradient (5 – 100%), whereby the enzymes were separated based on the ionic strength of the elution buffer. The elution profile shows eight distinct peaks after the IEX step. As shown in Figure 5.2, the bovine BSAL was present in fractions eluted at 10% NaCl concentration and labelled as **peak B**. These fractions were collected between the elution volumes of **175.0 mL** and **200.5 mL**. In total, 17 fractions (25.5 mL) were obtained from the IEX step. The protein concentration is 6.83 mg/mL, corresponding to 174.16 mg of total protein.

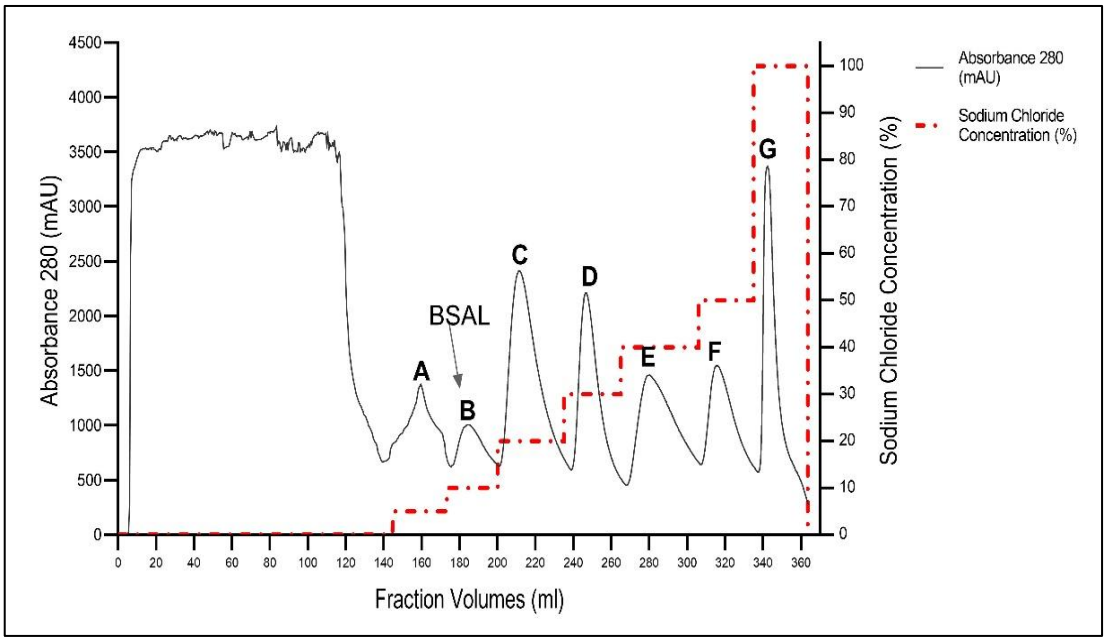


Figure 5.2 Anion–exchange Chromatography of Aqueous Crude Bovine Pancreatic Extract. The Purified Bovine BSAL was eluted at Peak B (10% NaCl concentration).

Note: The thin line shows the absorbance at a wavelength of 280nm during chromatography. The arrows marked peaks that showed the presence of bovine BSAL on the 1D–SDS PAGE with lipolytic activity. Tubes were pooled at 10% NaCl concentration, indicating the presence of active bovine BSAL. Column: Hi Trap Q Fast Flow column (pre–packed); flow rate: 2.4mL/min; mobile phase: 20mM Tris pH8, 20mM Tris NaCl pH8.

5.3.2 Protein and Peptide Identification of Bovine Bile–Salt Activated Lipase

1D–SDS PAGE analysis of the bovine BSAL from crude extract and post–IEX are shown in Figure 5.3. From the 1D–SDS PAGE, the crude extract displayed a broad and intense smear with multiple protein bands, reflecting the complex pancreatic protein composition prior to IEX. In contrast, after the single IEX step revealed a single, discrete band with an estimation of molecular weight at 60 kDa (**Lane 3**).

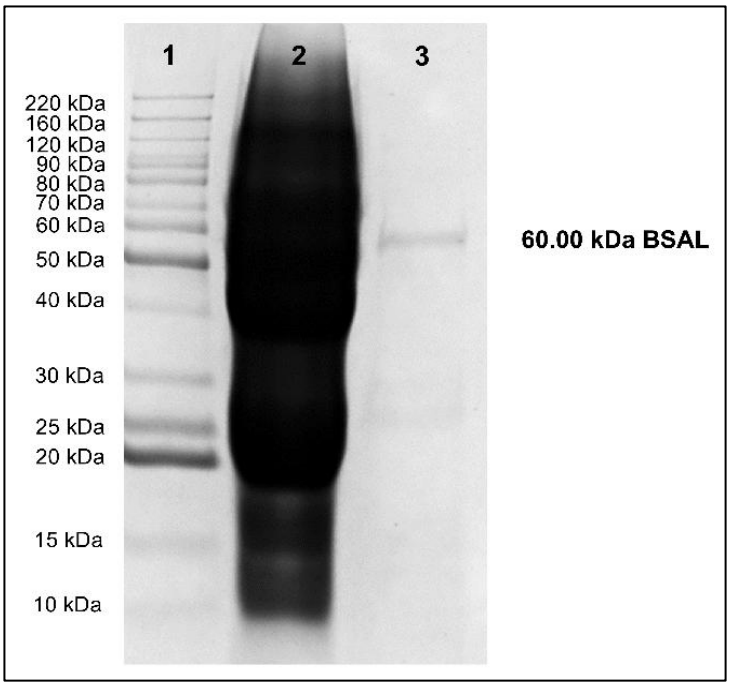


Figure 5.3 1D–SDS PAGE (Bis–Tris 12%) of Pure Bovine BSAL. Pure Bovine BSAL was approximately estimated to be 60 kDa (Lane 3).

Note: Lane 1: Benchmark^{TM} Unstained Protein Ladder; Lane 2: Crude extract; Lane 3: Purified BSAL obtained after Hi Trap Q Fast Flow chromatography.

Following IEX, the band expected to be bovine BSAL, was excised and destained for LC–MS/MS protein identification. Table 5.2 lists the protein identified from the LC–MS/MS analysis. The bovine pancreatic BSAL (Accession number: P30122) was identified as a hit by LC–MS/MS to have 30.9% protein coverage with a molecular mass of 65.12 kDa and calc pI 5.57. The predictive peptide sequences related to bovine BSAL characteristics were determined and selected as potential bovine pancreatic BSAL based on the percolator® algorithm with a q–value of less than 1% false discovery rate (FDR). The peptide identification results showed that 199 predictive peptides were obtained (data not shown). In the current study, ten predictive peptides

show similar characteristics to the same master protein of bovine pancreatic BSAL. The result obtained was confirmed with low FDR with Qvality q–value (>0.01), XCorr Sequest HT (>2.0), and percolator q–value Sequest HT value (>0.01). In general, the reported peptides contained one or no missed cleavage events. The peptide sequence, position in the master protein, charge, and molecular weight are listed in Table 5.3. Most of the predictive peptides have low molecular weight ranging from 1104.60 – 3378.94 Da and net charge of 2 to 3. Five of ten predictive peptide sequences undergo modifications during the sample handling process, as shown in Table 5.3, with frequent variable deamination and oxidation modifications, with less frequent fixed carbamidomethyl modifications. Only two cysteine carbamidomethylation (CAM) modified sites were identified (Peptide amino acid 82–109 **C**LQATLTQDSTYGNED**C**LYLNIWVPQGR, proposed CAM on C82 and C97; Peptide amino acid 234–256 AISQSGVGL**C**PWAIQQDPLFWAK, proposed CAM on C243).

Table 5.2
Protein Identification from the LC–MS/MS

No	Accession Number	Protein Identified	No of Peptides	Coverage (%)	Molecular Weight (kDa)	Calc PI
1	P00727	Cytosol aminopeptidase OS=Bos taurus OX=9913 GN=LAP3 PE=1 SV=3	25	68.02	56.25	6.48
2	P21856	Rab GDP dissociation inhibitor alpha OS=Bos taurus OX=9913 GN=GDI1 PE=1 SV=1	16	60.85	50.53	5.14
3	Q2HJH1	Aspartyl aminopeptidase OS=Bos taurus OX=9913 GN=DNPEP PE=1 SV=1	18	52.02	51.80	6.92
4	P30122	Bile salt–activated lipase (Fragment) OS=Bos taurus OX=9913 GN=CEL PE=1 SV=2	10	30.99	65.12	5.57
5	A3KMV5	Ubiquitin–like modifier–activating enzyme 1 OS=Bos taurus OX=9913 GN=UBA1 PE=2 SV=1	15	24.67	117.76	5.77

Table 5.3
Peptide Sequence Prediction of Bovine Pancreatic BSAL via LC–MS/MS.

No	Annotated Sequence	Confidence	Modifications	Charge	Position in Master Protein	Theo. MH+ [Da]	Qvality q–value	XCorr Sequest HT	Percolator q–Value Sequest HT
1	[R].TGDP**N**TGHSTVPA**N**WDPYTLEDD**N**YLEI**N**K.[Q]	High	1x Deaminated [N] 2x Deaminated [N14; N24]	2	492–521	3378.49	0	6.54	0
2	[R].VGPLGFLSTGDS**N**LPG**N**YGLWD**Q**H**M**AIAWVK.[R]	High	1xOxidation [M25] 1xDeamidated [N/Q] 2xDeamidated [N17; Q/N]	3	163–193	3361.62	0	6.64	0
3	[R].AIS**Q**SGVGL**C**PWAI**QQ**DPLFWAK.[R]	High	1xDeamidated [Q] 1xCarbamidomethyl [C10]	3	234–256	2572.30	0	5.76	0
4	[R].**C**L**Q**ATLT**Q**DSTYG**N**ED**C**LYL**N**IWVPQGR.[K]	High	1xDeamidated [Q/N] 2xCarbamidomethyl [C1; C17]	3	82–109	3315.54	0	3.56	0
5	[K].T**M**VDLETDILFLIPTK.[I]	High	1xOxidation [M2]	2	401–416	1864.99	0	4.25	0
6	[R].GNVIVVTFNYR.[V]	High	–	2	152–162	1281.70	0	3.75	0
7	[K].LSLFGDSIDIFK.[G]	High	–	2	38–49	1354.73	0	2.64	0
8	[K].LPLGSTEYPK.[L]	High	–	2	290–299	1104.60	0	2.73	0
9	[K].SANTYTYLFSQPSR.[M]	High	–	2	428–441	1634.78	0	4.62	0
10	[K].QDVTEEDFYK.[L]	High	–	2	355–364	1273.56	0	2.64	0

Note: Description of Bovine Pancreatic BSAL peptide sequence prediction. The bold symbol represents the possible site of fixed and variable modifications. The confidence level for the identified protein was determined by the false discovery rate (FDR) and interpreted as high–confidence hits, which were 99% accurate. The charge is the sum of positive (basic) and negative (acidic) charge residues in neutral pH. Position in Master Protein is the location of the annotated predictive peptide sequence in the protein. Theo. MH+ [Da] is the protonated monoisotopic mass of the peptides in Daltons. Qvality q–value and Percolator q–Value Sequest HT are calculated from the number of target and decoy proteins and the minimum FDR is required for a hit to be considered correct (Qvality q–values and Percolator q–Value Sequest HT > 0.01 are considered high–confidence hits). XCorr Sequest HT indicates the number of fragment ions that are common to two different peptides with the same precursor mass and calculates the cross–correlation (XCorr) for all candidate peptides in search (XCorr value > 2 is considered favourable).

5.3.3 Lipolytic Enzyme Assay

The lipolytic activity was measured for all bovine crude extract and IEX samples using lipase activity assay described. The pNP standard curve was constructed to determine the lipase activity of bovine BSAL, with the R^2 value of 0.99 (Appendix 5). Table 5.4 summarizes the purification and lipolytic enzyme activity measured for bovine BSAL in crude extract, and IEX samples. The protein concentration of purified bovine BSAL, as calculated from the $A_{280,}$ was 6.83 mg/mL.

Table 5.4
Purification of Bovine Pancreatic BSAL

Purification stage	Volume (mL)	A_{280}	Protein content (mg)	*Specific lipolytic activity (U/mg)	Total lipolytic activity (U)	Yield (%)	Purification Fold
Crude extract	200.0	57.30	11460.00	0.207 (0.1245)	2372.22	100.00	1.00
IEX (*Peak B – 10% NaCl*)	25.5	6.83	174.16	0.222 (0.1772)	38.66	1.63	1.07

Note: *Mean (SD). Specific lipolytic activity of porcine pancreatic lipase (1 mg/mL) = 0.223 (0.1913) U/mg.
Extinction Coefficient = ~106230 $M^{-1}cm^{-1}$.

The one–step IEX purification of bovine BSAL resulted in a modest enrichment of lipolytic activity. This indicated that the enzymes responsible for lipolytic activity was highly presented in the crude extract sample. The crude extract exhibited a specific lipolytic activity of 0.207 U/mg, which increased slightly to 0.222 U/mg following IEX, corresponding to a purification fold of 1.07. This postulated that there was very little loss of lipase during the delipidation process.

Lipase activity was also compared using a commercially available porcine pancreatic lipase as a positive control. The concentration of the porcine pancreatic lipase was standardised to 1 mg/mL and yielded 0.0223 U/mg of the specific lipolytic activity. Importantly, this suggests that the one–step IEX purification of bovine BSAL is comparable to that of the porcine origin, indicating functional equivalence between the bovine and porcine enzymes under the assay conditions employed. Hence, the pancreatic bovine BSAL has a strong potential as a Halal enzyme replacement, specifically for pancreatic lipase.

5.4 Discussion

This study employed a one–step purification of IEX, 1D–SDS PAGE, LC–MS/MS, and lipase activity assay to characterise bovine pancreatic BSAL. Previous work has reported the success of bovine pancreatic BSAL extraction and purification together with enzyme assay activity, N–terminal sequencing, and glycoprotein confirmation (Tanaka *et al.,* 1999). The work presented herein successfully extracted and purified the bovine pancreatic BSAL and confirmed protein identification via LC–MS/MS, with the enzyme assay activity compared against the established porcine lipase.

Firstly, the bovine pancreatic crude extract was subjected to IEX, and a single peak was eluted at 10% NaCl concentration (**peak B**), which has been confirm to contain active BSAL lipolytic activities. Therefore, the use of a second column was unnecessary. The elution profiles of the BSAL enzyme are shown in Figure 5.2. A summary of the BSAL purification results is presented in Table 5.4. Purified fractions obtained from the one–step purification yielded a modest increase in the specific lipolytic activity than the crude extract. Previously, pancreatic lipase was reported to have more significant similarity in molecular weight, similar amino–acid composition, and common antigenic determinants among mammalian lipases such as human, porcine, bovine, and ovine (Caro *et al.,* 1981). On top of that, the specific lipase activity of bovine BSAL is comparable with that of porcine pancreatic lipase, which has been discovered in this study, despite some arguments that lipases will have distinct lipolytic activity and specificity between different biological sources (Shahani *et al.,* 1976). This discovery proves that purified bovine BSAL can be suggested as an alternative to porcine BSAL, considering that its specific lipolytic activity is similar to commercial porcine pancreatic lipase.

Bovine pancreatic BSAL is a glycoprotein with 597 amino acids and 65.12 kDa in molecular weight, as reported in the protein database system (PDB). In this study, the molecular weight of purified BSAL was determined by gel electrophoresis and confirmed with the LC–MS/MS. As shown in Figure 5.3, the purified product revealed a single band with approximately 60.0 kDa on the 1D–SDS PAGE, and 65.12 kDa was confirmed with the LC–MS/MS of the molecular weight. This corresponds to the previous finding that the molecular weight of purified bovine pancreatic BSAL ranged from 61.2 kDa to 65.5 kDa (Chen *et al.,* 1998). In another study, bovine pancreatic

BSAL was reported to have a molecular weight of 63.0 kDa, as estimated by the 1D–SDS PAGE (Iijima *et al.,* 1998). This finding was also consistent with other research, whereby the 1D–SDS PAGE of the purified BSAL from defatted *Pyloric caeca* pancreatic tissue was seen as a homogenous band at 60.0 kDa (Gjellesvik *et al.,* 1992). In contrast, the molecular weight of purified porcine pancreatic BSAL was reported to be slightly larger in the range of 70 to 85 kDa (Momsen & Bockman, 1977; Rudd *et al.,* 1987). Meanwhile, the molecular weight of purified rat pancreatic BSAL was reported to be 70 kDa (Calame *et al.,* 1974). Several mammalian BSALs were reported to have similar specificities and kinetic properties. However, the inconsistency of the physical properties and heterogeneity, including pI and molecular weight, have been controversial findings for BSAL from different animal sources (Rudd *et al.,* 1987). It is speculated that although they may have similar protein cores, BSALs from different sources are subjected to varying degrees of modifications in various hosts, leading to molecular weight variations (Abouakil *et al.,* 1988). Generally, glycans may contribute up to 30% of the molecular weight of glycoproteins (Puranik *et al.,* 2022). Previously, the electrophoretic characterisation of the native bovine BSAL revealed the presence of N–linked sugars, which escalated the number of isoelectric forms and average pI, as well as the changes in the mass–to–charge ratio (Chen *et al.,* 1998). Therefore, the expected size of the protein of interest is influenced by post–translational glycosylation modification. Alternatively, the variations of the C–terminal region of BSAL have also been reported to contribute towards differences in the molecular weight (Gjellesvik *et al.,* 1992).

This work aims to identify the bovine pancreatic BSAL that could benefit pharmaceutical and medical applications, mainly to cater for Halal requirements. The LC–MS/MS proteomic analysis showed a positive protein identification, resulting in ten predictive peptide sequences showing 30.9% bovine pancreatic BSAL protein coverage to the same protein with the accession number P30122. It is difficult to compare the extent of proteome coverage in this study with previous studies that have focused on crystallisation (Chen *et al.,* 1998) and N–terminal amino acid sequencing (Tanaka *et al.,* 1999) of bovine pancreatic BSAL. Mass spectrometry helps detect the peptide as the amino acid sequence is unique to the candidate protein and provides better selectivity (Chiu *et al.,* 2017; Rauh, 2012).

The existing literature on bovine BSAL purification is limited and relatively dated. The latest report on BSAL extraction and purification was two decades ago, reporting on the affinity binding sites of pancreatic BSAL in pancreatic and intestinal tissue of rats (Bruneau *et al.,* 2000). Although there have been scientific reports on successful BSAL purification from bovine, this study presents a single–step purification of bovine pancreatic BSAL. Previously, bovine BSAL was isolated in a pure form by lyophilisation of fresh bovine pancreas, sucrose solution enzyme extraction, ammonium sulphate, and acetone fractional precipitation, followed by GFC on Sephadex G–100 (Shahani *et al.,* 1976). In another study by Tanaka *et al*. (1999), the bovine BSAL was purified from a defatted pancreas with 50 mM sodium phosphate, pH 7.5, containing 0.5 mM PMSF and 2 mM benzamidine as an extraction buffer. Rudd *et al*. (1987), used different extraction buffers made up of 0.1 M sodium acetate buffer pH 4.8 containing 0.9% NaCl, 0.2% Triton X–100, 3 mM sodium taurocholate, 2 mM benzamide hydrochloride, 0.2 mM phenylmethylsulfonyl fluoride, 2mM hydrocinnamic acid, and 0.5 mM Nα–benzoyl–D, L–arginine was added with proteinase inhibitors were used during the BSAL extraction from frozen porcine pancreas. In the same study, the ammonium precipitation was done before running on Sephacryl S–200, followed by TSK 3000 SW columns to purify the porcine pancreatic BSAL (Rudd *et al.,* 1987). The use of frozen pancreas was also observed in a study by Momsen & Brockman (1977), followed by Sephadex G–150 GFC, which is used to obtain purified porcine BSAL. Besides using fresh frozen pancreas as starting material, the pancreatic juice has been previously collected from dogs using a cannula, followed by ammonium precipitation, and applied to a DEAE–cellulose column and concentrated utilising a PM–10 membrane filter (Lee, 1978). However, the cannulation process from the pancreatic duct for the pancreatic juices collection raises animal concerns, especially when using a non-invasive alternative (Steiner & Williams, 2002).

A quick method using affinity chromatography of cholate–derivatized Sepharose successfully purified BSAL from bovine and porcine commercial crude and human milk whey has also been reported (Moore *et al.,* 1996). Despite the various approaches, the findings are surprisingly consistent, with the molecular weight obtained for bovine pancreatic BSAL being approximately 60 kDa. In summary, various purification methods are available, as well as the choice of starting material, extraction buffer, and columns used to purify pancreatic BSAL successfully. However, the study herein offers a more straightforward approach with minimal purification steps and

directly using fresh bovine pancreas that would have gone to waste as part of the slaughtering process. This results in an improved yield of BSAL with the specific lipolytic activity of purified bovine BSAL comparable to commercial porcine pancreatic lipase.

5.5 Conclusion

BSAL was successfully purified and characterised from bovine (*Bos taurus*) fresh pancreatic tissue. The specific lipolytic activity of bovine BSAL was slightly enhanced after the one–step IEX to 0.222 U/mg (1.63–fold). The specific lipolytic activity of the purified BSAL was equivalent to porcine lipase, with minimal difference observed between the two. Overall, the results of this study indicate that LC–MS/MS analysis followed by peptide prediction allows rapid peptides identification of bovine pancreatic BSAL. This enables the extraction and purification process to obtain purified BSAL to be carried out effectively. Therefore, further studies on the current topic are recommended to determine the properties of bovine BSAL as a possible alternative for porcine lipase.

CHAPTER 6
PURIFICATION AND CHARACTERIZATION OF SHEEP (*OVIS ARIES*) PANCREATIC TRIACYLGLYCEROL LIPASES

6.1 Introduction

Lipase is one of the omnipresent enzymes with excellent stability found in nature has been isolated from various sources (Jawed *et al.,* 2019). Lipases are crucial for lipid digestion and provide the highest dietary source of calories (Oliveira *et al.,* 2024). The most common function of lipase is to break down triglycerides (TAG) into glycerol and free fatty acids (Pirahanchi & Sharma, 2023). The substantial growth of the international industrial enzyme market is projected to increase from $6.4 billion in 2021 to an estimated $8.7 billion in 2026 (Vardar–Yel *et al.,* 2024) in which lipases are the leading key players due to their versatility and myriad functions in numerous industrial applications – food, pharmaceutical, medicine, and chemical industries (Jawed *et al.,* 2019; Vardar–Yel *et al.,* 2024). Based on the market value, lipases constitute the third–largest enzyme group after proteases and carbohydrases (Navvabi *et al.,* 2018). Furthermore, lipases are one of the essential enzymes in pharmaceuticals due to their effectiveness in organic synthesis involving hydrolytic or esterification reactions, mainly in producing enantiopure drugs such as profens and atenolol (Contesini *et al.,* 2020). Lipase has also shown notable function and great potential in medical settings, such as designing therapeutic substitutes and diagnostic aids (Jawaid & Forsmark, 2019) for cancer, atherosclerosis, cystic fibrosis, and Alzheimer's disease (Ezema *et al.,* 2023). Intensive investigations on lipases have been conducted to solve nutritional problems secondary to the improper digestion of dietary fats (Szkopek *et al.,* 2024). The abnormal levels of pancreatic enzymes, including lipase, have become one of the diagnostic measures for pancreatic diseases (Gültepe *et al.,* 2016). Together with other classes of pancreatic enzymes, namely protease and amylase, they are synergistically essential for an excellent digestive system (Hou & Shimada, 2009) and become as the main components in pancreatic enzyme replacement therapy for exocrine pancreatic insufficiency (EPI) treatment and are appointed as the best medical care for pancreatic cancer patients (Harvey *et al.,* 2021). Pancreatic lipase is essential mainly because it is involved in up to 90% of fat digestion (Oliveira *et al.,* 2024).

One of the significant pancreatic lipases is the triacylglycerol lipases (TL, EC 3.1.1.3), sometimes referred to as triacylglycerol ester hydrolases, triacylglycerol hydrolases, and triglyceride lipase (Jawed *et al.,* 2019). According to the enzyme commission (EC) number system, TL is classified as a hydrolase responsible for hydrolysis reactions (Palmer & Bonner, 2011). TL is widely produced by animals, plants, and microorganisms such as bacteria, yeast, and fungi (Ezema *et al.,* 2023; Taipa *et al.,* 1992). It is a ubiquitous enzyme with considerable physiological significance and industrial potential (Sharma *et al.,* 2001). A wide range of molecular sizes, substrates, catalytic rates, and positional specificities have been observed from different sources of TLs (Kim *et al.,* 1997). TL is important for TAG digestion in humans (Dolinsky *et al.,* 2004). TAG acts as a natural energy reservoir component that will be utilized during cellular energy crises in the human body and other species (Ravotti *et al.,* 2020). The metabolic turnover of TAG requires an esterase that favours hydrolysis by water–soluble esterase (Jawed *et al.,* 2019). During the interfacial activation, the oil–water interface characterized and distinguished the lipase from the esterase (Kim *et al.,* 1997). In addition, the diversity of TLs has different fatty acid preferences, resulting in various rates and extents of triacylglycerol substrate hydrolysation (Calder, 2016). Animal lipases are usually found in the pancreas and digestive tracts (Hou & Shimada, 2009). TLs are the primary lipases secreted by the pancreas that are important for breaking down dietary lipids into unesterified fatty acids and monoglycerides (Chen *et al.,* 2012). It is critically vital for the exocrine pancreas to synthesize and secrete several lipolytic enzymes, which work with gastric lipase to achieve complete dietary fat digestion and absorption (Li *et al.,* 2007).

Domestic sheep, members of the Bovidae family, are widely distributed in Malaysia for livestock agriculture. Despite being small, it is essential as it provides alternative protein sources. The meat contains abundant essential amino acids and trace elements crucial for optimal human health, as it has fewer calories and lower cholesterol (Ding *et al.,* 2024). However, some sheep organs are not fully leveraged and disposed of together with the billions of tons of biological waste generated by slaughterhouses annually worldwide, which leads to potential pollution (Li *et al.,* 2012). Thus, the sheep pancreas, a by–product of the meat industry, can be employed as an alternative source for Halal digestive enzymes, specifically focusing on lipase applications. This would add value and function to the sheep pancreas, besides reducing waste and its management costs.

The pancreas has been reported as an EPI treatment by directly consuming its raw form. This method is rarely used as the preparation of the raw pancreas could be difficult and pose infections and disease transmission risks (Szkopek *et al.,* 2024). Therefore, it is encouraged to extract and purify lipases from animals, such as the sheep pancreas, before they can be consumed in powder, tablet, or capsule form. Slaughtered sheep presents as a Halal alternative as the demand for Halal–certified products has significantly increased from both Muslim and non–Muslim consumers, particularly with respect to Halal pharmaceutical products (Aziz *et al.,* 2014), which has a projected market value of US$3.2 trillion by 2024 (American Halal Foundation, 2024).

Porcine was one of the significant sources of pancreatic lipase from animal hosts. The extraction and purification of the porcine pancreatic lipase started as early as the second half of the 19th century (Caro *et al.,* 1981; Iijima *et al.,* 1998; Rudd *et al.,* 1987). The latest study of TL reports on the bioinformatics findings of *Aspergillus flavus* TL isolated from the decaying seed of *Cucumeropsis manni* (Ezema *et al.,* 2023). To highlight, microbial lipase from bacteria, fungi, and yeast is the current primary source of lipase and is essential in various industries, including pharmaceuticals (Vardar–Yel *et al.,* 2024; Vivek *et al.,* 2022). Although many microbial lipases are currently available, they are still inadequate in fulfilling the requirements of most industries. This is because microbial lipase may act differently regarding behaviour and functionality than animal lipase. Hence, using enzymes from Halal animals, such as sheep pancreas, as a lipase source should be considered to meet the existing needs.

Although many reports on the extraction and purification of TL have been extensively studied before, limited information has been published specifically on TL digestive enzymes in Bovidae species. Furthermore, the purification study of sheep TL was reported more than sixty years ago (Arienti *et al.,* 1974; Canioni *et al.,* 1975). In comparison with this effort, little work has been done on the purification of TL from sheep pancreas. The main goal of the current study is to present an updated and simplified purification technique of TL from the fresh sheep pancreas, which was subsequently confirmed by seventeen predictive peptide sequences with sheep TL characteristics via LC–MS/MS with the TL lipolytic activity determination. This evaluation will shed light on the usefulness of sheep TL as an alternative to porcine based, particularly for therapeutic purposes.

6.2 Materials and Methods

The sheep Triacylglycerol Lipase (TL) purification scheme is summarised as in Figure 6.1.

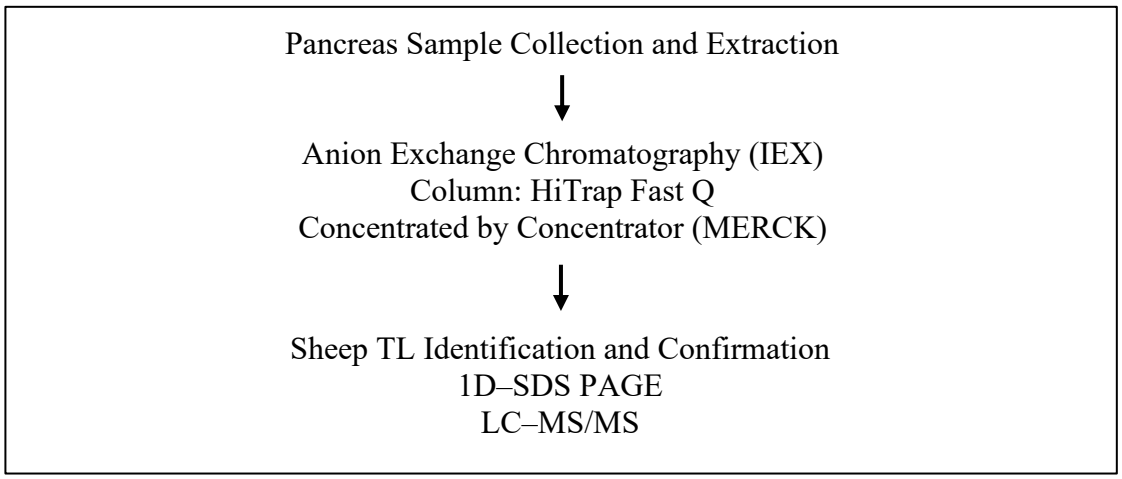


Figure 6.1 Sheep Triacylglycerol Lipase (TL) Purification Scheme.

6.2.1 Extraction and Purification of Sheep Triacylglycerol Lipase

Sheep pancreas was collected freshly from slaughtered animals of Abattoir Complex, Department of Veterinary Services (DVS), Shah Alam, Malaysia (Coordinates: 3.05, 101.51), and stored on ice. There was no available information on the supplier or animal records from the abattoir. Nevertheless, it was determined that all the animals were male with an estimated age between 6 to 12 months.

The pancreases were washed with tap water upon receiving. Then, the pancreas was dissected free from adherent fat and connective tissues with a scalpel blade (Elamin *et al.,* 2014). The pancreas was cut into smaller pieces on ice, and the tissue slices were washed with a 50 mM Tris pH 7.4 buffer containing 0.1 M sodium chloride (NaCl) to remove blood (Al–Ajlan & Bailey, 1999). The bovine pancreas collection and pancreatic crude extraction were done on the same day. Approximately 120 g – 160 g of pancreas samples were homogenized using a laboratory blender (Tefal – France), 1 min at low speed and 1 min at high speed (Bradley *et al.,* 1994).

Then, sheep pancreatic tissues were suspended in 20 mL of extraction buffer (50 mM Tris pH 7.4, 2 mM Ethylenediaminetetraacetic acid (EDTA) pH 8, 10 mM HEPES pH 7.4, 1% Triton X–100, and 150 mM NaCl) and vortexed for 10 mins before

centrifugation at 4000 rpm for 2 mins. The supernatants were collected and added with 70% (v/v) ethanol, bringing a total of 25 mL. The mixture was vortexed for 10 secs, and 2 mL of 5 µg/mL of aprotinin of aprotinin as a protease inhibitor was added to the samples. Aprotinin is a serine protease inhibitor and essential in inhibiting endogenous serine proteolytic activity. The suppression of the non–targeted proteases preserved the enzymatic activities of the targeted proteins. This helps to mitigate the risk of proteolytic degradation of the targeted enzymes, whereby the recovery of intact soluble proteases was maximised in the collected supernatant during the extraction procedure. The samples were centrifuged at 14,000 rpm for 20 mins before collecting the supernatant to recover soluble proteins. The protein concentration was measured and stored at –20^{o}C until further use.

6.2.2 Purification of Sheep Triacylglycerol Lipase

The purification is a critical step in this study to isolate the targeted enzymes. Following the preparation of the pancreatic tissue extraction, the sheep crude pancreatic extract was subjected to a one–step anion exchange chromatography (IEX) purification to isolate the sheep TL based on surface net charge. No further purification step was done after the IEX since the sheep TL was successfully purified at this stage.

The purification step was performed at room temperature on the second day (within 24 hours) following the crude extraction. Sheep pancreatic TL was further purified by IEX on a pre–packed HiTrap Q Fast Flow column containing a Sepharose–based resin (strong anion exchanger) (bed height 1.6 cm, column diameter 2.5 cm, column volume 5 mL) using an AKTA Avant^{TM} chromatography system (Cytiva – USA). The column equilibration process began by replacing the column's ethanol storage with distilled water to remove the preservative. Subsequently, the column was washed and equilibrated with the start buffer. The 20 mM Tris pH 8 was used as the start buffer, and 20 mM Tris 1 M NaCl pH 8 was used as the elution buffer. The sample was filtered using 0.45 µm and 0.25 µm cellulose acetate pore membrane filters (Merck – Germany). A total of 160 mL filtered sample was applied to the column in buffer A, and the column was washed until the absorbance monitored at 280 nm returned to baseline. The pancreatic enzymes were eluted using an elution buffer at a 2.4 mL/min flow rate, and 1.5 mL fractions were collected.

The IEX was chosen to separate the proteins depending on their ability to interact with a specific positive charge resin where negative charge proteins will bound to the resin. Generally, the proteins were eluted by increasing the ionic strength (salt concentration) of the elution buffer. In this study, the salt ions compete with the bound proteins for the positive charges on the surface of resin, which induced the elution of the bound proteins. As a result, the protein with lower net charge will elute first, following with higher net charge of protein that retained longer as it requires higher ionic strength of elution buffer to be eluted at the selected pH. Since sheep TL possesses an isoelectric point equal to 6.33, the IEX is performed using buffers with higher pH (pH 8).

Initially, a preliminary linear gradient IEX was conducted to determine the optimal ionic strength required to identify the best NaCl concentration for isolating each targeted enzyme. Subsequently, a NaCl step gradient was applied to purify and isolate the targeted enzymes within a single cycle of the IEX procedure. This allows distinct peak separation and efficient removal of contaminants at lower ionic strengths before eluting the targeted enzymes at their specific targeted salt concentrations. The IEX purification was repeated at least three times, and the chromatogram profiling was constructed based on the mean absorbance values.

The elution buffer composition was set up as a step gradient at 5%, 10%, 20%, 30%, 40%, 50%, and 100% sodium chloride (NaCl) to elute the bovine BSAL. Each fraction representing different peaks was run on 1–dimensional sodium dodecyl sulphate–polyacrylamide gel electrophoresis (1D–SDS PAGE) for molecular weight determination. The sheep TL was eluted at 20% of salt concentration. Fractions containing protease activity based on the molecular weight were pooled and concentrated using a 30,000 MW and 50,000 MW Amicon® Ultra Centrifugal Filter (MERCK – Germany).

6.2.3 Protein and Peptide Identification of Sheep Triacylglycerol Lipase

6.2.3.1 Determination of Protein Concentration

The total protein concentration of total crude pancreatic extract and purified fraction samples from IEX were measured. Absorbance was measured at 280 nm (A_{280}) using a NanoDrop® ND–1000 UV–Vis Spectrophotometer (Thermo Fisher Scientific – US). The obtained concentration values (mg/mL) were subsequently utilised to calculate the total protein content (mg) and were essential for determining the proteolytic enzymatic activity (U/mg) of the samples.

6.2.3.2 One–Dimensional Sodium Dodecyl Sulfate Polyacrylamide Gel Electrophoresis (1D–SDS PAGE)

The molecular mass of purified bovine pancreatic BSAL was estimated by 1D–SDS PAGE using NuPAGE 4–12% mini protein gel of Bis–Tris electrophoresis system in X Cell SureLock Mini–Cell (Invitrogen – US) stained with Coomassie Brilliant Blue stain (Invitrogen – US).

The sample was prepared as described in Table 6.1. The protein mixtures were prepared by adding protein sample (x µl), 4X NuPAGE LDS Sample Buffer (2.5 µl), 10X NuPAGE Reducing agent (1 µl), and Ultrapure water (y µl) in a 1.5 mL Eppendorf tube. The protein volume needed was calculated using the dilution formula (M1V1 = M2V2) based on the initial concentration of the protein. Then, Ultrapure water was added, bringing a 10 µl volume for sample preparation. The protein sample was heated at 70^{o}C for 10 mins before loading into the wells. The 1X NuPAGE MES SDS Running Buffer was prepared by adding 50 mL of 20X MES SDS Running Buffer to 950 mL of distilled water. The gel electrophoresis system was set up at 200 V (constant voltage) and 125 mA (current). The electrophoretic separation was conducted for approximately 35 to 45 minutes to ensure the complete resolution of the protein bands.

Table 6.1
Sample Preparation for SDS–PAGE

Chemicals	Volume (µl)
Protein Concentration	20 mg/mL
Protein Sample	*x*
NuPAGE LDS Sample Buffer (4X)	2.5
NuPAGE Reducing agent (10X)	1.0
Ultrapure water	*y*
Final Volume	**10.0**

The gel was transferred into a clean container and added with 50 mL of distilled water. Then, the gel was microwaved at high power for 1 min and shaken for 1 min. The steps were repeated twice. Then, the gel was added with Safely Blue Safe stain (Invitrogen – US) liquid. The gel was microwaved again at high for 45 secs and shaken for 5 mins. The gel was washed with distilled water and shaken for 10 mins before viewing with ChemiDoc™ Imaging System (BioRad – US).

6.2.3.3 Liquid Chromatography–Mass Spectrometry (LC–MS/MS)

Protein bands were further identified using liquid chromatography–mass spectrometry (LC–MS/MS). Before the LC–MS/MS procedure, trypsin gel digestion was carried out. Then, a total of 5 µL sample was injected into Dionex Ultimate 3000 RSLCnano Orbitrap Fusion (Thermo Fisher Scientific – US) with EASY–Spray Acclaim PepMapTM C18 100 A0 (2 µm particle size, 50 µm id x 15 cm) separation column. The sample was eluted with LC–MS grade water, 0.1% formic acid (A), and ACN, 0.1% formic acid (B), at a 250 nL/min flow rate. The elution gradient was 5%–40% B for 91 min, 2 min to 85% B, 3 min at 85% B, 1 min at 5% B, and 4 min at 5% B. The full scan spectra were collected by Orbitrap MS (OTMS) scan mass ranging from 310 – 1800 m/z with 50 ms maximum injection. The spectra were analyzed by ion trap MS (ITMS) with 250 ms maximum injection. The LC–MS/MS data was analyzed using Thermo Scientific™ Proteome Discoverer™ Software Version 2.1. The results were matched with the database downloaded from UniProt. The variable modifications were oxidation (M) and acetyl (N–terminal), with fixed modification of carbamidomethyl (C). All peptides were validated using the percolator® algorithm, based on a q–value of less than 1% false discovery rate (FDR). The LC–MS/MS

analysis was performed at the Proteomic Laboratory, Malaysian Genome and Vaccine Institute, Bangi, Malaysia.

6.2.4 Lipolytic Enzyme Assay

The lipolytic activity of crude extracts and purified fractions from IEX were determined using the modified method from previous studies (Vardar Yel, 2021; Vo *et al.,* 2022) alongside the commercial porcine pancreatic lipase (Sigma Aldrich – Germany) as a positive control. Lipase activity was evaluated through the conversion of 4–nitrophenyl Palmitate (pNPP) into p–nitrophenol (pNP) product formation, which resulted in enzymatic reaction (Vo *et al.,* 2022).

The pNP calibration standard curve was construct to determine the enzyme concentration tested. The pNPP was used as substrate. The pNP standard curve was established by preparing 50 mM stock solution of pNPP in 1 mL acetonitrile (ACN). Subsequently, a series of 8 serial dilutions were prepared in 25 mM sodium phosphate ($NaPO_4$) pH 7 from the working standard, 5–fold dilutions were employed to ensure the standard curve spanned the full range of detectable lipase activity. The final volume for each dilution was adjusted to a final volume of 600 µL. The pNP standard curve of linear scale of absorbance at 405 nm against concentration (mM) was constructed as recommended by the previous study.

The standard assay contained 10 µL of lipase sample, 150 µL of substrates, and 40 µL of 25 mM $NaPO_4$ buffer pH 7. The 25 mM $NaPO_4$ buffer pH 7 and ACN mixture was used as a blank. The lipolytic assay was performed in a 96–well microplate with a 200 µL reaction volume, incubated at 25°C. Finally, the absorbances at 405 nm were measured periodically at 1, 5, 10, 15, 30, 45, 60, 90 and 120 mins using microplate reader. The experiments were conducted in triplicates.

The enzyme concentration of the crude extract and purified sample were quantified by extrapolating the absorbance values of the samples against a pNP standard curve. The lipolytic activity was calculated based on the formula given.

$$Specific\ lipolytic\ activity\ \left(\frac{U}{mg}\right) = \frac{Total\ lipolytic\ activity\ (U)}{Total\ Protein\ content\ (mg)} \qquad 6.1$$

One unit of lipase is defined as the amount of enzyme that will generate 1.0 µmole of pNP from the pNPP reaction per minute at 25°C as measured at 405 nm using a SpectraMax iD5 Multi–mode Microplate reader (Molecular Devices – USA).

6.3 Results

6.3.1 Extraction and Purification of Sheep Triacylglycerol Lipase

Sheep pancreatic TL was successfully purified from the fresh pancreatic tissue by pancreatic tissue delipidation, protein extraction, and IEX. Total of 160 mL of filtered sheep crude extract was loaded onto the pre–packed HiTrap Q Fast Flow column. Figure 6.2 illustrates the elution pattern of IEX on the pre–packed HiTrap Q Fast Flow column. The IEX elution was performed with a step NaCl gradient (5 – 100%), whereby the enzymes were separated based on the ionic strength of the elution buffer. The elution profile shows eight distinct peaks after the IEX step. As shown in Figure 6.2, the sheep TL was present in fractions eluted at 20% NaCl concentration and labelled as **peak C**. These fractions were collected between the elution volumes of **166.0 mL** and **188.5 mL**. In total, 15 fractions (22.5 mL) were obtained from the IEX step, yielding a protein concentration of 7.31 mg/mL, corresponding to 164.48 mg of total protein.

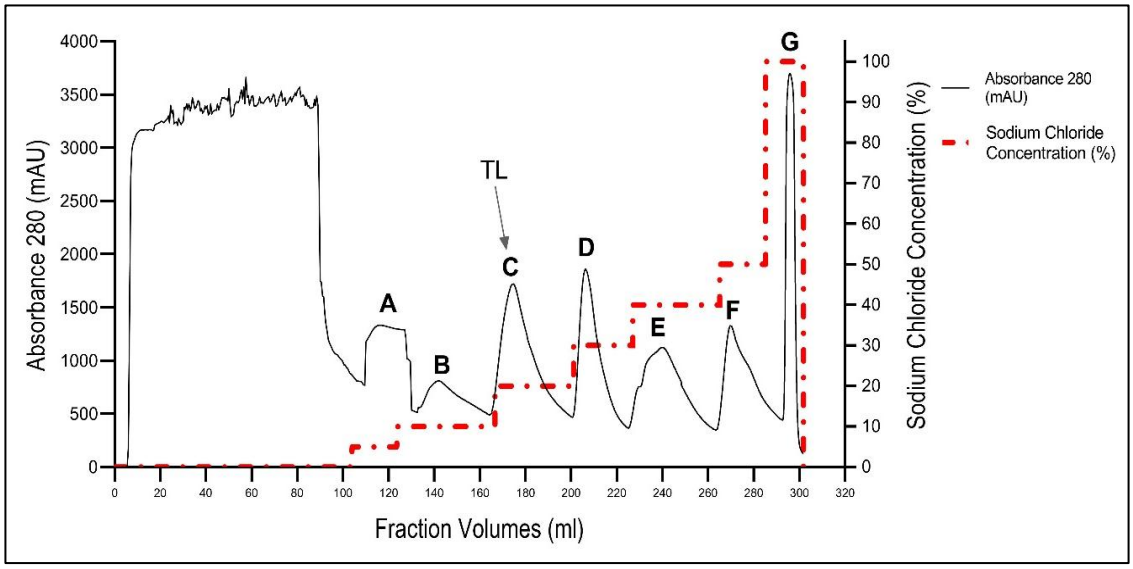


Figure 6.2 Anion–exchange Chromatography of Aqueous Crude Sheep Pancreatic Extract. The Purified Sheep TL was eluted at Peak C (20% NaCl concentration).

Note: The thin line shows the absorbance at a wavelength of 280nm during chromatography. The arrows marked peaks that revealed the presence of sheep TL on the 1D–SDS PAGE with lipolytic activity. Tubes were pooled at 20% NaCl concentration, indicating the presence of active sheep TL. Column: Hi Trap Q Fast Flow column (pre–packed); flow rate: 2.4mL/min; mobile phase: 20mM Tris pH8, 20mM Tris NaCl pH8.

6.3.2 Protein and Peptide Identification of Sheep Triacylglycerol Lipase

1D–SDS PAGE analysis of the sheep TL from crude extract and post–IEX are shown in Figure 6.3. From the 1D–SDS PAGE, the crude extract displayed a broad and intense smear with multiple protein bands, reflecting the complex pancreatic protein composition prior to IEX. In contrast, after the single IEX step revealed a single, discrete band with an estimation of molecular weight at 53 kDa (**Lane 3**).

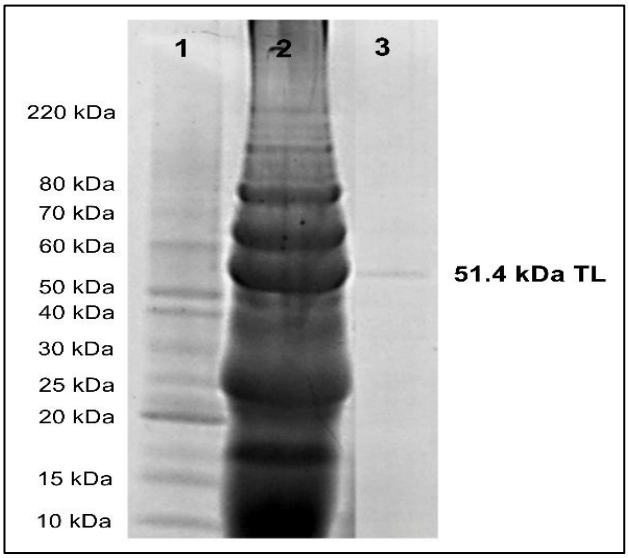


Figure 6.3 1D–SDS PAGE (Bis–Tris 12%) of Pure Sheep TL. Pure Sheep TL was approximately estimated to be 53 kDa (Lane 3).

Note: Lane 1: Benchmark™ Unstained Protein Ladder; Lane 2: Crude extract; Lane 3: Diluted crude extract (10x); and Lane 4: Purified TL obtained after Hi Trap Q Fast Flow chromatography. The gel (Bis–Tris 12%) was stained with Coomassie blue.

The single band, expected to be sheep TL, was excised and destained for LC–MS/MS protein and peptide identification. Table 6.2 lists the proteins identified from the LC–MS/MS analysis. The sheep pancreatic TL (Accession number: W5Q512) with 66.09% protein coverage was identified through the LC–MS/MS analysis. The quality of the purified TL was validated by mass spectrometry, whereby the calculated molecular mass was 51.4 kDa and calc pI 5.62. The protein band was identified as sheep pancreatic TL and confirmed with LC–MS/MS through the molecular weight and predictive peptide sequences identified and validated using the percolator® algorithm, based on a q–value of less than 1% false discovery rate (FDR). The peptide sequence, position in the master protein, charge, and molecular weight are listed in Table 6.3. A

total of 144 predictive peptides were identified (data not shown). Only seventeen predictive peptides that have similar sheep pancreatic TL master protein characteristics reported on low FDR with Qvality q–value (>0.01), XCorr Sequest HT (>2.0), and percolator q–value Sequest HT value (>0.01) (Table 6.3) were selected. Most of the predictive peptides have a net charge between 2 and 4 with a low molecular weight below 4488.12 Da. Eight of seventeen predictive peptide sequences undergo frequent fixed carbamidomethyl modifications and variable deamination but low variable oxidation modifications during the sample handling.

Table 6.2
Protein Identification from the LC–MS/MS

No	Accession Number	Protein Identified	No of Peptides	Coverage (%)	Molecular Weight (kDa)	Calc PI
1	W5Q5I2	Triacylglycerol lipase OS=Ovis aries OX=9940 GN=LOC101103610 PE=3 SV=1	17	66.09	51.403	5.62
2	A0A836D393	Glutathione reductase OS=Ovis aries OX=9940 GN=JEQ12_013800 PE=3 SV=1	9	34.52	52.025	7.64
3	W5PL89	Glutathione–disulfide reductase OS=Ovis aries OX=9940 GN=GSR PE=4 SV=1	8	36.19	46.181	7.5
4	W5P9B8	Chymotrypsinogen A–like OS=Ovis aries OX=9940 GN=LOC114112429 PE=4 SV=1	5	36.12	27.489	8.09
5	W5Q219	Cationic trypsin OS=Ovis aries OX=9940 GN=LOC101112049 PE=4 SV=1	6	43.65	26.46	7.71

Table 6.3
Peptide Sequence Prediction of Sheep Pancreatic TL via LC–MS/MS

No	Annotated Sequence	Confidence	Modifications	Charge	Position in Master Protein	Theo. MH+ [Da]	Qvality q–value	XCorr Sequest HT	Percolator q–Value Sequest HT
1	[R].ITGLDPAEPYF**Q**GTPELVR.[L]	High	1xDeamidated [Q12]	2	190–208	2104.06	0	5.25	0
2	[K].**N**ALS**Q**IVDIDGIWEGTR.[GD]	High	1xDeamidated [N/Q]	2	258–274	1887.94	0	3.87	0
3	[K].FLWY**N**NVINPTLPK.[V]	High	1xDeamidated [N]	2	418–431	1719.91	0	3.13	0
4	[R].IVGAEVAYLVDVLK.[QS]	High	–	2	140–153	1488.87	0	4.82	0
5	[R].VTGHILVSLFGDKGNSK.[Q]	High	–	3	369–385	1771.97	0	5.49	0
6	[R].VTGHILVSLFGDK.[G]	High	–	3	369–381	1385.78	0	3.70	0
7	[K].**Q**YEIF**N**GTLKPDSTES**N**EFDSDVDVGVL**Q**K.[V]	High	1xDeamidated [N/Q] 2xDeamidated [Q/N]	3	386–415	3376.56	0	6.69	0
8	[K].ITVEAYDG**Q**VFDF**C**S**Q**DTVR.[E]	High	1xDeamidated [Q] 1xCarbamidomethyl [C14]	2	427–456	2351.05	0	5.02	0
9	[R].LDPSDA**Q**FVDVIHTDAAP**M**IP**N**LGFG**M**SQVVG HLDFFPNGGK.[E]	High	2xDeamidated [Q/N] 2xOxidation [M19; M27]	4	209–250	4488.12	0	3.72	0
10	[R].FLLYT**N**E**N**P**N**N**N**F**Q**EIVADASIIA**N**S**N**FK.[T]	High	1xDeamidated [N/Q]	3	55–82	3187.56	0	5.83	0
11	[R].FVIHGFTDKGDE**N**WL**Q**SI**C**K.[N]	High	1xDeamidated [N/Q] 1xCarbamidomethyl [C19]	3	89–108	2395.14	0	3.88	0
12	[K].**C**FP**C**PSEG**C**P**Q**M**M**GHYADRFPGK.[T]	High	1xDeamidated [Q11] 1xOxidation [M12] 3xCarbamidomethyl [C1; C4; C9]	4	314–335	2614.07	0	3.06	0
13	[R].DFVA**C**NHLR.[S]	High	1xCarbamidomethyl [C5]	2	275–283	1131.54	0	2.25	0
14	[R].EEVLLTLNP**C**.[–]	High	1xCarbamidomethyl [C10]	2	457–466	1187.6	0	3.06	0
15	[R].LG**C**FSDDSPWAGTIERPLK.[V]	High	1xCarbamidomethyl [C3]	3	24–42	2149.04	0	3.14	0
16	[K].GDENWLQSI**C**K.[N]	High	1xCarbamidomethyl [C10]	2	98–108	1349.62	0	3.14	0
17	[K].YYADSIL**N**PDGFAGFP**C**ASYSDFSA**N**K.[C]	High	1xDeamidated [N] 1xCarbamidomethyl [C17]	3	287–313	2978.28	0	5.09	0

Note: Description of Sheep Pancreatic TL peptide sequence prediction. The bold symbol represents the possible site of fixed and variable modifications during the sample handling process. The confidence level for the identified protein was determined by the false discovery rate (FDR) and interpreted as high–confidence hits, which were 99% accurate. The charge is the sum of positive (basic) and negative (acidic) charge residues in neutral pH. Position in Master Protein is the location of the annotated predictive peptide sequence in the protein. Theo. MH+ [Da] is the protonated monoisotopic mass of the peptides in Daltons. Qvality q–value and Percolator q–Value Sequest HT are calculated from the number of target and decoy proteins, and the minimum FDR is required for a hit to be considered correct (Qvality q–values and Percolator q–Value Sequest HT > 0.01 are considered high–confidence hits). XCorr Sequest HT indicates the number of fragment ions that are common to two different peptides with the same precursor mass and calculates the cross–correlation (XCorr) for all candidate peptides in search (XCorr value >2 is considered favorable).

6.3.3 Lipolytic Enzyme Assay

The lipolytic activity was measured for all bovine crude extract and IEX samples using lipase activity assay described. The pNP standard curve was constructed to determine the lipase activity of sheep TL, with the R^2 value of 0.99 (Appendix 5). Table 6.4 summarizes the purification and lipolytic enzyme activity measured for sheep TL in the crude extract and IEX samples. The protein concentration of purified sheep TL, as calculated from the $A_{280,}$ was 7.31 mg/mL.

Table 6.4
Purification of Sheep Pancreatic TL

Purification stage	Volume (mL)	A_{280}	Protein content (mg)	Specific lipolytic activity (U/mg)	Total lipolytic activity (U)	Yield (%)	Purification Fold
Crude extract	160.0	47.24	7560.00	0.640	4838.40	100.00	1.00
IEX (*Peak C – 20% NaCl*)	22.5	7.31	164.48	0.136	22.36	0.46	0.21

Note: Specific lipolytic activity of porcine pancreatic lipase (1 mg/mL) = 0.223 U/mg

From the Table 6.4, the specific lipolytic activity showed a marked declined after one–step IEX purification as compared to the crude extract, indicating a loss of lipase during the procedure. The crude extract exhibited a high specific lipolytic activity of 0.640 U/mg, showing a substantial proportion catalytically active of the total protein present. In contrast, the purified sheep TL have a much lower specific lipolytic activity of 0.136 U/mg, correspond to 0.21–fold. The significant reduction in the specific lipolytic activity suggest that IEX did not enriched the targeted sheep TL.

The activity was also compared against a commercially available porcine pancreatic lipase as a positive control. The concentration of the porcine pancreatic lipase was standardized to 1 mg/mL and yielded 0.223 U/mg of specific lipolytic activity. This suggests that the final product of sheep TL purification has a lower specific TL lipolytic activity of 0.136 U/mg. However, the crude sheep pancreatic extract recorded higher specific lipolytic activity as the starting material volume and the protein concentration were higher before purification. These findings suggest that sheep crude extract pancreatic could be utilized for lipase replacement for Halal enzyme alternative.

6.4 Discussion

The results here confirmed that the sheep pancreas contained TL. Sheep TL was purified from 160 mL of pancreatic crude extract using one–step of IEX purification. The elution profiles of the TL enzyme are shown in Figure 6.2. A single peak was eluted at 20% NaCl concentration (peak C), containing declined active TL lipolytic activities after purified with Hi Trap Q Fast Flow column. Although the sheep TL was successfully isolated and observed as a single band on 1D–SDS PAGE, the specific lipolytic activity of the purified sheep TL was significantly reduced to 0.21–fold as compared to the sheep crude extract sample (Table 6.4). In comparison, the crude extract yielded the highest specific lipolytic activity recovery compared to the IEX sample. Thus, the utilization of IEX purification technique to isolate TL from sheep pancreatic was not effective since the lipolytic enzymatic activity was recorded low.

This notable decline in the specific lipolytic activity of purified sheep TL during purification can be attributed to several concurrent factors. Temperature and exposure time are critical dependencies for enzyme denaturation. These two factors contribute to short or long terms enzyme instability, which correlates to enzyme conformational changes and affects enzyme activity (Kabir & Ju, 2023). In this study, the IEX purification was not conducted under cold conditions, which may have accelerated thermal denaturation during the process. However, the denaturation temperatures of the enzymes vary from one enzyme to another (Robinson, 2015).

Other than that, in previous microbial lipase studies, a 50% loss of lipase activity has been reported due to chromatography hydrophobic interaction (Taipa *et al.,* 1992). This could contribute to the loss of lipolytic activity during purification. In addition, several steps, such as ultrafiltration and precipitation, including chromatography processes, may have contributed to the loss of product in each step involved (Sukohidayat *et al.,* 2018). Furthermore, the presence of metal ions in some enzymes is critical as they enhance the enzyme–specific activity and influence enzyme stability (Sharon *et al.,* 1998). The introduction of metal ions such as calcium and magnesium is believed to escalate the enzyme activity by acting as a binding link between the enzyme and substrate to form an active site during the lipolytic assay (Sharma *et al.,* 2017; Vijayaraghavan *et al.,* 2016).

Previously, the exclusion of magnesium from the growth media of *Pseudomonas aeruginosa* KKA5 showed a 50% reduction in lipase activity (Duan *et al.,* 2023). Other than that, the introduction of calcium, another example of divalent ion can also escalate the enzyme performance acting as a binding link between the lipase and its substrate (Abdelaziz *et al.,* 2025). In this study, no supplementation of metal ions during extraction, purification or in the lipolytic enzyme assay was done. It is suggested to assess the impacts of different types and concentrations of metal ions on the lipolytic activity of the purified sheep TL sample.

Additionally, the resemblance in molecular weight, amino–acid composition, and antigenic determinants among mammalian pancreatic lipases such as human, porcine, bovine, and ovine has been reported (Caro *et al.,* 1981). The mammalian pancreatic lipase molecular weight range was reported to be around 45 to 60 kDa (Canioni *et al.,* 1975; Lehner & Verger, 1997; Taipa *et al.,* 1992; Vandermeers *et al.,* 1974). Previously, extensive N–terminal homology with identical cysteinyl residues has been observed in human and porcine lipases (Caro *et al.,* 1981). In the same study, two sulfhydryl groups acting as antigenic determinants were observed in these lipases (Caro *et al.,* 1981). On the contrary, different biological sources of lipase have been shown to exhibit distinct lipolytic activity and specificity (Shahani *et al.,* 1976). The molecular weight of purified sheep pancreatic TL was determined by gel electrophoresis. As shown in Figure 6.3, the purified product revealed a single band on the 1D–SDS PAGE with a molecular weight of approximately 53 kDa, comparable to the 52.2 kDa molecular weight of sheep TL in the Protein Database System (PDB) and 51.4 kDa calculated mass from LC–MS/MS analysis. Previously, the molecular weight of sheep pancreatic TL was estimated to be approximately 49.2 kDa by gel filtration compared to the reference protein (Canioni *et al.,* 1975). Based on the literature, the mass of TL varies according to the biological source; for example, 25 kDa in *Aspergillus oryza* (Toida *et al.,* 1998), 30 kDa in *Pseudomonas aeruginosa* (Sharon *et al.,* 1998), 32 kDa in *Pseudomonas fluorescens* (Sugiura *et al.,* 1977), 40 kDa in *Mycobacterium phlei* (Paznokas & Kaplan, 1977), 46 to 48 kDa in human (Taipa *et al.,* 1992; Vandermeers *et al.,* 1974), porcine (Lehner & Verger, 1997), and 48 to 67kDa in bovine (Wolf *et al.,* 1978).

Different authors have purified and measured the lipolytic activity of the pancreatic TL. However, the updated literature on the sheep pancreatic TL is limited. Although there have been earlier reports of the success of sheep pancreatic TL purification, this study employed a different method of pancreatic extraction with a single–step purification. The latest report on TL extraction and purification from sheep pancreas was from 1975, using ammonium precipitation, acetone treatment, ion exchange, and GFC (Canioni *et al.,* 1975). In the case of bovine during the year 1972, the TL was purified from the pancreas and pancreatic juice, starting with ammonium sulfate fractionization, chromatography on DEAE–cellulose (pH 7), and CM–cellulose (pH 5), and finally GFC on Sephadex G–100 (Julien *et al.,* 1972). In another study of bovine, later in the year 1978, the TL was extracted from the thyroid gland and was purified by co–sedimentation with lysosomes, followed by detergent solubilization and run on Sephadex G–200 and carboxymethyl cellulose chromatography (Wolf *et al.,* 1978). Another study on porcine liver microsome TL in the year 1997 also used different methods of extraction and purification, where the enzymes were solubilized with zwitterionic detergent and followed by sequential chromatography on Q–Sepharose, hydroxyapatite, Affi–Gel heparin, and Mono–Q (Lehner & Verger, 1997). On the other hand, the study of human pancreatic TL from the year 1974 was isolated from pancreatic juice using different types of columns such as Sephadex G–25, diethylaminoethyl–cellulose, carboxymethyl–cellulose, and Sephadex G–75 (Vandermeers *et al.,* 1974). The purification techniques used to extract microbial sources of TL were also reported to be different from those in our study. For example, ammonium sulfate precipitation followed by chromatography on Sephadex G–75 and DEA–Sephadex was utilized to purify TL from *Penicillium cyclopium* (Chahinian *et al.,* 2000). The same methods were used to purify TL from *Pseudomonas fluorescens* (Sugiura *et al.,* 1977). In another study, TL from *Aspergillus oryzae* was purified using ammonium sulfate fractionation, acetone precipitation, IEX, and GFC (Toida *et al.,* 1998). Meanwhile, the purification method of TL from *Mycobacterium phlei* was carried out by 5% Triton X–100 cell suspension and IEX on two successive DEAE–cellulose columns (Paznokas & Kaplan, 1977). Overall, numerous purification strategies have been employed for TL extraction and purification purposes, including

the choice of starting material, buffer selection for extraction, and different kinds of columns used to purify the pancreatic TL.

Hence, this study offers more straightforward methods with a minimum purification step that utilize fresh sheep pancreas as a starting material. Although the sheep pancreatic TL was successfully purified using a single–step purification, surprisingly, the result was consistent with the previous reports. The findings presented herein also revealed that the sheep pancreatic crude extract has a better specific lipolytic activity that is 3–fold higher than the commercial porcine pancreatic lipase and 5–fold higher than the purified sample from the IEX. This suggests that the crude extract is a better source of TL in the sheep pancreas. In the future, this current study may offer beneficial information to scale up and increase the yield of TL purification by using IEX.

6.5 Conclusion

In conclusion, TL was successfully purified and characterized from fresh pancreatic tissues in sheep (*Ovis aries*). The specific lipolytic activity of sheep TL was notably reduced after the one–step IEX to 0.136 U/mg (0.21–fold). The pancreatic crude extract recorded higher specific lipolytic activity, which is three times higher than the positive control. The sheep pancreatic TL was confirmed with LC–MS/MS with peptide identification. In short, the crude sheep pancreatic TL could be an alternative to porcine lipase. Therefore, further investigation on the current topic is recommended to determine the biochemical properties of sheep TL and their potential related to Halal pharmaceutical products.

CHAPTER 7
BOVINE (*BOS TAURUS)* AND SHEEP *(OVIS ARIES)* PANCREATIC ALPHA–AMYLASE EXTRACTION AND PURIFICATION

7.1 Introduction

Domestic bovine and sheep are members of the Bovidae family, broadly distributed as livestock in Malaysia for Halal meat consumption. The pancreas is one of the animal organs that are not fully utilized and often discarded as waste. It is one of the Mammalian pancreatic tissues that are non–edible and produced in large quantities by the meat industry. Thus, the improper handling of animal organs discarded as waste is contributing to the accumulation of biological waste that leads to potential environmental pollution (Li *et al.,* 2012). Thus, the bovine and sheep pancreas, a by–product of the meat industry, could serve as an alternative source for Halal digestive enzymes, especially amylase. Although porcine pancreatic enzymes currently dominate the market due to their high activity and availability; however, their non–Halal status restricts use among Muslim consumers, escalating the need for alternative Halal sources such as bovine and sheep pancreas. In addition, among Muslim and non–Muslim consumers, the awareness has increased in demanding good–quality and Halal–certified products, including medicine and health supplements (Aziz *et al.,* 2014). Halal pharmaceutical products have gained the interest of non–Muslim consumers because these products are considered cleaner and healthier (Sudarsono & Nugrowati, 2020). The exocrine pancreas glands' alkaline secretions, including α–amylase, trypsin, chymotrypsin, and carboxypeptidase, are important for the small intestine's carbohydrates, proteins, and fat breakdown (Rafaqat *et al.,* 2023).

Amylase is the predominant pancreatic exocrine secretory–granule zymogen (Doyon *et al.,* 2002). Alpha–Amylases (α 1–4 glucan 4–glucanohydrolase, EC 3.2.1.1) catalyze the hydrolysis of α (1–4) glycosidic linkages of starch and are widely distributed in nature, being found in bacteria, plants, and animals (Böswald *et al.,* 2023; Rydberg *et al.,* 2008). The investigations on amylase had started as early as the 1800s

and held the attention of investigators for over 150 years (Koyama *et al.,* 2000; Zakowski & Bruns, 1985). Norby demonstrated the first separation of pancreatic (P–amylase) and salivary isozymes (S–amylase) in 1964. The amylase isozymes have been appointed as a diagnostic marker for pancreatic or parotid diseases (Koyama *et al.,* 2000). These amylases share a 97%–99 % amino acid sequence identity and are composed of three domains: the catalytic domain (A domain), the signal peptide (B domain), and the C–terminal region (C domain) (Doyon *et al.,* 2002; Takashima & Amano, 2012).

To date, the extraction and the purification of the pancreatic Alpha–Amylase from bovine and sheep were done many years ago in the mid–1970s (Banks *et al.,* 1976; Ettalibi *et al.,* 1975). In this present study, attempts were made to extract and purify AMYP from bovine and sheep fresh pancreas using a single purification step, anion exchange chromatography with the current purification system technology. However, despite following an optimized protocol, the extraction and purification process did not yield detectable or active alpha–amylase from either bovine or sheep pancreas. The almost complete absence of a measurable clearing zone representing amylolytic activity and specific protein bands corresponding to AMYP in chromatographic fractions, SDS–PAGE, and LC–MS/MS analyses indicates that the extraction and purification were unsuccessful. This outcome highlights the need for further optimization of extraction conditions and purification strategies to reduce possible degradation or low abundance of AMYP in the tested samples. Nonetheless, this study provides valuable insights into the limitations and challenges associated with the use of these animal sources for Halal enzyme production.

7.2 Materials and Methods

The bovine and sheep Alpha–Amylase (AMYP) purification scheme was summarised as in Figure 7.1.

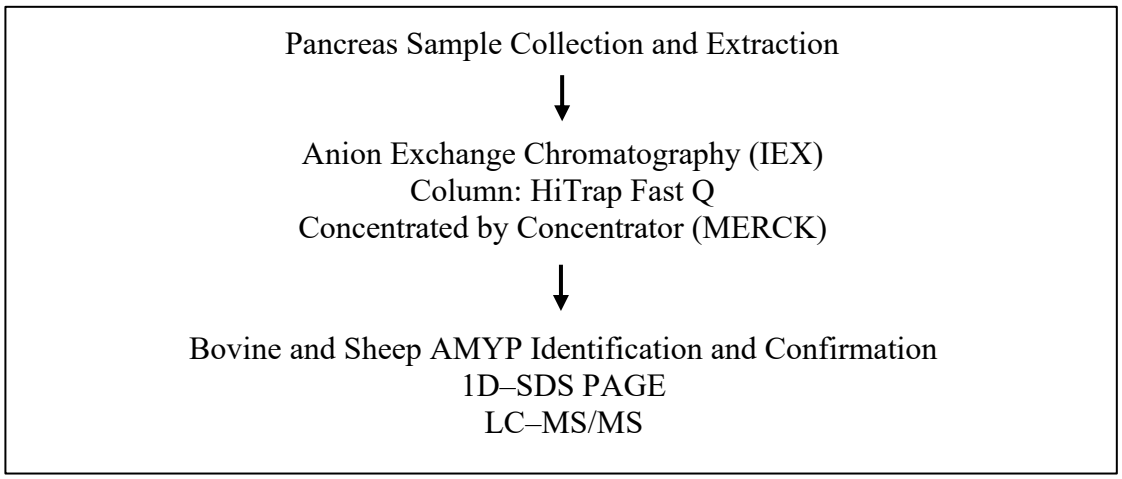


Figure 7.1 Bovine and Sheep Alpha–Amylase (AMYP) Purification Scheme.

7.2.1 Extraction and Purification of Bovine and Sheep Alpha–Amylase

Randomized bovine and sheep pancreas was collected freshly from slaughtered animals of Abattoir Complex, Department of Veterinary Services (DVS), Shah Alam (Coordinates: 3.05, 101.51), Malaysia, and stored on ice. There was no available information on the supplier or animal records from the abattoir. Nevertheless, it was determined that all the animals were male with an estimated age more than 2 years for bovine and between 6 to 12 months for sheep.

The pancreases were washed with tap water upon receiving. Then, the pancreas was dissected free from adherent fat and connective tissues with a scalpel blade (Elamin *et al.,* 2014). The pancreas was cut into smaller pieces on ice, and the tissue slices were washed with a 50 mM Tris pH 7.4 buffer containing 0.1 M sodium chloride (NaCl) to remove blood (Al–Ajlan & Bailey, 1999). The bovine and sheep pancreases collection and pancreatic crude extraction were done on the same day. Approximately 120 g – 160 g of pancreas samples were homogenized using a laboratory blender (Tefal – France), 1 min at low speed and 1 min at high speed (Bradley *et al.,* 1994).

Then, bovine and sheep pancreatic tissues were suspended in 20 mL of extraction buffer (50 mM Tris pH 7.4, 2 mM Ethylenediaminetetraacetic acid (EDTA) pH 8, 10 mM HEPES pH 7.4, 1% Triton X–100, and 150 mM NaCl) and vortexed for 10 mins before centrifugation at 4000 rpm for 2 mins. The supernatants were collected and added with 70% (v/v) ethanol, bringing a total of 25 mL. The mixture was vortexed for 10 secs, and 2 mL of 5 µg/mL of aprotinin of aprotinin as a protease inhibitor was added to the samples. Aprotinin is a serine protease inhibitor and essential in inhibiting endogenous serine proteolytic activity. The suppression of the non–targeted proteases preserved the enzymatic activities of the targeted proteins. This helps to mitigate the risk of proteolytic degradation of the targeted enzymes, whereby the recovery of intact soluble proteases was maximised in the collected supernatant during the extraction procedure. The samples were centrifuged at 14,000 rpm for 20 mins before collecting the supernatant to recover soluble proteins. The protein concentration was measured and stored at –20^{o}C until further use.

7.2.2 Purification of Bovine and Sheep Alpha–Amylase

The purification is a critical step in this study to isolate the targeted enzymes. Following the preparation of the pancreatic tissue extraction, the bovine and sheep crude pancreatic extracts were subjected to one–step anion exchange chromatography (IEX) purification to isolate the bovine and sheep AMYP based on surface net charge. No further purification step was done after the IEX since, both bovine and sheep AMYP was unsuccessfully purified and identified at this stage.

The purification step was performed at room temperature on the second day (within 24 hours) following the crude extraction. Bovine and sheep pancreatic AMYP was purified by IEX on a pre–packed HiTrap Q Fast Flow column containing a Sepharose–based resin (strong anion exchanger) (bed height 1.6 cm, column diameter 2.5 cm, column volume 5 mL) using an AKTA Avant^{TM} chromatography system (Cytiva – USA). The column equilibration process began by replacing the column's ethanol storage with distilled water to remove the preservative. Subsequently, the column was washed and equilibrated with the start buffer.

The 20 mM Tris pH 8 was used as the start buffer, and 20 mM Tris 1 M NaCl pH 8 was used as the elution buffer. The sample was filtered using 0.45 μm and 0.25 μm cellulose acetate pore membrane filters (Merck – Germany). A total of 160 – 200 mL filtered sample was applied to the column in buffer A, and the column was washed until the absorbance monitored at 280 nm returned to baseline. The pancreatic enzymes were eluted using an elution buffer at a 2.4 mL/min flow rate, and 1.5 mL fractions were collected.

The IEX was chosen to separate the proteins depending on their ability to interact with a specific positive charge resin where negative charge proteins will bound to the resin. Generally, the proteins were eluted by increasing the ionic strength (salt concentration) of the elution buffer. In this study, the salt ions compete with the bound proteins for the positive charges on the surface of resin, which induced the elution of the bound proteins. As a result, the protein with lower net charge will elute first, following with higher net charge of protein that retained longer as it requires higher ionic strength of elution buffer to be eluted at the selected pH. Respectively, bovine and sheep AMYP possesses an isoelectric point equal to 5.97 and 4.95, the IEX is performed using buffers with higher pH (pH 8).

Initially, a preliminary linear gradient IEX was conducted to determine the optimal ionic strength required to identify the best NaCl concentration for isolating each targeted enzyme. Subsequently, a NaCl step gradient was applied to purify and isolate the targeted enzymes within a single cycle of the IEX procedure. This allows distinct peak separation and efficient removal of contaminants at lower ionic strengths before eluting the targeted enzymes at their specific targeted salt concentrations. The IEX purification was repeated at least three times, and the chromatogram profiling was constructed based on the mean absorbance values.

The elution buffer composition was set up as a step gradient at 5%, 10%, 20%, 30%, 40%, 50%, and 100% sodium chloride (NaCl) to elute the bovine BSAL. Each fraction representing different peaks was run on 1–dimensional sodium dodecyl sulphate–polyacrylamide gel electrophoresis (1D–SDS PAGE) for molecular weight determination. Fractions containing amylolytic activity based on the molecular weight were pooled and concentrated using a 30,000 MW and 50,000 MW Amicon® Ultra Centrifugal Filter (MERCK – Germany).

7.2.3 Bovine and Sheep Alpha–Amylase Protein and Peptide Identification

7.2.3.1 Determination of Protein Concentration

The total protein concentration of total crude pancreatic extract and purified fraction samples from IEX were measured. Absorbance was measured at 280 nm (A_{280}) using a NanoDrop® ND–1000 UV–Vis Spectrophotometer (Thermo Fisher Scientific – US). The obtained concentration values (mg/mL) were subsequently utilised to calculate the total protein content (mg) and were essential for determining the proteolytic enzymatic activity (U/mg) of the samples.

7.2.3.2 One–Dimensional Sodium Dodecyl Sulfate Polyacrylamide Gel Electrophoresis (1D–SDS PAGE)

The molecular mass of purified bovine and sheep pancreatic AMYP was estimated by 1D–SDS PAGE using NuPAGE 4–12% mini protein gel of Bis–Tris electrophoresis system in X Cell SureLock Mini–Cell (Invitrogen – US) stained with Coomassie Brilliant Blue stain (Invitrogen – US).

The sample was prepared as described in Table 7.1. The protein mixtures were prepared by adding protein sample (x µl), 4X NuPAGE LDS Sample Buffer (2.5 µl), 10X NuPAGE Reducing agent (1 µl), and Ultrapure water (y µl) in a 1.5 mL Eppendorf tube. The protein volume needed was calculated using the dilution formula (M1V1 = M2V2) based on the initial concentration of the protein. Then, Ultrapure water was added, bringing a 10 µl volume for sample preparation. The protein sample was heated at 70^{o}C for 10 mins before loading into the wells. The 1X NuPAGE MES SDS Running Buffer was prepared by adding 50 mL of 20X MES SDS Running Buffer to 950 mL of distilled water. The gel electrophoresis system was set up at 200 V (constant voltage) and 125 mA (current). The electrophoretic separation was conducted for approximately 35 to 45 minutes to ensure the complete resolution of the protein bands.

Table 7.1
Sample Preparation for SDS–PAGE

Chemicals	Volume (µl)
Protein Concentration	20 mg/ml
Protein Sample	*x*
NuPAGE LDS Sample Buffer (4X)	2.5
NuPAGE Reducing agent (10X)	1.0
Ultrapure water	*y*
Final Volume	**10.0**

The gel was transferred into a clean container and added with 50 ml of distilled water. Then, the gel was microwaved at high power for 1 min and shaken for 1 min. The steps were repeated twice. Then, the gel was added with Safely Blue Safe stain (Invitrogen – US) liquid. The gel was microwaved again at high for 45 secs and shaken for 5 mins. The gel was washed with distilled water and shaken for 10 mins before viewing with ChemiDoc™ Imaging System (BioRad – US).

7.2.3.3 Liquid Chromatography–Mass Spectrometry (LC–MS/MS)

Only protein band from sheep IEX was further identified using liquid chromatography–mass spectrometry (LC–MS/MS). Before the LC–MS/MS procedure, trypsin gel digestion was carried out. Then, a total of 5 µL sample was injected into Dionex Ultimate 3000 RSLCnano Orbitrap Fusion (Thermo Fisher Scientific – US) with EASY–Spray Acclaim PepMapTM C18 100 A0 (2 µm particle size, 50 µm id x 15 cm) separation column. The sample was eluted with LC–MS grade water, 0.1% formic acid (A), and ACN, 0.1% formic acid (B), at a 250 nL/min flow rate. The elution gradient was 5%–40% B for 91 min, 2 min to 85% B, 3 min at 85% B, 1 min at 5% B, and 4 min at 5% B. The full scan spectra were collected by Orbitrap MS (OTMS) scan mass ranging from 310 – 1800 m/z with 50 ms maximum injection. The spectra were analyzed by ion trap MS (ITMS) with 250 ms maximum injection. The LC–MS/MS data was analyzed using Thermo Scientific™ Proteome Discoverer™ Software Version 2.1. The results were matched with the database downloaded from UniProt. The variable modifications were oxidation (M) and acetyl (N–terminal), with fixed modification of carbamidomethyl (C). All peptides were validated using the percolator® algorithm,

based on a q–value of less than 1% false discovery rate (FDR). The LC–MS/MS analysis was performed at the Proteomic Laboratory, Malaysian Genome and Vaccine Institute, Bangi, Malaysia.

7.2.4 Amylolytic Enzyme Assay

Amylase activity was evaluated by starch hydrolysis plate assay. Muller–Hinton agar (MHA) was used for this plate assay. The detail composition of the MHA can be referred in Appendix 6. The MHA was prepared by mixing 7.6 g of MHA powder with 200 mL of distilled water. Then, the mixture was boiled to completely dissolve the medium. The medium was then sterilised using an autoclave, the machine was set at 121°C for 15 mins. After the autoclave was done, the agar solution was poured onto petri dishes and allowed to solidify. Once the MHA plates were solidified, the prepared MHA were stored at 2 – 8°C before use.

The sterilised cork borer was used to create circular holes on the MHA surfaces. Then, a total of 50 µL of each sample was poured into the designated holes made by the cork borer. The samples were allowed to dry at room temperature. The plate was then incubated at 37°C for 24 – 48 hrs. After incubation, the plates were flooded with Gram's iodine solution. After 1 – 2 mins, the excess Gram's iodine solution was removed from the plate. The clearing zone was observed and measured. The clearing zone serves as a qualitative indicator for amylolytic activity, where the samples contain amylase and can break down the starch. Meanwhile, no clearing zone indicates no amylolytic activity. The presence, size, and clarity of this zone are used to infer the level of enzymatic activity. A well–defined and large clearing zone typically suggests strong amylase production, while a faint or small zone may indicate low enzymatic output. Three starch hydrolysis plate assays were examined for each bovine and sheep samples.

7.3 Results

7.3.1 Extraction and Purification of Bovine Alpha–Amylase

Bovine pancreatic crude pancreatic extract was subjected to purification from fresh pancreatic tissue through delipidation, protein extraction, and IEX. Total of 200 mL of filtered bovine crude extract was loaded onto the pre–packed HiTrap Q Fast Flow column. Figure 7.2 shows the bovine pancreatic crude extract elution profile of IEX using a pre–packed HiTrap Q Fast Flow column. The IEX elution was performed with a step NaCl gradient (5 – 100%), whereby the enzymes were separated based on the ionic strength of the elution buffer. The elution profile shows eight distinct peaks after the IEX step. However, none of the fractions contained the targeted bovine AMYP pancreatic enzyme. No visible bands at the targeted molecular weight (57kDa) were observed across the fractions from each gradient, representing 10%, 20%, 30%, 40%, 50%, and 100% of NaCl concentration in the 1D–SDS PAGE (Figure 7.3).

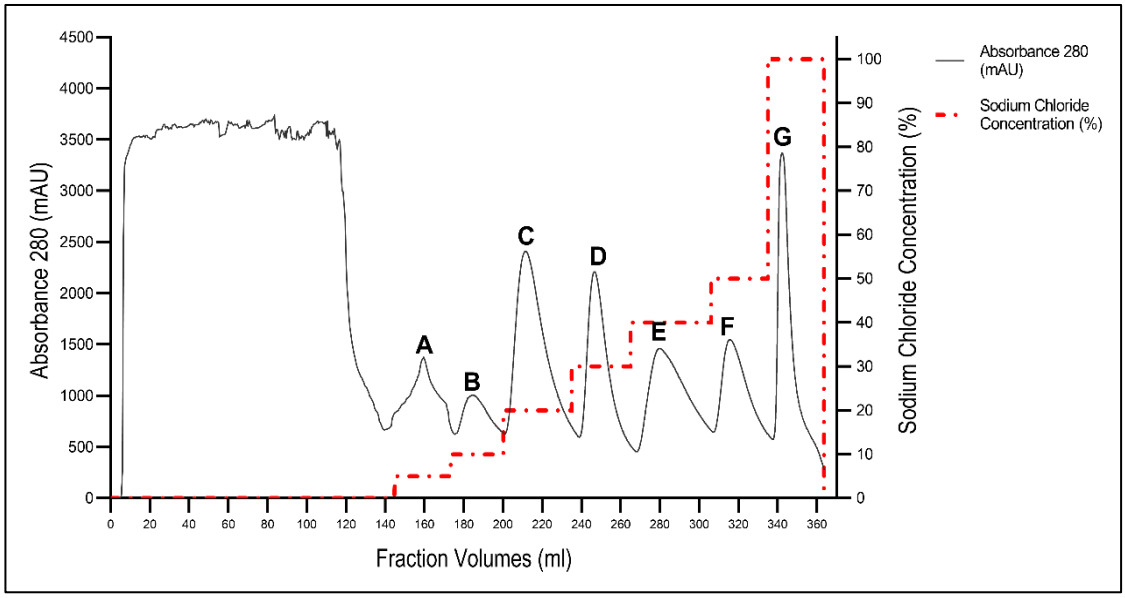


Figure 7.2 Anion–exchange Chromatography of Aqueous Crude Bovine Pancreatic Extract. There was no Bovine AMYP identified across NaCl gradient.

Note: The chromatogram represents the absorbance of the bovine crude extract at 280nm. Column: Hi Trap Q Fast Flow column (pre–packed); flow rate: 2.4mL/min; mobile phase: 20mM Tris pH8, 20mM Tris NaCl pH8.

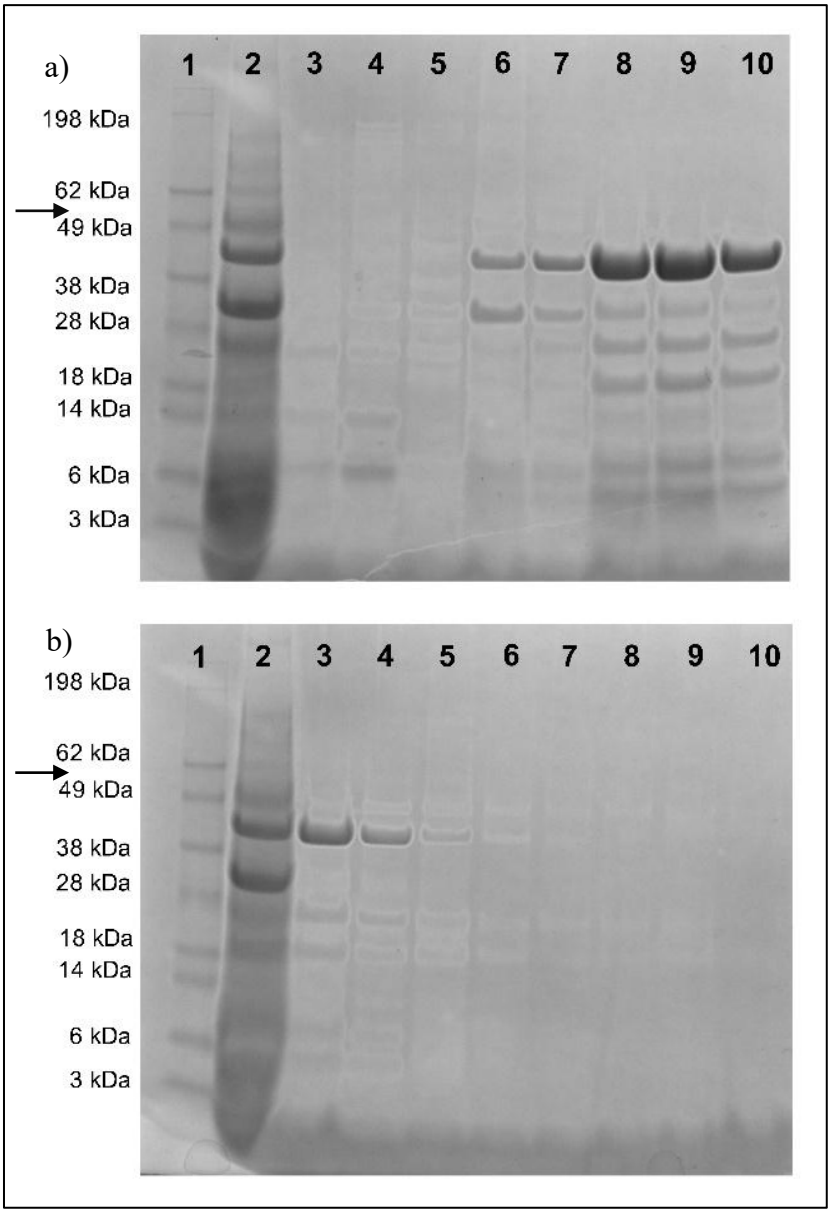


Figure 7.3 1D–SDS PAGE (Bis–Tris 12%) of Bovine Crude Extract. There was no Bovine AMYP identified across at the targeted molecular weight (57 kDa).

Note: a) Lane 1: SeeBlue® Pre–Stained Protein Standard; Lane 2: Crude Extract; Lane 3: 10% Fraction; Lane 4: 10% Fraction; Lane 5: 10% Fraction; Lane 6: 20% Fraction; Lane 7: 20% Fraction; Lane 8: 30% Fraction; Lane 9: 30% Fraction; and Lane 10: 30% Fraction. b) Lane 1: SeeBlue® Pre–Stained Protein Standard; Lane 2: Crude Extract; Lane 3: 30% Fraction; Lane 4: 40% Fraction; Lane 5: 40% Fraction; Lane 6: 40% Fraction; Lane 7: 50% Fraction; Lane 8: 50% Fraction; Lane 9: 50% Fraction; and Lane 10: 100% Fraction. The gel (Bis–Tris 12%) was stained with Coomassie blue.

7.3.2 Extraction and Purification of Sheep Alpha–Amylase

Sheep pancreatic crude pancreatic extract was subjected to purification from fresh pancreatic tissue through delipidation, protein extraction, and IEX. Figure 7.4 shows the sheep pancreatic crude extract elution profile of IEX using a prepacked HiTrap Q Fast Flow column. The IEX elution was performed with a step NaCl gradient (5 – 100%), whereby the enzymes were separated based on the ionic strength of the elution buffer. The elution profile shows eight distinct peaks after the IEX step. The fractions containing targeted sheep AMYP were pooled however, none of the fractions contained the targeted sheep AMYP pancreatic enzyme although there are visible bands estimated to be 60 kDa were observed across the fraction from gradient representing 30% (**Peak C**) and 40% (**Peak D**) of NaCl concentration in the 1D–SDS PAGE (Figure 7.5b, **Lane 5, 6, and 7**).

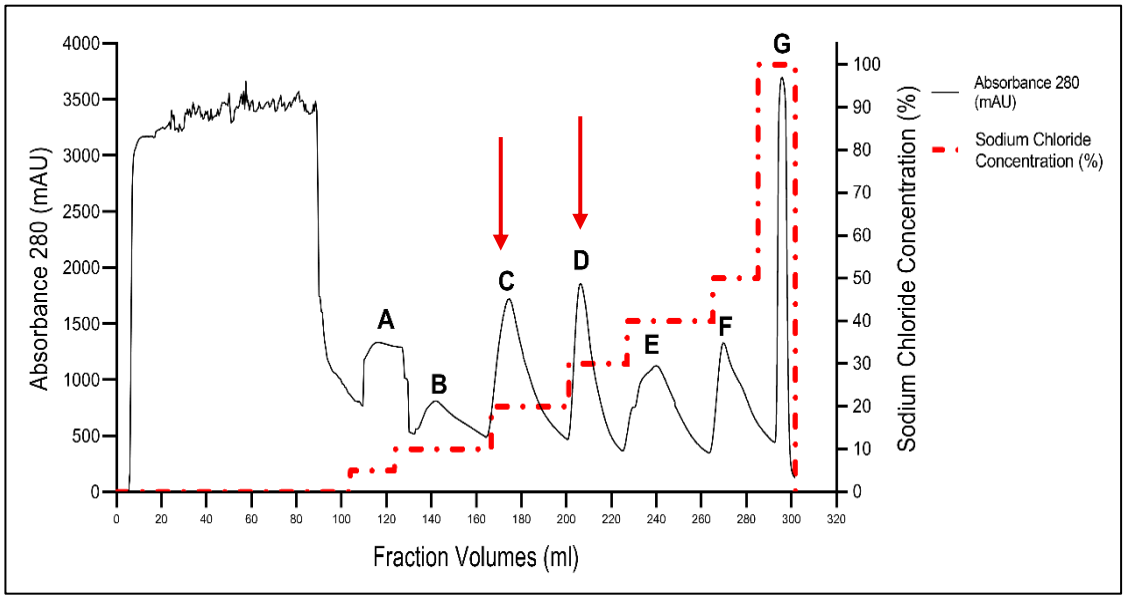


Figure 7.4 Anion–exchange Chromatography Of Aqueous Crude Sheep Pancreatic Extract. The predicted Sheep AMYP was eluted at Peak C (20% NaCl concentration) and at Peak D (30% NaCl concentration).

Note: The chromatogram represents the absorbance of the sheep crude extract at 280nm. Column: Hi Trap Q Fast Flow column (pre–packed); flow rate: 2.4mL/min; mobile phase: 20mM Tris pH8, 20mM Tris NaCl pH8.

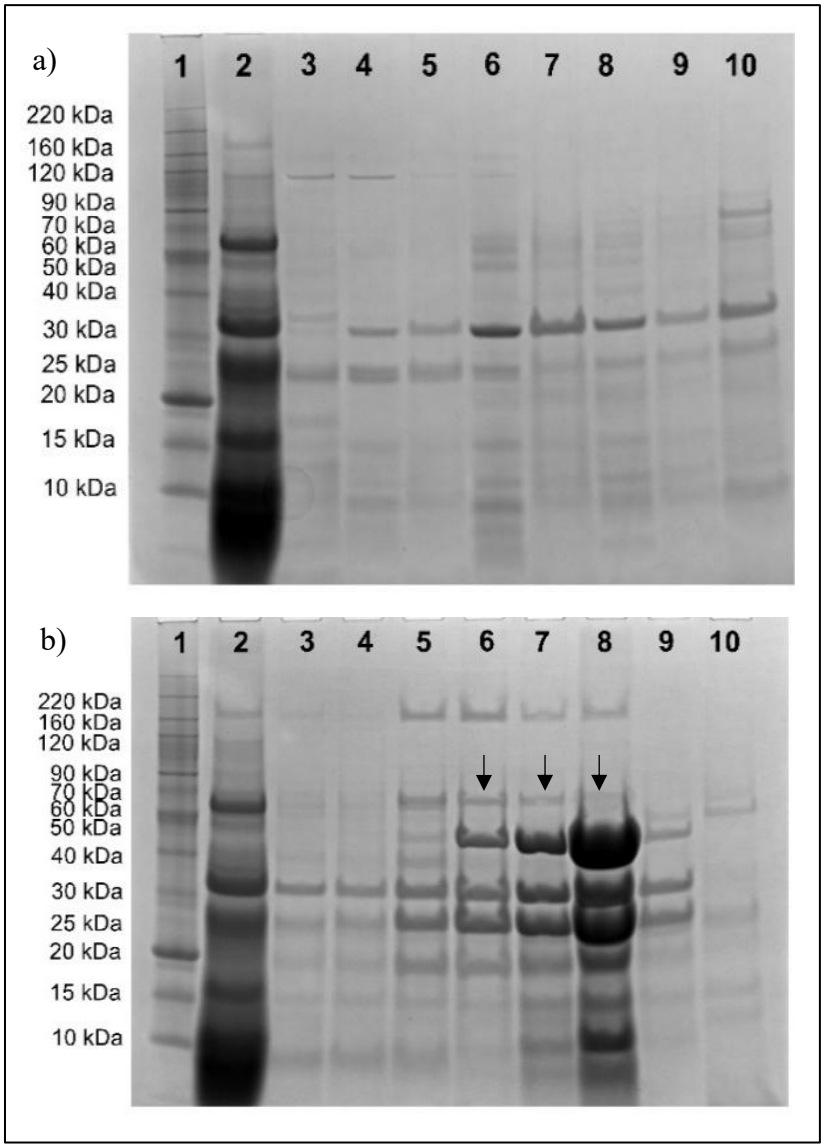


Figure 7.5 1D–SDS PAGE (Bis–Tris 12%) of Sheep Crude Extract. The Sheep AMYP was predicted to be approximately 57 kDa (b: Lane 5,6, and 7).

Note: a) Lane 1: Benchmark™ Unstained Protein Ladder; Lane 2: Crude Extract; Lane 3: 10% Fraction; Lane 4: 10% Fraction; Lane 5: 10% Fraction; Lane 6: 10% Fraction; Lane 7: 20% Fraction; Lane 8: 20% Fraction; Lane 9: 20% Fraction; and Lane 10: 20% Fraction. b) Lanel 1: Benchmark™ Unstained Protein Ladder; Lane 2: Crude Extract; Lane 3: 30% Fraction; Lane 4: 30% Fraction; Lane 5: 30% Fraction; Lane 6: 40% Fraction; Lane 7: 40% Fraction; Lane 8: 50% Fraction; Lane 9: 50% Fraction; and Lane 10: 100% Fraction. The gel (Bis–Tris 12%) was stained with Coomassie blue.

The band, expected to be sheep AMYP, was excised and destained for LC–MS/MS protein and peptide identification. However, the LC–MS/MS findings indicated that the targeted enzyme of interest, which is sheep AMYP, was not detected in this analysis. Despite the application of standard protein extraction, tryptic digestion, and high–resolution mass spectrometric analysis, no unique peptides were corresponding to the target protein passed the established identification thresholds. Instead, peptides matching a different protein known as a sheep pancreatic TL (Accession number – W5Q5I2) were consistently identified with high confidence, based on multiple unique peptides and strong peptide–spectrum matches (data not shown). The protein identification and peptide sequence prediction of sheep pancreatic TL via LC–MS/MS can be accessed through Table 6.3.

7.3.3 Amylolytic Enzyme Assay

The amylolytic activity was observed and measured using the starch hydrolysis on MHA for crude extract and pooled IEX samples. The α–amylase from porcine pancreas (1mg/mL) (Sigma Aldrich – Germany) was used as a positive control. The clear zone indicates the presence of amylase in the samples. The starch hydrolysis results of bovine and sheep samples are shown in Figure 7.6, Table 7.2 and Table 7.3, list the diameter of the clearing zone produced by bovine and sheep samples, respectively. Both bovine and sheep pancreatic crude extracts produced a consistent diameter of approximately 28 mm in diameter of the clearing zone. Similarly, to the positive control, the diameter of the clearing zone produced was also approximately 27 mm. The clearing zones produced by bovine and sheep pancreatic crude extracts were nearly identical to those of the positive control, demonstrating equivalent amylolytic activity on the MHA plate. Meanwhile, both the purified samples of bovine and sheep have shown less than 12 mm in diameter of the clearing zone. Therefore, the purified samples from the IEX showed low amylase content compared to the crude extracts. From the starch hydrolysis on the MHA, the crude pancreatic extracts from bovine and sheep can be suggested as an alternative source for pancreatic amylase.

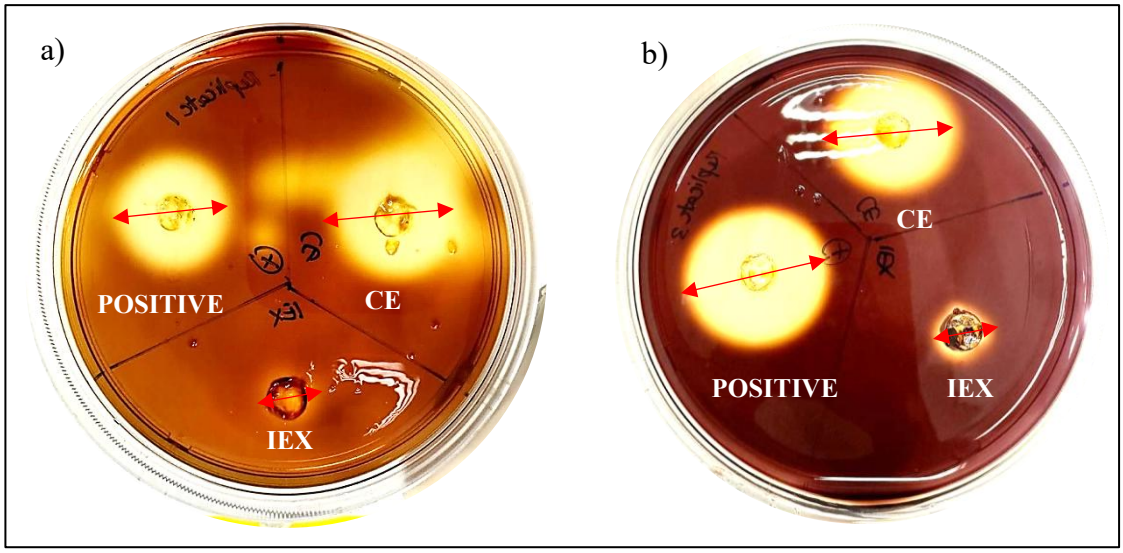


Figure 7.6 Starch hydrolysis of a) Bovine and b) Sheep samples on MHA.

Note: Crude extract (CE), Anion exchange chromatography (IEX) and Positive control – α–amylase from porcine pancreas.

Table 7.2
Starch Hydrolysis of Bovine Samples on MHA

Samples	Clearing Zone (mm)			
	Plate 1	Plate 2	Plate 3	Mean
Positive Control	27	28	28	27.6
Crude Extract	27	27	26	26.7
IEX	11	10	10	10.3

Table 7.3
Starch Hydrolysis of Sheep Samples on MHA

Samples	Clearing Zone (mm)			
	Plate 1	Plate 2	Plate 3	Mean
Positive Control	28	28	29	28.3
Crude Extract	26	27	28	27.0
IEX	12	12	11	11.7

7.4 Discussion

Enzymes are purified for various reasons, such as to fully characterize or to mass produce for commercial purposes (Dako *et al.,* 2012). This is the latest report on the AMYP purification from bovine and sheep fresh pancreas tissue samples. The earliest research began to investigate on the bovine and sheep extraction and purification of pancreatic AMYP was done in the mid–1970s (Banks *et al.,* 1976; Ettalibi *et al.,* 1975). Both of these studies reported on the successful of the pancreatic AMYP purification. Conversely to the previous findings, the attempt to extract and purify the pancreatic AMYP was unsuccessful in both bovine and sheep pancreatic samples.

Although extensive research has been conducted on amylase applications, no recent report on the extraction and purification of pancreatic amylase. In this study, the pancreatic tissues from bovine and sheep were processed for the crude extract and subjected to a one–step IEX. No visible band at the targeted size (57 kDa) across the fractions from different NaCl concentrations on the 1D–SDS PAGE from bovine crude extract. Meanwhile, there are visible bands expected to be sheep pancreatic AMYP at the targeted size of approximately 57 kDa on the 1D–SDS PAGE (Figure 7.5b – **Lanes 5, 6, and 7**) from the sheep crude extract. However, the LC–MS/MS analysis confirmed that these bands do not contain the predicted sheep pancreatic AMYP. Thus, no further purification steps were taken since the targeted enzymes are absent in this sample. The unexpected identification of sheep TL instead of sheep AMYP within the same excised gel band can be attributed to their high similarity in isoelectric point (pI) and molecular weights (MW). This could be postulated that a high abundance of TL has been co–eluted during the one–step IEX and co–migrated on the 1D–SDS PAGE. Consequently, the dominant presence of this stable TL has masked any potentially degraded or low–abundant AMYP within that specific fraction. This leads to the sheep TL definitive high–confidence identification during the LC–MS/MS analysis.

Generally, there are no set protocols to purify different enzymes. The protocols of the purification can be customized and designed according to the enzyme of interest characteristic and behaviour. In addition, the literature focusing on the ruminant pancreatic AMYP purification is limited. The research to date highlights the purification of Alpha–Amylase from microorganisms and plants (Abdelmalek *et al.,* 2025; Pawar *et*

al., 2025; Zhang *et al.,* 2025). In this study, attempts to extract and purify pancreatic AMYP from fresh bovine and sheep pancreas using a one–step IEX did not yield detectable levels of active enzyme. The absence of significant enzymatic activity of the purified samples, as evidenced by the lack of clearing zones on MHA as well as no protein bands detected on 1D–SDS PAGE for bovine and confirmed by LC–MS/MS for sheep corresponding to AMYP, indicates the unanticipated findings of the current extraction and IEX purification approach.

There are several possible contributing factors attributed to the unsuccessful extraction and purification of the bovine and sheep pancreatic AMYP. Firstly, the selection of one–step purification step strategy, although efficient in theory, may not have been sufficient to isolate AMYP from a complex mixture of pancreatic proteins and inhibitors present in bovine and sheep tissues. Although it is advisable to use the minimum number of steps during the purification procedure to minimize the enzyme activity losses does not reflect our findings. The previous study employed multi–step purification protocols, including salt fractionation, GFC, and IEX, which likely contributed to higher purity and yield of AMYP (Banks *et al.,* 1976; Ettalibi *et al.,* 1975). In contrast, this study utilises the fresh pancreatic bovine and crude extract directly to the IEX.

The inability to isolate bovine and sheep AMYP suggests that one–step IEX was inadequate for resolving the enzyme from the highly complex pancreatic matrix. Given that the pancreatic crude extract contains an enormous range of digestive enzymes and inhibitors, it is probable that contaminants possessing pI similar and MW to AMYP bound to the column and eluted at the same salt concentration, thereby preventing effective isolation. This limitation contrasts with historical studies that successfully purified ruminant amylase by employing multi–step protocols, including ammonium sulphate precipitation and GFC, to reduce sample complexity prior to or alongside chromatographic separation. Consequently, the absence of these preliminary pre–fractionation steps in the current protocol likely resulted in the AMYP being masked by other proteins or lost among the high volume of contaminants during the elution process.

Other factors, such as the enzyme stability from the fresh pancreas to crude extraction and purification, also need to be performed under controlled conditions, which includes form the time of sample collection and extraction to purification, the buffer pH, and temperature must be considered as the amylase is sensitive can be degraded easily leading to loss of activity over time. The purification was done under room temperature and this may have contributed to the enzyme's instability, as temperature and exposure time are critical dependencies for enzyme denaturation. Consequently, conducting the purification under cold conditions could help to preserve the enzyme's structural integrity and activity by minimizing the risk of degradation and inactivation caused by proteolytic effects during the isolation process. To add, the enzyme instability may also happen due to loss of an inactivating cofactor or inactivation of the enzyme caused by the proteolytic effects (Vijayaraghavan *et al.,* 2016). Some enzymes require a divalent metal, such as Magnesium or Calcium, to enhance the enzyme–specific activity and influence enzyme stability (Sharon *et al.,* 1998). Recent evidence suggests that the inclusion of divalent metal ions, specifically Ca2+ and Mg2+, had a positive effect on the activity of the enzyme (Zafar *et al.,* 2025).

Furthermore, the fresh pancreas tissue samples were randomly collected from the abattoir. There was no details information on animal age, breed, gender, animal's nutrition, and diet. The differences in animal age, breed, diet, or tissue handling between this and previous studies could also affect enzyme abundance and integrity. The experimental design does not involve the control animal feed intake, and the variation in animal feed could vary from different animals, which may have impacted to variability in the enzyme production and expression, including the amylase. Previous studies demonstrate that the starch feed will increase the production of Alpha–Amylase content in ruminants (Harmon, 1992). In another study, the supplementation of starch in the feeding system was reported to increase the Alpha–Amylase activity (Xu *et al.,* 2009). It is also possible that variations in AMYP isoforms among different species or individuals contribute to challenges in purification.

The recent advancement in purification technology was indeed expected to improve the purification efficiency; however, our findings suggest that modifications in the extraction and purification protocols are necessary. Future recommendations for the pancreatic AMYP extraction and purification from bovine and sheep could be improved

by protease inhibitors, optimizing buffer compositions, adjusting ionic strength and pH, or adding additional purification steps, such as affinity chromatography, to enhance enzyme stability and recovery.

7.5 Conclusion

In conclusion, AMYP was not successfully purified and characterized from fresh pancreatic tissues in bovine (*Bos* taurus) and sheep (*Ovis aries*). The pancreatic crude extract recorded higher amylolytic activity when compared to the positive control based on the formation of a clear zone on the MHA. The absence of bovine pancreatic AMYP was confirmed with 1D–SDS PAGE, where no visible band was at the targeted molecular weight, and sheep pancreatic AMYP was further confirmed with LC–MS/MS after the IEX, with no matching protein and peptide identifications that is related to sheep AMYP. Overall, the unsuccessful extraction and purification in this study highlight the complexity of isolating functional pancreatic AMYP from bovine and sheep pancreas. Therefore, further investigation is recommended on the optimization of the purification method to purify AMYP in both bovine and sheep pancreatic tissue before it can be suggested as an alternative substitute, as Halal–certified enzymes to porcine enzymes in medical and pharmaceutical applications.

CHAPTER 8
PANCREATIC ENZYMES BIOINFORMATICS *IN–SILICO* ANALYSIS AND EXPERIMENTAL GLYCOSYLATION PROFILING

8.1 Introduction

Proteins are complex macromolecules that have an essential role in cellular activity (Singh *et al.,* 2016). The comprehensive analysis of these functional proteins is critical to determine their biological functions, that leads to a better understanding of their mechanisms and roles within the body. With the advancement and rapid evolution of computational biology, bioinformatic *in–silico* tools have emerged as highly advanced and essential methods to analyse proteins. These computational approaches empower researchers and scientist to efficiently predict protein sequences, three-dimensional (3D) model structures, and evaluate complex biochemical properties prior to conducting experiments in the lab.

With profound modern bioinformatics platforms available online and offline enable in depth protein characterisation. Fundamental protein information such as amino acid sequences, molecular weights (MW), and isoelectric points (pI) can be gathered from comprehensive databases like UniProt and the Expasy servers. Furthermore, advanced sequence homology modelling utilizing tools like pBLAST allows for precise multiple and pairwise sequence alignments, enabling researchers to identify evolutionary relationships and find the most suitable template models for the targeted proteins. Following that, an accurate 3D protein structures can be generated using these templates on online servers such as SWISS-Model. Then, the quality of the 3D protein structure can be validated through MolProbity scores, Ramachandran plot and Root Mean Square Deviation (RMSD).

One of the most critical applications of these advanced *in–silico* tools is the evaluation of Post-Translational Modifications (PTMs) such as glycosylation. PTMs immensely increase the functional diversity of the proteome and dictate enzyme

stability, folding, solubility, and molecular trafficking (Ramazi & Zahiri, 2021). By utilizing prediction servers like GlycoPred, NetNGlyc, and NetOGlyc, bioinformatic approaches can precisely forecast potential N-linked (NLG) and O-linked (OLG) glycosylation sites based on consensus sequences. Coupled with advanced molecular visualization software like PyMOL, researchers and scientist can visually map these predicted glycosylation sites to determine whether they are exposed on the protein's outer surface or buried deep within its structure. The analysis and knowledge of the protein are important to determine its function, leading to a better understanding of its role and mechanism in the human body (Singh *et al.,* 2016).

Thus, the bioinformatic tools can help to predict the sequence and structure to understand the other properties of glycoproteins, such as their functional and biochemical properties. These tools help to identify glycosylation sites, predict the type of glycan modifications, and model their 3D structures, which are crucial for studying how glycoproteins interact with other molecules and their role in various biological processes. Although these bioinformatic *in–silico* analyses provide powerful predictions and insights, it is essential to evaluate the findings with wet lab experimental data. The experimental data will help to confirm and validate the findings. The combination of the *in–silico* and wet lab experimental findings will provide a more comprehensive and accurate understanding of the glycosylation of the pancreatic enzymes of interest.

In the present work, we evaluated and characterized the pancreatic enzymes of interest, such as Carboxypeptidase A1 (CBPA1), Bile–Salt Activated Lipase (BSAL), Triacylglycerol Lipase (TL), and Alpha–Amylase (AMYP) using the *in–silico* bioinformatic approach. In this study, the potential N–glycosylation and O–glycosylation positions in the pancreatic enzyme of interest, such as bovine and sheep, were analysed with a comparison to the human and porcine, 3D protein structures were predicted, and a 3D glycoproteins model was constructed. At the same time, the glycoprotein wet lab assessment via 1D–SDS PAGE and specialized staining was also carried out to visualize the glycoprotein from the bovine and sheep samples alongside the human prostate and commercial porcine enzyme as positive controls.

8.2 Materials and Methods

This study consists of two major parts. The first part focused on bioinformatic approaches for *in–silico* glycosylation prediction and visualization. Its goal was to gather all the protein information, such as functions, molecular weight (MW), isoelectric point (pI), sequences, structure, and predict and visualize the glycosylation site of the selected pancreatic enzyme of interest. The second part focused on the experimental glycosylation profiling of the pancreatic enzymes of interest. The glycosylation profiling used a unique glycosylation staining method with a glycoprotein enrichment technique to assess the glycosylation state of the pancreatic enzymes of interest.

8.2.1 *In–Silico* Glycosylation Assessment

8.2.1.1 Gathering Selected Protein Information

The amino acid sequences of pancreatic enzymes of interest – Carboxypeptidase A1 (CBPA1), Bile–Salt Activated Lipase (BSAL), Triacylglycerol Lipase (TL), and Alpha–Amylase (AMYP) from bovine, sheep, porcine, and human were obtained from online databases: UniProt (https://www.uniprot.org/). The name of the protein was keyed into the database search box. Protein information, such as accession numbers (ID), functions, sequences, and length of amino acid sequences was successfully gathered. Additional protein information, such as molecular weight (MW) and isoelectric point (pI) of all the selected proteins, was obtained from the Expasy (https://web.expasy.org/compute_pi/) online server. The FASTA sequences obtained from UniProt were used as sequence templates for MW and pI information execution.

8.2.1.2 Sequence and Structure Analysis of Homology Modeling

After gathering all the protein information, the study continued with sequence and structure analysis of the pancreatic enzymes of interest such as Carboxypeptidase A1 (CBPA1), Bile–Salt Activated Lipase (BSAL), Triacylglycerol Lipase (TL) and Alpha–Amylase (AMYP) from different variants available, such as bovine, sheep, porcine, and human. The sequence homology modelling was done using two steps: multiple Sequence Alignment and Pairwise Sequence Alignment. These methods are crucial to determine the best template for all selected pancreatic enzymes of interest.

a) Multiple and Pairwise Sequence Alignment

Sequence alignment tools known as Basic Local Alignment Search Tool (pBLAST) (https://blast.ncbi.nlm.nih.gov/Blast.cgi) search was carried out to identify the most suitable template for all pancreatic enzymes of interest. The main and template protein sequences were aligned for the multiple and pairwise sequence analysis, and the pBLAST generated the results directly. This step will determine one template model with a high similarity percentage for each pancreatic enzyme of interest for the subsequent analysis. At the same time, the PDB file was downloaded from the PDB database (https://www.rcsb.org/), and the homology modelling crystal structure was utilized. The resolution value, Ångström (Å), was considered to determine the quality of the protein structure. The protein template structure less than 2.30 Å was considered a high–quality structure.

The FASTA sequence of each pancreatic enzyme of interest was keyed in to be aligned with the template model candidate sequence. The FASTA sequences of the template candidates were obtained from the Research Collaboratory for Structural Bioinformatics Protein Data Bank (RCSB PDB) database (https://www.rcsb.org/). The next step used one template deduced from this step for each pancreatic enzyme.

b) Protein Modeling

The protein modelling was performed using the SWISS–Model (https://swissmodel.expasy.org/) online server on the targeted pancreatic enzyme of interest. The targeted protein FASTA sequence was used as input. The quality of the 3D protein model structure templates was measured and selected based on MolProbity score, Ramachandran plot and Root Mean Square Deviation (RMSD). A lower MolProbity score indicates a higher quality structure with fewer steric clashes, more favourable Ramachandran plot with better overall geometry structure. The MolProbity score between 1.5 to 3.0 is considered a good score. For the Ramachandran plot, three items, the 'fully allowed or favoured part,' 'outer limit or allowed part,' and the 'disallowed part', were considered (Singh *et al.,* 2016, Kumar & Sharma, 2020). The structure is considered stable when most atoms fall into the fully allowed part.

Additionally, the overall structural accuracy of the generated models can be validated by calculating the RMSD. The RMSD measures the average deviation of protein atomic positions of the superimposed generated 3D model structure and its corresponding experimental template (Ishabiyi *et al.,* 2026). The high structural similarity and stability, a lower RMSD value is required with ≤ 2.0 Å generally accepted as the minimum threshold for a high–quality homology model.

c) Glycosylation Sites Prediction and Visualization

Two major types of glycosylation, N–linked (NLG) and O–linked (OLG) glycosylation were predicted using an available online server. The NLG occurs on asparagine (N) residues within an N–X–S or N–X–T sequence (X is any amino acid other than P – proline or D – aspartic Acid) (An *et al.,* 2017). The OLG occurs on the side chain hydroxyl oxygen of serine (S) or threonine (T) residues.

GlycoPred Server (https://comp.chem.nottingham.ac.uk/glyco/) was used to determine possible NLG and OLG sites. The threshold was set to 0.5 to predict high–potential sites for both NLG and OLG site prediction. In addition, NetNGlyc 1.0 (https://services.healthtech.dtu.dk/services/NetNGlyc–1.0/) and NetOGlyc 4.0 (https://services.healthtech.dtu.dk/services/NetOGlyc–4.0/) were also used to predict

the NLG and OLG, respectively. Generally, for both NLG and OLG predicted from the NetGlyc server, scores more than 0.5 indicate positive prediction of glycosylation sites. The FASTA sequences of the main proteins were required to run the glycosylation sites prediction, and the results were generated automatically by the online server. Finally, when the possible NLG and OLG sites were identified, PyMOL software was used to visualize the glycosylation location of all sites. This software assists in visualizing and locating the glycosylation sites on the protein sequence and structure, whether they are buried deep inside the protein or on the surface of the protein. Figure 8.1 summarizes the workflow for *in–silico* characterization and glycosylation assessment of pancreatic enzymes.

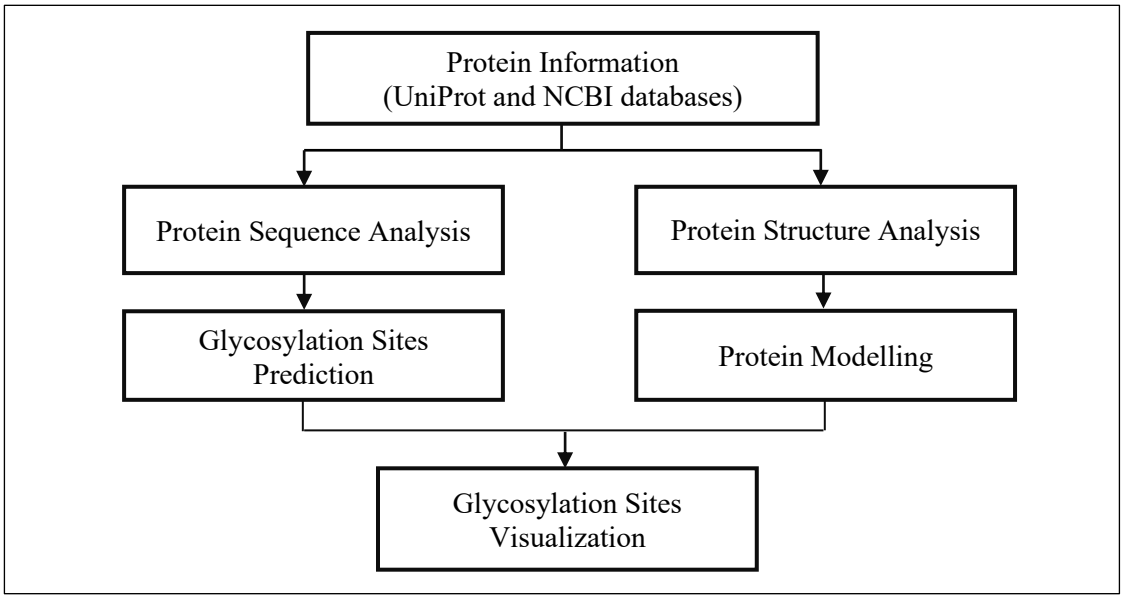


Figure 8.1 *In–silico* Characterization and Glycosylation Site Prediction of Pancreatic Enzymes.

8.2.2 Experimental Glycosylation Profiling and Visualization

8.2.2.1 Glycosylation Profiling via *1D–SDS PAGE*

The MW of the purified pancreatic enzymes (bovine CBPA1, sheep CBPA1, bovine BSAL and sheep TL) from the purification steps were estimated by 1D–SDS PAGE done using NuPAGE 4–12% mini protein gel of Bis–Tris electrophoresis system in X Cell SureLock Mini–Cell (Invitrogen – US). Three different types of staining: Coomassie Brilliant Blue stain (Invitrogen – US), Pro–Q ® Emerald 300 Glycoprotein stain (Molecular Probes®), and Sypro Ruby stain were used.

Specifically, the Pro–Q ® Emerald 300 Glycoprotein stain was utilized to selectively visualize carbohydrate moieties present on the purified pancreatic enzyme. The presence of glycosylation will be detected when the carbohydrate moieties were oxidized with periodate solution, forming reactive aldehyde groups that reacts towards the fluorescent stain. In contrast, Coomassie Brilliant Blue and Sypro Ruby stains were employed to visualize the total protein content, serving as controls to verify the presence of the purified enzymes, regardless of their glycosylation status. Consequently, the detection of glycosylation was determined by aligning the bands; a protein was considered glycosylated if a fluorescent band observed in the Pro–Q ® Emerald 300 stained gel corresponded to the same molecular weight band identified in the total protein stains.

For the 1D–SDS PAGE, the sample was prepared as described in Table 8.1. The protein mixtures were prepared by adding protein sample (x µl), 4X NuPAGE LDS Sample Buffer (2.5 µl), 10X NuPAGE Reducing agent (1 µl), and Ultrapure water (y µl) in a 1.5 mL Eppendorf tube. The protein volume needed was calculated using the dilution formula (M1V1=M2V2) based on the initial concentration of the protein. Then, Ultrapure water was added, bringing a 10 µl volume for sample preparation. The protein sample was heated at 70^{o}C for 10 mins before loading into the wells. The 1X NuPAGE MES SDS Running Buffer was prepared by adding 50 mL of 20X MES SDS Running Buffer to 950 mL of distilled water. The gel electrophoresis system was set up at 200 V (constant voltage) and 125 mA (current). The time it takes for the protein to separate completely is about 35–45 mins.

Table 8.1
Sample Preparation for SDS–PAGE

Chemicals	Volume (µl)
Protein Concentration	20 mg/mL
Protein Sample	*x*
NuPAGE LDS Sample Buffer (4X)	2.5
NuPAGE Reducing agent (10X)	1.0
Ultrapure water	*y*
Final Volume	**10.0**

8.2.2.2 Glycoprotein Enrichment via *Glycosylation Isolation Kit*

The glycoprotein enrichment was done using the Glycosylation Isolation Kit, Con A (Thermo Scientific – US). The 1X Binding/Wash buffer was prepared by adding 460 µL 5X Binding/Wash buffer with 1840 µL of ultrapure water for one sample. The column was inserted into a collection tube. The Con A Lectin resin binds specifically to glucose, and mannose was gently swirled to obtain a homogenous suspension. A total of 200 µL of 50% resin slurry was transferred to the column using a wide–bore pipette tip. The column was centrifuged at 1000 x g for 1 min to remove the storage buffer. The collection tube was reused until before fraction collection. The column was placed in the collection tube, and 200 µL of 1X Binding/Wash buffer was added to the resin. The top cap was closed, the column was centrifuged at 1000 x g for 1 min, and the rinse was discarded. This step was repeated two times. The bottom cap was placed on the column, and the sample was added to the resin. The samples were prepared by adding 40 µL of 5X Binding/Wash Buffer with 20 µL of sample and 140 µL of ultrapure water. The top cap was closed, and the column was incubated at room temperature for 10 mins with an end–over–end rotator. Then, the top and bottom caps were removed from the column, and the column was placed into the collection tube. The top was replaced. The column was centrifuged at 1000 x g for 1 min, and the flow–through was collected into a new Eppendorf tube. The column was reinserted and added to the resin with 200 µL of 1X Binding/Wash buffer. The column was capped and centrifuged at 1000 x g for 1 min, and the flow–through was collected using the same Eppendorf tube. This step was repeated one time. The bottom cap of the column was placed and added

with 200 µL of 1X Binding/Wash buffer to the column and incubated at room temperature for 5 mins on the end–over–end rotator. The top and bottom caps were removed from the column. The column was placed in the collection tube, and the top cap was replaced. The column was centrifuged at 1000 x g for 1 min, and the rinse was collected in the same Eppendorf tube. These fractions were assigned as an unbound sample (Fraction 1).

The bottom cap was replaced on the column, and 200 µL of 1X Elution buffer was added to the resin. The column was capped. It was then incubated at room temperature for 5 mins on the end–over–end rotator. The top and bottom caps were removed from the column. The column was placed in the new collection tube, and the top cap was replaced. The column was centrifuged at 1000 x g for 1 min. The flow–through was collected using the new Eppendorf tube. This step was repeated two times. The elute was collected using the same new Eppendorf tube. These fractions were assigned as a bound sample (Fraction 2). The eluted glycoproteins were stored immediately on ice for immediate use.

8.2.2.3 Glycoprotein Acetone Precipitation

The required volume of acetone was cooled to –20°C. The unbound and bound glycoprotein samples were placed in the acetone–compatible tubes. Four times the sample volumes of cold –20°C acetone was added to the glycoprotein sample tubes. The tubes were vortexed and incubated at –20ºC for 60 mins. Then, the tubes were centrifuged at 13000 – 15000 x g. The supernatants were decanted and adequately disposed of, and extra care was taken not to dislodge the protein pellet. The acetone evaporated from the uncapped tubes at room temperature for 30 mins.

8.2.2.4 Glycosylation Staining

a) Coomassie Brilliant Blue staining

The gel was transferred into a clean container and added to 50 mL of distilled water. Then, the gel was microwaved at high power for 1 min and shaken for 1 min. The steps were repeated twice. Then, the gel was added with Safely Blue Safe stain (Invitrogen – US) liquid. The gel was microwaved again at high for 45 secs and shaken for 5 mins. The gel was washed with distilled water and shaken for 10 mins.

b) Pro–Q ® Emerald 300 Glycoprotein staining

The gel was stained using Pro–Q ® Emerald 300 Glycoprotein Gel and Blot Stain Kit (Invitrogen – US). The CandyCane^{TM} Glycoprotein Molecular Weight Standard (Invitrogen – US) was used as the protein ladder. The gel was transferred into a clean container. The gel was fixed with 25 mL of Fix solution and incubated at room temperature with gentle agitation on an orbital shaker for 10 – 20 mins. This step was repeated once more. The gel was washed with 100 mL of washing solution with gentle agitation for 10 – 20 mins. This step was repeated once more. The gel was oxidized with 25 mL of oxidizing solution with gentle agitation for 30 mins. Then, the gel was washed with 100mL of washing solution with gentle agitation. This step was repeated twice more. The fresh Pro–Q ® Emerald 300 Glycoprotein staining solution was prepared by adding 500µL of Pro–Q ® Emerald 300 stock solution with 25 mL of staining buffer. The gel was incubated with 25 mL of the Pro–Q ® Emerald 300 Glycoprotein staining solution while gently agitating for 90 – 120 mins. The gel was washed with 100 mL of washing solution at room temperature for 15 – 20 mins. This step was repeated once more. The same gel was used for the following staining method.

c) Sypro Ruby Staining

The gel was transferred into a clean container. The gel was fixed in 25 mL of fixing solution. The fixing solution comprised 50% methanol and 7% acetic acid. The gel was gently agitated for 30 mins. The fixing solution was discarded and added with 25 mL of Sypro Ruby staining solution (Invitrogen – US) incubated in the dark (covered with aluminium foil) and gentle agitation on an orbital shaker overnight. Then, the gel was washed with 50 mL of washing solution. The washing solution comprised 10% methanol and 7% acetic acid. The gel was rinsed with distilled water twice for 5 mins before imaging.

8.3 Results

8.3.1 *In–silico* Characterization and Glycosylation Prediction.

The *in–silico* investigation was compared the pancreatic enzymes of interest based on homology modelling of sequence and structure. At the same time, these *in–silico* findings also help with preliminary glycosylation prediction before the glycosylation state of the pancreatic enzyme of interest can be validated. Carboxypeptidase A1 (CBPA1) was successfully extracted and purified as a protease from bovine and sheep. For lipase, Bile–Salt Activated Lipase (BSAL) and Triacylglycerol Lipase (TL) were successfully extracted and purified from bovine and sheep, respectively. However, the Alpha–Amylase (AMYP) was not successfully extracted and purified from bovine and sheep. Table 8.2 shows the protein information of the pancreatic enzymes of interest, such as accession numbers (ID), functions, sequences, MW, and pI. Three classes of pancreatic enzymes of interest were investigated: protease, lipase, and amylase. The protein information included all the pancreatic enzymes of interest from bovine, sheep, pig, and human hosts.

For CBPA1, the MW ranged from 46.9 to 47.2 kDa. There were also no differences in amino acid numbers except for less than one amino acid in sheep. The pI ranged from 5.13 to 5.45 for the CBPA1 protease class. For BSAL, the MW varied between 65.0 to 79.3 kDa, with pI ranging from 5.13 to 5.92. For TL, the MW ranged from 50.0 to 52.2 kDa with pI between 5.73 to 6.33. And lastly, for amylase, the MW ranged from 56.9 to 57.7 kDa, and the pI ranged from 4.95 to 6.6.

The MW of the studied enzymes of interest shows considerable variation, with BSAL exhibiting the highest MW range (65.0–79.3 kDa) and CBPA1 the lowest (46.9–47.2 kDa). This suggests differences in structural complexity and potential functional roles among the enzymes. The pI also varied, with CBPA1 and BSAL having similar lower pI values (around 5.13–5.45 and 5.13–5.92, respectively), while TL and amylase displayed slightly higher pI ranges (up to 6.33 and 6.60, respectively). These variations in pI indicate differences in the net charge of the enzymes at physiological pH, potentially influencing their solubility, stability, and interactions within the biological system.

Table 8.2
Protein Information of Pancreatic Enzymes of Interest

Enzyme Class	Enzyme Protein ID	Molecular Weight (Da)	Isoelectric Point (pI)	Amino Acid Length	Function(s)
Protease (Carboxypeptidase A1) Other names: Carboxypeptidase A1 precursor	CBPA1_BOVIN UniProt ID: P00730	47082.06	5.33	419	• Catalyses the release of a C–terminal amino acid • Metallocarboxypeptidase activity • Zinc ion binding • Leukotriene metabolic process • Proteolysis
	W5P5N4_SHEEP UniProt ID: W5P5N4	46898.00	5.33	418	
	CBPA1_PIG UniProt ID P09954	47235.25	5.13	419	
	CBPA1_HUMAN UniProt ID: P15085	47140.27	5.45	419	
Lipase (Bile–salt Activated Lipase) Other names: Bile salt–activated lipase precursor Bile salt–stimulated lipase Carboxyl ester lipase Cholesterol esterase Pancreatic lysophospholipase Sterol esterase	CEL_BOVIN UniProt ID: P30122	65162.00	5.32	597	• Catalyzes the hydrolysis of a wide range of substrates, including cholesteryl esters, phospholipids, lysophospholipids, di– and tri–acylglycerols, and fatty acid esters of hydroxy fatty acids (FAHFA) • Preferentially hydrolyses FAHFAs with the ester bond further away from the carboxylate. • Has an essential role in the complete digestion of dietary lipids and their intestinal absorption, along with the absorption of fat–soluble vitamins.
	A0A286ZKB1_PIG UniProt ID: A0A286ZKB1	70923.00	5.92	652	
	CEL_HUMAN UniProt ID: P19835	79322.00	5.13	753	

Lipase (Triacylglycerol Lipase) Other name: Pancreatic Lipase Pancreatic triacylglycerol lipase	W5Q6H9_SHEEP UniProt ID: W5Q6H9	52240.00	6.33	470	• Plays an important role in fat metabolism. • It preferentially splits the esters of long–chain fatty acids at positions 1 and 3, producing mainly 2–monoacylglycerol and free fatty acids. • Shows considerably higher activity against insoluble emulsified substrates than against soluble ones.
	LIPP_PIG UniProt ID: P00591	50084.00	5.73	450	
	LIPP_HUMAN UniProt ID: P16233	51157.00	6.27	456	
Amylase (Alpha–amylase)	F1MJQ3_BOVIN UniProt ID: F1MJQ3	56957.00	5.97	506	• Endohydrolysis of (1–>4)–alpha–D–glucosidic linkages in polysaccharides containing three or more (1–>4)–alpha–linked D–glucose units.
	W5QBL8_SHEEP UniProt ID: W5QBL8	57360.00	4.95	511	
	AMYP_PIG UniProt ID: P00690	57086.00	6.52	511	
	AMYP_HUMAN UniProt ID: P04746	57707.00	6.60	511	

Note: The pancreatic enzymes of interest in protein information, including protein ID, functions, molecular weight, and amino acid length were obtained from the UniProt database (https://www.uniprot.org/). The isoelectric point was calculated from the Expasy website (https://web.expasy.org/compute_pi/).

8.3.2 Sequence Analysis

The sequence analysis was done on the candidate protein templates to choose the best protein template. The candidates of the template proteins were obtained from the RCSB database and then aligned with the protein of interest to find the best protein template.

8.3.2.1 Multiple and Pairwise Sequence Alignment

The results for multiple and pairwise sequence alignment are explained below, while the alignment results are shown in the appendixes (Appendix 7 – Appendix 9). All of the selected protein templates have high resolution with a resolution value less than 2.30 Å. However, human TL and porcine TL have slightly higher than 2.30 Å resolution values, which are 2.80 Å and 2.46 Å, respectively. Their structure was still considered a high–quality structure as compared to other protein templates available. The details of each protein template for the Carboxypetidase A1 (CBPA1), Bile–Salt Activated Lipase (BSAL), Triacylglycerol Lipase (TL), and Alpha–Amylase (AMYP) protein of interest were listed in Table 8.3, Table 8.4,Table 8.5, and Table 8.6, respectively, and are explained below. However, the resolution for both porcine BSAL and bovine AMYP was not mentioned as the data was not available in either RCSB PDB or SWISS–Model protein databases. This may be due to a lack of sequence homology to known templates, a lack of high–resolution templates, or no experimental structure or template available.

Table 8.3 lists the CBPA1 protein templates. For bovine CBPA1, three template proteins were selected, such as 2CTC, 1HDQ, and 3KGQ have a 100% alignment percentage with the target protein. The resolution of the template proteins chosen was below 2.30 Å, showing a good resolution of structure visualization. 2CTC was chosen as the protein template for bovine CBPA1 as it has a 1.40 Å resolution value. For sheep CBPA1, only one template protein was selected as only one template protein was available, which is 5OM9 with 83% alignment percentage. The resolution of the 5OM9 template protein is 1.80 Å, and it is below 2.30 Å, showing a good resolution of structure visualization. For human CBPA1, three template proteins were selected, such as 3FJU, 5OM9, and 6I6Z have a 100% alignment percentage with the target protein. The resolution of the template proteins chosen was below 2.30 Å, showing a good resolution of structure visualization. 6I6Z was chosen as the protein template for human CBPA1 as it has a 1.72 Å resolution value. For porcine CBPA1, only one template protein was selected as only one template protein was available, which is 1PCA with 90% of alignment percentage. The resolution of the 1PCA template protein is 2.00 Å, and it is below 2.30 Å, showing a good resolution of structure visualization.

Table 8.3
CBPA1 Protein Templates

Host	Protein Template	Percentage Identity	Resolution
Bovine	**2CTC**	100	1.40 Å
	1HDQ	100	2.30 Å
	3KGQ	100	1.70 Å
Sheep	**5OM9**	83	1.80 Å
Human	3FJU	100	1.80 Å
	5OM9	100	1.80 Å
	6I6Z	100	1.72 Å
Porcine	**1PCA**	90	2.00 Å

Note: The highlighted protein templates were selected for protein modelling.

The BSAL protein templates were listed as in Table 8.4. For bovine BSAL, three template proteins were selected, such as 2BCE, 1AQL, and 1AKN have more than 99% alignment percentage with the target protein. The resolution of the template proteins chosen was below 2.30 Å, showing a good resolution of structure visualization. 2BCE was chosen as the protein template for bovine BSAL as it has a 1.60 Å resolution value. For human BSAL, three template proteins were selected, such as 1F6W, 6H18, and 6H1A have more than 99% alignment percentage with the target protein. The resolution of the template proteins chosen was below 2.30 Å, showing a good resolution of structure visualization. 6H1A was chosen as the protein template for human BSAL as it has a 1.75 Å resolution value.

Table 8.4
BSAL Protein Templates

Host	Protein Template	Percentage Identity	Resolution
Bovine	**2BCE**	99	1.60 Å
	1AQL	100	2.80 Å
	1AKN	100	2.80 Å
Human	1F6W	99	2.30 Å
	6H18	99	1.85 Å
	6H1A	99	1.75 Å

Note: The highlighted protein templates were selected for protein modelling.

Table 8.5 lists the TL protein templates. For Sheep TL, only one template protein was selected as only one template protein was available, which is 1BU8 with a 77% alignment percentage. The resolution of the 1BU8 template protein is 1.80 Å, and it is below 2.30 Å, showing a good resolution of structure visualization. For human TL, three template proteins were selected, such as 1LPA, 1N8S, and 1LPB have more than 100% alignment percentage with the target protein. The resolution of the template proteins chosen was 2.46, still showing a good resolution for structure visualization. 1LPB was chosen as the protein template for human TL as it has the lowest Å resolution value among the templates. For Porcine TL, only one template protein was selected as only one template protein was available, which is 1ETH with a 99% alignment percentage. The resolution of the 1ETH template protein is 2.8 Å is still showing a good resolution for structure visualization.

Table 8.5
TL Protein Templates

Host	Protein Template	Percentage Identity	Resolution
Sheep	**1BU8**	77	1.80 Å
Human	1LPA	100	3.04 Å
	1N8S	100	3.04 Å
	1LPB	100	2.46 Å
Porcine	**1ETH**	99	2.80 Å

Note: The highlighted protein templates were selected for protein modelling.

Alpha–Amylase protein templates were listed in Table 8.6. For Sheep AMYP, only one template protein was selected as only one template protein was available, which is 1KB3 with 87% alignment percentage. The resolution of the 1KB3 template protein is 2.10 Å, and it is below 2.30 Å, showing a good resolution for structure visualization. For human AMYP, three template proteins were selected, such as 4X9Y, 5U3A, and 5VA9 have 100% alignment percentage with the target protein. The resolution of the template proteins chosen was below 2.30 Å, showing a good resolution of structure visualization. 5U3A was chosen as the protein template for human AMYP as it has the lowest resolution value (0.95 Å). For porcine AMYP, three template proteins were selected, such as 1UA3, 3L2M, and 1HX0 have more than 99% alignment percentage with the target protein. The resolution of the template proteins chosen was below 2.30 Å, showing a good resolution for structure visualization. Thus, 1HX0 was selected as a protein template for porcine AMYP as it has a 1.38 Å resolution value.

Table 8.6
AMYP Protein Templates

Host	Protein Template	Percentage Identity	Resolution
Sheep	**1KB3**	87	2.10 Å
Human	4X9Y	100	1.07 Å
	5U3A	100	0.95 Å
	5VA9	100	2.55 Å
Porcine	1UA3	100	2.01 Å
	3L2M	100	1.97 Å
	1HX0	100	1.38 Å

Note: The highlighted protein templates were selected for protein modelling.

8.3.3 Structure Analysis

8.3.3.1 Protein Modelling

Protein homology modelling of the three pancreatic enzymes of interest using the SWISS–Model server (Figure 8.2 – Figure 8.5). After the protein was modelled, its structure was then aligned with all template protein candidates available at once. From this, the aligned region can be visualized. The alignment ensures the modelled structure is as accurate as possible by transferring information from a known template and increases the reliability of the homology model. The coloured regions showed the aligned region for better visualization.

Figure 8.2 illustrates the 3D superimposition of the predicted CBPA1 homology models onto their corresponding high–resolution experimental templates. The coloured segments within each structure map out the specific backbone regions where the generated model accurately aligns with the known templates. For bovine (Figure 8.2, a) and human (Figure 8.2, d) CBPA1, three templates of 2CTC, 1HDQ, and 3KGQ (for bovine) and 3FJU, 5OM9 and 6I6Z (for human) were aligned and superimposed demonstrates highly conserved backbone architecture with near–identical α/β folding patterns across all models, while the small ball–and–stick representations correspond to crystallographic water molecules and bound ligands or catalytic components which is known as Zinc ions resolved within the active–site region, confirming preservation of the metalloprotease catalytic framework. Meanwhile, for sheep (Figure 8.2, b), and porcine CBPA1 (Figure 8.2, c), there was only a single template available. Thus, no superimposed of template for these host. There were also no water molecules and bound ligands or catalytic component were observed.

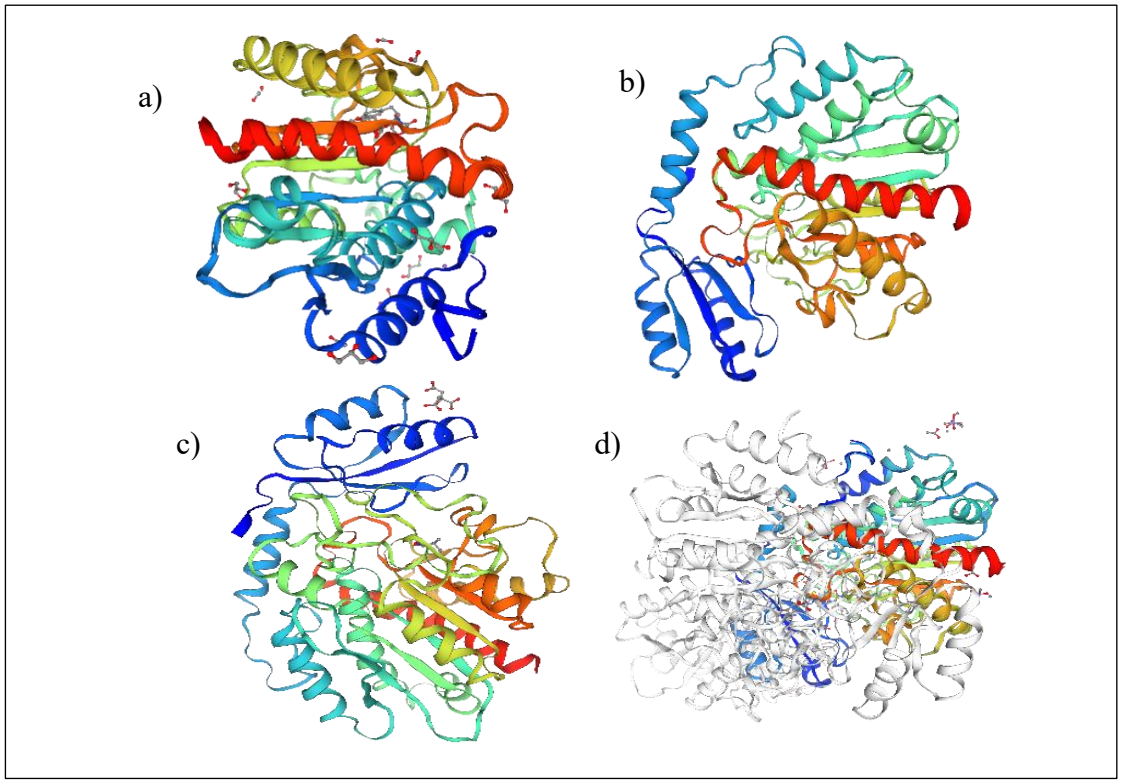


Figure 8.2 Structure Alignment for CBPA1 a) Bovine, b) Sheep, c) Porcine and d) Human with Template Candidates.

Figure 8.3 illustrates the 3D superimposition of the predicted BSAL homology models onto their corresponding high–resolution experimental templates. The coloured segments within each structure map out the specific backbone regions where the generated model accurately aligns with the known templates. For bovine (Figure 8.3, a) and human BSAL (Figure 8.3, b), three templates of 2BCE, 1AQL and 1AKN (for bovine) and 1F6W, 6H18 and 6H1A (for human) were aligned and superimposed. The structural alignment of both bovine and human BSAL templates highlights a highly conserved α/β–hydrolase fold, exhibiting significant backbone superimposition across the catalytic core and lid regions. In addition, the ball–and–stick structures found within these models represent bound ligands, coordinated ions, substrate analogues, and crystallographic water molecules, all of which are crucial for defining and stabilizing the architecture of the active site.

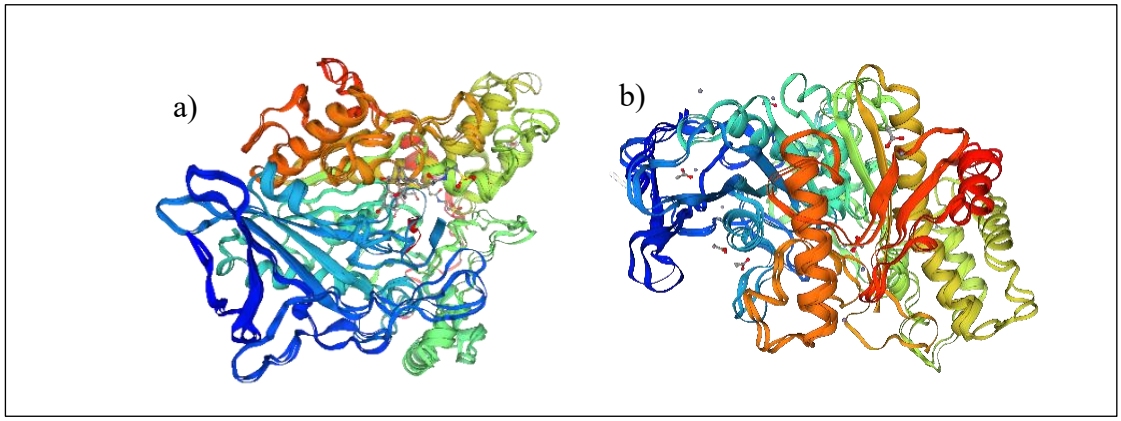


Figure 8.3 Structure Alignment for BSAL a) Bovine and b) Human with Template Candidates.

Figure 8.4 illustrates the 3D superimposition of the predicted TL homology models onto their corresponding high–resolution experimental templates. The coloured segments within each structure map out the specific backbone regions where the generated model accurately aligns with the known templates. For sheep (Figure 8.4, a), and porcine TL (Figure 8.4, c), there was only a single template available. Thus, no superimposed of template for these host. There were no water molecules and bound ligands or catalytic component were observed in sheep TL but presented in porcine TL. Meanwhile for human TL, three templates of 1LPA, 1N85, and 1LPB were aligned and superimposed highlights a strictly conserved α/β–hydrolase fold with precise backbone alignment across both the catalytic domain and the lid region. The accompanying ball–and–stick structures represent bound ligands, substrate analogs, inhibitors, coordinated Calcium ions for structural stability, and crystallographic water molecules, all of which are essential for delineating and stabilizing the active site.

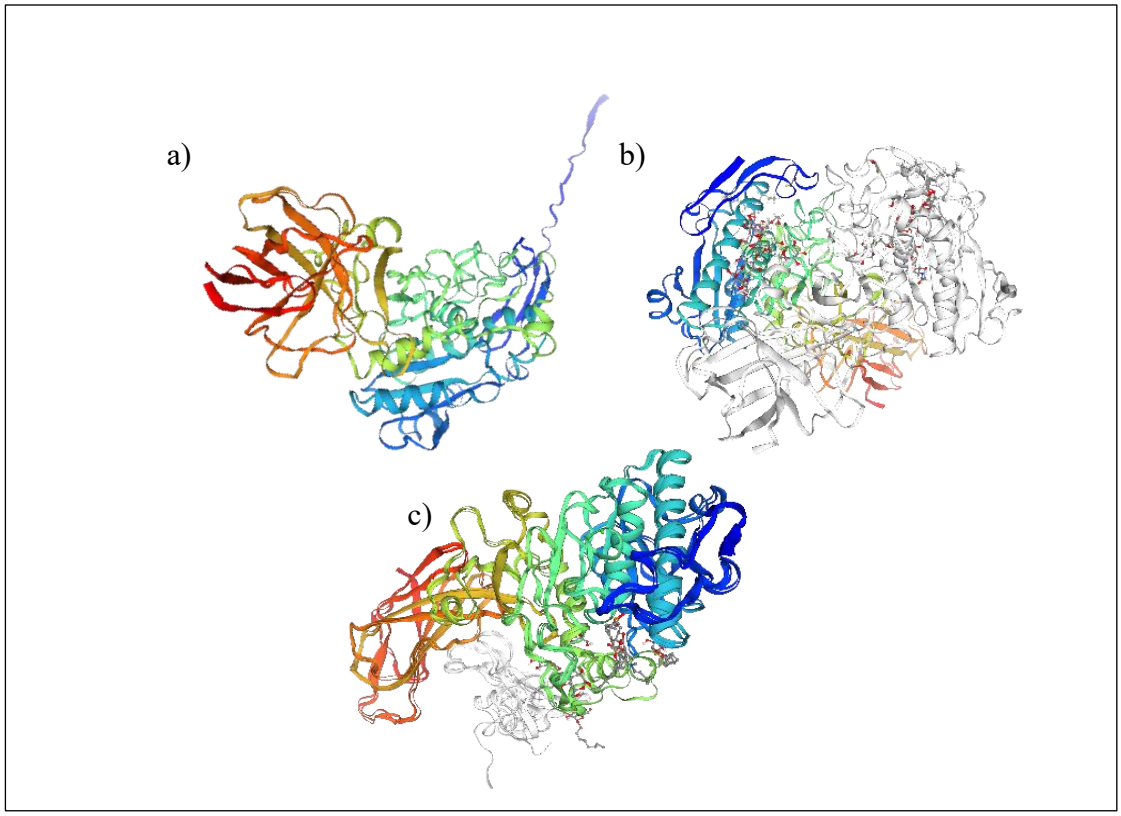


Figure 8.4 Structure Alignment for TL a) Sheep, b) Human and c) Porcine with Template Candidates.

Figure 8.5 illustrates the 3D superimposition of the predicted AMYP homology models onto their corresponding high–resolution experimental templates. The coloured segments within each structure map out the specific backbone regions where the generated model accurately aligns with the known templates. For sheep (Figure 8.5, a), there was only a single template available. Thus, no superimposed of template for these host. There were no water molecules and bound ligands or catalytic component were observed in sheep AMYP. Meanwhile, for porcine (Figure 8.5, b) and human AMYP (Figure 8.5, v), three templates of 1UA3, 3L2M and 1HX0 (for porcine) and 4X9Y, 5U3A and 5VA9 (for human) were aligned and superimposed demonstrates a highly conserved $(\beta/\alpha)_8$–barrel catalytic core with strong backbone. In addition, the ball–and–stick representations correspond to bound carbohydrate ligands or substrate analogues within the active–site cleft, coordinated Calcium and Chloride ions essential for structural stability and catalytic efficiency, as well as crystallographic water molecules contributing to active–site architecture.

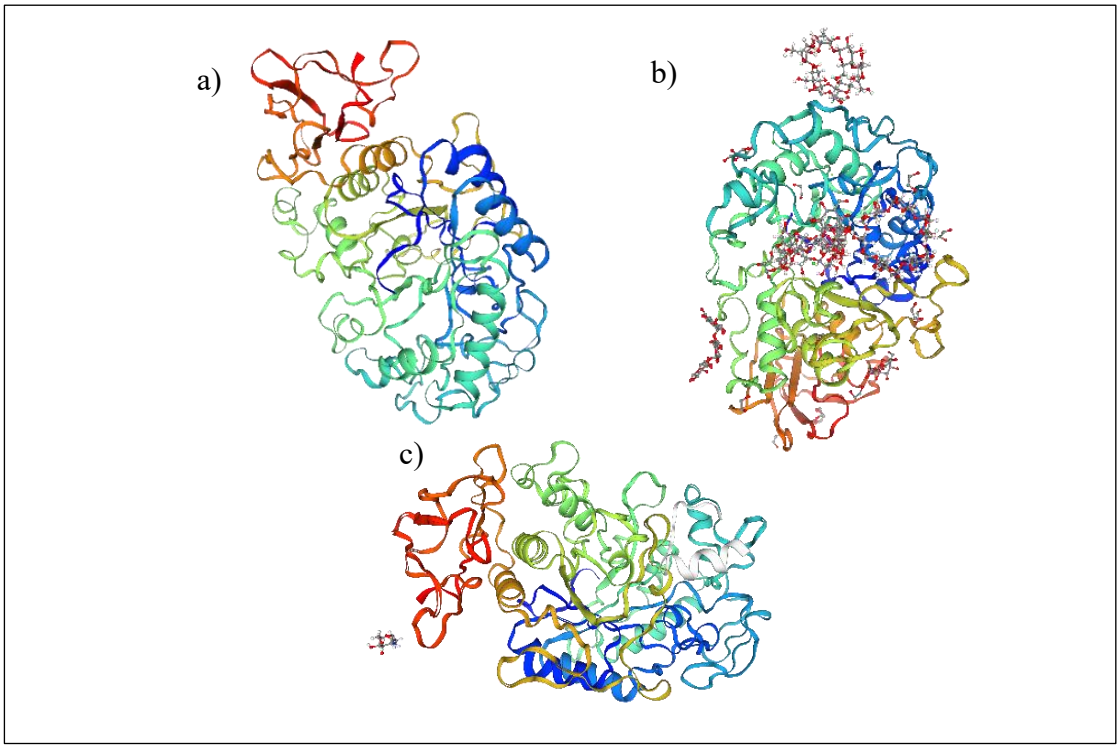


Figure 8.5 Structure Alignment for AMYP a) Sheep, b) Porcine and c) Human with Template Candidates.

8.3.3.2 Template Protein Structure Validation

MolProbity score, Ramachandran plot and RMSD were the parameters used to validate the selected template structure. The results of the template protein structure validation were tabulated in .

Table 8.7. Based on the structure validation results, the template structure for CBPA1 classes is feasible as the MolProbity score is less than 3.00 with more than 95% of Ramachandran favoured values. For BSAL classes, the template structures are also feasible as the MolProbity score is less than 3.00 and with more than 96% of Ramachandran favoured value. Next, for TL classes, sheep TL and human TL are feasible as the MolProbity is less than 3.00 and the Ramachandran favoured value is more than 93%. Although the porcine TL has a slightly higher MolProbity score (3.87), the template is considered feasible, considering the Ramachandran favoured value is more than 80%. Finally, for AMYP classes, the templates have high Ramachandran favoured value (>96%) with MolProbity value less than 3.0. Thus, all of the selected templates for the AMYP classes are considered a feasible structure. These concludes that majority of residues were located in the most favoured regions, which supports the structural accuracy of the predicted model.

Finally, the RMSD value indicates strong structural conservation across all the protein of interest. This metric further strengthens the validation of the generated 3D models by measuring the average spatial distance between the alpha–carbon backbones of the superimposed model and its corresponding experimental template. The generated CBPA1 models for all species exhibit remarkably low RMSD values (0.13–0.65 Å) demonstrating excellent backbone superimposition and high structural similarity to their selected templates, which reflects the highly conserved catalytic architecture of pancreatic metalloproteases. For BSAL, the human model showed strong structural agreement (0.90 Å), whereas bovine BSAL exhibited a higher RMSD (2.70 Å). This suggests greater conformational deviation, which may be associated with intrinsic flexibility of lipase domains. Furthermore, for TL, sheep and human models presented low RMSD values (0.14–0.80 Å), indicating acceptable structural conservation, while porcine TL showed negligible RMSD (0.00 Å), consistent with near–identical structural

alignment to its reference template. Similarly, AMYP models displayed consistently low RMSD values (0.28–0.80 Å), confirming strong preservation of the α–amylase fold across species. Overall, the RMSD values support high structural similarity and reliable backbone alignment for CBPA1, TL and AMYP, alongside comparatively greater, yet justifiable, conformational deviation observed in bovine BSAL. Ultimately, these reported RMSD values confirm that the SWISS–Model generated highly accurate and stable 3D protein structures for the *in–silico* analysis. Thus, all of the selected templates are of high quality and can be used for 3D protein modelling and visualization of the *in–silico* glycosylation sites prediction. The protein models of CBPA1, BSAL, TL, and AMYP are shown in Figure 8.6, Figure 8.7, Figure 8.8, and Figure 8.9, respectively.

Table 8.7
Protein Structure Validation

Host	MolProbity Score	Ramachandran Favoured	Ramachandran Outliers	RMSD
Bovine CBPA1	1.93	96.39%	0.33%	0.21 Å
Sheep CBPA1	1.28	96.24%	0.75%	0.13 Å
Porcine CBPA1	2.68	95.50%	0.50%	0.65 Å
Human CBPA1	1.15	96.88%	0.33%	0.47 Å
Bovine BSAL	2.03	96.01%	0.19%	2.70 Å
Human BSAL	1.31	97.09%	0.00%	0.90 Å
Sheep TL	1.60	96.22%	0.89%	0.14 Å
Porcine TL	3.87	81.78%	4.20%	0.00 Å
Human TL	2.82	93.40%	1.32%	0.80 Å
Sheep AMYP	1.48	96.56%	0.00%	0.80 Å
Porcine AMYP	1.75	97.17%	0.20%	0.28 Å
Human AMYP	0.61	97.97%	0.00%	0.34 Å

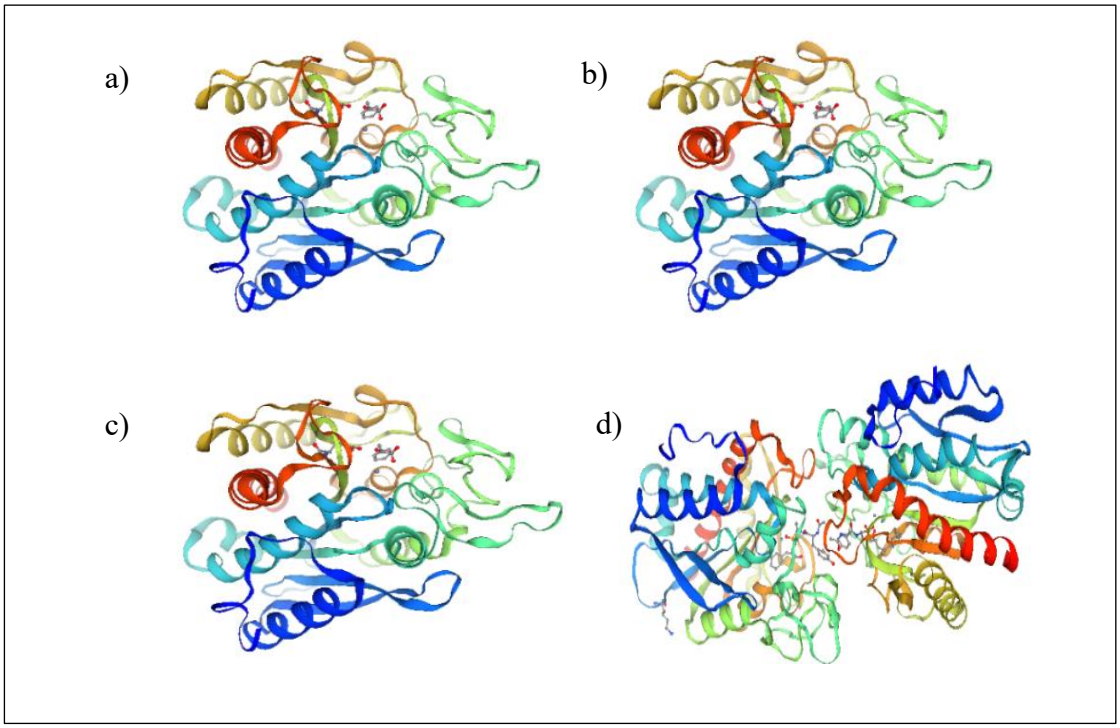


Figure 8.6 3D Model of CBPA1.

Note: a) Bovine, b) Sheep, c) Porcine, and c) Human

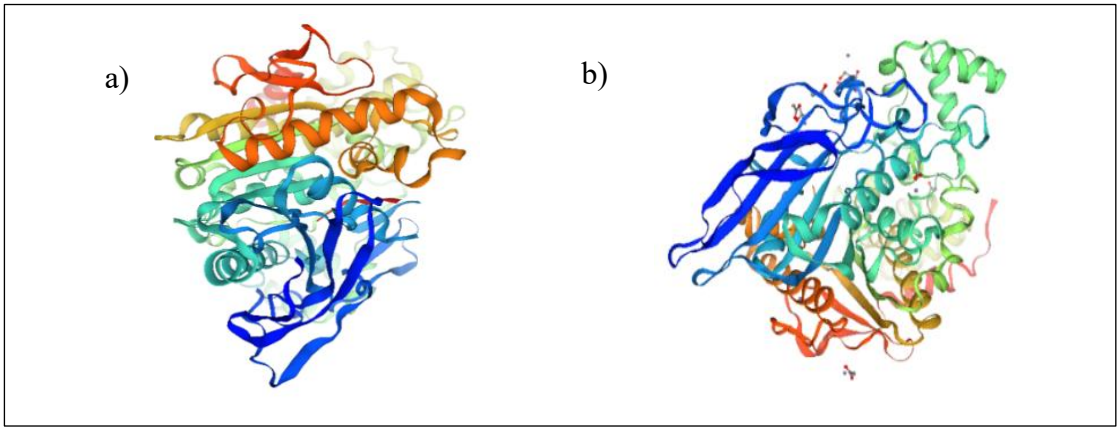


Figure 8.7 3D Model of BSAL.

Note: a) Bovine and b) Human

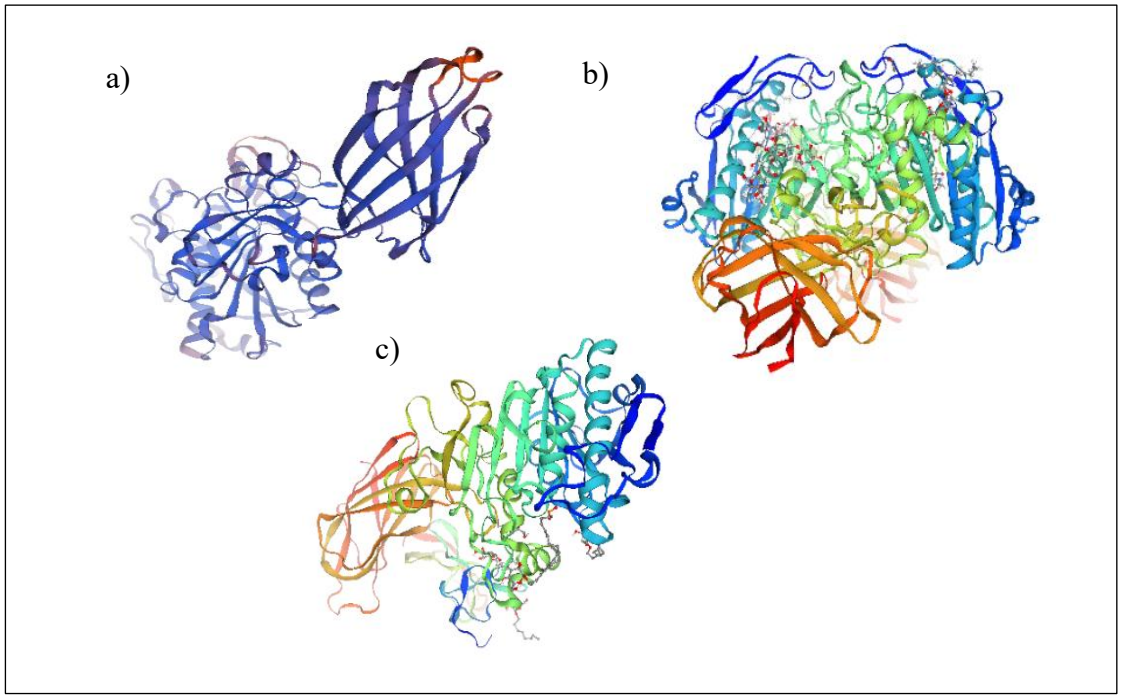


Figure 8.8 3D Model of TL.

Note: a) Sheep, b) Porcine, and c) Human

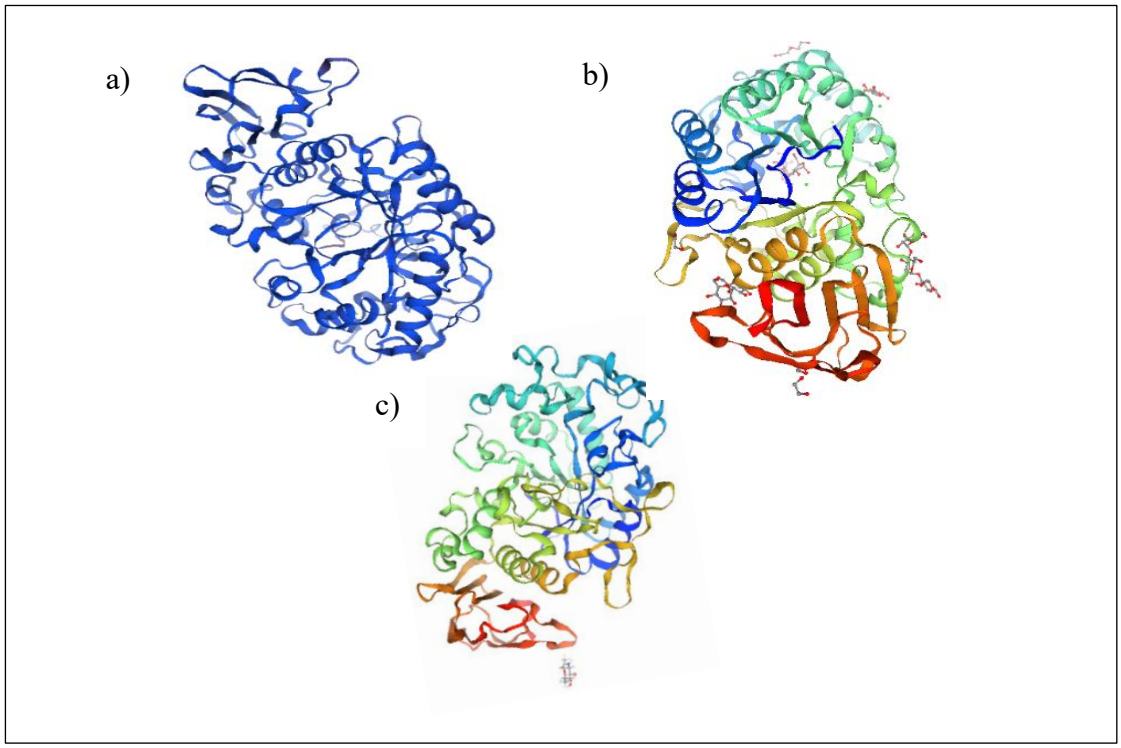


Figure 8.9 3D Model of AMYP.

Note: a) Sheep, b) Porcine, and c) Human

8.3.4 Glycosylation Bioinformatics Assessment

8.3.4.1 Potential Glycosylation Sites Prediction

Table 8.8, Table 8.9, Table 8.10, and Table 8.11 shows the prediction of all potential glycosylation sites in all of the enzymes of interest, such as CBPA1, BSAL, TL, and AMYP, respectively, from different hosts such as bovine, sheep, porcine, and human. The results for N–linked glycosylation (NLG) sites were obtained based on two different servers, which are Net–Nglyc 1.0 and GlycoPred. Meanwhile, the O–linked glycosylation (OLG) sites were obtained from Net–OGlyc 4.0 and GlycoPred. However, only some of the glycosylation sites for the enzymes of interest were successfully predicted with GlycoPred, as this website page is under maintenance. Thus, the prediction cannot be continued to be executed using this server.

Table 8.8 presents the summary for the NLG and OLG sites' predictions for the CBPA1 enzymes of bovine, sheep, porcine, and human. The Net–Nglyc 1.0 server showed higher NLG sites prediction for all samples compared to the Glyco Pred server. All of the CBPA1 samples from bovine, sheep, porcine, and human have consensus NLG, which is NYA 118, executed using the Net–Nglyc 1.0 server. Meanwhile, the Glyco Pred server predicted more OLG sites prediction all samples compared to Net–Oglyc 4.0. There was no OLG consensus predicted among all the samples. For bovine CBPA1, three NLG sites were mentioned in both servers, which are NTF 115, NNL 416, and NLY 417. For porcine and human, only one NLG sites were mentioned in both servers, which are NYA 118 and NPH 139, respectively. Next, three sites of OLG were mentioned in both servers, such as SRA 109, STN 113, and SSS 267 for bovine. Two OLG sites were mentioned for porcine (TST 114 and STF 115) and human (SRA 109 and STD 113).

Table 8.8
Prediction of Potential Glycosylation Sites for CBPA1

No	Enzyme of Interest	Glycosylation Site			
		N–linked		O–linked	
		Net–Nglyc 1.0	Glyco Pred	Net–Oglyc 4.0	Glyco Pred
1	**Bovine CBPA1**	**NTF 115**, **NYA 118**, NRP 168, NPD 222, NRL 233, NRN 254, NWD 256, NSE 281, NFK 298, NQV 298, NQV 330, NQG 370, **NNL 416**, **NLY 417** (14)	**NTF 115 NNL 416 NLY 417** (3)	SLQ 71, SQS 107, **SRA 109**, **STN 113**, TFN 116, TRS 239, **SSS 267**, SSP 268, SPC 269, TYH 274 (10)	SVL 8, TVK 38, SPI 61, SLL 95, **SRA 109**, **STN 113**, TNT 114, TYH 121, SYE 151, STG 163, TGV 188, TED 197, SLC 246, **SSS 267**, SET 272, SEV 282, SIV 288, TEL 327, SAV 335, SGG 361, TFE 378, SQI 394 (22)
2	**Sheep CBPA1**	**NYA 118**, NRP 168, NPD 222, NRL 233, NPC 268, NSE 280, NFK 297 (7)	–	SLQ 71, SQS 107, SRA 109, STD 113, TDS 114, SFN 116, TRS 239, SSN 266, SNP 267, TYH 273 (10)	–
3	**Porcine CBPA1**	**NYA 118**, NRP 168, NLD 212, NPD 222, NRM 233, NPC 269, NSE 281, NIK 298 (8)	**NYA 118**, NDH 294, NHP 416 (3)	SQG 107, TTS 113, **TST 114**, **STF 115**, TFN 116, TRS 239, SGS 244, SSN 267, SNP 268 (9)	**TST 114**, **STF 115**, TYH 121, SSY 150, SYE 151, SGV 188 TED 197, SGS 246, SSN 267, SET 272, SEV 282, SIV 288 SLY 342, SGG 361, TYN 368, SFE 378, TGR 384, SQI 394, TWL403 (19)
4	**Human CBPA1**	**NYA 118**, **NPH 139**, NTY 150, NPD 222, NRM 233, NPC 269, NSE 281, NIK 298, NYG 349 (9)	**NPH 139**, NHP 416 (2)	**SRA 109**, **STD 113**, TRS 239, SHT 241, SGA 264, SSN 267, SNP 268 (7)	SVA 29, SPI 61, SIQ 71, SHG 81, SYE 85, SLL 95, **SRA 109**, **STD 113**, TYH 121, SKI 144, STG 163, TGG 164, SGV 188, TLD 212, TNR 232, SLC 246, SSN 267, SET 272, SEV 282, SIV 288, TEP 320, TAL 338, SLY 342, SGS 361, TID 364, TYS 368, SQG 370, TFE 378, SQI 394, TWL 403 (30)

Note: The underlined sequence shows the consensus glycosylation site across samples. The bold sequence shows the same glycosylation site across the servers used.

Table 8.9 presents the summary for the NLG and OLG sites' predictions for the BSAL enzymes of bovine, porcine, and human, using Net–NGlyc 1.0 and Net–OGlyc 4.0 to predict NLG and OLG sites, respectively. The OLG is more frequent compared to NLG sites in porcine and human BSAL. Conversely, bovine BSAL recorded higher NLG compared to OLG sites. The bovine, porcine, and human BSAL shared eleven NLG consensus sequences as seen in Table 8.9. Meanwhile, only one consensus sequence, which is TLK, was observed across bovine, porcine, and human BSAL.

Table 8.9
Prediction of Potential Glycosylation Sites for BSAL

No	Enzyme of Interest	Glycosylation Site	
		N–linked	**O–linked**
		Net–Nglyc 1.0	Net–Oglyc 4.0
1	**Bovine BSAL** PTM – 2 glycosylation sites, No reported glycan (UniProt) N–linked (GlcNAc...) asparagine (205, 379)	NKK 35, NED 95, NIW 102, NFL 136, NYL 140, NVI 153, NYR 160, NLP 175, NYG 179, NIE 195, NKG 227, NLY 320, NAA 324, NDM 335, NSN 351, NKQ 353, NTY 430, NFA 488, NTG 496, NWD 505, NYL 515, NKQ 520, NSM 526, NYL 535, NSQ 563, NSG 574 (26)	TLK 72, STV 500, TVP 501, TSA 551, SAG 552, SLL556, SQA 564, SPV 567, SGA 575, TEP 579, SAG 582 (11)
2	**Porcine BSAL** Unreview (UniProt) No database for protein modelling (template)	NKK 111, NIW 178, NFL 212, NYL 216, NVI 229, NYR 236, NLP 251, NYG 255, NKG 303, NLY 396, NAA 400, NDM 411 (12)	SWQ 15, TLG 49, SRL 52, TRR 60, TWR 68, TLK148, SSV 544, TGD 605, SEA 608, TPA 611, TGD 616, TPA 622, TGD 627, SEA 630, TPA 633, SDA 639 (17)
3	**Human BSAL** PTM – N– & O–glycosylated (UniProt) N–linked (GlcNAc...) (complex) asparagine (207) O–linked (GalNAc...) threonine (558, 569, 579, 607, 618, 629, 640, 651, 662, 673)	NKK 37, NPQ 64, NFK 79, NIW 104, NFL 138, NNY 141, NYL 142, NVI 155, NYR 162, NLP 177, NYG 181, NIA 197, NKG 229, NPL 252, NLY 322, NAA 326, NNM 337, NMD 338, NKG 353, NKK 356, NKK 399, NAK 427, NFA 490, NMG 498, NSG 515, NFL 537 (26)	TLK 74, SAV 502, THW 506, TTE 512, TEN 513, TDQ 553, TPV 558, TGD 563, SEA 566, TPV 569, TGD 574, SET 577, TAP 579, TGD 585, SGA 588, TGD 596, SGA 599, TGD 607, SGA 610, TGD 618, SGA 621, TGD 629, SGA 632, TGD 640, S GA643, TGD 651, SGA 654, TGD 662, SGA 665, TGD 673, TGD 684, SGA 687, TGD 695, SGA 698, TPT 704, TGD 706, SET 709, TAP 711, TGD 717, SGA 720, TGD 728, SEA 731, TDD 739, SKE 742 (44)

Note: The underlined sequence shows the consensus glycosylation site across samples.

The summary of potential glycosylation sites for sheep, porcine, and human TL was presented in Table 8.10. The NLG and OLG for TL were only analysed using Net–Nglyc 1.0 and Net–Oglyc 4.0, respectively. From the analysis, the NLG sites are more regular than the OLG sites in all samples. The sheep, porcine, and human share three NLG consensus sequences, which are NVH, NGG, and NPD. Only one OLG site was mentioned for both sheep (SNF 82) and human (TER 37), but none for porcine.

Table 8.10
Prediction of Potential Glycosylation Sites for TL

No	Enzyme of Interest	Glycosylation Site	
		N–linked	**O–linked**
		Net–Nglyc 1.0	Net–Oglyc 4.0
1	**Sheep TL**	NEN 62, NPN 64, NNY 66, NYQ 67, NFQ 83, NCI 120, NTR 140, NVH 165, NGG 249, NIL 260, NGI 269, NPD 296, NTG 348, NFT 354, NGN 384, NSK 386, NLF 429, NFC 452 (18)	SNF 82 (1)
2	**Porcine TL** PTM – 1 glycosylation site, No reported glycan (UniProt) N–linked (GlcNAc...) asparagine (167)	NCI 101, NVH 146, NLG 213, NGG 230, NHL 263, NPD 277, NKC 295, NFA 335, NSR 366, NNV 406, NVI 407, NDG 426 (12)	–
3	**Human TL** PTM – 1 glycosylation site, No reported glycan (UniProt) N–linked (GlcNAc...) asparagine (183)	NTR 52, NEN 60, NPN 62, NNF 64, NFQ 65, NFK 80, NRK 84, NWL 101, NVC 105, NLF 109, NCI 117, NIR 137, NVH 162, NGT 183, NLG 229, NGG 246, NIL 257, NHL 279, NPD 293, NVF 306, NKC 311, NDV 336, NFA 351, NKG 379, NSK 382, NEF 401, NNV 421, NVI 422, NPT 425, NVG 441, NFC 447 (31)	TER 37 (1)

Note: The underlined sequence shows the consensus glycosylation site across samples.

The potential NLG and OLG glycosylation sites for bovine, sheep, porcine, and human AMYP were summarized in Table 8.11. The NLG sites' prediction is more frequent as compared to the OLG sites' prediction in all samples. The bovine, sheep, porcine, and human shared fifteen NLG and three OLG consensus sequences, as shown in Table 8.11. For porcine, there are two NLG (NPS 68 and NND 445) and one OLG (SAW 147) site that were mentioned in both servers. Next, for human, there are three NLG (NDW 370, NND 445, and NGN 474) and two OLG (TCG 129 and TIN 386) sites that were mentioned in both servers.

Table 8.11
Prediction of Potential Glycosylation Sites for AMYP

No	Enzyme of Interest	Glycosylation Site			
		N–linked		O–linked	
		Net–Nglyc 1.0	Glyco Pred	Net–Nglyc 4.0	Glyco Pred
1	**Bovine AMYP**	NAV 63, NNV 102, NVG 103, NHM 115, NPG 135, NGE 160, NLN 231, NGR 265, NWG 294, NQR316, NDW 370, NNN 377, NNG 378, NGV 379, NPD 388, NMV 408, NVV 414, NGS 427, NQV 430, NND 445, NDD 446, NCT 476, NSA 496 (23)	–	TSS 126, STC 128, TCG 129, SYF 132, TRD 138, SGW 147, TGN 158, TIN 386 (8)	–
2	**Sheep AMYP**	NEN 61, NVV 63, NES 90, NNV102, NVG 103, NHM 115, NPG 135, NDG 152, NGE 160, NVA 167, NRL 199, NLN 231, NTS 233, NGL 265, NWG 294, NRA 305, NHD 313, NQR 316, NDW 370, NNN 377, NNG 378, NGV 379, NAD 388, NDW 395, NMV 408, NVV 414, NWW 423, NGS 427, NQV 430, NKG 438, NND 445, NND 445, NDD 446, NRC 475, NSA 496 (35)	–	TSS 126, STC 128, TCG 129, SYF 132, TRD 138, SGW 147, TIN 386 (7)	–

3	**Porcine AMYP** PTM – 1 glycosylation site, No reported glycan (UniProt) N–linked (GlcNAc...) asparagine (427)	NEN 61, NIV 63, **NPS 68**, NEN 90, NEF 92, NNV 102, NVG 103, NHM 115, NPG 135, NRE 138, NDG 152, NDP 167, NKL 199, NLN 231, NTN 233, NWF 235, NGR 265, NWG 294, NHD 313, NQR 316, NFV 362, NGQ 365, NDW 370, NNN 377, NNG 378, NGV 379, NAD 388, NDW 395, NMV 408, NVV 414, NWW 423, NGS 427, NQV 430, NRG 438, **NND 445**, NDD 446, NSC 475, NSA 496 (38)	NIV 63, **NPS 68**, NDP 167, NHD 313, NGQ 365, NDW 365, NNN 370, NQV 427, **NND 445** (9)	TCG 129, SYC 132, **SAW 147**, TAS 158, SGG 160, TIN 386 (6)	SAF 8, **SAW 147**, SYN 165, TNW 234, SRP 241, SSE 259, SSY 356, TCG 386, STL 453, TLQ 454, TGL 457, SDG 486, SIS 493, SAE 497, SKL 509 (15)
4	**Human AMYP** PTM – 1 glycosylation site, No reported glycan (UniProt) N–linked (GlcNAc...) asparagine (476)	NTQ 20, NEN 61, NPF 68, NED 90, NMV 96, NNV 102, NVG 103, NHM 115, NAV 120, NPG 135, NDG 152, NYN 165, NDA 167, NHL 199, NLN 231, NSN 233, NWF 235, NGR 265, NGE 285, NWG 294, NHD 313, NQR 316, NGN 365, NDV 367, **NDW 370**, NNN 377, NNG 378, NGV 379, NPD 388, NDW 395, NMV 408, NVV 414, NWY 423, NGS 427, NQV 430, NRG 438, **NND 445**, **NGN 474**, NCT 476, NSA 496 (40)	NVA 63, NHL 199, NHD 313, **NDW 370**, NGS 427, **NND 445**, **NGN 474** (7)	**TCG 129**, SRD 138, SGW 147, **TIN 386** (4)	SAG 123, SST 127, STC 128, **TCG 129**, TQV 170, TGL 178, SKP 241, SSY 356, **TIN 386**, SLT 452, TLQ 457, SDG 485, SIS 493, SAE 497, SKL 509 (15)

Note: The underlined sequence shows the consensus glycosylation site across samples. The bold sequence shows the same glycosylation site across the servers used.

8.3.4.2 Potential Glycosylation Sites Location

Figure 8.10 (CBPA1), Figure 8.11 (BSAL), Figure 8.12 (TL), and Figure 8.13 (AMYP) show the visualization of potential glycosylation sites in all of the pancreatic enzymes from different hosts such as bovine, sheep, porcine, and human. For this step, only one software was used, which is PyMOL. The selected protein templates for each of the enzymes of interest were used to construct the structure on PyMOL. The location of the potential glycosylation sites for the NLG and OLG was also constructed on the template protein structure. The highlighted spheres in yellow colour indicate the potential N–linked glycosylation sites, red–coloured spheres indicate the potential O–linked glycosylation sites. The exposed glycosylation sites were highlighted for the glycosylation sites prediction.

Figure 8.10 shows the NLG and OLG potential glycosylation sites highlighted in yellow and red spheres, respectively. Based on the possible glycosylation site, the NLG is more abundant and appears to be more clustered and more exposed on the membrane surfaces compared to the OLG in bovine CBPA1, which may suggest a high density of glycosylation region. For sheep CBPA1, OLG is more exposed on the surface to NLG as it resides in a deeper location of the protein. Next, most of the OLG sites' prediction of porcine CBPA1 are visible and exposed to the outer surface of the protein membrane; meanwhile, the NLG is more localized and partially buried within the structure. Lastly, for the human CBPA1, both the NLG and OLG were exposed clearly on the membrane surface.

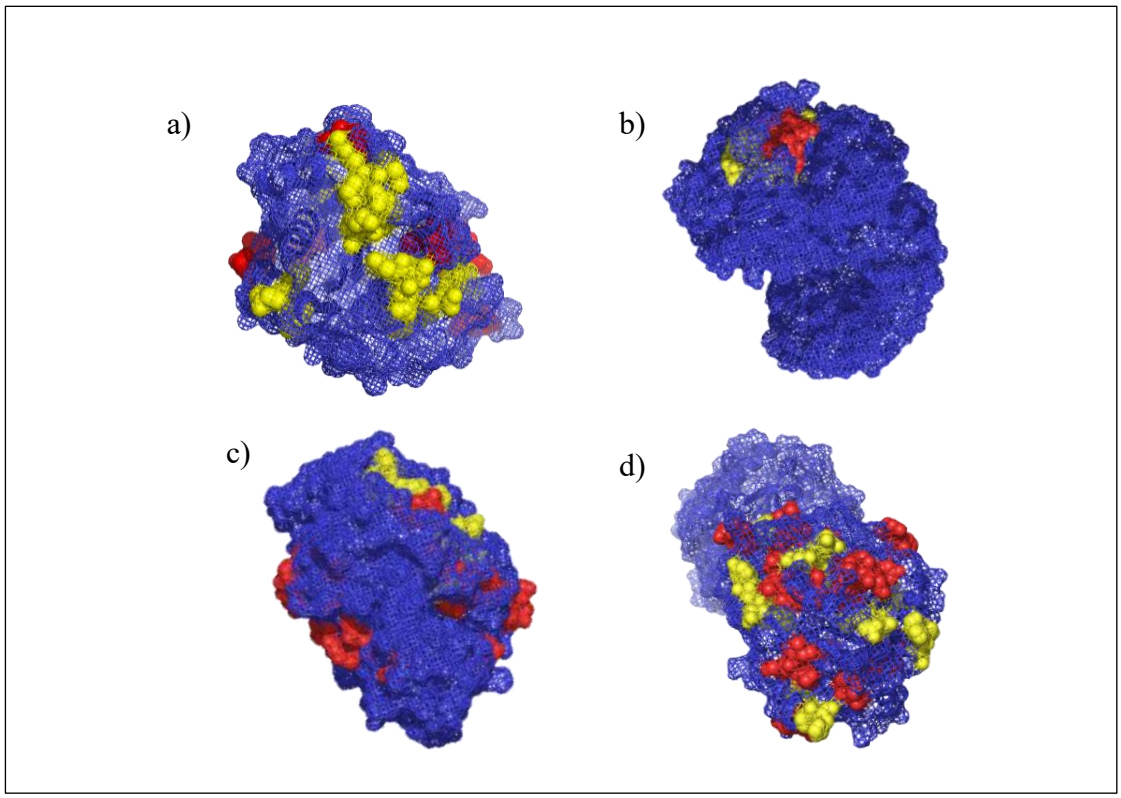


Figure 8.10 CBPA1 Potential Glycosylation Site Locations.

Note: a) Bovine, b) Sheep, c) Porcine, and d) Human. Yellow–coloured spheres indicate the potential N–linked glycosylation sites, red–coloured spheres indicate the potential O–linked glycosylation sites.

The potential NLG and OLG sites prediction for BSAL was visualized as in Figure 8.11 for bovine and human. However, the porcine BSAL glycosylation site prediction analysis can only be done based on the primary amino acid sequence, since the template structure is not available in the RCSB and SwissProt protein databases. The NLG and OLG potential glycosylation sites are highlighted in yellow and red spheres, respectively. There are numerous NLG sites on the outer surface and buried within the protein structure of bovine BSAL. The OLG sites were more exposed and located proximately near the NLG on the exposed region. Whereas, the human BSAL also has a higher frequency of NLG than OLG sites and is exposed on the protein surface. The OLG sites were also exposed on the protein surface and highly connected with the NLG sites.

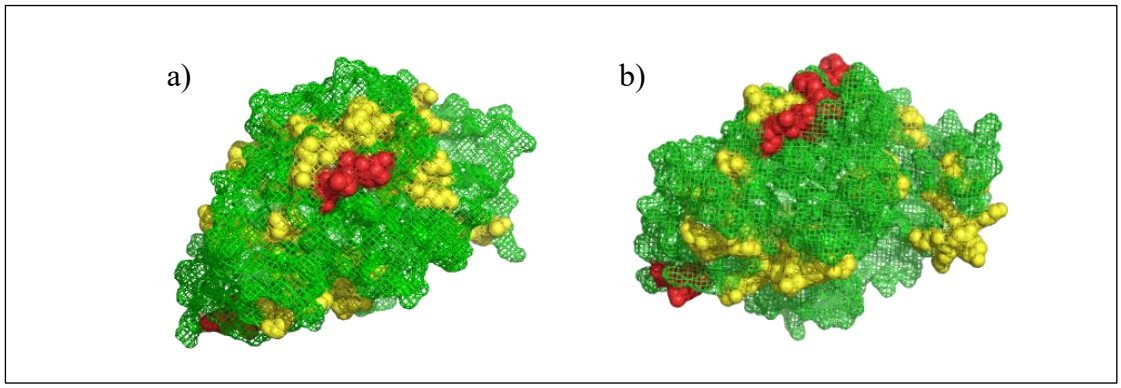


Figure 8.11 BSAL Potential Glycosylation Site Locations.

Note: a) Bovine and b) Human. Yellow–coloured spheres indicate the potential N–linked glycosylation sites, red–coloured spheres indicate the potential O–linked glycosylation sites.

Figure 8.12 illustrates the potential glycosylation sites location for TL in sheep, porcine, and human. The NLG and OLG potential glycosylation sites are highlighted in yellow and red spheres, respectively. The NLG sites were more frequent and highly exposed on the protein surface in sheep TL. The OLG was less frequent but still appeared and interacted with NLG on the exposed region of the protein surface. Next, there were no OLG sites predicted in the amino acid sequences, so there was no OLG sites were visualized in the protein structure of porcine TL. The NLG sites were also not exposed on the protein surface; instead, they were localized in the inner surface of the protein. Lastly, for human TL, it is highly glycosylated with NLG, where some were exposed on the surface and some were localized in the inner surface of the protein. Meanwhile, the OLG was less frequent than the NLG but exposed on the protein surface.

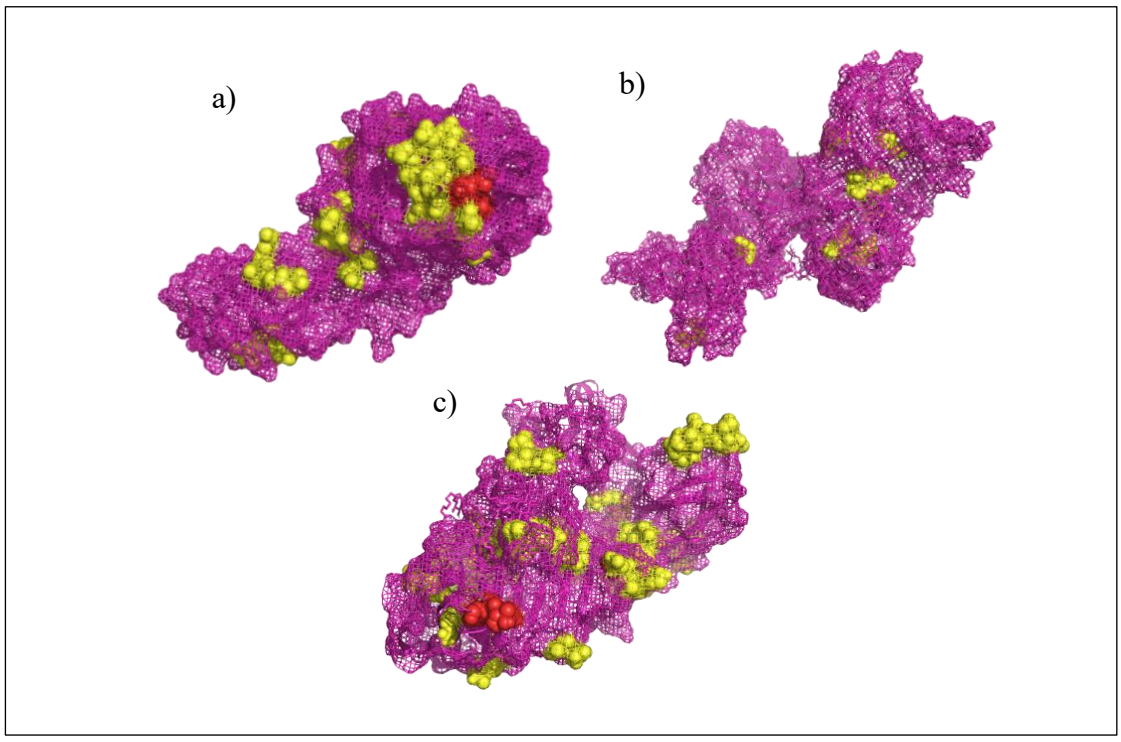


Figure 8.12 TL Potential Glycosylation Site Locations.

Note: a) Sheep, b) Porcine, and c) Human. Yellow–coloured spheres indicate the potential N–linked glycosylation sites, red–coloured spheres indicate the potential O–linked glycosylation sites.

Figure 8.13 presents the glycosylation sites prediction for sheep, porcine, and human AMYP. However, the bovine AMYP glycosylation site prediction analysis can only be done based on the primary amino acid sequence, since the template structure is not available in the RCSB and SwissProt protein databases. The NLG and OLG potential glycosylation sites are highlighted in yellow and red spheres, respectively. The NLG sites were more frequent in sheep AMYP, however, most of the NLG sites were localized in the inner protein surface. Meanwhile, although the OLG sites are less frequent but it is highly exposed on the protein surface. Next, for porcine AMYP, both NLG and OLG sites were highly exposed on the protein surface and had a strong interaction between them. Lastly, for the human AMYP, the high density of the NLG sites was exposed on the protein surface. Similarly, to the OLG sites, it is less frequent than NLG sites but is still exposed on the protein surface, and some of them have interacted with nearby NLG sites.

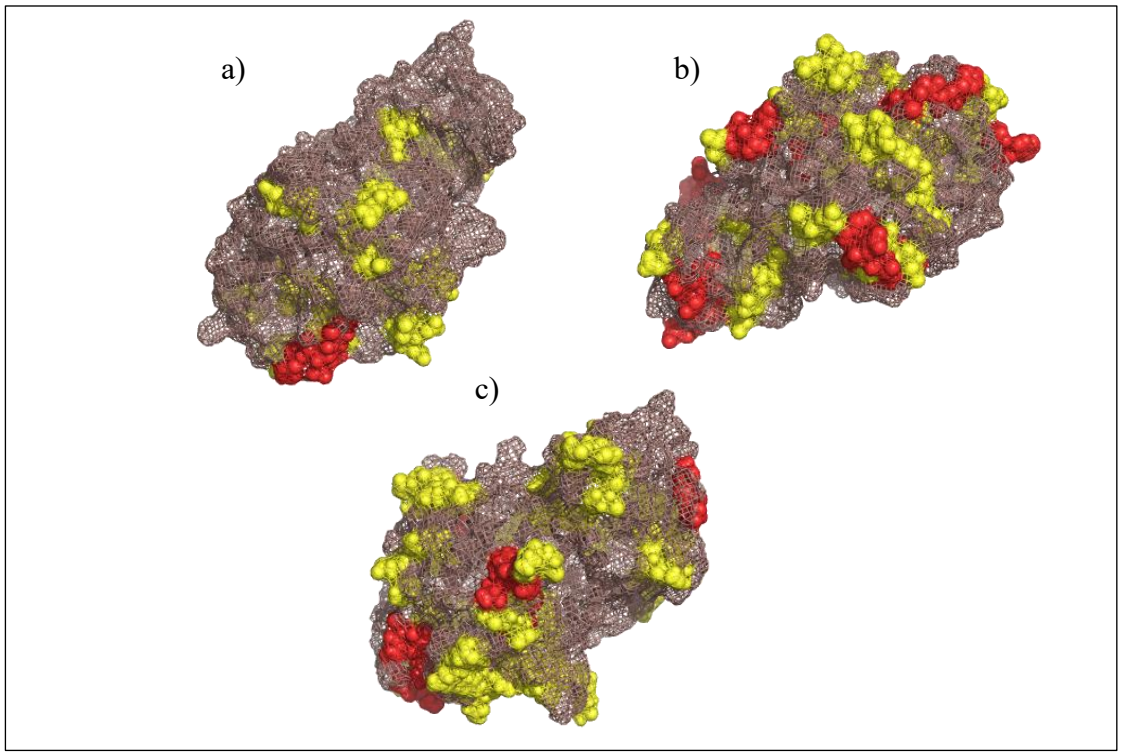


Figure 8.13 AMYP Potential Glycosylation Site Locations.

Note: a) Sheep, b) Porcine, and c) Human. Yellow–coloured spheres indicate the potential N–linked glycosylation sites, red–coloured spheres indicate the potential O–linked glycosylation sites.

8.3.5 Glycosylation Experimental Assessment

8.3.5.1 Protease Glycosylation Assessment for Bovine and Sheep Pancreatic Enzyme Sequential Purification

Figure 8.14 presents the 1D–SDS PAGE results of bovine and sheep CBPA1 sequential purification using three different types of staining, such as Coomassie Brilliant Blue staining, Pro–Q ® Emerald 300 Glycoprotein staining, and Sypro Ruby staining. From the results, the Coomassie Brilliant Blue stained the total protein from the bovine and sheep crude extract samples (Figure 8.14a – **Lane 3 and 6**) as well as the porcine pancreatin (Figure 8.14a – **Lane 2 and 9**). The purified sample of CBPA1 from the anion exchange chromatography (IEX) and gel filtration chromatography (GFC) was also visible at the targeted molecular weight for both bovine (Figure 8.14a – **Lane 4 and 5**) and sheep (Figure 8.14a – **Lane 7 and 8**). However, for Pro–Q ® Emerald 300 Glycoprotein staining, only crude extracts from bovine and sheep showed multiple solid bands (Figure 8.14b – **Lane 3 and 6**). The Pro–Q ® Emerald 300 Glycoprotein staining aims to stain any available glycoprotein in the sample. The same molecular weight of the targeted CBPA1 in both bovine sheep was visible in the crude extract samples, but the bands were absent in the purified samples. Since the targeted CBPA1 were present in the Coomassie Brilliant Blue staining and also in the Pro–Q ® Emerald 300 Glycoprotein staining in crude extract samples, it is postulated that the purified CBPA1 is a low–abundance glycoprotein. Thus, no bands were observed in both purified samples in the Pro–Q ® Emerald 300 Glycoprotein staining. Then, the same gel was destained and finally stained with Sypro Ruby staining. However, only crude extracts from bovine and sheep showed solid multiple bands (Figure 8.14c – **Lane 3 and 6**).

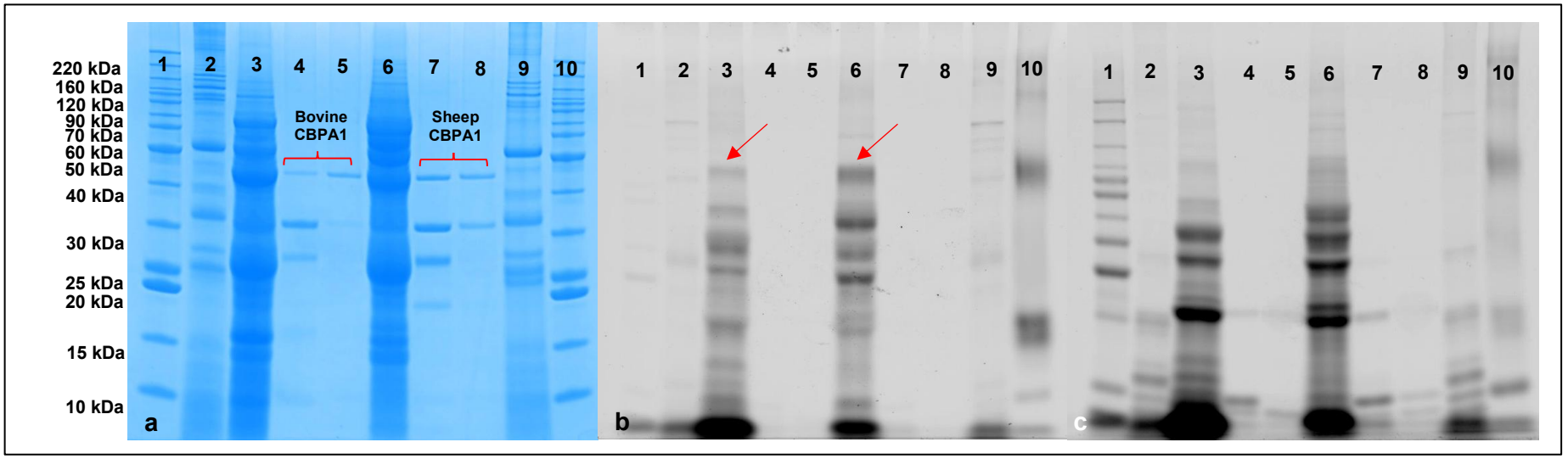


Figure 8.14 1D–SDS PAGE (Bis–Tris 12%) of Bovine and Sheep CBPA1 Sequential Purification. a) Coomassie Brilliant Blue staining, b) Pro–Q ® Emerald 300 Glycoprotein staining, and c) Sypro Ruby staining.

Note: Lane 1 and Lane 10 (Gel A): Benchmark™ Protein Ladder, Lane 2 and Lane 9: Positive Control (Porcine Pancreatin), Lane 3: Bovine Pancreatic Crude Extract, Lane 4: Bovine Anion Exchange Chromatography, Lane 5: Bovine Size Exclusion Chromatography, Lane 6: Sheep Pancreatic Crude Extract, Lane 7: Sheep Anion Exchange Chromatography, Lane 8: Sheep Size Exclusion Chromatography, and Lane 10 (Gel B and C): Candy Cane™ Protein Ladder.

8.3.5.2 Lipase Glycosylation Assessment for Bovine and Sheep Pancreatic Enzyme Sequential Purification

Figure 8.15 presents the 1D–SDS PAGE results of bovine BSAL and sheep TL sequential purification using three different types of staining, such as Coomassie Brilliant Blue staining, Pro–Q ® Emerald 300 Glycoprotein staining, and Sypro Ruby staining. From the 1D–SDS PAGE results, the Coomassie Brilliant Blue stained the total protein of all samples (Figure 8.15a). A protein band at the targeted molecular weight was observed, indicating the presence of bovine BSAL (Figure 8.15a – **Lane 4**). Meanwhile, there was no visible band at the targeted molecular weight representing the sheep TL in this sample. Next, the same set of samples was run on the 1D–SDS PAGE and stained with Pro–Q ® Emerald 300 Glycoprotein staining to detect the presence of glycoprotein. However, for Pro–Q ® Emerald 300 Glycoprotein staining, only crude extracts from bovine and sheep, as well as the porcine lipase, showed multiple bands (Figure 8.15b). Overall, from the glycoprotein staining, it can be deduced that the purified samples may be unglycosylated protein, as the crude extract sample also showed no visible solid band at the same targeted molecular weight. Then, the same gel was destained and finally stained with Sypro Ruby staining. However, only crude extracts from bovine and sheep, and porcine lipase were recovered showed multiple bands (Figure 8.15c).

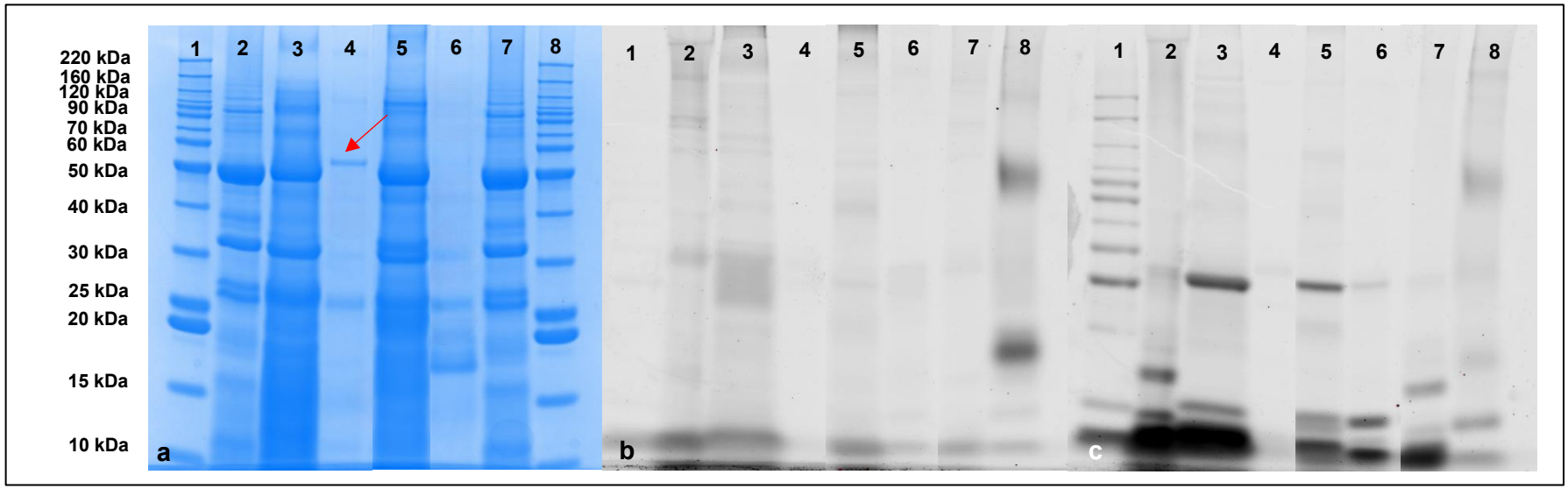


Figure 8.15 1D–SDS PAGE (Bis–Tris 12%) of Bovine BSAL and Sheep TL Sequential Purification. a) Coomassie Brilliant Blue staining, b) Pro–Q ® Emerald 300 Glycoprotein staining, and c) Sypro Ruby staining.

Note: Lane 1 and Lane 8 (Gel A): Benchmark™ Protein Ladder, Lane 2 and Lane 7: Positive Control (Porcine Lipase), Lane 3: Bovine Pancreatic Crude Extract, Lane 4: Bovine Anion Exchange Chromatography, Lane 5: Sheep Pancreatic Crude Extract, Lane 6: Sheep Anion Exchange Chromatography, and Lane 8 (Gel B and C): Candy Cane™ Protein Ladder.

8.3.5.3 Glycoprotein Enrichment for Bovine and Sheep Pancreatic Crude Extract

The bovine and sheep crude extracts were further analysed with a Glycosylation Isolation Kit, Con A, and stained with Coomassie Brilliant Blue. Con A specifically binds to mannose and glucose residues on N–linked glycoproteins. The Con A–enriched fraction primarily retained high–mannose and hybrid–type N–glycans, consistent with Con A's specificity. The samples were also concentrated with acetone precipitation for a better yield of protein concentration. The human prostate was used as a positive control to compare with the bovine and sheep crude extract samples.

As shown in Figure 8.16, the human prostate is a good glycoprotein positive control, as multiple bands representing the glycosylated protein in the bound fraction were visualized in the 1D–SDS PAGE (Figure 8.16 – **Lane 4**). Next, for the bovine sample, three bands were observed, and one of them is postulated to be at the CBPA1 targeted molecular weight (Figure 8.16 – **Lane 7**). Similarly, for the sheep sample, three bands were observed, and one of them is also postulated to be at the CBPA1 targeted molecular weight (Figure 8.16 – **Lane 10**). From the glycoprotein enrichment result, it is proposed that only purified CBPA1 was considered as a glycosylated protein.

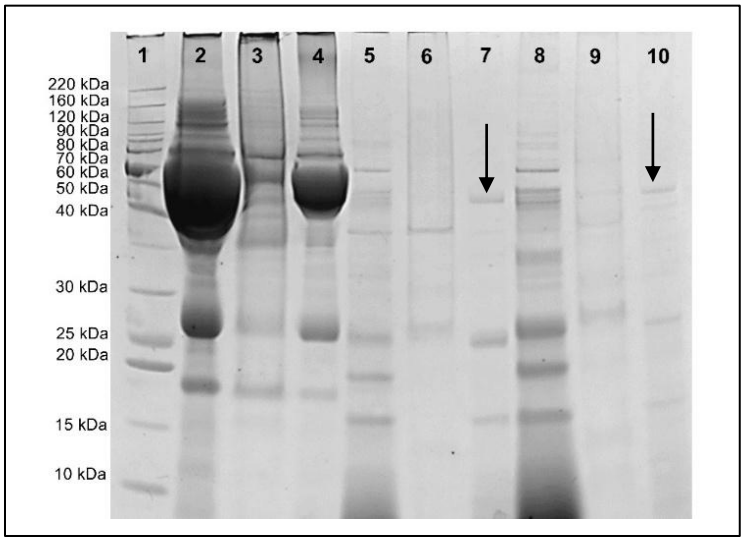


Figure 8.16 1D–SDS PAGE (Bis–Tris 12%) of Bovine and Sheep Pancreatic Crude Extract Glycoprotein Enrichment.

Note: Lane 1: Benchmark^{TM} Protein Ladder, Lane 2: Human prostate, Lane 3: Unbound Human prostate, Lane 4: Bound Human prostate, Lane 5: Fresh Bovine Crude Extract, Lane 6: Unbound Fresh Bovine Crude Extract, Lane 7: Bound Fresh Bovine Crude Extract, Lane 8: Fresh Sheep Crude Extract, Lane 9: Unbound Fresh Sheep Crude Extract and Lane 10: Bound Fresh Sheep Crude Extract.

8.4 Discussion

Glycosylation is a critical post–translational modification (PTM) that influences protein folding, stability, and function (Pienkowski *et al.,* 2025). It is the most prevalent PTM in enzymes (Kiribayeva *et al.,* 2024). For enzymes such as proteases, lipases, and amylases, glycosylation is essential for facilitating correct folding, enhancing resistance to proteolysis, and supporting efficient enzymatic activity within the harsh digestive environment (Esmail & Manolson, 2021; Goettig, 2016). Furthermore, it is important to understand these specific modifications for developing new therapeutic biomolecules, as aberrant or incompatible glycosylation can result in reduced enzymatic activity, a limited circulation half–life, and lead to unwanted immunogenicity. The primary motivation is to elucidate these structural details focusing on the glycosylation status from the current reliance on porcine based Pancreatic Enzyme Replacement Therapy (PERT).

Based on the presented in the previous chapters of this thesis, bovine and sheep has been shown to be a functional source and could be served as a highly promising Halal compliant alternative for PERT replacement in the future. However, the purified enzymes from bovine and sheep sources need to confidently validated as viable functional substitutes for porcine enzymes. Thus, it is necessary to comprehensively compare their biochemical and structural profiles. In this study, we employed a combination of *in–silico* bioinformatic analysis and experimental findings approaches to investigate the glycosylation status of these pancreatic enzymes, namely, CBPA1, BSAL, TL, and AMYP. This study represents a current and updated report on the glycosylation analysis of the purified pancreatic enzymes from bovine and sheep in comparison to porcine and human.

Prior to the *in–silico* glycosylation analysis, the protein information of the pancreatic enzymes of interest such as accession numbers (ID), functions, sequences, length of amino acid sequences, molecular weight (MW) and isoelectric point (pI) was obtained from the Expasy online server. These information of *in–silico* bioinformatic characterization provides critical structural and biochemical insights that rationalize the physical behaviour, stability, and isolation outcomes of the targeted pancreatic enzymes during the experimental purification processes. Furthermore, these *in–silico*

bioinformatic information helps to strategize the experimental purification processes by providing essential physicochemical baseline data, specifically the theoretical MW and pI. The selection of anion exchange chromatography (IEX) and gel filtration chromatography (GFC) technique was initially based on the *in–silico* bioinformatic characterization findings. In addition, the choices of the start buffer, elution buffer and mobile phase for the selected purification methods were optimized based on the theoretical MW and pI information to ensure successful binding on the columns used.

The *in–silico* analysis has successfully generated and validated the 3D protein model structure for each class of the pancreatic enzymes for bovine, sheep, porcine and human validated by acceptable range of MolProbity score, Ramachandran plot and Root Mean Square Deviation (RMSD). Then, the *in–silico* prediction of the glycosylation sites were analysed using GlycoPred, NetNGlyc 1.0, and NetOGlyc 4.0 servers enabled the potential NLG and OLG sites. These predictions were then visualized using PyMol software in the context of protein structure by utilizing a protein template of each enzyme of interest. The glycoprotein enrichment was done, followed by staining to validate the computational findings. The experimental findings provide strong evidence for the computational approach for glycosylation analysis. Two types of glycosylation sites, which are NLG and OLG, were observed in all enzymes of interest.

The *in–silico* glycosylation analysis also suggested that all enzymes were predicted to have more N–glycan sites compared to O–glycan sites, except undetected OLG for porcine TL. There has been no recent study that investigated the glycosylation state of these pancreatic enzymes, such as CBPA1, BSAL, TL, and AMYP from bovine and sheep. One of the studies available was on bovine pancreatic BSAL mass spectrometric characterization and glycosylation profiling (Wang *et al.,* 1998). Interestingly, this study identified 26 potential NLG sites using glycosylation site prediction in bovine BSAL, which is significantly higher than the 2 NLG sites reported in a previous study using mass spectrometry–based glycoproteomic analysis. This discrepancy may be attributed to different methodologies employed, which is mass spectrometry provides direct evidence of glycosylation, and this study only used computational prediction tools, such as GlycoPred and NetNGlyc 1.0, that can only detect all theoretically N–linked glycosylatable motifs based on sequence and structural features. Next, this study indicated that there are NLG and OLG sites predicted on

human BSAL. However, only OLG with nine threonine residues and less than one serine was reported to be glycosylated previously in a human milk BSAL sample (Wang *et al.,* 1995). The porcine TL was reported as a glycoprotein, and the glycan moiety was bound to asparagine 166, which is consistent with the study findings that only NLG sites were predicted (Bianchetta *et al.,* 1979). Other than that, human AMYP was predicted to be N–linked and O–linked glycosylated, but the previous study reported that it was only N–linked glycosylated at asparagine 461, analysed with electrospray ionization mass spectrometry (Rydberg *et al.,* 1999). No direct comparison based on the previous study can be made on other pancreatic enzymes of interest since the literature is limited.

Although the possible N–linked and O–linked glycosylation sites were successfully predicted and visualized using the PyMol software, the glycoprotein enrichment and staining were done to further validate the glycosylation status of the pancreatic enzymes. The Concanavalin A (Con A) lectin–based glycoprotein enrichment kit was used since the *in–silico* glycosylation analysis revealed that enzymes were heavily N–linked glycosylated. This is because, Con A lectin exhibits a high, specific binding affinity for mannose and glucose residues, which are the fundamental building blocks of high–mannose and hybrid–type N–glycans. Therefore, this lectin–based enrichment method was the most biologically appropriate and targeted choice to isolate the specific N–linked glycoproteins as predicted by the *in–silico* glycosylation analysis.

Surprisingly, only bovine and sheep CBPA1 are suggested to be glycosylated after the glycoprotein enrichment, and on the 1D–SDS PAGE staining results, as there were bands observed at the expected size of approximately 45–47 kDa (Figure 8.16 – **Lane 7 and Lane 10**) from the crude extract samples. Before glycoprotein enrichment, there were no visible bands were observed on the crude extract and purified samples for both bovine and sheep samples, as seen in Figure 8.14 and Figure 8.15, respectively. It is postulated that the glycoprotein concentration was low, and it is also possible that the available glycans were masked by abundant non–glycosylated protein present in the samples. This is supported by the LC–MS/MS findings, where non–glycosylated peptides are more abundant and they dominate the spectra analysed through the mass spectrometry (Saraswat *et al.,* 2021).

The Con A enrichment method specifically addresses this limitation whereby the glycopeptides carrying the target glycan structures were retained on the lectin support, while non–glycosylated peptides, incompatible glycans, and other interfering contaminants such as detergents and salts were effectively washed away, which improved the quality of the glycoprotein staining. The Con A enrichment was successful in visualizing the targeted bands of bovine and sheep CBPA1 from the crude extract samples on the 1D–SDS PAGE. Thus, it is suggested that the glycan presented in both bovine and sheep CBPA1 was bound to the lectin. Commonly, glycopeptides carrying the glycan structures that have affinity toward the selected lectins will be retained on the lectin supports, and non–glycosylated peptides or non–targeted glycopeptides will flow through (Ongay *et al.,* 2012). In addition, only glycan or glycoprotein with specific mannose or glucose residues will bind to the lectin and be eluted as bound glycoprotein. The lectin binding specificity is an important factor and is determined by the ability to recognize the specific monosaccharides, such as mannose or glucose (Sondej *et al.,* 2009). This method is only suitable for the N–linked glycans detection, as the incompatible glycans and non–glycosylated proteins will be washed away during the enrichment procedure. Moreover, the selection of the Con A enrichment method helps to justified on the heavily N–linked glycosylated during the *in–silico* predictions.

While the computational and experimental findings of this study provide preliminary insights into the glycosylation status of bovine and sheep pancreatic enzymes (CBPA1, BSAL, TL and AMYP), a direct comparison with current literature presents a critical challenge. To date, there is a substantial lack of recent studies investigating the structural characterization and glycosylation profiles of CBPA1, BSAL, TL, and AMYP from Halal animal sources. Historically, the fundamental characterization of these mammalian enzymes peaked between the 1970s and late 1990s. In recent decades, the scientific focus has predominantly shifted toward microbial and recombinant enzyme sources for industrial applications, or toward the clinical utility of these enzymes, such as utilizing CBPA1 as a diagnostic marker for pancreatic carcinoma (Ishimoto–Namiki *et al.,* 2023; Said *et al.,* 2020; Uhlig *et al.,* 2022). Consequently, the available literature for comparative glycosylation analysis is largely historical.

In addition, there is still a lack of information on the attached glycan of the purified pancreatic enzymes. The utilization of *in–silico* glycosylation analysis and the application on the traditional method of lectin–based enrichment may serve as an excellent and robust qualitative screening tool to prove glycosylation status. Therefore, further investigation still needs to be conducted, focusing on the attached glycan information and how it could influence protein function, stability, and cellular interactions (Saraswat *et al.,* 2021).

8.5 Conclusion

In conclusion, this study investigates the prediction and structural visualization of N– and O–linked glycosylation sites of pancreatic enzymes such as CBPA1, BSAL, TL, and AMYP using an *in–silico* approach. Glycosylation was further validated through specialized glycosylation staining techniques and glycoprotein enrichment protocols. All of the enzymes demonstrated a predominant N–linked glycosylation compared to O–linked glycosylation, except for porcine TL, which shows no detectable O–linked sites in the computational analysis. Among the purified enzymes, only CBPA1 was experimentally confirmed to be glycosylated following the glycoprotein enrichment using Con A enrichment, suggesting its biological relevance and potential PTM. To strengthen these findings, future research should integrate mass spectrometry–based glycoproteomic approach to comprehensively elucidate the complex structure to identify glycosylation sites and glycan structures by using high–end machines, such as Ultra Performance Liquid Chromatography could be an added point before these purified enzymes could be appointed as a Halal alternative to porcine enzymes for industrial applications.

CHAPTER 9
CONCLUSION AND RECOMMENDATION

9.1 Introduction

The first part of this study was designed to extract and purify the bovine (*Bos taurus*) and sheep (*Ovis aries*) pancreatic enzymes from fresh pancreas, namely Carboxypeptidase A1 (CBPA1), Bile–Salt Activated Lipase (BSAL), Triacylglycerol Lipase (TL), and Alpha–Amylase (AMYP). The extraction and the purification were successfully done from fresh pancreas to crude extraction, and purification via anion exchange chromatography (IEX) for CBPA1, BSAL, TL, and AMYP. The gel filtration chromatography (GFC) was done to further purify the CBPA1. As a result, successful purification of CBPA1 from both bovine and sheep, BSAL from bovine, and TL from sheep. These pancreatic enzymes were identified and confirmed with LC–MS/MS analysis as bovine CBPA1 (P00730), sheep CBPA1 (W5P5N4), bovine BSAL (P30122), and sheep TL (W5Q5I2). However, the AMYP was unsuccessfully purified and identified from bovine and sheep samples.

The second section focuses on the enzymatic activities of bovine and sheep purified pancreatic enzymes with commercialize porcine enzymes as a positive control. In general, all of the purified enzymes' activities were comparable to the positive control. The specific proteolytic activities of the purified bovine CBPA1 from IEX samples were approximately 32–fold higher than those of porcine pancreatin. The sheep IEX samples demonstrated a greater specific proteolytic activity with an increase of 55–fold than the porcine pancreatin. On the other hand, the specific lipolytic activity of the purified BSAL was equivalent to porcine lipase, with minimal difference observed between these two samples. Meanwhile, the sheep pancreatic TL crude extract recorded three times higher specific lipolytic activity than the porcine lipase. Lastly, for AMYP, the bovine and sheep pancreatic crude extract recorded higher amylolytic activity when compared to the porcine α amylase based on the larger clear zone formation on the MHA. In summary, enzyme activities can be varied depending on the stage of sample processing, with changes observed from the crude extract through to the purified form.

The last part of this study combines both *in–silico* and experimental findings to investigate the glycosylation status of the pancreatic enzymes studied. The *in–silico* analysis revealed higher similarity in homology modelling of the purified pancreatic enzyme from bovine and sheep in comparison to porcine and human. The *in–silico* glycosylation demonstrated that all of the enzymes have a predominant N–linked glycosylation compared to O–linked glycosylation, except for porcine TL, which shows no detectable O–linked sites. Only CBPA1 was experimentally postulated to be glycosylated following enrichment, suggesting its biological relevance and potential post–translational modification (PTM).

9.2 Conclusion and Recommendation

This research extends our knowledge to the current understanding of pancreatic enzyme extraction and purification focusing on bovine and sheep. Among the purified pancreatic enzymes, sheep CBPA1 and bovine BSAL are strongly suggested for the PERT replacements as it shows potent enzymatic activities when compared to the positive porcine standards. In addition to isolate key pancreatic enzymes such as CBPA1, BSAL, and TL, this study incorporates glycosylation state prediction analyses, providing preliminary insights into potential PTM that may influence enzyme function. However, detailed glycan structural analysis for the purified enzymes is absence which has become a limitation in this study. Deep glycan analysis is critical for elucidating the specific glycan moieties may influence enzyme stability and activity. Unfortunately, the study did not include the glycan structure analysis. It would be significant scientific interest to compare the glycan profiles of the purified bovine and sheep pancreatic enzymes with those from porcine sources as a positive control. By understanding the structural and functional implications of glycosylation could reveal unique characteristics that either enhance or limit the use of non–porcine alternatives. Future research should prioritize in–depth glycan structure characterization, employing high–resolution mass spectrometry analytical techniques such as Ultra Performance Liquid Chromatography. This would strengthen the case for adopting bovine or ovine pancreatic enzymes as viable substitutes for porcine enzymes in industrial, particularly where religious, ethical, or supply–related concerns limit the porcine enzyme usage.

REFERENCES

Abdelaziz, A. A., Abo-Kamar, A. M., Elkotb, E. S., & Al-Madboly, L. A. (2025). Microbial lipases: advances in production, purification, biochemical characterization, and multifaceted applications in industry and medicine. *Microbial Cell Factories*, *24*(40), 1–20.

Abdelraheem, E. M. M., Busch, H., Hanefeld, U., & Tonin, F. (2019). Biocatalysis explained: From pharmaceutical to bulk chemical production. *Reaction Chemistry and Engineering*, 1–30.

Abouakil, N., Mas, E., Bruneau, N., Benajiba, A., & Lombardo, D. (1993). Bile salt-dependent lipase biosynthesis in rat pancreatic AR 4-2 J cells. Essential requirement of N-linked oligosaccharide for secretion and expression of a fully active enzyme. *Journal of Biological Chemistry*, *268*(34), 25755–25763.

Abouakil, N., Rogalska, E., Bonicel, J., & Lombardo, D. (1988). Purification of pancreatic carboxylic-ester hydrolase by immunoaffinity and its application to the human bile-salt-stimulated lipase. *Biochimica et Biophysica Acta (BBA) - Lipids and Lipid Metabolism*, *961*, 299–308.

Adams, C. W., Allison, D. E., Flagella, K., Presta, L., Clarke, J., Dybdal, N., McKeever, K., & Sliwkowski, M. X. (2006). Humanization of a recombinant monoclonal antibody to produce a therapeutic HER dimerization inhibitor, pertuzumab. *Cancer Immunology, Immunotherapy*, *55*(6), 717–727.

Adhikari, N., Amin, Sk. A., & Jha, T. (2020). Collagenases and gelatinases and their inhibitors as anticancer agents. In Satya P. Gupta (Ed.), *Cancer-Leading Proteases*. Academic Press. https://doi.org/10.1016/B978-0-12-818168-3.00010-3.

Ahasan, A. S. M. L., Invernizzi, G., Farina, G., Pilotto, A., Barbé, F., Bontempo, V., Rossi, R., Bellagamba, F., Lecchi, C., Savoini, G., & Agazzi, A. (2018). The effects of superoxide dismutase-rich melon pulp concentrate on inflammation, antioxidant status and growth performance of challenged post-weaning piglets. *Animal*, *13*(1), 136–143.

Ahmad, A. N., Abidin, U. F. U. Z., Othman, M., & Rahman, R. A. (2018). Overview of the halal food control system in Malaysia. *Food Control*, *90*, 352–363.

Akinfemiwa, O., Zubair, M., & Muniraj Thiruvengadam. (2023). Amylase. In *StatPearls [Internet]*. Treasure Island (FL): StatPearls Publishing. https://www.ncbi.nlm.nih.gov/books/NBK557738/

Al-Ajlan, A., & Bailey, G. S. (1999). Purification and some properties of camel carboxypeptidase B. *Molecular and Cellular Biochemistry*, *201*, 105–110.

Al-Bedak, O. A. M., Moharram, A. M., Ameen, F., Stephenson, S. L., Idres, M. M. M., & Yasser, M. M. (2025). Optimizing conditions for augmented production of amylase by *Talaromyces islandicus* AUMC 11391. *Electronic Journal of Biotechnology*, *75*, 39–48.

Alexandre-Heymann, L., Yaker, F., Lassen, P. B., Dubois-Laforgue, D., & Larger, E. (2024). Pancreatic enzyme replacement therapy in subjects with exocrine pancreatic insufficiency and diabetes mellitus: a real-life, case–control study. *Diabetology and Metabolic Syndrome*, *16*(39), 1–10.

Alhajj, M., Zubair, M., & Farhana Affiliations, A. (2023). Enzyme Linked Immunosorbent Assay. In *StatPearls [Internet]*. Treasure Island (FL): StatPearls Publishing. https://www.ncbi.nlm.nih.gov/books/NBK555922/

Alhazmi, L. S., & Alshehri, W. A. (2025). Purification and biochemical characterization of α-Amylase from newly isolated *Bacillus Cereus* strain and its application as an additive in breadmaking. *Polish Journal of Microbiology*, *74*(1), 48–59.

Alina, A. R., Illiyin, M. A. N., Juraini, J., Salmah, Y., Mashitoh, A. S., & Imtinan, A. K. (2012). Detection of non-halal plasma transglutaminase in selected surimi-based products by using sandwich ELISA method. *World Applies Sciences Journal 17*, 39–44.

Alipal, J., Mohd Pu'ad, N. A. S., Lee, T. C., Nayan, N. H. M., Sahari, N., Basri, H., Idris, M. I., & Abdullah, H. Z. (2021). A review of gelatin: Properties, sources, process, applications, and commercialisation. *Materials Today: Proceedings*, *42*, 240–250.

Aloulou, A., Puccinelli, D., De Caro, A., Leblond, Y., & Carrière, F. (2007). A comparative study on two fungal lipases from *Thermomyces lanuginosus* and *Yarrowia lipolytica* shows the combined effects of detergents and pH on lipase adsorption and activity. *Biochimica et Biophysica Acta - Molecular and Cell Biology of Lipids*, *1771*, 1446–1456.

American Halal Foundation. (2024). *The Untapped Market For Halal Pharmaceuticals*. https://halalfoundation.org/the-untapped-market-for-halal-pharmaceuticals/

American Lung Association. (2020). *Learn about Cystic Fibrosis*. https://www.lung.org/lung-health-diseases/lung-disease-lookup/cystic-fibrosis/learn-about-cystic-fibrosis

American Medical Association. (2017). Pancreatic enzyme replacement products. *JAMA - Journal of the American Medical Association*, *318*(19), 1929.

An, H. J., Froehlich, J. W., & Lebrilla, C. B. (2009). Determination of glycosylation sites and site-specific heterogeneity in glycoproteins. *Current Opinion in Chemical Biology*, *13*(4), 421–426.

An, H. J., Froehlich, J. W., & Lebrilla, C. B. (2017). Determination of glycosylation sites and site-specific heterogeneity in glycoproteins hyun. *Russian Chemical Bulletin*, *66*(5), 882–885.

Anish, A. K. (2022). Halal food industry in world: Opportunity and challenges. *SSRN Electronic Journal*.

Antonini, F., Crippa, S., Falconi, M., Macarri, G., & Pezzilli, R. (2017). Pancreatic enzyme replacement therapy after gastric resection: An update. *Digestive and Liver Disease*, *50*, 1–5.

Arey, B. J. (2012). The role of glycosylation in receptor signaling. . In Petrescu Stefana (Ed.), *Glycosylation*. InTechOpen. https://www.intechopen.com/chapters/39461

Ariff, O. M., Sharifah, N. Y., & Hafidz, A. W. (2015). Status of beef industry of Malaysia. *Malaysian Journal of Animal Science*, *18*(2), 1–21.

Arham, Q. L., Yasri, Y., & Abror, A. (2026). A bibliometric study on the implementation of Halal practices in West Sumatera with VOSviewer. *Jurnal Manajemen Motivasi*, *22*, 622–629.

Arienti, G., Harrison, F. A., & Leat, W. M. F. (1974). The lipase activity of sheep pancreatic juice. *Quarterly Journal of Experimental Physiology and Cognate Medical Sciences*, *59*, 351–359.

Ashkar, M., Geremia, J., Baldwin, Z., Edwards, M. L., Zhang, Y., Garcia-Horton, V., Yang, M., Shen, E., Dylla, D. E., Sanchez Gonzalez, Y., & Barkin, J. A. (2025). Prescribing patterns and perceptions of pancreatic enzyme replacement therapy

among healthcare providers: A Prospective United States healthcare providers survey. *Advances in Therapy*, 1–20.

Assidi, M., Dufort, I., Ali, A., Hamel, M., Algriany, O., Dielemann, S., & Sirard, M. A. (2008). Identification of potential markers of oocyte competence expressed in bovine cumulus cells matured with follicle-stimulating hormone and/or phorbol myristate acetate in vitro. *Biology of Reproduction*, *79*, 209–222.

Augé, N., Rebaï, O., Lepetit-Thévenin, J., Bruneau, N., Thiers, J.-C., Mas, E., Lombardo, D., Negre-Salvayre, A., & Vérine, A. (2003). Pancreatic bile salt-dependent lipase induces smooth muscle cells proliferation. *Circulation*, *108*, 86–91.

Aziz, N. A., Ibrahim, I., & Raof, N. A. (2014). The need for legal intervention within the Halal pharmaceutical industry. *Procedia - Social and Behavioral Sciences*, *121*, 124–132.

Aziz, S. (2018). Pancreatitis in children: A diagnosis missed in Pakistan? *Journal of the Pakistan Medical Association*, *68*(8), 1154–1156.

Bacha, A. Ben, Gargouri, Y., Bezzine, S., & Mejdoub, H. (2006). Purification and biochemical characterization of phospholipase A2 from dromedary pancreas. *Biochimica et Biophysica Acta - General Subjects*, *1760*, 1202–1209.

Banchhor, M., & Saraf, S. (2008). Potentiality of Papain as an Antiaging Agent in cosmetic formulation. *Pharmacognosy Reviews*, *2*(4), 266–270.

Bangarh, R., Khatana, C., Kaur, S., Sharma, A., Kaushal, A., Siwal, S. S., Tuli, H. S., Dhama, K., Thakur, V. K., Saini, R. V., & Saini, A. K. (2023). Aberrant protein glycosylation: Implications on diagnosis and Immunotherapy. *Biotechnology Advances*, *66*.

Banks, W., Mazumder, N. K., & Spooner, R. L. (1976). The action pattern of bovine pancreatic alpha-amylase. *Int. J. Biochem*,*7*, 107–110.

Bartel, M. J., Asbun, H., Stauffer, J., & Raimondo, M. (2015). Pancreatic exocrine insufficiency in pancreatic cancer: A review of the literature. *Digestive and Liver Disease*, *47*, 1013–1020.

Bartels, R. H., Meyer, S. L., Stehmann, T. A., Bourdon, C., Bandsma, R. H. J., & Voskuijl, W. P. (2016). Both exocrine pancreatic insufficiency and signs of pancreatic inflammation are prevalent in children with complicated severe acute malnutrition: An observational study. *Journal of Pediatrics*, *174*, 165–170.

Basso, M. F., Valencia-Jiménez, A., Celso, F. Lo, Gerhardt, I. R., Higgins, T. J. V., & Grossi-de-Sa, M. F. (2025). Exploring plant α-Amylase inhibitors: Mechanisms and potential application for insect pest control. *Biotechnology Journal*, *20*(e70098).

Bellomo, T. L. (2020). Exocrine pancreatic insufficiency: Can this be the cause of your patient's GI symptoms? *Nursing*, *50*(3), 41–45.

Ben Abdelmalek, I., Alhmdi, T. A. A., Ben Bacha, A., & Krayem, N. (2025). Unlocking the therapeutic potential of *Saussurea costus*: purification and functional characterization of α-amylase inhibitors. *Frontiers in Bioengineering and Biotechnology*, *13*.

Berry, A. J. (2014). Pancreatic enzyme replacement therapy during pancreatic insufficiency. *Current Gastroenterology Reports*, *29*(3), 101–108.

Berton, A., Rouvellac, S., Robert, B., Rousseau, F., Lopez, C., & Crenon, I. (2012). Effect of the size and interface composition of milk fat globules on their in vitro digestion by the human pancreatic lipase: Native versus homogenized milk fat globules. *Food Hydrocolloids*, *29*(1), 123–134.

Bharathi, D., Rajalakshmi, G., & Komathi, S. (2019). Optimization and production of lipase enzyme from bacterial strains isolated from petrol spilled soil. *Journal of King Saud University - Science*, *31*(4), 898–901.

Bianchetta, J. D., Bidaud, J., Guidoni, A. A., Bonicel, J. J., & Rovery, M. (1979). Sequence of the first 234 amino acids of porcine pancreatic lipase. *European Journal of Biochemistry*, *97*, 395–405.

Birhanu, A. G. (2023). Mass spectrometry-based proteomics as an emerging tool in clinical laboratories. In *Clinical Proteomics* (Vol. 20, Number 32, pp. 1–20). BioMed Central Ltd.

Bond, J. S. (2019). Proteases: History, discovery, and roles in health and disease. *Journal of Biological Chemistry*, *294*(5), 1643–1651.

Borowitz, D., Goss, C. H., Limauro, S., Konstan, M. W., Blake, K., Casey, S., Quittner, A. L., & Murray, F. T. (2006). Study of a novel pancreatic enzyme replacement therapy in pancreatic insufficient subjects with cystic fibrosis. *Journal of Pediatrics*, *149*(5).

Böswald, L. F., Kienzle, E., Matzek, D., Schmitz, M., & Popper, B. A. (2023). Comparative analysis of pancreatic amylase activity in laboratory rodents. *Scientific Reports*, *13*(17299), 1–8.

Bradley, G., Naude, R. J., Muramoto, K., Yamauchi, F., & Oelofsen, W. (1994). Ostrich (*Struthio Camelus*) Carboxypeptidase A: Purification, Characterization Kinetic Properties and of the Pancreatic Enzyme. *Int. J. Biochem*, *26*(4), 555–564.

Brennan, G. T., & Saif, M. W. (2019). Pancreatic enzyme replacement therapy: A concise review. *JOP : Journal of the Pancreas*, *20*(5), 121–125.

Britannica. (2020). *Zymogen*. https://www.britannica.com/science/zymogen

Bruneau, N., Lombardo, D., & Bendayan, M. (2000). The affinity binding sites of pancreatic bile salt-dependent lipase in pancreatic and intestinal tissues. *Journal of Histochemistry & Cytochemistry*, *48*(2), 267–276.

Busnardo, A. C., Didio, L. J. A., Tidrick, R. T., & Thomford, N. R. (1983). History of the pancreas. *American Journal of Surgery*, *146*(5), 539–550.

Cade, J. E., & Hanison, J. (2017). The pancreas. *Anaesthesia and Intensive Care Medicine*, *18*, 527–531.

Calame, K. B., Gallo, L., Cheriathundam, E., Vahouny, G. V., & Treadwell, C. R. (1974). Purification and properties of subunits of sterol ester hydrolase from rat pancreas. *Archives of Biochemistry and Biophysics*, *168*, 57–65.

Calder, P. C. (2016). Fatty acids: Metabolism. *Encyclopedia of Food and Health* (pp. 632–644). Elsevier Ltd.

Canioni, P., Benajiba, A., Julien, R., Rathelot, J., Benabdeljlil, A., & Sarda, L. (1975). Ovine pancreatic lipase : Purification and some properties. *Biochimie*, *57*, 35–41.

Capurso, G., Traini, M., Piciucchi, M., Signoretti, M., & Arcidiacono, P. G. (2019). Exocrine pancreatic insufficiency: Prevalence, diagnosis, and management. *Clinical and Experimental Gastroenterology*, *12*, 129–139.

Caro, A. D. E., Bonicel, J., & Guy, O. (1981). Comparative studies of human and porcine pancreatic lipases: N-terminal sequences, sulfhydryl groups and interfacial activity. *Biochimie*, *63*, 799–801.

Chabot, J. A., Tsai, W. Y., Fine, R. L., Chen, C., Kumah, C. K., Antman, K. A., & Grann, V. R. (2010). Pancreatic proteolytic enzyme therapy compared with gemcitabine-

based chemotherapy for the treatment of pancreatic cancer. *Journal of Clinical Oncology*, *28*(12), 2058–2063.

Chahinian, H., Vanot, G., Ibrik, A., Rugani, N., Sarda, L., & Comeau, L. C. (2000). Production of extracellular lipases by *Penicillium cyclopium* purification and Characterization of a partial acylglycerol lipase. *Bioscience, Biotechnology and Biochemistry*, *64*(2), 215–222.

Chandra, P., Enespa, Singh, R., & Arora, P. K. (2020). Microbial lipases and their industrial applications: a comprehensive review. *Microbial Cell Factories*, *19*(169), 1–42.

Chapman, J., Ismail, A. E., & Dinu, C. Z. (2018). Industrial applications of enzymes: Recent advances, techniques, and outlooks. *Catalysts*, *8*(6), 20–29.

Chaudhary, A., Domínguez-Muñoz, J. E., Layer, P., & Lerch, M. M. (2020). Pancreatic exocrine insufficiency as a complication of gastrointestinal surgery and the impact of pancreatic enzyme replacement therapy. *Digestive Diseases*, *38*(1), 53–68.

Chen, B., Liu, W., Li, Y., Ma, B., Shang, S., & Tan, Z. (2022). Impact of N-linked glycosylation on therapeutic proteins. *Molecules*, *27*(24), 1-10.

Chen, C.-X., Zhang, Y.-Y., Yang, J., Yan, M.-H., Jie, Y., & Jiang, S. (2024). An overview of progress in the application of recombinant collagen in cosmetics. *Journal of Dermatologic Science and Cosmetic Technology*, *1*(4), 1–2.

Chen, J. C. H., Miercke, L. J. W., Krucinski, J., Starr, J. R., Saenz, G., Wang, X., Spilburg, C. A., Lange, L. G., Ellsworth, J. L., & Stroud, R. M. (1998). Structure of Bovine Pancreatic Cholesterol Esterase at 1.6 Å: Novel structural features involved in lipase activation. *Biochemistry*, *37*(15), 5107–5117.

Chen, K. Y., Chang, S. Sen, & Chen, C. Y. C. (2012). In silico identification of potent pancreatic triacylglycerol lipase inhibitors from traditional chinese medicine. *PLoS ONE*, *7*(9), 1–11.

Cheng, T. H., Ismail, N., Kamaruding, N., Saidin, J., & Danish-Daniel, M. (2020). Industrial enzymes-producing marine bacteria from marine resources. *Biotechnology Reports*, *27*(e00482), 1–9.

Chiu, H.-H., Tsai, I.-L., Lu, Y.-S., Lin, C.-H., & Kuo, C.-H. (2017). Development of an LC-MS/MS method with protein G purification strategy for quantifying

bevacizumab in human plasma. *Analytical and Bioanalytical Chemistry*, *409*(28), 6583–6593.

Choi, J. M., Han, S. S., & Kim, H. S. (2015). Industrial applications of enzyme biocatalysis: Current status and future aspects. *Biotechnology Advances*, *33*(7), 1443–1454.

Christie, D. L., Cleverly, D. R., & O'Connor, C. J. (1991). Human milk bile-salt stimulated lipase. Sequence similarity with rat lysophospholipase and homology with the active site region of cholinesterases. *FEBS Letters*, *278*(2), 190–194.

Claghorn, K. V. (2019). *Pancreatic enzyme replacement therapy (PERT)*. Oncolink. https://www.oncolink.org/support/nutrition-and-cancer/during-and-after-treatment/pancreatic-enzyme-replacement-therapy-pert

Clauser, E., Gardell, S. J., Craik, C. S., MacDonald, R. J., & Rutter, W. J. (1988). Structural characterization of the rat carboxypeptidase A1 and B genes. Comparative analysis of the rat carboxypeptidase gene family*. *The Journal of Biological Chemistry*, *263*(33), 17837–17845.

Contesini, F. J., Davanço, M. G., Borin, G. P., Vanegas, K. G., Cirino, J. P. G., de Melo, R. R., Mortensen, U. H., Hildén, K., Campos, D. R., & Carvalho, P. de O. (2020). Advances in recombinant lipases: application in the pharmaceutical industry. *Industrial Biocatalysis: Challenges and Opportunities*, *10*, 1–33.

Cruickshank, A. H. (1986). The normal pancreas. *In Pathology of the Pancreas* (pp. 275–276). Springer, London. https://doi.org/10.1007/978-1-4471-3329-2_1

Cui, N., Hu, M., & Khalil, R. A. (2017). Biochemical and biological attributes of matrix metalloproteinases. *Progress in Molecular Biology and Translational Science*, *147*, 1–73.

Cui, Y., Jiao, Y., Wang, K., He, M., & Yang, Z. (2019). A new prognostic factor of breast cancer: High carboxyl ester lipase expression related to poor survival. *Cancer Genetics*, *239*, 54–61.

Dako, E., Bernier, A.-M., Thomas, A., & Jankowski, C. K. (2012). The problems associated with enzyme purification. In *Chemical Biology* (pp. 20–40). InTech. https://doi.org/10.5772/33307

Date, K., Satoh, A., Iida, K., & Ogawa, H. (2015). Pancreatic α-amylase controls glucose assimilation by duodenal retrieval through N-glycan-specific binding, endocytosis, and degradation. *Journal of Biological Chemistry*, *290*(28), 17439–17450.

Dawson, H. D., Chen, C., Gaynor, B., Shao, J., & Urban, J. F. (2017). The porcine translational research database: A manually curated, genomics and proteomics-based research resource. *BMC Genomics*, *18*(1), 1–13.

Dawson, H. D., Loveland, J. E., Pascal, G., Gilbert, J. G. R., Uenishi, H., Mann, K. M., Sang, Y., Zhang, J., Carvalho-Silva, D., Hunt, T., Hardy, M., Hu, Z., Zhao, S. H., Anselmo, A., Shinkai, H., Chen, C., Badaoui, B., Berman, D., Amid, C., … Tuggle, C. K. (2013). Structural and functional annotation of the porcine immunome. *BMC Genomics*, *14*(1).

De Caro, J., Boudouard, M., Bonicel, J., Guidoni, A., Desnuelle, P., & Rovery, M. (1981). Porcine pancreatic lipase. Completion of the primary structure. *BBA - Protein Structure*, *671*(2), 129–138.

De La Iglesia-García, D., Huang, W., Szatmary, P., Baston-Rey, I., Gonzalez-Lopez, J., Prada-Ramallal, G., Mukherjee, R., Nunes, Q. M., Enrique Domínguez-Muñoz, J., & Sutton, R. (2017). Efficacy of pancreatic enzyme replacement therapy in chronic pancreatitis: Systematic review and meta-Analysis. *Gut*, *66*(8), 1474–1486.

De Wolf, M., Lagrou, A., Hilderson, H. J., & Dierick, W. (1978). Acid triacylglycerol lipase from bovine thyroid gland. *Lipids*, *13*(9), 598–604.

Dennis, E. A., Cao, J., Hsu, Y. H., Magrioti, V., & Kokotos, G. (2011). Phospholipase A2 enzymes: Physical structure, biological function, disease implication, chemical inhibition, and therapeutic intervention. *Chemical Reviews*, *111*(10), 6130–6185.

Dimesa, A. M., Coban, M. A., & Shoari, A. (2026). Matrix Metalloproteinases in Hepatocellular Carcinoma: Mechanistic Roles and Emerging Inhibitory Strategies for Therapeutic Intervention. *Cancers*, *18*(2), 288.

Dindyal, S., & Spalding, D. (2019). Pancreatic cancer Key points. *Medicine*, *47*(7), 433–439.

Ding, W., Lu, Y., Xu, B., Chen, P., Li, A., Jian, F., Yu, G., & Huang, S. (2024). Meat of Sheep: Insights into Mutton Evaluation, Nutritive Value, Influential Factors, and Interventions. *Agriculture*, *14*(1060), 1–26.

Do Nascimento, J. R. O., Júnior, A. V., Bassinello, P. Z., Cordenunsi, B. R., Mainardi, J. A., Purgatto, E., & Lajolo, F. M. (2006). Beta-amylase expression and starch degradation during banana ripening. *Postharvest Biology and Technology*, *40*(1), 41–47.

Dolinsky, V. W., Gilham, D., Alam, M., Vance, D. E., & Lehner, R. (2004). Triacylglycerol hydrolase: Role in intracellular lipid metabolism. *Cellular and Molecular Life Sciences*, *61*(13), 1633–1651.

Domínguez-Muñoz, J. (2011). Pancreatic enzyme replacement therapy for pancreatic exocrine insufficiency: When is it indicated, what is the goal and how to do it? *Advances in Medical Sciences*, *56*(1), 1–5.

Dominguez-Muñoz, J. E., Vujasinovic, M., de la Iglesia, D., Cahen, D., Capurso, G., Gubergrits, N., Hegyi, P., Hungin, P., Ockenga, J., Paiella, S., Perkhofer, L., Rebours, V., Rosendahl, J., Salvia, R., Scheers, I., Szentesi, A., Bonovas, S., Piovani, D., Löhr, J. M., … Witt, H. (2025). European guidelines for the diagnosis and treatment of pancreatic exocrine insufficiency: UEG, EPC, EDS, ESPEN, ESPGHAN, ESDO, and ESPCG evidence-based recommendations. *United European Gastroenterology Journal*, *13*(1), 125–172.

Doyon, Y., Home, W., Daull, P., & Bel, D. L. E. (2002). Effect of C-domain N-glycosylation and deletion on rat pancreatic α -amylase secretion and activity. *Biochemistry*, *264*, 259–264.

Drag, M., & Salvesen, G. S. (2010). Emerging principles in protease-based drug discovery. *Nature Reviews Drug Discovery*, *9*(9), 690–701.

Duan, R., Zhang, J., Liu, L., Cui, W., & Regenstein, J. M. (2018). The functional properties and application of gelatin derived from the skin of channel catfish (*Ictalurus punctatus*). *Food Chemistry*, *239*, 464–469.

Duan, X., Zhai, W., Li, X., Wu, S., Wang, Y., Wang, L., Basang, W., Zhu, Y., & Gao, Y. (2023). Preparation, purification, and biochemical of fat-degrading bacterial enzymes from pig carcass compost and its application. *BMC Biotechnology*, *23*(1), 1–14.

Dunleavy, L., Al-Mukhtar, A., & Halliday, V. (2018). Pancreatic enzyme replacement therapy following surgery for pancreatic cancer: An exploration of patient self-management. *Clinical Nutrition ESPEN*, *26*, 97–103.

Eatemadi, A., Aiyelabegan, H. T., Negahdari, B., Mazlomi, M. A., Daraee, H., Daraee, N., Eatemadi, R., & Sadroddiny, E. (2017). Role of protease and protease inhibitors in cancer pathogenesis and treatment. *Biomedicine and Pharmacotherapy*, *86*, 221–231.

Eigler, T., & Ben-Shlomo, A. (2014). Somatostatin system: Molecular mechanisms regulating anterior pituitary hormones. *Journal of Molecular Endocrinology*, *53*(1).

Elamin, B. A., Al-Maleki, A., Ismael, M. A., & Ayoub, M. A. (2014). Purification and functional characterization of pancreatic insulin from camel (*Camelus dromedarius*). *Saudi Journal of Biological Sciences*, *21*(6), 574–581.

Ellis, H. (2013). Anatomy of the pancreas and the spleen. *Surgery (United Kingdom)*, *31*(6), 263–266.

Elmansy, E. A., Asker, M. S., El-Kady, E. M., Hassanein, S. M., & El-Beih, F. M. (2018). Production and optimization of α-amylase from thermo-halophilic bacteria isolated from different local marine environments. *Bulletin of the National Research Centre*, *42*(1).

Elsässer, B., Zauner, F. B., Messner, J., Soh, W. T., Dall, E., & Brandstetter, H. (2017). Distinct Roles of Catalytic Cysteine and Histidine in the Protease and Ligase Mechanisms of Human Legumain As Revealed by DFT-Based QM/MM Simulations. *ACS Catalysis*, *7*(9), 5585–5593.

Ermis, E. (2017). Halal status of enzymes used in food industry. *Trends in Food Science & Technology*, *64*, 69–73.

Esmail, S., & Manolson, M. F. (2021). Advances in understanding N-glycosylation structure, function, and regulation in health and disease. *European Journal of Cell Biology*, *100*(7–8).

Ettalibi, M., Abdeljlil, A. Ben, & Marchis-Mouren, G. (1975). Purification and characterization of ovine pancreatic α - amylase. *Biochimie*, *57*(9), 995–999.

Ezema, B. O., Omeje, K. O., Bill, R. M., Goddard, A. D., Sabinus, S. O., & Fernandez-Castane, A. (2023). Bioinformatic characterization of a triacylglycerol lipase produced by *Aspergillus flavus* isolated from the decaying seed of *Cucumeropsis mannii*. *Journal of Biomolecular Structure and Dynamics*, *41*(6), 2587–2601.

Fan, H., Fang, N., Yang, B., Xian, H., & Li, Z. (2025). Spectrochimica Acta Part A: Molecular and Biomolecular Spectroscopy Fluorescence lifetime imaging of human pancreatic lipase activity using a novel probe for early diagnosis of severe acute pancreatitis. *Spectrochimica Acta Part A: Molecular and Biomolecular Spectroscopy*, *326*.

Ferrone, M., Raimondo, M., & Scolapio, J. S. (2007). Pancreatic enzyme pharmacotherapy. *Pharmacotherapy*, *27*(6), 910–920.

Fieker, A., Philpott, J., & Armand, M. (2011). Enzyme replacement therapy for pancreatic insufficiency: Present and future. *Clinical and Experimental Gastroenterology*, *4*(1), 55–73.

Fischer, J. (2016). Manufacturing halal in Malaysia. *Contemporary Islam*, *10*(1), 35–52.

Fjeld, K., Masson, E., Lin, J. H., Michl, P., Stokowy, T., Gravdal, A., El Jellas, K., Steine, S. J., Hoem, D., Johansson, B. B., Dalva, M., Ruffert, C., Zou, W. Bin, Li, Z. S., Njølstad, P. R., Chen, J. M., Liao, Z., Johansson, S., Rosendahl, J., … Molven, A. (2020). Characterization of CEL-DUP2: Complete duplication of the carboxyl ester lipase gene is unlikely to influence risk of chronic pancreatitis. *Pancreatology*, *20*(3), 377–384.

Folk, J. E., & Schirmer, E. W. (1963). The Porcine Pancreatic Carboxypeptidase A System*. *Journal of Biological Chemistry*, *238*(12), 3884–3894.

Fortune Business Insight. (2022). *Halal Food and Beverages Market 2021 – 2028*.

Frulloni, L., Falconi, M., Gabbrielli, A., Gaia, E., Graziani, R., Pezzilli, R., Uomo, G., Andriulli, A., Balzano, G., Benini, L., Calculli, L., Campra, D., Capurso, G., Cavestro, G. M., De Angelis, C., Ghezzo, L., Manfredi, R., Malesci, A., Mariani, A., … Vantini, I. (2010). Italian consensus guidelines for chronic pancreatitis. *Digestive and Liver Disease*, *42*(SUPPL. 6), S381–S406.

Fung, D., Razi, A., Pandos, M., Velez, B., Fermin Perez, E., Adams, L., Rawson, S., Walsh, R. M., & Hanna, J. (2025). Evidence supporting a catalytic pentad mechanism for the proteasome and other N-terminal nucleophile enzymes. *Nature Communications*, *16*(1).

Gagyi, E. B., Obeidat, M., Tari, E., Váncsa, S., Veres, D. S., Banovcin, P., Hegyi, P. J., Hegyi, P., & Eross, B. (2025). Progression from acute to chronic pancreatitis in

children: a systematic review and meta-analysis. *Clinical and Experimental Pediatrics*.

Gagyi, E. B., Teutsch, B., Veres, D. S., Pálinkás, D., Vörhendi, N., Ocskay, K., Márta, K., Hegyi, P. J., Hegyi, P., & Erőss, B. (2024). Incidence of recurrent and chronic pancreatitis after acute pancreatitis: a systematic review and meta-analysis. *Therapeutic Advances in Gastroenterology*, *17*.

Gallego, R. G., Blanco, J. L. J., Thijssen-van Zuylen, C. W. E. M., Gotfredsen, C. H., Voshol, H., Duus, J., Schachner, M., & Vliegenthart, J. F. G. (2001). Epitope diversity of N-Glycans from bovine peripheral myelin glycoprotein p0 revealed by mass spectrometry and nano probe magic angle spinning 1H NMR spectroscopy. *Journal of Biological Chemistry*, *276*(33), 30834–30844.

Ganeshpurkar, A., Makar, S., Kumar, D., Jana, S., & Singh, S. K. (2020). Aspartic proteases: Potential drug targets for anticancer drug development. In S. P. Gupta (Ed.), *Cancer-Leading Proteases*. Academic Press. https://doi.org/10.1016/B978-0-12-818168-3.00005-X.

Gardner, T. B., Adler, D. G., Forsmark, C. E., Sauer, B. G., Taylor, J. R., & Whitcomb, D. C. (2020). ACG Clinical Guideline. *The American Journal of Gastroenterology*, 1.

Gazaway, E., Kandel, R., Grant, O. C., & Woods, R. J. (2025). Are N-linked glycans intrinsically disordered? *Current Opinion in Structural Biology*, *93*.

Gjellesvik, D. R., Lombardo, D., & B.T., W. (1992). Pancreatic bile salt dependent lipase from cod (*Gadus morhua*): Purification and properties. *Biochimica et Biophysica Acta (BBA) - Lipids and Lipid Metabolism*, *1124*(2), 123–134.

Goettig, P. (2016). Effects of glycosylation on the enzymatic activity and mechanisms of proteases. *International Journal of Molecular Sciences*, *17*(12), 1969.

Goldstein, S. M., Kaempfer, C. E., Kealey, J. T., & Wintroub, B. U. (1989). Human mast cell carboxypeptidase. Purification and characterization. *Journal of Clinical Investigation*, *83*(5), 1630–1636.

Gomez-Guillen, M. C., Gimenez, B., Lopez-Caballero, M. E., & Montero, M. P. (2011). Functional and bioactive properties of collagen and gelatin from alternative sources: A review. *Food Hydrocolloids*, *25*(8), 1813–1827.

Gómez-villegas, P., Vigara, J., Romero, L., Gotor, C., Raposo, S., Gonçalves, B., & Léon, R. (2021). Biochemical characterization of the amylase activity from the new haloarchaeal strain *Haloarcula sp.* Hs isolated in the odiel marshlands. *Biology*, *10*(4).

Goncharova, K., Ushakova, G., Kovalenko, T., Osadchenko, I., Skibo, G., & Pierzynowski, S. G. (2015). Diet supplemented with pancreatic-like enzymes of microbial origin restores the hippocampal neuronal plasticity and behaviour in young pigs with experimental exocrine pancreatic insufficiency. *Journal of Functional Foods*, *14*, 270–277.

Gonzalez, N. J. (2014). The history of the enzyme treatment of cancer. *Alternative Therapies in Health and Medicine*, *20*, 30–44.

González-Sánchez, V., Amrani, R., González, V., Trigo, C., Picó, A., & de-Madaria, E. (2017). Diagnosis of exocrine pancreatic insufficiency in chronic pancreatitis: 13C-Mixed Triglyceride Breath Test versus Fecal Elastase. *Pancreatology*, *17*(4), 580–585.

Google (2026). NotebookLM. [Large language model]. https://notebooklm.google/.

Gopinath, S. C. B., Anbu, P., Arshad, M. K., Lakshmipriya, T., Voon, C. H., Hashim, U., & Chinni, S. V. (2017). Biotechnological Processes in Microbial Amylase Production. *BioMed Research International*, *2017*.

Grand View Research. (2022). *Halal Food And Beverage Market 2022 – 2030*.

Griffin, S. M., Alderson, D., & Farndon, J. R. (1989). Acid resistant lipase as replacement therapy in chronic pancreatic exocrine insufficiency: A study in dogs. *Gut*, *30*(7), 1012–1015.

Groenen, M. A. M., Archibald, A. L., Uenishi, H., Tuggle, C. K., Takeuchi, Y., Rothschild, M. F., Rogel-Gaillard, C., Park, C., Milan, D., Megens, H. J., Li, S., Larkin, D. M., Kim, H., Frantz, L. A. F., Caccamo, M., Ahn, H., Aken, B. L., Anselmo, A., Anthon, C., … Schook, L. B. (2012). Analyses of pig genomes provide insight into porcine demography and evolution. *Nature*, *491*(7424), 393–398.

Guasch, A., Coll, M., Avilés, F. X., & Huber, R. (1992). Three-dimensional structure of porcine pancreatic procarboxypeptidase A. A comparison of the A and B

zymogens and their determinants for inhibition and activation. *Journal of Molecular Biology*, *224*(1), 141–157.

Gültepe, I., Başaranoɨlu, M., Zorlu, M., Şenyiɨit, A., Taşkale, E. Z., Zarali, S., Atay, K., & Köroɨlu, E. (2016). Low lipase levels as an independent marker of pancreatic cancer: A frequently neglected condition in clinical setting. *Turkish Journal of Gastroenterology*, *27*(2), 197–200.

Günther, T., Tulipano, G., Dournaud, P., Bousquet, C., Csaba, Z., Kreienkamp, H. J., Lupp, A., Korbonits, M., Castaño, J. P., Wester, H. J., Culler, M., Melmed, S., & Schulz, S. (2018). International union of basic and clinical pharmacology. CV. somatostatin receptors: Structure, function, ligands, and new nomenclature. *Pharmacological Reviews*, *70*(4), 763–835.

Gupta, S. P., & Gupta, S. D. (2020). Cancer-leading proteases: An introduction. In S. P. Gupta (Ed.), *Cancer-Leading* Proteases. Academic Press. https://shop.elsevier.com/books/cancer-leading-proteases/gupta/978-0-12-818168-3

Hacein-Bey-Abina, S., Le Deist, F., Carlier, F., Bouneaud, C., Hue, C., De Villartay, J.-P., Thrasher, A. J., Wulffraat, N., Sorensen, R., Dupuis-Girod, S., Fischer, A., Davies, E. G., Kuis, W., Leiva, L., & Cavazzana-Calvo, M. (2002). Sustained correction of X-linked severe combined immunodeficiency by ex vivo gene therapy. *New England Journal of Medicine*, *346*(16), 1185–1193.

Halal Malaysia Official. (2020). *Definition of Halal*. http://www.halal.gov.my/v4/index.php?data=bW9kdWxlcy9uZXdzOzs7Ow==&utama=panduan&ids=gp1

Hameed, A. M., Lam, V. W. T., & Pleass, H. C. (2015). Significant elevations of serum lipase not caused by pancreatitis: A systematic review. *Hpb*, *17*(2), 99–112.

Harish, B. S., & Uppuluri, K. B. (2020). Serine proteases leading to prostate cancer: Structures, functions, and development of anticancer drugs. In S. P. Gupta (Ed.), *Cancer-Leading Proteases* (pp. 215–242). Academic Press. https://doi.org/10.1016/B978-0-12-818168-3.00008-5.

Harmon, D. L. (1992). Impact of nutrition on pancreatic exocrine and endocrine secretion in ruminants: a review. *Journal of Animal Science*, *70*(4), 1290–1301.

Harvey, P. R., McKay, S. C., Wilkin, R. J. W., Layton, G. R., Powell-Brett, S., Okoth, K., Trudgill, N., Roberts, K. J., Baker, G., Brom, M. K., Brown, Z., Farrugia, A., Haldar, D., Kalisvaart, M., Marley, A., Pande, R., Patel, R., Stephenson, B. T. F., Baillie, C., … Jones, C. (2021). Pancreatic enzyme replacement therapy in patients with pancreatic cancer: A national prospective study. *Pancreatology*, *21*(6), 1127–1134.

Hayee, B. H., Watson, K., Campbell, S., Simpson, A., Farrell, E., Hutchings, P., Macedo, P., Perrin, F., Whelan, K., & Elston, C. (2019). A high prevalence of chronic gastrointestinal symptoms in adults with cystic fibrosis is detected using tools already validated in other GI disorders. *United European Gastroenterology Journal*, *7*(7), 881–888.

He, M., Zhou, X., & Wang, X. (2024). Glycosylation: mechanisms, biological functions and clinical implications. *Signal Transduction and Targeted Therapy*, *9*(1), 1–33.

Headon, D. R., & Walsh, G. (1994). The industrial production of enzymes. *Biotechnology Advances*, *12*(4), 635–646.

Hediana, Y., & Rusdiana, T. (2021). Indonesian Halal Pharmaceutical: Challenges and Market Opportunities. *Indonesian Journal of Pharmaceutics*, *3*(3), 99–115.

Henry, B. M., Skinningsrud, B., Saganiak, K., Pękala, P. A., Walocha, J. A., & Tomaszewski, K. A. (2019). Development of the human pancreas and its vasculature — An integrated review covering anatomical, embryological, histological, and molecular aspects. *Annals of Anatomy*, *221*, 115–124.

Henzel, W. J., Watanabe, C., & Stults, J. T. (2003). Protein identification: The origins of peptide mass fingerprinting. *Journal of the American Society for Mass Spectrometry*, *14*(9), 931–942.

Herdiana, Y., Sofian, F. F., Shamsuddin, S., & Rusdiana, T. (2024). Towards halal pharmaceutical: Exploring alternatives to animal-based ingredients. *Heliyon*, *10*(1), 1–19.

Hong, G. P., Min, S. G., & Jo, Y. J. (2019). Anti-oxidative and anti-aging activities of porcine by-product collagen hydrolysates produced by commercial proteases: Effect of hydrolysis and ultrafiltration. *Molecules*, *24*(6).

Hou, C. T., & Shimada, Y. (2009). Lipases. In M. Schaechter (Ed.), *Encyclopedia of Microbiology* (3rd ed., pp. 385–392). Academic Press. https://doi.org/10.1016/B978-012373944-5.00153-X.

Hou, S., Zhang, Y., Xu, J., Bai, J., Liu, J., Xie, J., & Xu, T. (2020). Residue Asn21 acts as a switch for calcium binding to modulate the enzymatic activity of human phospholipase A2 group IIE. *Biochimie*, *176*, 117–121.

Hou, Y., Chen, X., Tolmachova, T., Ernst, S. A., & Williams, J. A. (2013). EPI64B Acts as a GTPase-activating protein for Rab27B in pancreatic acinar cells. *Journal of Biological Chemistry*, *288*(27), 19548–19557.

Hui, D. Y., & Howles, P. N. (2002). Carboxyl ester lipase. *Journal of Lipid Research*, *43*(12), 2017–2030.

Ianiro, G., Pecere, S., Giorgio, V., Gasbarrini, A., & Cammarota, G. (2016). Digestive Enzyme Supplementation In Gastrointestinal Diseases. *Current Drug Metabolism*, *17*(2), 187–193.

Iijima, N., Tanaka, S., & Ota, Y. (1998). Purification and characterization of bile salt-activated lipase from the hepatopancreas of red sea bream, *Pagrus major*. *Fish Physiology and Biochemistry*, *18*, 59–69.

Imrie, C. W., Connett, G., Hall, R. I., & Charnley, R. M. (2010). Review article: Enzyme supplementation in cystic fibrosis, chronic pancreatitis, pancreatic and periampullary cancer. *Alimentary Pharmacology and Therapeutics*, *32*(SUPPL. 1), 1–25.

Industry ARC. (2021). *Halal Market - Forecast (2017-2025)*.

Ishabiyi, F. O., Umar, H. I., Dutta, T., Onyinye, O. C., Damola, O. D., Budagova, L., Temesgen, D., Bourhia, M., Bello, R. O., Alyami, E. M., Alsolami, M., & Almohammed, O. A. (2026). Establishing FDA-approved oncology drugs as GPR176 inhibitor through homology modelling, molecular docking, MMGBSA, DFT, and molecular dynamics simulation. *Scientific Reports*, *16*(1).

Ishimoto-Namiki, U., Ino, Y., Esaki, M., Shimada, K., Saruta, M., & Hiraoka, N. (2023). Novel Insights into Immunohistochemical Analysis for acinar cell neoplasm of the pancreas: Carboxypeptidase A2, Carboxypeptidase A1, and glycoprotein 2. *American Journal of Surgical Pathology*, *47*(5), 525–534.

Islamic Services of America. (2023). *A Glimpse into The Global Halal Industry [2023]*. https://www.isahalal.com/news-events/blog/glimpse-global-halal-industry-2023

Ismail, O. Z., & Bhayana, V. (2017). Lipase or amylase for the diagnosis of acute pancreatitis? *Clinical Biochemistry*, *50*(18), 1275–1280.

Jadach, B., Mielcarek, Z., & Osmałek, T. (2024). Use of collagen in cosmetic products. *Current Issues in Molecular Biology*, *46*(3), 2043–2070.

Janeček, Š., Svensson, B., & MacGregor, E. A. (2014). α-Amylase: An enzyme specificity found in various families of glycoside hydrolases. *Cellular and Molecular Life Sciences*, *71*(7), 1149–1170.

Jankowski, W. M., Jakub, F., & Tarasiuk-Zawadzka, A. (2025). Molecular mechanisms and pathophysiological implications of mucin-type O-glycosylation dysregulation in colorectal cancer progression. *Naunyn-Schmiedeberg's Arch Pharmacol*, *13049–13063*.

Jawaid, S., & Forsmark, C. E. (2019). Exocrine pancreatic insufficiency following acute pancreatitis: True association or EPI phenomenon? *Digestive Diseases and Sciences*, *64*(7), 1731–1733.

Jawed, A., Singh, G., Kohli, S., Sumera, A., Haque, S., Prasad, R., & Paul, D. (2019). Therapeutic role of lipases and lipase inhibitors derived from natural resources for remedies against metabolic disorders and lifestyle diseases. *South African Journal of Botany*, *120*, 25–32.

Jelski, W., & Mroczko, B. (2019). Biochemical diagnostics of pancreatic cancer - Present and future. *Clinica Chimica Acta, 498,* 47-51.

Ji, Y., Li, Y., & Wang, J. (2026). Glycosylation in cancer: diversity, functions, potential as diagnostic biomarkers and therapeutic targets. *Medicine Plus*, 1–13.

Jitonnom, J., & Sontag, C. (2012). Comparative study on activation mechanism of carboxypeptidase A1, A2 and B: First insights from steered molecular dynamics simulations. *Journal of Molecular Graphics and Modelling*, *38*, 298–303.

Johansson, B. B., Fjeld, K., El Jellas, K., Gravdal, A., Dalva, M., Tjora, E., Ræder, H., Kulkarni, R. N., Johansson, S., Njølstad, P. R., & Molven, A. (2018). The role of the carboxyl ester lipase (CEL) gene in pancreatic disease. *Pancreatology*, *18*(1), 12–19.

Johns, J. D., & Rowe, S. M. (2019). The effect of CFTR modulators on a cystic fibrosis patient presenting with recurrent pancreatitis in the absence of respiratory symptoms: A case report. *BMC Gastroenterology*, *19*(1), 10–13.

Johnson, M. (2012). Protein Modification Protocol. *Labome*, *2*(118), 1.

Julien, R., Canioni, P., Rathelot, J., Sarda, L., & Plummer, T. H. (1972). Studies on bovine pancreatic lipase and colipase. *Biochimica et Biophysica Acta (BBA) - Lipids and Lipid Metabolism*, *280*(2), 215–224.

Kabir, M. F., & Ju, L. K. (2023). On optimization of enzymatic processes: Temperature effects on activity and long-term deactivation kinetics. *Process Biochemistry*, *130*(January), 734–746.

Karabasanavar, N. S., Singh, S. P., Kumar, D., & Shebannavar, S. N. (2014). Detection of pork adulteration by highly-specific PCR assay of mitochondrial D-loop. *Food Chemistry*, *145*, 530–534.

Karahalil, E. (2020). Principles of halal-compliant fermentations: Microbial alternatives for the halal food industry. *Trends in Food Science & Technology*, *98*, 1–9.

Karia, N., Asaari, M. H. A. H., Mohamad, N., & Kamaruddin, S. (2015). Assessing Halal logistics competence: An Islamic-based and resource-based view. *IEOM 2015 - 5th International Conference on Industrial Engineering and Operations Management, Proceeding*, 1–6.

Karve, T. M., & Cheema, A. K. (2011). Small Changes Huge Impact: The Role of Protein Posttranslational Modifications in Cellular Homeostasis and Disease. *Journal of Amino Acids*, *2011*, 1–13.

Kawaguchi, N., Date, K., Suzuki, Y., Tomita, C., Naradate, R., Higami, T., Nakamura, K., Aikawa, K., & Ogawa, H. (2018). A novel protocol for the preparation of active recombinant human pancreatic lipase from Escherichia coli. *Journal of Biochemistry*, *164*(6), 407–414.

Kelsey, R., Manderson Koivula, F. N., McClenaghan, N. H., & Kelly, C. (2019). Cystic Fibrosis–Related Diabetes: Pathophysiology and Therapeutic Challenges. *Clinical Medicine Insights: Endocrinology and Diabetes*, *12*.

Kemik, O., Kemik, A. S., Sumer, A., Beğenik, H., Dülger, A. C., Purisa, S., & Tuzun, S. (2012). Serum procarboxypeptidase A and carboxypeptidase A levels in pancreatic disease. *Human and Experimental Toxicology*, *31*(5), 447–451.

Kerfelec, B., Chapus, C., & Puigserver, A. (1985). Existence of ternary complexes of procarboxypeptidase A in the pancreas of some ruminant species. *European Journal of Biochemistry*, *151*(3), 515–519.

Khan, S., Ullah, M. W., Siddique, R., Nabi, G., Manan, S., Yousaf, M., & Hou, H. (2016). Role of recombinant DNA technology to improve life. *International Journal of Genomics*, *2016*.

Kiczak, L., Tomaszek, A., Bania, J., Paslawska, U., Zacharski, M., Noszczyk-nowak, A., Janiszewski, A., Skrzypczak, P., Ardehali, H., Jankowska, E. A., & Ponikowski, P. (2013). Expression and complex formation of MMP9, MMP2, NGAL, and TIMP1 in porcine myocardium but not in skeletal muscles in male pigs with tachycardia-induced systolic heart failure. *BioMed Research International*, *2013*, 1–12.

Kim, K. K., Song, H. K., Shin, D. H., Hwang, K. Y., & Sun, S. W. (1997). The crystal structure of a triacylglycerol lipase from *Pseudomonas cepacia* reveals a highly open conformation in the absence of a bound inhibitor. *Structure*, *5*, 173–185.

Kim, T., Kim, S., Kang, W. Y., Baek, H., Jeon, H. Y., Kim, B. Y., Kim, C. G., & Kim, D. (2011). Porcine amniotic fluid as possible antiwrinkle cosmetic agent. *Korean Journal of Chemical Engineering*, *28*(9), 1839–1843.

Kiribayeva, A., Silayev, D., Akishev, Z., Baltin, K., Aktayeva, S., Ramankulov, Y., & Khassenov, B. (2024). An impact of N-glycosylation on biochemical properties of a recombinant α-amylase from *Bacillus licheniformis*. *Heliyon*, *10*(6), e28064.

Koh, J., Victor, A. F., Howell, M. L., Yeo, J. G., Qu, Y., Selover, B., Waite-Cusic, J., & Dallas, D. C. (2020). Bile salt-stimulated lipase activity in donor breast milk influenced by pasteurization techniques. *Frontiers in Nutrition*, *7*(November), 1–7.

Kohlmeier, M. (2015). Absorption, transport, and retention. In *Nutrient Metabolism* (2nd ed., pp. 37–93). Academic Press. https://doi.org/10.1016/B978-0-12-387784-0.00003-1.

Konstan, M. W., Wagener, J. S., Wilschanski, M., Laki, I., Boas, S. R., Sands, D., Gangal, M., Martin, R. S., Shanahan, W., & Pennington, J. (2018). A comparison of liprotamase, a non-porcine pancreatic enzyme replacement therapy, to porcine

extracted pancrelipase in a noninferiority randomized clinical trial in patients with cystic fibrosis. *Clinical Investigation*, *08*(04), 147–154.

Kovacheva-Slavova, M., Siminkovitch, S., Genov, J., Golemanov, B., Mitova, R., Gecov, P., Svinarov, D., & Vladimirov, B. (2017). Pancreatic enzyme replacement therapy in patients with pancreatic exocrine insufficiency. *Pancreatology*, *17*(4), S39.

Koyama, I., Komine, S. I., Yakushijin, M., Hokari, S., & Komoda, T. (2000). Glycosylated salivary α-amylases are capable of maltotriose hydrolysis and glucose formation. *Comparative Biochemistry and Physiology - B Biochemistry and Molecular Biology*, *126*(4), 553–560.

Krem, M. M., & Cera, E. Di. (2001). Molecular markers of serine protease evolution. *The EMBO Journal*, *20*(12), 3036-3045.

Krupa, L., Bajka, B., Staroń, R., Dupont, D., Singh, H., Gutkowski, K., & Macierzanka, A. (2020). Comparing the permeability of human and porcine small intestinal mucus for particle transport studies. *Scientific Reports*, *10*(1), 1–12.

Kumar, N., & Srivastava, R. (2024). Deep learning in structural bioinformatics: current applications and future perspectives. *Briefings in Bioinformatics*, *25*(3).

Kumar, R., Mehta, D., Mishra, N., Nayak, D., & Sunil, S. (2020). Molecular sciences role of host-mediated post-translational modifications (PTMs) in RNA virus pathogenesis. *International Journal of Molecular Sciences*, *22*(323), 1–7.

Kumar, S., & Chakravarty, S. (2018). Amylases. In C. S. Nunes & V. Kumar (Eds.), *Enzymes in Human and Animal Nutrition: Principles and Perspectives* (pp. 163–180). Academic Press. https://doi.org/10.1016/B978-0-12-805419-2.00008-3.

Kumar, V., Singh, D., Sangwan, P., & Gill, P. K. (2014). Global Market Scenario of Industrial Enzymes. In V. Beniwal & A. K. Sharma (Eds.), *Industrial Enzymes Trends, Scope and Relevance* (pp. 173–196). Nova Science Publishers. https://www.researchgate.net/publication/268892217_Global_scenario_of_industrial_enzyme_market.

Kumosa, L. S., Zetterberg, V., & Schouenborg, J. (2018). Gelatin promotes rapid restoration of the blood brain barrier after acute brain injury. *Acta Biomaterialia*, *65*, 137–149.

Labow, R. S., Adams, K. A. H., & Lynn, K. R. (1983). Porcine cholesterol esterase, a multiform enzyme. *Biochimica et Biophysica Acta (BBA) - Protein Structure and Molecular Enzymology*, *749*(1), 32–41.

Lacko, A. G., & Neurath, H. (1970). Studies on procarboxypeptidase a and carboxypeptidase a of the spiny pacific dogfish (*Squalus acanthias*). *Biochemistry*, *9*(24), 4680–4690.

Laher, I. (2020). Handbook of healthcare in the Arab world. In *Handbook of Healthcare in the Arab World*. Springer International Publishing.

Lambre, C., Baviera, J. M. B., Bolognesi, C., Cocconcelli, P. S., Crebelli, R., Gott, D. M., Grob, K., Lampi, E., Mengelers, M., Mortensen, A., Riviere, G., Steffensen, I.-L., Tlustos, C., Loveren, H. Van, Vernis, L., Zorn, H., Gundert-Remy, U., Herman, L., Turck, D., … Chesson, A. (2021). Safety evaluation of food enzyme trypsin from porcine pancreas. *EFSA Journal*, *19*(6), 1–13.

Landers, A., Brown, H., & Strother, M. (2019). The effectiveness of pancreatic enzyme replacement therapy for malabsorption in advanced pancreatic cancer, a pilot study. *Palliat Care, 12*(1178224218825270), 1–7.

Latip, M. A. A., Nordin, N. F. H., & C, G.-F. (2019). Microbes from Antarctica as a source for understanding cold adaptive Halal enzymes. *Journal of Halal Industry and Services*, *2*(1), 1–8.

Lee, D. Y., Lee, S. Y., Kang, H. J., Park, Y., & Hur, S. J. (2021). Development of effective heparin extraction method from pig by-products and analysis of their bioavailability. *Journal of Animal Science and Technology*, *62*(6), 933–947.

Lee, P. C. (1978). Comparative studies of canine colipase and lipases from bovine, porcine, canine, human and rat pancreases. *Comparative Biochemistry and Physiology Part B: Comparative Biochemistry*, *60*(4), 373–378.

Lehner, R., & Verger, R. (1997). Purification and characterization of a porcine liver microsomal triacylglycerol hydrolase. *Biochemistry*, *36*(7), 1861–1868.

Lestari, W., Octavianti, F., Jaswir, I., & Hendri, R. (2019). Plant-based substitutes for gelatin. In Hassan Faridah, Osman Ismah, Kassim Erne Suzila, Haris Balkis, & Hassan Rohana (Eds.), *Contemporary Management and Science Issues in the Halal Industry*. (1st ed., pp. 319–322). Springer Singapore. https://doi.org/10.1007/978-981-13-2677-6

Li, J. L., Yu, Q. L., Zhang, L., Liu, L. L., & Guo, Z. Bin. (2012). Purification and characteristics of trypsin from the pancreas of tibetan sheep. *Journal of Food Biochemistry*, *36*(1), 122–128.

Li, M., Yuan, Y., Han, X., Liu, X., Zhang, W., & Hao, J. (2022). Antioxidant mitoquinone alleviates chronic pancreatitis via anti-fibrotic and antioxidant effects. *Journal of Inflammation Research*, *15*, 4409–4420.

Li, X., Lindquist, S., Lowe, M., Noppa, L., & Hernell, O. (2007). Bile salt–stimulated lipase and pancreatic lipase-related protein 2 are the dominating lipases in neonatal fat digestion in mice and rats. *Pediatric Research*, *62*(5), 537–541.

Lim, D. W., Yoon, T. S., Han, K. H., Sajjad, S., Shin, H. S., & Kang, S. (2023). Improved separation in horizontal protein SDS-PAGE with double-deck flat electrodes and a field inversion gel electrophoresis module. *Methods and Protocols*, *6*(6).

Lin, C. C., Chiou, T. K., & Sung, W. C. (2015). Characteristics of gelatin from giant grouper (*Epinephelus Lanceolatus*) skin. *International Journal of Food Properties*, *18*(11), 2339–2348.

Lindquist, S., Andersson, E.-L., Lundberg, L., & Hernell, O. (2012). Bile salt-stimulated lipase plays an unexpected role in arthritis development in rodents. *PLoS ONE*, *7*(10), 1–9.

Lindquist, S., Wang, Y., Andersson, E. L., Grebe, S. T., Alenius, G. M., Rantapää-Dahlqvist, S., Lundberg, L., & Hernell, O. (2023). Effects of bile salt-stimulated lipase on blood cells and associations with disease activity in human inflammatory joint disorders. *PLoS ONE*, *18*(8), 1–15.

Liu, T. T., Liu, X. T., Chen, Q. X., & Shi, Y. (2020). Lipase inhibitors for obesity: A review. *Biomedicine and Pharmacotherapy*, *128*.

Liu, X., & Kokare, C. (2017). Microbial enzymes of use in industry. In G. Brahmachari, *Biotechnology of Microbial Enzymes: Production, Biocatalysis and Industrial Applications* (pp. 267–298). Academic Press. https://doi.org/10.1016/B978-0-12-803725-6.00011-X.

Lombardo, D. (2001). Bile salt-dependent lipase: its pathophysiological implications. *Biochimica et Biophysica Acta (BBA) - Molecular and Cell Biology of Lipids*, *1533*(1), 1–28.

Lombardo, D., Silvy, F., Crenon, I., Martinez, E., Collignon, A., Beraud, E., & Mas, E. (2018). Pancreatic adenocarcinoma, chronic pancreatitis, and MODY-8 diabetes: is bile salt-dependent lipase (or carboxyl ester lipase) at the crossroads of pancreatic pathologies? *Oncotarget*, *9*(15), 12513–12533.

López-Otín, C., & Bond, J. S. (2008). Proteases: Multifunctional enzymes in life and disease. *Journal of Biological Chemistry*, *283*(45), 30433–30437.

Lourenço, C. B., Ataide, J. A., Cefali, L. C., Novaes, L. C. d. L., Moriel, P., Silveira, E., Tambourgi, E. B., & Mazzola, P. G. (2016). Evaluation of the enzymatic activity and stability of commercial bromelain incorporated in topical formulations. *International Journal of Cosmetic Science*, *38*(5), 535–540.

Lubis, H. N., Mohd-Naim, N. F., Alizul, N. N., & Ahmed, M. U. (2016). From market to food plate: Current trusted technology and innovations in halal food analysis. *Trends in Food Science & Technology*, *58*, 55–68.

Lumibao, J. C., Tremblay, J. R., Hsu, J., & Engle, D. D. (2022). Altered glycosylation in pancreatic cancer and beyond. *Journal of Experimental Medicine*, *219*(6), 1–13.

Ma, K., Cai, X., Zhou, Y., Wang, Y., & Jiang, T. (2017). In vitro and in vivo evaluation of tetracycline loaded chitosan-gelatin nanosphere coatings for titanium surface functionalization. *Macromolecular Bioscience*, *17*(2), 1–9.

Macierzanka, A., Torcello-Gómez, A., Jungnickel, C., & Maldonado-Valderrama, J. (2019). Bile salts in digestion and transport of lipids. *Advances in Colloid and Interface Science*, *274*, 102045.

Mahadevan, V. (2019). Anatomy of the pancreas and spleen. *Surgery (United Kingdom)*, *37*(6), 297–301.

Maldonado-Valderrama, J., Wilde, P., Macierzanka, A., & Mackie, A. (2011). The role of bile salts in digestion. *Advances in Colloid and Interface Science*, *165*(1), 36–46.

Manson, W. G., & Weaver, L. T. (1997). Fat digestion in the neonate. *Archives of Disease in Childhood - Fetal and Neonatal Edition*, *76*(3), 206–211.

Marengo, M., Pezzilli, D., Gianquinto, E., Fissore, A., Oliaro-Bosso, S., Sgorbini, B., Spyrakis, F., & Adinolfi, S. (2022). Evaluation of porcine and *Aspergillus oryzae* α-Amylases as Possible Model for the Human Enzyme. *Processes*, *10*(4).

Market Research. (2020). *Global Exocrine Pancreatic Insufficiency Market Trends, Applications, Analysis, Growth, and Forecast to 2027*. 4–9. https://marketresearch.biz/report/exocrine-pancreatic-insufficiency-market/#request-for-customization

Market Research. (2021a). *Global Halal Cosmetics and Personal Care Market 2021 – 2025*. *https://www.marketresearch.com/Infiniti-Research-Limited-v2680/Global-Halal-Cosmetics-Personal-Care-40800704/*

Market Research. (2021b). *Global Halal Pharmaceuticals Market Growth 2021 – 2026*. *https://www.marketresearch.com/APO-Research-Inc-v4273/Global-Halal-Pharmaceuticals-Forecast-43749855/*

Market Watch. (2019). *Global Exocrine Pancreatic Insufficiency Market Competitive Strategies, Regional Analysis Forecast 2028*. https://www.marketwatch.com/press-release/global-exocrine-pancreatic-insufficiency-market-competitive-strategies-regional-analysis-forecast-2028-2019-02-22

Market.us. (2022). *Halal Pharmaceuticals Market 2029 – 2028*. https://market.us/report/halal-pharmaceutical-market/

Masaki, H. (2010). Role of antioxidants in the skin: Anti-aging effects. *Journal of Dermatological Science*, *58*(2), 85–90.

Mayberry, J. F. (2014). Digestive enzyme supplements: replacement therapy for individuals unwilling to take porcine products. *British Journal of Hospital Medicine*, *75*(8).

Mendes, A. A., Oliveira, P. C., & de Castro, H. F. (2012). Properties and biotechnological applications of porcine pancreatic lipase. *Journal of Molecular Catalysis B: Enzymatic*, *78*, 119–134.

Mennitt, D. (2012). What is the current FDA-approved therapy to treat pancreatic insufficiency for children with cystic fibrosis? *NASN School Nurse (Print)*, *27*(2), 67–68.

Miller, A. L., Garcia, P. L., & Yoon, K. J. (2020). Developing effective combination therapy for pancreatic cancer : An overview. *Pharmacological Research*, 155, 104740.

Minussi, R. C., Pastore, G. M., & Durán, N. (2002). Potential applications of laccase in the food industry. *Trends in Food Science and Technology*, *13*(6–7), 205–216.

Mishra, M., Tiwari, S., & Gomes, A. V. (2017). Protein purification and analysis: Next generation western blotting techniques. *Expert Review of Proteomics*, *14*(11), 1037–1053.

Mittal, S., & Saluja, D. (2015). Protein post-translational modifications: Role in protein structure, function and stability. In L. R. Singh, T. A. Dar, & P. Ahmad (Eds.), *Proteostasis and Chaperone Surveillance* (pp. 188). Springer New Delhi. https://doi.org/10.1007/978-81-322-2467-9

Miyagawa, S., Maeda, A., Kawamura, T., Ueno, T., Usui, N., Kondo, S., Matsumoto, S., Okitsu, T., Goto, M., & Nagashima, H. (2014). A comparison of the main structures of N-glycans of porcine islets with those from humans. *Glycobiology*, *24*(2), 125–138.

Mohd Azmi, S. I., Kumar, P., Sharma, N., Sazili, A. Q., Lee, S. J., & Ismail-Fitry, M. R. (2023). Application of plant proteases in meat tenderization: Recent trends and future prospects. *Foods*, *12*(6).

Momsen, W. E., & Brockman, H. L. (1977). Purification and characterization of cholesterol esterase from porcine pancreas. *Biochimica et Biophysica Acta (BBA) - Lipids and Lipid Metabolism*, *486*(1), 103–113.

Moore, A. N. J., Vakos, H., Neville, T. A. M., Tonge, P., Arya, P., & Burton, G. W. (1996). A quick method for purifying bile salt-activated lipases. *Biotechnology Techniques*, *10*(7), 523–528.

Moreau, J., Bouisson, M., Saint-Marc-Girardin, M. F., Pignal, F., Bommelaer, G., & Ribet, A. (1988). Comparison of fungal lipase and pancreatic lipase in exocrine pancreatic insufficiency in man. *Gastroenterologie Clinique et Biologique*, *12*(11), 787–792.

Morley, J. E. (2019). *Endocrine Function*. MSD Manuals. https://www.msdmanuals.com/home/hormonal-and-metabolic-disorders/biology-of-the-endocrine-system/endocrine-function

Moss, R. W. (2008). The life and times of John Beard, DSc (1858-1924). *Integrative Cancer Therapies*, *7*(4), 229–251.

Mottillo, E. P., Paul, G. M., Moore, H. P. H., & Granneman, J. G. (2014). Use of fluorescence microscopy to probe intracellular lipolysis. In O. A. MacDougald (Ed.), *Methods in enzymology* (Vol. 538, pp. 263–278). Academic Press. https://doi.org/10.1016/B978-0-12-800280-3.00015-3.

Munck, A., Duhamel, J. F., Lamireau, T., Le Luyer, B., Le Tallec, C., Bellon, G., Roussey, M., Foucaud, P., Giniès, J. L., Houzel, A., Marguet, C., Guillot, M., David, V., Kapel, N., Dyard, F., & Henniges, F. (2009). Pancreatic enzyme replacement therapy for young cystic fibrosis patients. *Journal of Cystic Fibrosis*, *8*(1), 14–18.

Munkley, J. (2019). The glycosylation landscape of pancreatic cancer (Review). *Oncology Letters*, *17*(3), 2569–2575.

Nagae, M., Nagata, M., Teramoto, M., Yamakawa, M., Matsuki, T., Ohnuki, K., & Shimizu, K. (2020). Effect of porcine placenta extract supplement on skin condition in healthy adult women: A randomized, double-blind placebo-controlled study. *Nutrients*, *12*(6), 1–12.

Nakahata, K., Matsunami, K., Kobayashi, C., Omori, T., Xu, H., Firdawes, S., Fukuzawa, M., & Miyagawa, S. (2008). Analysis of the serine protease function of porcine factor I produced by liver cells for xenotransplantation. *Transplant Immunology*, *19*, 30–36.

Nakano, M., Kakehi, K., Tsai, M. H., & Lee, Y. C. (2004). Detailed structural features of glycan chains derived from α1-acid glycoproteins of several different animals: The presence of hypersialylated, O-acetylated sialic acids but not disialy1 residues. *Glycobiology*, *14*(5), 431–441.

Navvabi, A., Razzaghi, M., Fernandes, P., Karami, L., & Homaei, A. (2018). Novel lipases discovery specifically from marine organisms for industrial production and practical applications. *Process Biochemistry*, *70*(April), 61–70.

Neurath, H., Bradshaw, R. A., Pétra, P. H., & Walsh, K. A. (1970). Bovine carboxypeptidase A-activation, chemical structure and molecular heterogeneity. *Philosophical Transactions of the Royal Society of London. Series B, Biological Sciences*, *257*(813), 159–176.

Nigam, P. S. (2013). Microbial enzymes with special characteristics for biotechnological applications. *Biomolecules*, *3*(3), 597–611.

Norazmi, M. N., & Lim, L. S. (2015). Halal pharmaceutical industry: opportunities and challenges. *Trends in Pharmacological Sciences*, *36*(8), 496–497.

Norouzian, D., Akbarzadeh, A., Scharer, J. M., & Moo Young, M. (2006). Fungal glucoamylases. *Biotechnology Advances*, *24*(1), 80–85.

Obe, D. A., & Fatoki, T. H. (2021). In silico evaluation of the structural dynamics beta-amylase from sweet potato (*Ipomoea batatas*). *Asian Journal of Biotechnology and Bioresource Technology*, 1–10.

Ogun, O. J., Thaller, G., & Becker, D. (2022). An overview of the importance and value of porcine species in sialic acid research. *Biology*, *11*(903), 1–17.

Ojha, A., Ojha, U., Mohammed, R., Chandrashekar, A., & Ojha, H. (2019). Current perspective on the role of insulin and glucagon in the pathogenesis and treatment of type 2 diabetes mellitus. *Clinical Pharmacology: Advances and Applications*, *11*, 57–65.

Olesen, S. S. (2019). Chronic pancreatitis and exocrine pancreatic insufficiency. *Medicine (United Kingdom)*, *47*(7), 428–432.

Olesen, S. S., Krarup, H., Poulsen, J. L., Christensen, J. H., Sheel, A. R. G., Sutton, R., Greenhalf, W., Halloran, C., & Drewes, A. M. (2019). Pancreas-specific plasma amylase for assessment and diagnosis of chronic pancreatitis: New insights on an old topic. *United European Gastroenterology Journal*, *7*(7), 955–964.

Oliveira, B. H. de, Bourlieu, C., Lecomte, J., Villeneuve, P., & Nascimento, V. M. G. do. (2024). Lipolysis of *Burkholderia lata* LBBIO-BL02 lipase in simulated human digestive environments: A candidate for enzyme replacement therapy. *Food Bioscience*, *58*(103737), 1–14.

Oliver, M. R., Frulloni, L., & Lo, J. (2013). Synopsis of recent guidelines on pancreatic exocrine insufficiency. *United European Gastroenterology Journal*, *1*(2), 79–83.

Olsen, D., Yang, C., Bodo, M., Chang, R., Leigh, S., Baez, J., Carmichael, D., Perälä, M., Hämäläinen, E. R., Jarvinen, M., & Polarek, J. (2003). Recombinant collagen and gelatin for drug delivery. *Advanced Drug Delivery Reviews*, *55*(12), 1547–1567.

Omar, M. S., Nur, M., Noor, F., Dalila, N., Mohd, F., Mokhtar, M., Faris, M., Zahari, H., Adzwa, N., & Adzni, M. (2022). Muslim and non-muslim students'

behavioural intention in consuming halal food. *International Journal of Technical Vocational and Engineering Technology*, *3*(2), 34–42.

Ongay, S., Boichenko, A., Govorukhina, N., & Bischoff, R. (2012). Glycopeptide enrichment and separation for protein glycosylation analysis. *Journal of Separation Science*, *35*(18), 2341–2372.

Onigbinde, S., Adeniyi, M., Daramola, O., Chukwubueze, F., Bhuiyan, M. M. A. A., Nwaiwu, J., Bhattacharjee, T., & Mechref, Y. (2025). Glycomics in human diseases and its emerging role in biomarker discovery. *Biomedicines*, *13*(8).

Othman, Y., Naimat, N., Ahmad Mustaffa, M. S., Awang, M. N., Abdul Rahman Shah, H., & Saifol, N. S. (2026). Regulatory issues in Halal certification of cosmetic products produced by original equipment manufacturers (OEM) in Malaysia. *PaperASIA*, *42*(1b).

Palmer, T., & Bonner, P. L. (2011). An introduction to enzymes. In *Enzymes* (2nd ed., pp. 2–13). Woodhead Publishing. https://doi.org/10.1533/9780857099921.1.2.

Pancreatic Cancer Action Network. (2020). *Pancreatic Enzymes*. https://www.pancan.org/facing-pancreatic-cancer/living-with-pancreatic-cancer/diet-and-nutrition/pancreatic-enzymes/

Pandol, S. J. (2015). Normal Pancreatic Function. *Pancreapedia*, 1–13.

Park, J.-Y., & Park, K.-M. (2022). Lipase and its unique selectivity: A mini-review. *Journal of Chemistry*, *2022*, 1–11.

Pascual, R., Burgos, F. J., Salva, M., Soriano, F., Mendez, E., & Aviles, F. X. (1989). Purification and properties of five different forms of human procarboxypeptidases. *European Journal of Biochemistry*, *179*(3), 609–616.

Pawar, R. A., Tanavade, A., Bhagat, S., Shetye, T., Kudalkar, S., & Khanvilkar, V. (2025). Production, purification and characterization of amylase using microorganism. *World Journal of Pharmaceutical Research*, *14*(05), 1376–1396.

Paznokas, J. L., & Kaplan, A. (1977). Purification and properties of a triacylglycerol lipase from *Mycobacterium phlei*. *Biochimica et Biophysica Acta (BBA) - Lipids and Lipid Metabolism*, *487*, 405–421.

Pérez-Silva, J. G., Español, Y., Velasco, G., & Quesada, V. (2016). The degradome database: Expanding roles of mammalian proteases in life and disease. *Nucleic Acids Research*, *44*(D1), D351–D355.

Peter, L., Jutta, K., & Lankisch, P. G. (2001). Pancreatic enzyme replacement therapy. *Current Gastroenterology Reports*, *3*(2), 101–108.

Pew Research Center Religion & Public Life. (2015). *The Future of World Religions: Population Growth Projections, 2010-2050*. 2010–2050. http://www.pewforum.org/2015/04/02/religious-projections-2010-2050/

Pezzilli, R., Caccialanza, R., Capurso, G., Brunetti, O., Milella, M., & Falconi, M. (2020). Pancreatic enzyme replacement therapy in pancreatic cancer. *Cancers*, *12*(2), 1–16.

Phukon, L. C., Chourasia, R., Kumari, M., Godan, T. K., Sahoo, D., Parameswaran, B., & Rai, A. K. (2020). Production and characterisation of lipase for application in detergent industry from a novel *Pseudomonas helmanticensis* HS6. *Bioresource Technology*, *309*(February), 123352.

Pienkowski, T., Wawrzak-Pienkowska, K., Tankiewicz-Kwedlo, A., Ciborowski, M., Kurek, K., & Pawlak, D. (2025). Leveraging glycosylation for early detection and therapeutic target discovery in pancreatic cancer. *Cell Death and Disease*, *16*(1).

Pierzynowska, K., Valverde-Piedra, J., Szymanczyk, S., Prykhod'ko, O., Pieszka, M., Kardas, M., Grochowska-Niedworok, E., Grabowski, T., Winiarczyk, M., & Pierzynowski, S. (2018). Pancreatic-like enzymes of microbial origin restore growth and normalize lipid absorption in a pig model with exocrine pancreatic insufficiency. *Archives of Medical Science*, *14*(2), 407–414.

Pirahanchi, Y., & Sharma, S. (2019). *Biochemistry, Lipase*. https://www.ncbi.nlm.nih.gov/books/NBK537346/

Pirahanchi, Y., & Sharma, S. (2023). *Biochemistry, Lipoprotein Lipase Pathophysiology*. StatPearls Publishing. https://www.ncbi.nlm.nih.gov/books/NBK537346/

Poreba, M. (2020). Protease-activated prodrugs: strategies, challenges, and future directions. *FEBS Journal*, *287*(10), 1936–1969.

Potel, C. M., Burtscher, M. L., Garrido-Rodriguez, M., Brauer-Nikonow, A., Becher, I., Le Sueur, C., Typas, A., Zimmermann, M., & Savitski, M. M. (2025). Uncovering protein glycosylation dynamics and heterogeneity using deep quantitative glycoprofiling (DQGlyco). *Nature Structural and Molecular Biology*, *32*(6), 1111–1126.

Powell-Brett, S., Carino, N. de L., & Roberts, K. (2020). Understanding pancreatic exocrine insufficiency and replacement therapy in Pancreatic Cancer. *European Journal of Surgical Oncology*, 539–544.

Pradini, D., Juwono, H., Madurani, K. A., & Kurniawan, F. (2018). A preliminary study of identification halal gelatin using quartz crystal microbalance (QCM) sensor. *Malaysian Journal of Fundamental and Applied Sciences*, *14*(3), 325–330.

Prasad, S., & Roy, I. (2017). Converting enzymes into tools of industrial importance. *Recent Patents on Biotechnology*, *12*(1), 33–56.

Precedence Research. (2022a). *Enzymes Market Size, Growth, Share, Trends, Report 2022 – 2030*. *https://www.precedenceresearch.com/enzymes-market*.

Precedence Research. (2022b). *Halal Cosmetics Market Report 2022 – 2030*. *https://www.precedenceresearch.com/halal-cosmetics-market*.

Precedence Research. (2022c). *Halal Ingredients Market Size, Share, Growth, Report 2022 – 2030*. *https://www.precedenceresearch.com/halal-ingredients-market*.

Puranik, A., Saldanha, M., Dandekar, P., & Jain, R. (2022). A comparison between analytical approaches for molecular weight estimation of proteins with variable levels of glycosylation. *Electrophoresis*, *43*(11), 1223–1232.

Qiu, Y., Sun, S., Yu, X., Zhou, J., Cai, W., & Qian, L. (2020). Carboxyl ester lipase is highly conserved in utilizing maternal supplied lipids during early development of zebrafish and human. *Biochimica et Biophysica Acta - Molecular and Cell Biology of Lipids*, *1865*(6), 158663.

Rafaqat, S., Hafeez, R., Mairaj, R., Saleem, A., & Rafaqat, S. (2023). Pancreatic biomarkers: Role in diabetes mellitus. *Journal of Pancreatology*, *6*(4), 169–177.

Rai, P. K., & Poddar, N. K. (2020). Serine proteases in ovarian cancer. In S. P. Gupta (Ed.), *Cancer-leading proteases* (pp. 183–213). Academic Press. https://doi.org/10.1016/B978-0-12-818168-3.00007-3.

Rajesh, C., Cummings, R. D., & Radhakrishnan, P. (2025). Unraveling the glyco-immunity nexus in pancreatic cancer. *Molecular Cancer*, *24*(211), 1–26.

Rakus, J. F., & Mahal, L. K. (2011). New technologies for glycomic analysis: toward a systematic understanding of the glycome. *Annual Review of Analytical Chemistry*, *4*, 367–392.

Ramazi, S., & Zahiri, J. (2021). Post-translational modifications in proteins: resources, tools and prediction methods. *Database*, *2021*(7), 1–20.

Ranke, F. F. B., Shinya, T. Y., Figueiredo, F. C., Núñez, E. G., Cabral, H., & Neto, P. O. (2020). Ethanol from rice byproduct using amylases secreted by *Rhizopus microsporus var. oligosporus*. Enzyme partial purification and characterization. *Journal of Environmental Management*, *266*(April).

Rauh, M. (2012). LC–MS/MS for protein and peptide quantification in clinical chemistry. *Journal of Chromatography B*, *883–884*, 59–67.

Ravotti, R., Worlitschek, J., Pulham, C. R., & Stamatiou, A. (2020). Triglycerides as novel phase-change materials: A review and assessment of their thermal properties. *Molecules*, *25*(23), 1–26.

Rebaï, O., Le Petit-Thevenin, J., Bruneau, N., Lombardo, D., & Vérine, A. (2005). In vitro angiogenic effects of pancreatic bile salt-dependent lipase. *Arteriosclerosis, Thrombosis, and Vascular Biology*, *25*(2), 359–364.

Reddy, S., Chandak, S. R., Sarkar, S., Shinde, R. K., & Chandak, M. S. (2024). Lateral Pancreaticojejunostomy in a Rare Case of Chronic Calcific Pancreatitis With Peripancreatic Pseudocyst in an 18-Year-Old Male: A Case Report. *Cureus*, *16*(5).

Regenstein, J. M. (2019). Kosher and Halal: how they affect muslim and jewish dietary practices. *Handbook of Eating and Drinking*, 1–22.

Rejeb, A., Rejeb, K., Zailani, S., Treiblmaier, H., & Hand, K. J. (2021). Integrating the Internet of Things in the halal food supply chain: A systematic literature review and research agenda. *Internet of Things*, *13*, 100361.

Reshidan, N. H., Affendy, N. B., Jonet, M. A., Lamasudin, D. U., Ariffin, Z. Z., Mat Zain, M., & Abd Hamid, U. M. (2025). Purification and characterisation of Bile-salt activated lipase (BSAL) enzyme from bovine (*Bos taurus*) pancreas. *Asia Pacific Journal of Molecular Biology and Biotechnology*, *33*(December 2024), 108–118.

Reshidan, N. H., Jonet, M. A., Zainal Ariffin, Z., & Abd Hamid, U. M. (2024). Purification and characterization of pancreatic carboxypeptidase A1 (CBPA1) of bovine (*Bos taurus*) and sheep (*Ovis aries*) for potential application as Halal enzymes. *Journal of Pancreatology*.

Robinson, P. K. (2015). Enzymes: principles and biotechnological applications. *Essays in Biochemistry*, *59*, 1–41.

Roder, P. V, Wu, B., Liu, Y., & Han, W. (2016). Pancreatic regulation of glucose homeostasis. *Experimental and Molecular Medicine*, *48*(3), 1–19.

Rose, C. A. (2017). Case examples from the gonzalez protocol for treatment of cancer. *Journal of Cancer Prevention & Current Research*, *8*(5), 8–10.

Roth, Z., Yehezkel, G., & Khalaila, I. (2012). Identification and quantification of protein glycosylation. *International Journal of Carbohydrate Chemistry*, *2012*, 1–10.

Rozengurt, E., & Eibl, G. (2026). Pancreatic cancer: molecular pathogenesis and emerging therapeutic strategies. *Signal Transduction and Targeted Therapy*, *11*(1).

Rudd, E. A., Mizuno, N. K., & Brockman, H. L. (1987). Isolation of two forms of carboxylester lipase (cholesterol esterase) from porcine pancreas. *Biochimica et Biophysica Acta (BBA) - Lipids and Lipid Metabolism*, *918*(2), 106–114.

Rydberg, E. H., Sidhu, G., Vo, H. C., Hewitt, J., Ct, H. C. F., Wang, Y., Numao, S., Macgillivray, R. T. A., Overall, C. M., Brayer, G. D., & Withers, S. G. (1999). Cloning, mutagenesis, and structural analysis of human pancreatic α-amylase expressed in pichia pastoris. *Protein Science*, *8*(3), 635–643.

Rydberg, E. H., Sidhu, G., Vo, H. C., Hewitt, J., Ct, H. C. F., Wang, Y., Numao, S., Macgillivray, R. T. A., Overall, C. M., Brayer, G. D., & Withers, S. G. (2008). Cloning, mutagenesis, and structural analysis of human pancreatic α-amylase expressed in pichia pastoris. *Protein Science*, *8*(3), 635–643.

Sahilah, A. M., Liyana, M. N. L., S., A., Aminah, A., & Khan, A. M. (2016). Halal authentication in Malaysia context : potential adulteration of non-Halal ingredients in meatballs and surimi products. *International Food Research Journal*, *23*(5), 1832–1838.

Said, S., Kurtin, P. J., Nasr, S. H., Graham, R. P., Dasari, S., Vrana, J. A., Yasir, S., Torbenson, M. S., Zhang, L., Mounajjed, T., Eric Chen, Z. M., Lee, H. E., & Wu, T. T. (2020). Carboxypeptidase A1 and regenerating islet-derived 1α as new markers for pancreatic acinar cell carcinoma. *Human Pathology*, *103*, 120–126.

Salin, M. L., & Wilson, W. W. (1981). Porcine superoxide dismutase Isolation and characterization of a relatively basic cuprozinc enzyme. *Molecular and Cellular Biochemistry*, *161*(3), 157–161.

Samanta, S. (2022). Structural and catalytical features of different amylases and their potential applications. *Jordan Journal of Biological Sciences*, *15*(2), 311–337.

Sándor, M., Thiel, F. G., Schmid, M., Demcsák, A., Morales Granda, N. C., Németh, B. C., Vajda, S., Hoerning, A., & Sahin-Tóth, M. (2022). Novel p.G250A mutation associated with chronic pancreatitis highlights misfolding-prone region in carboxypeptidase A1 (CPA1). *International Journal of Molecular Sciences*, *23*(24).

Sankararaman, S., Schindler, T., & Sferra, T. J. (2019). Management of exocrine pancreatic insufficiency in children. *Nutrition in Clinical Practice*, *34*(S1), S27–S42.

Sankari, A., & Sharma, S. (2024). Cystic Fibrosis. *In: StatPearls [Internet]*. StatPearls Publishing. https://www.ncbi.nlm.nih.gov/books/NBK493206/

Saraswat, M., Garapati, K., Mun, D. G., & Pandey, A. (2021). Extensive heterogeneity of glycopeptides in plasma revealed by deep glycoproteomic analysis using size-exclusion chromatography. *Molecular Omics*, *17*(6), 939–947.

Scheuerer, T., Herz, E., Srichuwong, S., & Weiss, J. (2025). Post-translational modifications of proteins and their effect on techno-functional properties for food applications. *Critical Reviews in Food Science and Nutrition,* 1–12.

Schjoldager, K. T., Narimatsu, Y., Joshi, H. J., & Clausen, H. (2020). Global view of human protein glycosylation pathways and functions. *Nature Reviews Molecular Cell Biology*, *21*(12), 729–749.

Schulten, H. J. (2025). Reviewing the developing significance of the serine protease PRSS23. *Frontiers in bioscience (Landmark edition), 30*(8), 27294.

Sendler, M., Mayerle, J., & Lerch, M. M. (2018). Molecular basis of diseases of the exocrine pancreas. *Molecular Pathology: The Molecular Basis of Human Disease*, 457–476.

Shahani, K. M., Khan, I. M., & Chandan, R. C. (1976). Bovine pancreatic lipase. I. Isolation, homogeneity, and characterization. *Journal of Dairy Science*, *59*(3), 369–375.

Sharath, A. K., Haque, N., & Prabhu, N. P. (2020). Spontaneous lid closure and substrate-induced lid opening dynamics of human pancreatic lipase-related protein 2: A computational study. *Journal of Molecular Structure*, *1217*, 128365.

Sharifpour, S., Fakhraee, S., & Behjatmanesh-ardakani, R. (2020). Insights into the mechanism of inhibition of phospholipase A2 by resveratrol: An extensive molecular dynamics simulation and binding free energy calculation. *Journal of Molecular Graphics and Modelling*, 107649.

Sharma, N., Ahlawat, Y. K., Stalin, N., Mehmood, S., Morya, S., Malik, A., Malathi, H., Nellore, J., & Bhanot, D. (2025). Microbial enzymes in industrial biotechnology: sources, production, and significant applications of lipases. *Journal of Industrial Microbiology and Biotechnology*, *52*, 1–22.

Sharma, P., Sharma, N., Pathania, S., & Handa, S. (2017). Purification and characterization of lipase by *Bacillus methylotrophicus* PS3 under submerged fermentation and its application in detergent industry. *Journal of Genetic Engineering and Biotechnology*, *15*(2), 369–377.

Sharma, R., Chisti, Y., & Banerjee, U. C. (2001). Production, purification, characterization, and applications of lipases. *Biotechnology Advances*, *19*(8), 627–662.

Sharon, C., Furugoh, S., Yamakido, T., Ogawa, H. I., & Kato, Y. (1998). Purification and characterization of a lipase from *Pseudomonas aeruginosa* KKA-5 and its role in castor oil hydrolysis. *Journal of Industrial Microbiology and Biotechnology*, *20*(5), 304–307.

Shayman, J. A., & Tesmer, J. J. G. (2019). Lysosomal phospholipase A2. *Biochimica et Biophysica Acta - Molecular and Cell Biology of Lipids*, *1864*(6), 932–940.

Shridas, P., & Webb, N. R. (2014). Diverse Functions of Secretory Phospholipases A 2. *Advances in Vascular Medicine*, *2014*, 1–11.

Shukla, D., Mandal, T., Saha, P., Kumar, D., Kumar, S., & Srivastava, A. K. (2020). Tumor-suppressive proteases revisited: Role in inhibiting tumor progression and metastasis. In S. P. Gupta (Ed.), *Cancer-leading proteases* (pp. 391–416). Academic Press. https://doi.org/10.1016/B978-0-12-818168-3.00014-0

Sikkens, E. C. M., Cahen, D. L., Kuipers, E. J., & Bruno, M. J. (2010). Pancreatic enzyme replacement therapy in chronic pancreatitis. *Best Practice and Research: Clinical Gastroenterology*, *24*(3), 337–347.

Simair, A. A., Qureshi, A. S., Khushk, I., Ali, C. H., Lashari, S., Bhutto, M. A., Mangrio, G. S., & Lu, C. (2017). Production and partial characterization of α-amylase enzyme from *Bacillus sp*. BCC 01-50 and potential applications. *BioMed Research International*, *2017*.

Simões, I., & Faro, C. (2004). Structure and function of plant aspartic proteinases. *European Journal of Biochemistry, 271*(11), 2067–2075.

Singh N., Upadhyay S., Jaiswar A., & Mishra N. (2016). Central bringing excellence in open access in silico analysis of protein. *JSM Bioinformatics, Genomics and Proteomics*, *1*(2), 1–7.

Smith, G. K., Banks, S., Blumenkopf, T. A., Cory, M., Humphreys, J., Laethem, R. M., Miller, J., Moxham, C. P., Mullin, R., Ray, P. H., Walton, L. M., & Wolfe, L. A. (1997). Toward antibody-directed enzyme prodrug therapy with the T268G mutant of human carboxypeptidase A1 and novel in vivo stable prodrugs of methotrexate*. *Journal of Biological Chemistry*, *272*(25), 15804–15816.

Sondej, M., Denny, P. A., Xie, Y., Ramachandran, P., Si, Y., Takashima, J., Shi, W., Wong, D. T., Loo, J. A., & Denny, P. C. (2009). Glycoprofiling of the human salivary proteome. *Clinical Proteomics*, *5*(1), 52–68.

Sorsa, T., Golub, L. M., Thomas, J. T., Leone, P., Anil, S., & Uitto, V. (2026). Matrix Metalloproteinases in Periodontal and Peri-Implant Diseases: Contribution to Their Pathogenesis, Diagnosis, and Treatment. *Journal of Periodontal Research*.

Srisantisaeng, P., Garnjanagoonchorn, W., Thanachasai, S., & Choothesa, A. (2013). Proteolytic activity from chicken intestine and pancreas: Extraction, partial characterization and application for hyaluronic acid separation from chicken comb. *Journal of the Science of Food and Agriculture*, *93*(13), 3390–3394.

Stapleton, D., Mews, C., Bulsara, M., Sherriff, J., & Sly, P. (2012). Pancreatic enzyme replacement therapy: Adherence to guidelines. *Journal of Coaching Education*, *5*(1), 2–3.

Steiner, J. M., & Williams, D. A. (2002). Purification of classical pancreatic lipase from dog pancreas. *Biochimie*, *84*(12), 1243–1251.

Steiner, J. M., Wilson, B. G., & Williams, D. A. (2003). Purification and partial characterization of feline classical pancreatic lipase. *Comparative Biochemistry and Physiology - B Biochemistry and Molecular Biology*, *134*(1), 151–159.

Stockley, A. J. (2014). Case report of exocrine pancreatic insufficiency in two palliative care patients. (X). *Sage* Journals.

Sudarsono, H., & Nugrowati, R. N. I. (2020). Determinants of the intention to consume halal food, cosmetics and pharmaceutical products. *The Journal of Asian Finance, Economics and Business*, *7*(10), 831–841.

Sugiura, M., Oikawa, T., Hirano, K., & Inukai, T. (1977). Purification, crystallization and properties of triacylglycerol lipase from Pseudomonas fluorescens. *Biochimica et Biophysica Acta (BBA)/Lipids and Lipid Metabolism*, *488*(3), 353–358.

Sukohidayat, N. H. E., Zarei, M., Baharin, B. S., & Manap, M. Y. (2018). Purification and characterization of lipase produced by *Leuconostoc mesenteroides subsp. mesenteroides* ATCC 8293 using an aqueous two-phase system (ATPS) composed of triton x-100 and maltitol. *Molecules*, *23*(1800), 1–17.

Szkopek, D., Pierzynowski, S. G., Pierzynowska, K., Zaworski, K., Kondej, A., Wychowański, P., Konieczka, P., Seklecka, B., Donaldson, J., Jank, M., & Woliński, J. (2024). A review: Pancreatic enzymes in the treatment of chronic pancreatic insufficiency in companion animals. *Journal of Veterinary Internal Medicine*, *38*(4), 1–8.

Szwiec, K., Goncharova, K., Valverde-Piedra, J. L., Ushakova, G., Kovalenko, T., Kardas, M., Świeboda, P., Osadchenko, I., Podgurniak, P., Grochulska-Niedworok, E., Winiarczyk, M., Lozinska, L., Filip, R., & Pierzynowski, S. (2015). Novel potential of pancreatic-like enzymes of microbial origin in exocrine pancreatic insufficiency – study on a pig model. *Journal of Pre-Clinical and Clinical Research*, *9*(1), 5–10.

Taipa, M. A., Aires-Barros, M. R., & Cabral, J. M. S. (1992). Purification of lipases. *Journal of Biotechnology*, *26*, 111–142.

Takashima, S., & Amano, J. (2012). Glycosylation and secretion of human α-amylases. *Advances in Biological Chemistry*, *02*(01), 10–19.

Tanaka, H., Mierau, I., & Ito, F. (1999). Purification and Characterization of Bovine Pancreatic Bile Salt-Activated Lipase. *Journal of Biochemistry*, *125*(5), 883–890.

Tandon, S., Sharma, A., Singh, S., Sharma, S., & Sarma, S. J. (2021). Therapeutic enzymes: Discoveries, Production and Applications. *Results in Chemistry*, 1–37.

Tang, C., Zhou, J., Song, Y., & Liu, S. (2025). Etiologies of exocrine pancreatic insufficiency. In *Gastroenterology Report*, *13*.

Tang, S., Tao, J., & Li, Y. (2024). Challenges and solutions for the downstream purification of therapeutic proteins. *Antibody Therapeutics, 7*(1), 1–12.

Tarafdar, A., Sirohi, R., Gaur, V. K., Kumar, S., Sharma, P., Varjani, S., Pandey, H. O., Sindhu, R., Madhavan, A., Rajasekharan, R., & Sim, S. J. (2021). Engineering interventions in enzyme production: Lab to industrial scale. *Bioresource Technology*, *326*, 124771.

Terzyan, S., Wang, C., Downs, D., Hunter, B., & Zhang, X. C. (2000). Crystal structure of the catalytic domain of human bile salt activated lipase. *Protein Science*, *9*(9), 1783–1790.

Tesfaye, E. L., Kumar, P., Jutur, P. P., Tefera, A. T., Jiru, T. M., & Gaur, N. A. (2025). The role of amylase in bioethanol production: advances in amylase-producing strains using CRISPR/Cas9 Technology. *Fuel Communications*, *23*, 100142.

Tian, M., Li, X., Yu, L., Qian, J. X., Bai, X. Y., Yang, J., Deng, R. J., Lu, C., Zhao, H., & Liu, Y. (2025). Glycosylation as an intricate post-translational modification process takes part in glycoproteins related immunity. *Cell Communication and Signaling, 23*(1).

Toida, J., Arikawa, Y., Kondou, K., Fukuzawa, M., & Sekiguchi, J. (1998). Purification and characterization of triacylglycerol lipase from *Aspergillus oryzae*. *Bioscience, Biotechnology, and Biochemistry*, *62*(4), 759–763.

Trang, T., Chan, J., & Graham, D. Y. (2014). Pancreatic enzyme replacement therapy for pancreatic exocrine insufficiency in the 21st century. *World Journal of Gastroenterology*, *20*(33), 11467–11485.

Trapnell, B. C., Chen, S., Khurmi, R., Bodhani, A., Kapoor, M., & Haupt, M. (2020). Hospitalization rates among patients with cystic fibrosis using pancreatic enzyme replacement therapy. *Chronic Respiratory Disease*, *17*, 147997311990061.

Trapnell, B. C., Strausbaugh, S. D., Woo, M. S., Tong, S., Silber, S. A., Mulberg, A. E., & Leitz, G. (2011). Efficacy and safety of PANCREAZE ® for treatment of exocrine pancreatic insufficiency due to cystic fibrosis. *Journal of Cystic Fibrosis*, *10*(5), 350–356.

Trezza, A., Cicaloni, V., Pettini, F., & Spiga, O. (2020). Potential roles of protease inhibitors in anticancer therapy. In S. P. Gupta (Ed.), *Cancer-leading proteases* (pp. 13–49). Academic Press. https://doi.org/10.1016/B978-0-12-818168-3.00002-4.

Trono, D. (2019). Recombinant enzymes in the food and pharmaceutical industries. *Biomass, Biofuels, Biochemicals: Advances in Enzyme Technology*, 349–387.

Tsuchiya, R., & Fujisawa, N. (1997). On the etymology of "pancreas." *International Journal of Pancreatology, 21*(3).

Turki, S., Ayed, A., Chalghoumi, N., Weekers, F., Thonart, P., & Kallel, H. (2010). An enhanced process for the production of a highly purified extracellular lipase in the non-conventional yeast Yarrowia lipolytica. *Applied Biochemistry and Biotechnology*, *160*(5), 1371–1385.

Uddin, S. M. K., Hossain, M. A. M., Sagadevan, S., Al Amin, M., & Johan, M. R. (2021). Halal and Kosher gelatin: Applications as well as detection approaches with challenges and prospects. *Food Bioscience*, *44*, 101422.

Uhlig, R., Contreras, H., Weidemann, S., Gorbokon, N., Menz, A., Büscheck, F., Luebke, A. M., Kluth, M., Hube-Magg, C., Hinsch, A., Höflmayer, D., Fraune, C., Möller, K., Bernreuther, C., Lebok, P., Sauter, G., Wilczak, W., Izbicki, J., Perez, D., … Clauditz, T. S. (2022). Carboxypeptidase A1 (CPA1) immunohistochemistry is highly sensitive and specific for acinar cell carcinoma (ACC) of the pancreas. *American Journal of Surgical Pathology*, *46*(1), 97–104.

Upadhyaya, S. R., Bashyal, J., Raut, B. K., & Parajuli, N. (2025). In silico study of therapeutic potential of natural polyphenol derivatives targeting pancreatic lipase. *Discover Chemistry*, *2*(1).

Vandermeers, A., Vandermeers-Piret, M. C., Rathé, J., & Christophe, J. (1974). On human pancreatic triacylglycerol lipase: Isolation and some properties. *BBA - Enzymology*, *370*, 257–268.

Vardar Yel, N. (2021). Investigation of the activity of lipase variants on different 4-nitrophenyl esters by spectrophotometric assay. *Caucasian Journal of Science*, *8*(2), 292–303.

Vardar-Yel, N., Tütüncü, H. E., & Sürmeli, Y. (2024). Lipases for targeted industrial applications, focusing on the development of biotechnologically significant aspects: A comprehensive review of recent trends in protein engineering. *International Journal of Biological Macromolecules*, *273*(132853), 1–16.

Verma, S., Dixit, R., & Pandey, K. C. (2016). Cysteine proteases: Modes of activation and future prospects as pharmacological targets. *Frontiers in Pharmacology, 7.*

Verma, S., & Tonk, R. K. (2020). Rhomboid proteases leading to cancer: Structures, functions, and inhibition. In S. P. Gupta (Ed.), *Cancer-Leading Proteases*. Academic Press. https://doi.org/10.1016/B978-0-12-818168-3.00012-7.

Vijayaraghavan, P., Raj, S. R. F., & Vincent, S. G. P. (2016). Industrial enzymes: Recovery and purification challenges. In G. S. Dhillon & S. Kaur (Eds.), *Agro-industrial wastes as feedstock for enzyme production* (pp. 95–110). Academic Press. https://doi.org/10.1016/B978-0-12-802392-1.00004-6.

Vilanova, M., Vendrell, J., Lopez, T., Cuchillo, C. M., & Avilés, F. X. (1985). Preparative isolation of the two forms of pig pancreatic pro-(carboxypeptidase A) and their monomeric carboxypeptidases A. *Biochemical Journal*, *229*(3), 605–609.

Vivek, K., Sandhia, G. S., & Subramaniyan, S. (2022). Extremophilic lipases for industrial applications: A general review. *Biotechnology Advances*, *60*(108002), 1–16.

Vo, C. V. T., Luu, N. V. H., Nguyen, T. T. H., Nguyen, T. T., Ho, B. Q., Nguyen, T. H., Tran, T.-D., & Nguyen, Q.-T. (2022). Screening for pancreatic lipase inhibitors: evaluating assay conditions using p -nitrophenyl palmitate as substrate. *All Life*, *15*(1), 13–22.

Wang, C. S., Dashti, A., Jackson, K. W., Yeh, J. C., Cummings, R. D., & Tang, J. (1995). Isolation and characterization of human milk bile salt-activated lipase c-tail fragmen. *Biochemistry*, *34*(33), 10639–10644.

Wang, C. S., Jackson, K. W., Dashti, A., Downs, D., Zhang, X., & Tang, J. J. N. (1998). Mass spectrometric characterization and glycosylation profile of bovine pancreatic bile salt-activated lipase. *Protein Expression and Purification*, *12*(2), 259–268.

Wang, C. S., & Hartsuck, J. A. (1993). Bile salt-activated lipase. A multiple function lipolytic enzyme. *Biochimica et Biophysica Acta (BBA) - Lipids and Lipid Metabolism*, *1166*(1), 1–19.

Wang, C. S., & Kloer, H.-U. (1983). Kinetic properties of human pancreatic carboxylesterase. *Biochimica et Biophysica Acta (BBA) - Lipids and Lipid Metabolism*, *754*(2), 142–149.

Wang, H., Sun, Z., Qi, Y., Hu, Y., Ni, Z., & Li, C. (2024). Update application of enzyme in food processing, preservation, and detection. *Food Bioengineering*, (July), 380–394.

Ward, O. P., Rao, M. B., & Kulkarni, A. (2009). *Proteases, Production*. 495–511.

Wei, H., Yan, L. H., Feng, W. H., Ma, G. X., Peng, Y., Wang, Z. M., Xiao, P. G., Facchini, P. J., Pandey, M. M., Rastogi, S., Rawat, A. K. S., Jeong, Y., Hong, S., Cho, S., Lee, W., Lee, S., Zahara, K., Tabassum, S., Sabir, S., … Activity, T. A. (2014). Antiproliferative properties of *Saussurea lappa* Clarke root extract in SH-SY5Y neuroblastoma cells via intrinsic apoptotic pathway. *Annual Review of Plant Physiology and Plant Molecular Biology*, *7*(1), 171–177.

Wilschanski, M., & Shaoul, R. (2014). Chronic pancreatitis. *Practical Algorithms in Pediatric Gastroenterology*, *9*(8), 102–103.

Winkler, F. K., D'Arcy, A., & Hunziker, W. (1990). Structure of human pancreatic lipase. *Nature*, *343*(6260), 771–774.

Winstead, N. S., & Wilcox, C. M. (2009). Clinical trials of pancreatic enzyme replacement for painful chronic pancreatitis - A review. *Pancreatology*, *9*(4), 344–350.

Witt, H., Beer, S., Rosendahl, J., Chen, J. M., Chandak, G. R., Masamune, A., Bence, M., Szmola, R., Oracz, G., Macek, M., Bhatia, E., Steigenberger, S., Lasher, D., Bühler, F., Delaporte, C., Tebbing, J., Ludwig, M., Pilsak, C., Saum, K., … Sahin-Tóth, M. (2013). Variants in CPA1 are strongly associated with early onset chronic pancreatitis. *Nature Genetics*, *45*(10), 1216–1220.

Wu, L., & Gao, C. (2023). Comprehensive overview the role of glycosylation of extracellular vesicles in cancers. *ACS Omega, 8*(50), 47380–47392.

Wu, X., Xu, M., Geng, M., Chen, S., Little, P. J., Xu, S., & Weng, J. (2023). Targeting protein modifications in metabolic diseases: molecular mechanisms and targeted therapies. *Signal Transduction and Targeted Therapy*, *8*(1), 220.

Xu, M., Du, S., Wang, J., Yu, Z. P., Harmon, D. L., & Yao, J. H. (2009). Influence of rumen escape starch on pancreatic exocrine secretion of goats. *Journal of Animal Physiology and Animal Nutrition*, *93*(1), 122–129.

Xu, P., Xu, S., He, C., & Khetan, A. (2020). Applications of small molecules in modulating productivity and product quality of recombinant proteins produced using cell cultures. *Biotechnology Advances*, *43*(June), 107577.

Yang, C., & Candelario-Jalil, E. (2017). Role of Matrix Metalloproteinases in Brain Edema. In J. Badaut & N. Plesnila (Eds.), *Brain edema: From molecular mechanisms to clinical practice* (pp. 199–215). Academic Press. https://doi.org/10.1016/B978-0-12-803196-4.00011-4.

Yang, N., Matthew, M. A., & Yao, C. (2023). Roles of Cysteine Proteases in Biology and Pathogenesis of Parasites. *Microorganisms*, *11*(6).

Yu, H., Chen, X., Yang, Y., Gu, M., Ren, K., & Wei, Z. (2025). Decoding glycosylation in neurodegenerative diseases: mechanistic insights and therapeutic opportunities. *FASEB Journal, 39*(20), 1–17.

Yu, X. W., Xu, Y., & Xiao, R. (2016). Lipases from the genus *Rhizopus*: Characteristics, expression, protein engineering and application. *Progress in Lipid Research*, *64*, 57–68.

Yu, Y., Hu, J., Miyaguchi, Y., Bai, X., Du, Y., & Lin, B. (2006). Isolation and characterization of angiotensin I-converting enzyme inhibitory peptides derived from porcine hemoglobin. *Peptides*, *27*, 2950–2956.

Yuswan, M. H., Aizat, W. M., Lokman, A. A., Desa, M. N. M., Mustafa, S., Junoh, N. M., Yusof, Z. N. B., Mohamed, R., Mohmad, Z., & Lamasudin, D. U. (2018). Chemometrics-Assisted Shotgun Proteomics for Establishment of Potential Peptide Markers of Non-Halal Pork (*Sus scrofa*) among Halal Beef and Chicken. *Food Analytical Methods*, *11*(12), 3505–3515.

Zabidi, A. R., Fauzi, F. N., Abd Razak, F. N., Rosli, D., Jamil, M. Z. M., Wan Ibrahim, W. K., & Yahaya, N. (2020). Screening porcine DNA in collagen cream cosmetic products. *Food Research*, *4*(February), 151–156.

Zafar, A., Masood, A., Rahman, Z., Hamid, A., Javed, M. H., Zulfiqar, A., Fatima, S., Makhdoom, M., & Aftab, M. N. (2025). Cloning, purification, and functional characterization of recombinant pullulanase from *Bacillus cereus* ATCC 14579 for improved detergent performance. *Journal of Surfactants and Detergents*, *28*(2), 263–276.

Zakowski, J. J., & Bruns, D. E. (1985). Biochemistry of human alpha amylase isoenzymes. *Critical Reviews in Clinical Laboratory Sciences*, *21*(4), 283–322.

Zechner, R., Zimmermann, R., Eichmann, T. O., Kohlwein, S. D., Haemmerle, G., Lass, A., & Madeo, F. (2012). FAT SIGNALS - Lipases and lipolysis in lipid metabolism and signaling. *Cell Metabolism*, *15*(3), 279–291.

Zelikson, R., Eilam-Rubin, G., & Kulka, R. G. (1971). The chymotrypsinogens and procarboxypeptidases of chick pancreas*. *Journal of Biological Chemistry*, *246*(19), 6115–6120.

Zentler-Munro, P. L., Assoufi, B. A., Balasubramanian, K., Cornell, S., Benoliel, D., Northfield, T. C., & Hodson, M. E. (1992). Therapeutic potential and clinical efficacy of acid-resistant fungal lipase in the treatment of pancreatic steatorrhoea due to cystic fibrosis. *Pancreas*, *7*(3), 311–319.

Zhang, B., Liu, J., Bao, N., Xue, H., Feng, H., Lu, Z., Zhang, D., Sun, W., Shapaer, T., Zhao, Z., Shang, D., Bao, C., & Chen, Y. (2026). Global, regional, and national burden and future projections of pancreatitis: A Joinpoint, APC, and ARIMA modeling analysis. *Clinical and Experimental Medicine*, *26*(1).

Zhang, H., Zhang, F., Wu, F., Guo, L., & Xu, X. (2025). Purification and Characterization of Endogenous α-Amylase from Glutinous Rice Flour. *Foods*, *14*(10), 1–14.

Zhang, L., Luo, S., & Zhang, B. (2016). Glycan analysis of therapeutic glycoproteins. *MAbs*, *8*(2), 205–215.

Zhang, N., Jiang, N., & Chen, Q. (2025). Key Regulators of Parasite Biology Viewed Through a Post-Translational Modification Repertoire. *Proteomics, 25*, 253–276.

Zhang, Q., Gong, X., Liu, H., & Yao, X. (2025). Application of computational methods in the drug discovery and development of Alzheimer's disease. *Acta Pharmaceutica Sinica B*, 1–27.

Zhang, Q., Han, Y., & Xiao, H. (2017). Microbial α-amylase: A biomolecular overview. *Process Biochemistry*, *53*, 88–101.

Zhong, J., Huang, M., Qiu, H., Seol, H., Yan, Y., Wang, S., & Li, N. (2025). Simple endoglycosidase-assisted peptide mapping workflow for characterizing non-consensus n-glycosylation in therapeutic monoclonal antibodies. *Journal of Pharmaceutical Sciences*, *114*(2), 1125–1132.

Zhong, Q., Xiao, X., Qiu, Y., Xu, Z., Chen, C., Chong, B., Zhao, X., Hai, S., Li, S., An, Z., & Dai, L. (2023). Protein posttranslational modifications in health and diseases: Functions, regulatory mechanisms, and therapeutic implications. *MedComm*, *4*(3), 1–112.

Zinck, S. S., Christensen, S. J., Jahola, D., Hyldgaard, C. H., Sørensen, O. B., Mohammadifar, M. A., & Meyer, A. S. (2026). α-Amylase mediated production of modified potato starch with distinct gel properties. *Food Hydrocolloids*, *170*, 1–15.

Zsóri, G., Illés, D., Terzin, V., Iványi, E., & Czakó, L. (2018). Exocrine pancreatic insufficiency in type 1 and type 2 diabetes mellitus: do we need to treat it? A systematic review. *Pancreatology*, *18*(5), 559–565.

APPENDICES

APPENDIX 1

Kelulusan Projek Menjalankan Projek Jabatan Perkhidmatan Veterinar

JABATAN PERKHIDMATAN VETERINAR
Department Of Veterinary Services
Kementerian Pertanian dan Industri Asas Tani
Wisma Tani, Blok Podium Lot 4G1 & 4G2
No. 28 Persiaran Perdana, Presint 4
62630 PUTRAJAYA
MALAYSIA

Tel : 603-8870 2000
Faks : 603-8888 6021
E-mel : prp@dvs.gov.my
Laman Web : www.dvs.gov.my

Ruj. Kami : JPV. BPI.600-1/7/1
Tarikh : 14 September 2020

DR UMI MARSHIDA BINTI ABDUL HAMID
Fakulti Sains Gunaan,
Universiti Teknologi MARA,
40450 Shah Alam,
Selangor Darul Ehsan.

Puan,

KELULUSAN UNTUK MENJALANKAN PROJEK PENYELIDIKAN *GLYCAN ANALYSIS OF PANCREATIC ENZYMES FROM HALAL FRESH PANCREAS SAMPLE OF BOVINE, SHEEP AND GOAT*

Dengan hormatnya saya merujuk kepada perkara tersebut di atas.

2. Sukacita dimaklumkan bahawa Jawatankuasa Penilaian Projek Penyelidikan (JPPP), Jabatan Perkhidmatan Veterinar **meluluskan** permohonan puan untuk menjalankan projek penyelidikan dengan kerjasama Bahagian Regulatori, DVS. Puan diminta untuk mengadakan perbincangan lanjut bersama bahagian tersebut bagi menentukan bentuk kerjasama dengan lebih terperinci.

3. Dimaklumkan juga sebarang data yang diperolehi daripada DVS adalah terhad untuk kegunaan projek penyelidikan *Glycan Analysis Of Pancreatic Enzymes From Halal Fresh Pancreas Sample Of Bovine, Sheep And Goat* sahaja. Adalah menjadi suatu kesalahan sekiranya data tersebut digunakan untuk tujuan selain kajian yang telah diluluskan.

4. Puan diminta untuk menghantar Laporan Kemajuan secara berkala dan Laporan Akhir kajian kepada urusetia JPPP sebagai makluman kajian-kajian yang dijalankan berkaitan dengan Jabatan Perkhidmatan Veterinar. Kegagalan dalam menghantar laporan akan memberi kesan kepada permohonan kerjasama pada masa akan datang. Selain dari itu, pegawai/penyelidik yang terlibat dalam projek ini hendaklah diberi kredit samada sebagai penulis bersama (co-author) atau disebut dalam penghargaan dalam penulisan yang bakal diterbitkan bergantung kepada sejauh mana penglibatan pegawai/penyelidik tersebut dalam projek/penulisan.

APPENDIX 2

List of Chemicals and Reagents

Chemicals / Reagents	Supplier
4–Nitrophenyl Palmitate (Lipase substrate)	Sigma Aldrich, Germany
Alpha–Amylase from Porcine Pancreas	Sigma Aldrich, Germany
Aprotinin	Cayman Chemical, USA
BenchMark™ Protein Ladder	Invitrogen, USA
Ethylenediaminetetraacetic acid (EDTA)	Systerm®, Malaysia
Ethanol (EtOH)	Sigma Aldrich, Germany
HEPES	Sigma Aldrich, Germany
Hydrochloric Acid (HCl)	Systerm®, Malaysia
Iodine	Thermo Fisher Scientific, US
Lipase from Porcine Pancreas	Sigma Aldrich, Germany
NuPAGE 4–12% Bis–Tris Electrophoresis System	Invitrogen, USA
NuPAGE MES SDS Running Buffer	Novex, USA
NuPAGE LDS Sample Buffer 4X	Novex, USA
NuPAGE Reducing Agent	Novex, USA
Pancreatin from Porcine Pancreas	Sigma Aldrich, Germany
Protease from Bovine Pancreas	Sigma Aldrich, Germany
SeeBlue® Plus2 Pre–Stained Standard	Novex, USA
Sodium Chloride (NaCl)	Systerm®, Malaysia
Sodium Hydroxide (NaOH)	Sigma Aldrich, Germany
Tris Buffer	Fisher Chemical, Canada
Triton X–100	Biotech

APPENDIX 3

List of Consumables, Apparatus, and Instruments

List of Laboratory Consumables

Consumables	Supplier
Eppendorf Tube	
Falcon Tube	
Microcentrifuge Tube (0.5mL, 1.0mL, 2.0mL)	

List of Laboratory Apparatus and Instruments

Apparatus and Instrument	Supplier
AKTA™ Avant Chromatography	Cytiva, USA
Centrifuge	Sigma, Germany
Flexpin Bench–Top centrifuge (CAX–370)	Tomy Tech USA Inc, USA
Hybrid Refrigerator centrifuge (TOMY LC–230)	Tomy Digital Biology Co., Ltd, Japan
IKA® MS 3 Vortex Nanophotometer™	IKA® Works (Asia) Sdn Bhd, Malaysia IMPLEN, Germany
Pipette	Eppendorf Asia Pacific Sdn Bhd, Malaysia
Shaking Water Bath (Julabo SW22)	JULABO GmbH, Germany
SDS–PAGE Electrophoresis	Invitrogen, USA
Thermo Shaker	Boeco, Germany
UV–Vis Spectrophotometer NanoPhotometer	Implen, Germany
Vacuum Filtration Machine	Rocker Scientific Co., Ltd., Taiwan
X Cell *SureLock* Mini–Cell	Invitrogen, USA

APPENDIX 4

Workflow Overview: A Visual Summary of Methodology



Fresh Bovine and Sheep Pancreas Collection
at Abattoir Complex, Department of Veterinary Services, Shah Alam



Crude Pancreatic Extraction



Sequential Enzyme Purification

Anion Exchange Chromatography (CBPA1, BSAL, TL and AMYP)
Column: HiTrap Fast Q Column
Gel Filtration Chromatography (CBPA1)
Column: HiLoad™ 16/6000 Superdex™ 200 pg Column

Glycosylation *In–silico* Analysis and

- Bioinformatic sequence and structure analysis
- Glycosylation sites prediction and visualization
- Glycosylation enrichment and staining

Enzyme Profiling

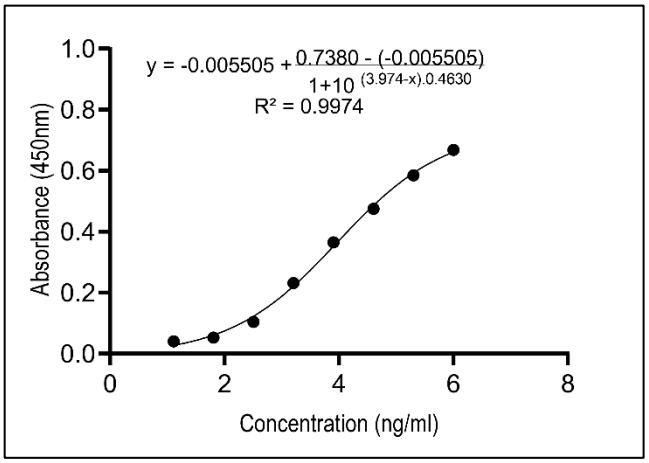
- 1D–SDS Page
- LC –MS/MS

Enzymatic Assay

- Protease assay
- Lipase assay
- Amylase assay

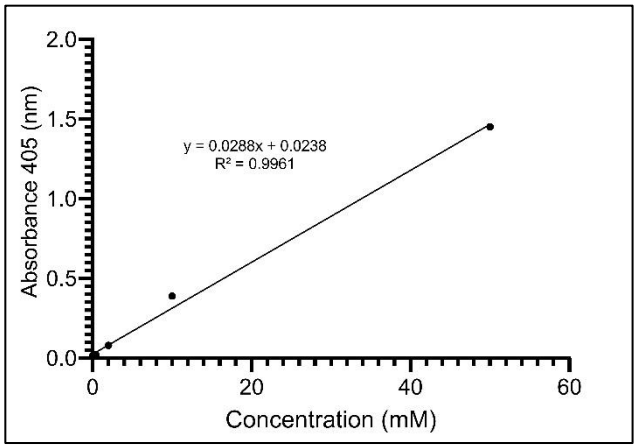
APPENDIX 5

Standard curve of Trypsin TPCK



Note: Absorbance at 450nm with Succinylated casein and 5% (w/v) 2,4,6–trinitobenzene sulfonic acid in methanol. Each point represents the mean value of duplicate determination.

Standard curve of p–Nitrophenol



Note: Absorbances at 405 nm were recorded at 25°C. Each point represents the mean value of triplicate determination.

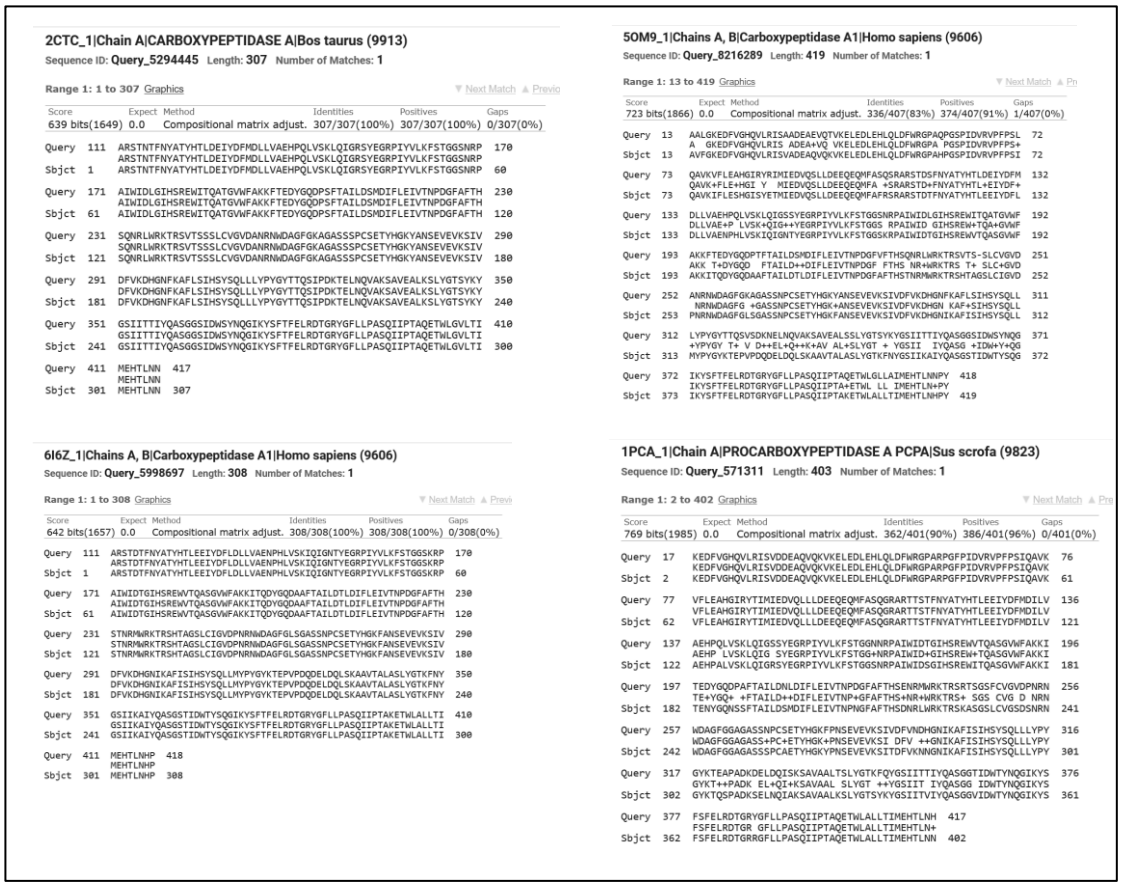
APPENDIX 6

Composition of Muller–Hinton Agar

Composition	Weight/L (g/L)
Beef extract	2.0
Acid Hydrolysate of Casein	17.5
Starch	1.5
Agar	17.0

APPENDIX 7

Multiple Sequence Alignment of CBPA1



2CTC_1|Chain A|CARBOXYPEPTIDASE A|Bos taurus (9913)

Sequence ID: **Query_5294445** Length: **307** Number of Matches: **1**

Range 1: 1 to 307 Graphics

Score	Expect	Method	Identities	Positives	Gaps
639 bits(1649)	0.0	Compositional matrix adjust.	307/307(100%)	307/307(100%)	0/307(0%)

```
Query  111  ARSTNTFNYATYHTLDEIYDFMDLLVAEHPQLVSKLQIGRSYEGRPIYVLKFSTGGSNRP  170
            ARSTNTFNYATYHTLDEIYDFMDLLVAEHPQLVSKLQIGRSYEGRPIYVLKFSTGGSNRP
Sbjct  1    ARSTNTFNYATYHTLDEIYDFMDLLVAEHPQLVSKLQIGRSYEGRPIYVLKFSTGGSNRP  60

Query  171  AIWIDLGIHSREWITQATGVWFAKKFTEDYGQDPSFTAILDSMDIFLEIVTNPDGFATH  230
            AIWIDLGIHSREWITQATGVWFAKKFTEDYGQDPSFTAILDSMDIFLEIVTNPDGFATH
Sbjct  61   AIWIDLGIHSREWITQATGVWFAKKFTEDYGQDPSFTAILDSMDIFLEIVTNPDGFATH  120

Query  231  SQNRLWRKTRSVTSSSLCVGVDANRNWDAGFGKAGASSSPCSETYHGKYANSEVEVKSIV  290
            SQNRLWRKTRSVTSSSLCVGVDANRNWDAGFGKAGASSSPCSETYHGKYANSEVEVKSIV
Sbjct  121  SQNRLWRKTRSVTSSSLCVGVDANRNWDAGFGKAGASSSPCSETYHGKYANSEVEVKSIV  180

Query  291  DFVKDHGNFKAFLSIHSYSQLLLYPYGYTTQSIPDKTELNQVAKSAVEALKSLYGTSYKY  350
            DFVKDHGNFKAFLSIHSYSQLLLYPYGYTTQSIPDKTELNQVAKSAVEALKSLYGTSYKY
Sbjct  181  DFVKDHGNFKAFLSIHSYSQLLLYPYGYTTQSIPDKTELNQVAKSAVEALKSLYGTSYKY  240

Query  351  GSIITTIYQASGGSIDWSYNQGIKYSFTFELRDTGRYGFLLPASQIIPTAQETWLGVLTI  410
            GSIITTIYQASGGSIDWSYNQGIKYSFTFELRDTGRYGFLLPASQIIPTAQETWLGVLTI
Sbjct  241  GSIITTIYQASGGSIDWSYNQGIKYSFTFELRDTGRYGFLLPASQIIPTAQETWLGVLTI  300

Query  411  MEHTLNN  417
            MEHTLNN
Sbjct  301  MEHTLNN  307
```

5OM9_1|Chains A, B|Carboxypeptidase A1|Homo sapiens (9606)

Sequence ID: **Query_8216289** Length: **419** Number of Matches: **1**

Range 1: 13 to 419 Graphics

Score	Expect	Method	Identities	Positives	Gaps
723 bits(1866)	0.0	Compositional matrix adjust.	336/407(83%)	374/407(91%)	1/407(0%)

```
Query  13   AALGKEDFVGHQVLRISAADEAEVQTVKELEDLEHLQLDFWRGPAQPGSPIDVRVPFPSL  72
            A  GKEDFVGHQVLRIS ADEA+VQ VKELEDLEHLQLDFWRGPA PGSPIDVRVPFPS+
Sbjct  13   AVFGKEDFVGHQVLRISVADEAQVQKVKELEDLEHLQLDFWRGPAHPGSPIDVRVPFPSI  72

Query  73   QAVKVFLEAHGIRYRIMIEDVQSLLDEEQEQMFASQSRARSTDSFNYATYHTLDEIYDFM  132
            QAVK+FLE+HGI Y  MIEDVQSLLDEEQEQMFA +SRARSTD+FNYATYHTL+EIYDF+
Sbjct  73   QAVKIFLESHGISYETMIEDVQSLLDEEQEQMFAFRSRARSTDTFNYATYHTLEEIYDFL  132

Query  133  DLLVAEHPQLVSKLQIGSSYEGRPIYVLKFSTGGSNRPAIWIDLGIHSREWITQATGVWF  192
            DLLVAE+P LVSK+QIG++YEGRPIYVLKFSTGGS RPAIWID GIHSREW+TQA+GVWF
Sbjct  133  DLLVAENPHLVSKIQIGNTYEGRPIYVLKFSTGGSKRPAIWIDTGIHSREWVTQASGVWF  192

Query  193  AKKFTEDYGQDPTFTAILDSMDIFLEIVTNPDGFVFTHSQNRLWRKTRSVTS-SLCVGVD  251
            AKK T+DYGQD  FTAILD++DIFLEIVTNPDGF FTHS NR+WRKTRS T+ SLC+GVD
Sbjct  193  AKKITQDYGQDAAFTAILDTLDIFLEIVTNPDGFATHSTNRMWRKTRSHTAGSLCIGVD  252

Query  252  ANRNWDAGFGKAGASSNPCSETYHGKYANSEVEVKSIVDFVKDHGNFKAFLSIHSYSQLL  311
             NRNWDAGFG +GASSNPCSETYHGK+ANSEVEVKSIVDFVKDHGN KAF+SIHSYSQLL
Sbjct  253  PNRNWDAGFGLSGASSNPCSETYHGKFANSEVEVKSIVDFVKDHGNIKAFISIHSYSQLL  312

Query  312  LYPYGYTTQSVSDKNELNQVAKSAVEALSSLYGTSYKYGSIITTIYQASGGSIDWSYNQG  371
            +YPYGY T+ V D++EL+Q++K+AV AL+SLYGT + YGSII  IYQASG +IDW+Y+QG
Sbjct  313  MYPYGYKTEPVPDQDELDQLSKAAVTALASLYGTKFNYGSIIKAIYQASGSTIDWTYSQG  372

Query  372  IKYSFTFELRDTGRYGFLLPASQIIPTAQETWLGLLAIMEHTLNNPY  418
            IKYSFTFELRDTGRYGFLLPASQIIPTA+ETWL LL IMEHTLN+PY
Sbjct  373  IKYSFTFELRDTGRYGFLLPASQIIPTAKETWLALLTIMEHTLNHPY  419
```

6I6Z_1|Chains A, B|Carboxypeptidase A1|Homo sapiens (9606)

Sequence ID: **Query_5998697** Length: **308** Number of Matches: **1**

Range 1: 1 to 308 Graphics

Score	Expect	Method	Identities	Positives	Gaps
642 bits(1657)	0.0	Compositional matrix adjust.	308/308(100%)	308/308(100%)	0/308(0%)

```
Query  111  ARSTDTFNYATYHTLEEIYDFLDLLVAENPHLVSKIQIGNTYEGRPIYVLKFSTGGSKRP  170
            ARSTDTFNYATYHTLEEIYDFLDLLVAENPHLVSKIQIGNTYEGRPIYVLKFSTGGSKRP
Sbjct  1    ARSTDTFNYATYHTLEEIYDFLDLLVAENPHLVSKIQIGNTYEGRPIYVLKFSTGGSKRP  60

Query  171  AIWIDTGIHSREWVTQASGVWFAKKITQDYGQDAAFTAILDTLDIFLEIVTNPDGFATH  230
            AIWIDTGIHSREWVTQASGVWFAKKITQDYGQDAAFTAILDTLDIFLEIVTNPDGFATH
Sbjct  61   AIWIDTGIHSREWVTQASGVWFAKKITQDYGQDAAFTAILDTLDIFLEIVTNPDGFATH  120

Query  231  STNRMWRKTRSHTAGSLCIGVDPNRNWDAGFGLSGASSNPCSETYHGKFANSEVEVKSIV  290
            STNRMWRKTRSHTAGSLCIGVDPNRNWDAGFGLSGASSNPCSETYHGKFANSEVEVKSIV
Sbjct  121  STNRMWRKTRSHTAGSLCIGVDPNRNWDAGFGLSGASSNPCSETYHGKFANSEVEVKSIV  180

Query  291  DFVKDHGNIKAFISIHSYSQLLMYPYGYKTEPVPDQDELDQLSKAAVTALASLYGTKFNY  350
            DFVKDHGNIKAFISIHSYSQLLMYPYGYKTEPVPDQDELDQLSKAAVTALASLYGTKFNY
Sbjct  181  DFVKDHGNIKAFISIHSYSQLLMYPYGYKTEPVPDQDELDQLSKAAVTALASLYGTKFNY  240

Query  351  GSIIKAIYQASGSTIDWTYSQGIKYSFTFELRDTGRYGFLLPASQIIPTAKETWLALLTI  410
            GSIIKAIYQASGSTIDWTYSQGIKYSFTFELRDTGRYGFLLPASQIIPTAKETWLALLTI
Sbjct  241  GSIIKAIYQASGSTIDWTYSQGIKYSFTFELRDTGRYGFLLPASQIIPTAKETWLALLTI  300

Query  411  MEHTLNHP  418
            MEHTLNHP
Sbjct  301  MEHTLNHP  308
```

1PCA_1|Chain A|PROCARBOXYPEPTIDASE A PCPA|Sus scrofa (9823)

Sequence ID: **Query_571311** Length: **403** Number of Matches: **1**

Range 1: 2 to 402 Graphics

Score	Expect	Method	Identities	Positives	Gaps
769 bits(1985)	0.0	Compositional matrix adjust.	362/401(90%)	386/401(96%)	0/401(0%)

```
Query  17   KEDFVGHQVLRISVDDEAQVQKVKELEDLEHLQLDFWRGPARPGFPIDVRVPFPSIQAVK  76
            KEDFVGHQVLRISVDDEAQVQKVKELEDLEHLQLDFWRGPARPGFPIDVRVPFPSIQAVK
Sbjct  2    KEDFVGHQVLRISVDDEAQVQKVKELEDLEHLQLDFWRGPARPGFPIDVRVPFPSIQAVK  61

Query  77   VFLEAHGIRYTIMIEDVQLLLDEEQEQMFASQGRARTTSTFNYATYHTLEEIYDFMDILV  136
            VFLEAHGIRYTIMIEDVQLLLDEEQEQMFASQGRARTTSTFNYATYHTLEEIYDFMDILV
Sbjct  62   VFLEAHGIRYTIMIEDVQLLLDEEQEQMFASQGRARTTSTFNYATYHTLEEIYDFMDILV  121

Query  137  AEHPQLVSKLQIGSSYEGRPIYVLKFSTGGNNRPAIWIDTGIHSREWVTQASGVWFAKKI  196
            AEHP LVSKLQIG SYEGRPIYVLKFSTGG+NRPAIWID+GIHSREW+TQASGVWFAKKI
Sbjct  122  AEHPALVSKLQIGRSYEGRPIYVLKFSTGGSNRPAIWIDSGIHSREWITQASGVWFAKKI  181

Query  197  TEDYGQDPAFTAILDNLDIFLEIVTNPDGFATHSENRMWRKTRSRTSGSFCVGVDPNRN  256
            TE+YGQ+ +FTAILD++DIFLEIVTNP+GFATHS+NR+WRKTRS+ SGS CVG D NRN
Sbjct  182  TENYGQNSSFTAILDSMDIFLEIVTNPNGFATHSDNRLWRKTRSKASGSLCVGSDSNRN  241

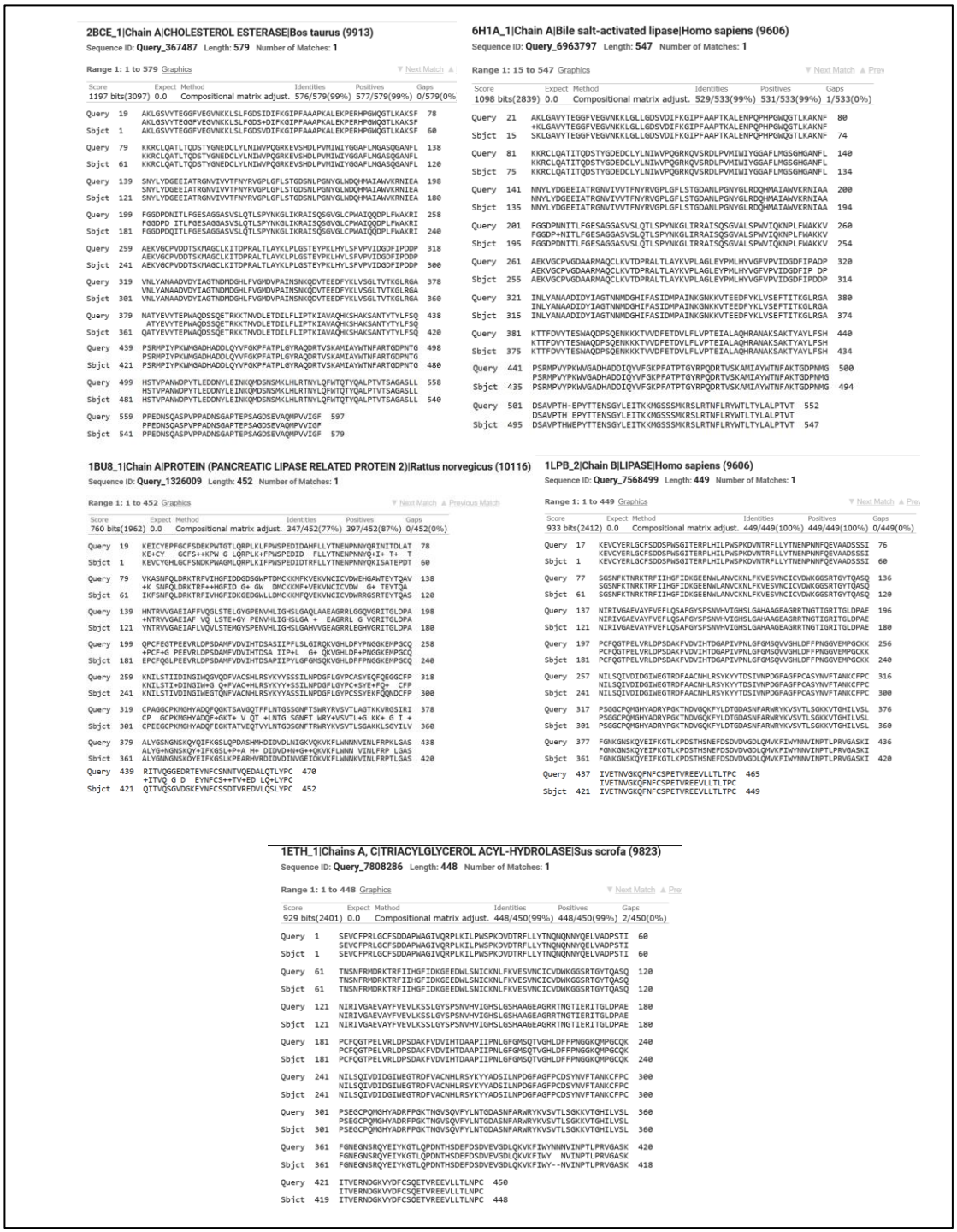
Query  257  WDAGFGGAGASSNPCSETYHGKFPNSEVEVKSIVDFVNDHGNIKAFISIHSYSQLLLYPY  316
            WDAGFGGAGASS+PC+ETYHGK+PNSEVEVKSI DFV ++GNIKAFISIHSYSQLLLYPY
Sbjct  242  WDAGFGGAGASSSPCAETYHGKYPNSEVEVKSITDFVKNNGNIKAFISIHSYSQLLLYPY  301

Query  317  GYKTEAPADKDELDQISKSAVAALTSLYGTKFQYGSIITTIYQASGGTIDWTYNQGIKYS  376
            GYKT++PADK EL+QI+KSAVAAL SLYGT ++YGSIIT IYQASGG IDWTYNQGIKYS
Sbjct  302  GYKTQSPADKSELNQIAKSAVAALKSLYGTSYKYGSIITVIYQASGGVIDWTYNQGIKYS  361

Query  377  FSFELRDTGRYGFLLPASQIIPTAQETWLALLTIMEHTLNH  417
            FSFELRDTGR GFLLPASQIIPTAQETWLALLTIMEHTLN+
Sbjct  362  FSFELRDTGRRGFLLPASQIIPTAQETWLALLTIMEHTLNN  402
```

APPENDIX 8

Multiple Sequence Alignment of BSAL and TL



2BCE_1|Chain A|CHOLESTEROL ESTERASE|Bos taurus (9913)

Sequence ID: **Query_367487** Length: **579** Number of Matches: **1**

Range 1: 1 to 579 Graphics

Score	Expect	Method	Identities	Positives	Gaps
1197 bits(3097)	0.0	Compositional matrix adjust.	576/579(99%)	577/579(99%)	0/579(0%

```
Query  19   AKLGSVVTEGGFVEGVNKKLSLFGDSIDIFKGIPFAAAPKALEKPERHPGWQGTLKAKSF  78
            AKLGSVVTEGGFVEGVNKKLSLFGDS+DIFKGIPFAAAPKALEKPERHPGWQGTLKAKSF
Sbjct  1    AKLGSVVTEGGFVEGVNKKLSLFGDSVDIFKGIPFAAAPKALEKPERHPGWQGTLKAKSF  60

Query  79   KKRCLQATLTQDSTYGNEDCLYLNIWVPQGRKEVSHDLPVMIWIYGGAFLMGASQGANFL  138
            KKRCLQATLTQDSTYGNEDCLYLNIWVPQGRKEVSHDLPVMIWIYGGAFLMGASQGANFL
Sbjct  61   KKRCLQATLTQDSTYGNEDCLYLNIWVPQGRKEVSHDLPVMIWIYGGAFLMGASQGANFL  120

Query  139  SNVLYDGEEIATRGNVIVVTFNYRVGPLGFLSTGDSNLPGNYGLWDQHMAIAWVKRNIEA  198
            SNVLYDGEEIATRGNVIVVTFNYRVGPLGFLSTGDSNLPGNYGLWDQHMAIAWVKRNIEA
Sbjct  121  SNVLYDGEEIATRGNVIVVTFNYRVGPLGFLSTGDSNLPGNYGLWDQHMAIAWVKRNIEA  180

Query  199  FGGDPDNITLFGESAGGASVSLQTLSPYNKGLIKRAISQSGVGLCPWAIQQDPLFWAKRI  258
            FGGDPD ITLFGESAGGASVSLQTLSPYNKGLIKRAISQSGVGLCPWAIQQDPLFWAKRI
Sbjct  181  FGGDPDQITLFGESAGGASVSLQTLSPYNKGLIKRAISQSGVGLCPWAIQQDPLFWAKRI  240

Query  259  AEKVGCPVDDTSKMAGCLKITDPRALTLAYKLPLGSTEYPKLHYLSFVPVIDGDFIPDDP  318
            AEKVGCPVDDTSKMAGCLKITDPRALTLAYKLPLGSTEYPKLHYLSFVPVIDGDFIPDDP
Sbjct  241  AEKVGCPVDDTSKMAGCLKITDPRALTLAYKLPLGSTEYPKLHYLSFVPVIDGDFIPDDP  300

Query  319  VNLYANAADVDYIAGTNDMDGHLFVGMDVPAINSNKQDVTEEDFYKLVSGLTVTKGLRGA  378
            VNLYANAADVDYIAGTNDMDGHLFVGMDVPAINSNKQDVTEEDFYKLVSGLTVTKGLRGA
Sbjct  301  VNLYANAADVDYIAGTNDMDGHLFVGMDVPAINSNKQDVTEEDFYKLVSGLTVTKGLRGA  360

Query  379  NATYEVVTEPWAQDSSQETRKKTMVDLETDILFLIPTKIAVAQHKSHAKSANTYTYLFSQ  438
             ATYEVVTEPWAQDSSQETRKKTMVDLETDILFLIPTKIAVAQHKSHAKSANTYTYLFSQ
Sbjct  361  QATYEVVTEPWAQDSSQETRKKTMVDLETDILFLIPTKIAVAQHKSHAKSANTYTYLFSQ  420

Query  439  PSRMPIYPKWMGADHADDLQYVFGKPFATPLGYRAQDRTVSKAMIAYWTNFARTGDPNTG  498
            PSRMPIYPKWMGADHADDLQYVFGKPFATPLGYRAQDRTVSKAMIAYWTNFARTGDPNTG
Sbjct  421  PSRMPIYPKWMGADHADDLQYVFGKPFATPLGYRAQDRTVSKAMIAYWTNFARTGDPNTG  480

Query  499  HSTVPANWDPYTLEDDNYLEINKQMDSNSMKLHLRTNYLQFWTQTYQALPTVTSAGASLL  558
            HSTVPANWDPYTLEDDNYLEINKQMDSNSMKLHLRTNYLQFWTQTYQALPTVTSAGASLL
Sbjct  481  HSTVPANWDPYTLEDDNYLEINKQMDSNSMKLHLRTNYLQFWTQTYQALPTVTSAGASLL  540

Query  559  PPEDNSQASPVPPADNSGAPTEPSAGDSEVAQMPVVIGF  597
            PPEDNSQASPVPPADNSGAPTEPSAGDSEVAQMPVVIGF
Sbjct  541  PPEDNSQASPVPPADNSGAPTEPSAGDSEVAQMPVVIGF  579
```

6H1A_1|Chain A|Bile salt-activated lipase|Homo sapiens (9606)

Sequence ID: **Query_6963797** Length: **547** Number of Matches: **1**

Range 1: 15 to 547 Graphics

Score	Expect	Method	Identities	Positives	Gaps
1098 bits(2839)	0.0	Compositional matrix adjust.	529/533(99%)	531/533(99%)	1/533(0%)

```
Query  21   AKLGAVVTEGGFVEGVNKKLGLLGDSVDIFKGIPFAAPTKALENPQPHPGWQGTLKAKNF  80
            +KLGAVVTEGGFVEGVNKKLGLLGDSVDIFKGIPFAAPTKALENPQPHPGWQGTLKAKNF
Sbjct  15   SKLGAVVTEGGFVEGVNKKLGLLGDSVDIFKGIPFAAPTKALENPQPHPGWQGTLKAKNF  74

Query  81   KKRCLQATITQDSTYGDEDCLYLNIWVPQGRKQVSRDLPVMIWIYGGAFLMGSGHGANFL  140
            KKRCLQATITQDSTYGDEDCLYLNIWVPQGRKQVSRDLPVMIWIYGGAFLMGSGHGANFL
Sbjct  75   KKRCLQATITQDSTYGDEDCLYLNIWVPQGRKQVSRDLPVMIWIYGGAFLMGSGHGANFL  134

Query  141  NNYLYDGEEIATRGNVIVVTFNYRVGPLGFLSTGDANLPGNYGLRDQHMAIAWVKRNIAA  200
            NNYLYDGEEIATRGNVIVVTFNYRVGPLGFLSTGDANLPGNYGLRDQHMAIAWVKRNIAA
Sbjct  135  NNYLYDGEEIATRGNVIVVTFNYRVGPLGFLSTGDANLPGNYGLRDQHMAIAWVKRNIAA  194

Query  201  FGGDPNNITLFGESAGGASVSLQTLSPYNKGLIRRAISQSGVALSPWVIQKNPLFWAKKV  260
            FGGDP+NITLFGESAGGASVSLQTLSPYNKGLIRRAISQSGVALSPWVIQKNPLFWAKKV
Sbjct  195  FGGDPDNITLFGESAGGASVSLQTLSPYNKGLIRRAISQSGVALSPWVIQKNPLFWAKKV  254

Query  261  AEKVGCPVGDAARMAQCLKVTDPRALTLAYKVPLAGLEYPMLHYVGFVPVIDGDFIPADP  320
            AEKVGCPVGDAARMAQCLKVTDPRALTLAYKVPLAGLEYPMLHYVGFVPVIDGDFIP DP
Sbjct  255  AEKVGCPVGDAARMAQCLKVTDPRALTLAYKVPLAGLEYPMLHYVGFVPVIDGDFIPDDP  314

Query  321  INLYANAADIDYIAGTNNMDGHIFASIDMPAINKGNKKVTEEDFYKLVSEFTITKGLRGA  380
            INLYANAADIDYIAGTNNMDGHIFASIDMPAINKGNKKVTEEDFYKLVSEFTITKGLRGA
Sbjct  315  INLYANAADIDYIAGTNNMDGHIFASIDMPAINKGNKKVTEEDFYKLVSEFTITKGLRGA  374

Query  381  KTTFDVYTESWAQDPSQENKKKTVVDFETDVLFLVPTEIALAQHRANAKSAKTYAYLFSH  440
            KTTFDVYTESWAQDPSQENKKKTVVDFETDVLFLVPTEIALAQHRANAKSAKTYAYLFSH
Sbjct  375  KTTFDVYTESWAQDPSQENKKKTVVDFETDVLFLVPTEIALAQHRANAKSAKTYAYLFSH  434

Query  441  PSRMPVYPKWVGADHADDIQYVFGKPFATPTGYRPQDRTVSKAMIAYWTNFAKTGDPNMG  500
            PSRMPVYPKWVGADHADDIQYVFGKPFATPTGYRPQDRTVSKAMIAYWTNFAKTGDPNMG
Sbjct  435  PSRMPVYPKWVGADHADDIQYVFGKPFATPTGYRPQDRTVSKAMIAYWTNFAKTGDPNMG  494

Query  501  DSAVPTH-EPYTTENSGYLEITKKMGSSSMKRSLRTNFLRYWTLTYLALPTVT  552
            DSAVPTH EPYTTENSGYLEITKKMGSSSMKRSLRTNFLRYWTLTYLALPTVT
Sbjct  495  DSAVPTHWEPYTTENSGYLEITKKMGSSSMKRSLRTNFLRYWTLTYLALPTVT  547
```

1BU8_1|Chain A|PROTEIN (PANCREATIC LIPASE RELATED PROTEIN 2)|Rattus norvegicus (10116)

Sequence ID: **Query_1326009** Length: **452** Number of Matches: **1**

Range 1: 1 to 452 Graphics

Score	Expect	Method	Identities	Positives	Gaps
760 bits(1962)	0.0	Compositional matrix adjust.	347/452(77%)	397/452(87%)	0/452(0%)

```
Query  19   KEICYEPFGCFSDEKPWTGTLQRPLKLFPWSPEDIDAHFLLYTNENPNNYQRINITDLAT  78
            KE+CY   GCFS++KPW G LQRPLK+FPWSPEDID  FLLYTNENPNNYQ+I+ T+  T
Sbjct  1    KEVCYGHLGCFSNDKPWAGHLQRPLKIFPWSPEDIDTRFLLYTNENPNNYQKISATEPDT  60

Query  79   VKASNFQLDRKTRFVIHGFIDGDSGKPTDMCKKMFKVEKVCNCICVDWEHGAWTEYTQAV  138
            +K SNFQLDRKTRF++HGFID G+ GW  DMCKKMF+VEKVCNCICVDW  G+ TEYTQA
Sbjct  61   IKFSNFQLDRKTRFIVHGFIDKGEDGWLLDMCKKMFQVEKVCNCICVDWRRGSRTEYTQAS  120

Query  139  HNTRVVGAEIAFFVQGLSTELGYGPENVHLIGHSLGAQLAAEAGRRLGGQVGRITGLDPA  198
            +NTRVVGAEIAF VQ LSTE+GY PENVHLIGHSLGA +  EAGRRL G VGRITGLDPA
Sbjct  121  YNTRVVGAEIAFLVQVLSTEMGYSPENVHLIGHSLGAHVVGEAGRRLEGHVGRITGLDPA  180

Query  199  QPCFEGTPEEVRLDPSDAMFVDVIHTDSASIIPFLSLGIRQKVGHLDFYPNGGKEMPGCQ  258
            +PCF+G PEEVRLDPSDAMFVDVIHTDSA IIP+L  G+ QKVGHLDF+PNGGKEMPGCQ
Sbjct  181  EPCFQGLPEEVRLDPSDAMFVDVIHTDSAPIIPYLGFGMSQKVGHLDFFPNGGKEMPGCQ  240

Query  259  KNILSTIIDINGIWQGVQDFVACSHLRSYKYYSSSILNPDGFLGYPCASYEQFQEGGCFP  318
            KNILSTI+DINGIW+G Q+FVAC+HLRSYKYY+SSILNPDGFLGYPC+SYE+FQ+  CFP
Sbjct  241  KNILSTILDINGIWEGTQNFVACNHLRSYKYYASSILNPDGFLGYPCSSYEEFQKDQCFP  300

Query  319  CPAGGCPKMGHYADQFQGKTSAVGQTFFLNTGSSGNFTSWRYRVSVTLAGTKKVRGSIRI  378
            CP  GCPKMGHYADQF+GKT+ V QT +LNTG SGNFT WRY+VSVTL+G KK+ G I +
Sbjct  301  CPEEGCPKMGHYADQFEGKTATVEQTVYLNTGDSGNFTRWRYKVSVTLSGAKKLSGYILV  360

Query  379  ALYGSNGNSKQYQIFKGSLQPDASHMHDIDVDLNIGKVQKVKFLWNNNVINLFRPKLGAS  438
            ALYG+NGNSKQY+IFKGSL+P+A H+ DIDVD+N+G++QKVKFLWNN VINLFRP LGAS
Sbjct  361  ALYGNNGNSKQYEIFKGSLKPEARHVRDIDVDINVGEIQKVKFLWNNKVINLFRPTLGAS  420

Query  439  RITVQGGEDRTEYNFCSNNTVQEDALQTLYPC  470
            +ITVQ G D  EYNFCS++TV+ED LQ+LYPC
Sbjct  421  QITVQSGVDGKEYNFCSSDTVREDVLQSLYPC  452
```

1LPB_2|Chain B|LIPASE|Homo sapiens (9606)

Sequence ID: **Query_7568499** Length: **449** Number of Matches: **1**

Range 1: 1 to 449 Graphics

Score	Expect	Method	Identities	Positives	Gaps
933 bits(2412)	0.0	Compositional matrix adjust.	449/449(100%)	449/449(100%)	0/449(0%)

```
Query  17   KEVCYERLGCFSDDSPWSGITERPLHILPWSPKDVNTRFLLYTNENPNNFQEVAADSSSI  76
            KEVCYERLGCFSDDSPWSGITERPLHILPWSPKDVNTRFLLYTNENPNNFQEVAADSSSI
Sbjct  1    KEVCYERLGCFSDDSPWSGITERPLHILPWSPKDVNTRFLLYTNENPNNFQEVAADSSSI  60

Query  77   SGSNFKTNRKTRFIIHGFIDKGEENWLANVCKNLFKVESVNCICVDWKGGSRTGYTQASQ  136
            SGSNFKTNRKTRFIIHGFIDKGEENWLANVCKNLFKVESVNCICVDWKGGSRTGYTQASQ
Sbjct  61   SGSNFKTNRKTRFIIHGFIDKGEENWLANVCKNLFKVESVNCICVDWKGGSRTGYTQASQ  120

Query  137  NIRIVGAEVAYFVEFLQSAFGYSPSNVHVIGHSLGAHAAGEAGRRTNGTIGRITGLDPAE  196
            NIRIVGAEVAYFVEFLQSAFGYSPSNVHVIGHSLGAHAAGEAGRRTNGTIGRITGLDPAE
Sbjct  121  NIRIVGAEVAYFVEFLQSAFGYSPSNVHVIGHSLGAHAAGEAGRRTNGTIGRITGLDPAE  180

Query  197  PCFQGTPELVRLDPSDAKFVDVIHTDGAPIVPNLGFGMSQVVGHLDFFPNGGVEMPGCKK  256
            PCFQGTPELVRLDPSDAKFVDVIHTDGAPIVPNLGFGMSQVVGHLDFFPNGGVEMPGCKK
Sbjct  181  PCFQGTPELVRLDPSDAKFVDVIHTDGAPIVPNLGFGMSQVVGHLDFFPNGGVEMPGCKK  240

Query  257  NILSQIVDIDGIWEGTRDFAACNHLRSYKYYTDSIVNPDGFAGFPCASYNVFTANKCFPC  316
            NILSQIVDIDGIWEGTRDFAACNHLRSYKYYTDSIVNPDGFAGFPCASYNVFTANKCFPC
Sbjct  241  NILSQIVDIDGIWEGTRDFAACNHLRSYKYYTDSIVNPDGFAGFPCASYNVFTANKCFPC  300

Query  317  PSGGCPQMGHYADRYPGKTNDVGQKFYLDTGDASNFARWRYKVSVTLSGKKVTGHILVSL  376
            PSGGCPQMGHYADRYPGKTNDVGQKFYLDTGDASNFARWRYKVSVTLSGKKVTGHILVSL
Sbjct  301  PSGGCPQMGHYADRYPGKTNDVGQKFYLDTGDASNFARWRYKVSVTLSGKKVTGHILVSL  360

Query  377  FGNKGNSKQYEIFKGTLKPDSTHSNEFDSDVDVGDLQMVKFIWYNNVINPTLPRVGASKI  436
            FGNKGNSKQYEIFKGTLKPDSTHSNEFDSDVDVGDLQMVKFIWYNNVINPTLPRVGASKI
Sbjct  361  FGNKGNSKQYEIFKGTLKPDSTHSNEFDSDVDVGDLQMVKFIWYNNVINPTLPRVGASKI  420

Query  437  IVETNVGKQFNFCSPETVREEVLLTLTPC  465
            IVETNVGKQFNFCSPETVREEVLLTLTPC
Sbjct  421  IVETNVGKQFNFCSPETVREEVLLTLTPC  449
```

1ETH_1|Chains A, C|TRIACYLGLYCEROL ACYL-HYDROLASE|Sus scrofa (9823)

Sequence ID: **Query_7808286** Length: **448** Number of Matches: **1**

Range 1: 1 to 448 Graphics

Score	Expect	Method	Identities	Positives	Gaps
929 bits(2401)	0.0	Compositional matrix adjust.	448/450(99%)	448/450(99%)	2/450(0%)

```
Query  1    SEVCFRRLGCFSDDAPWAGIVQRPLKILPWSPKDVDTRFLLYTNQNQNNYQELVADPSTI  60
            SEVCFRRLGCFSDDAPWAGIVQRPLKILPWSPKDVDTRFLLYTNQNQNNYQELVADPSTI
Sbjct  1    SEVCFRRLGCFSDDAPWAGIVQRPLKILPWSPKDVDTRFLLYTNQNQNNYQELVADPSTI  60

Query  61   TNSNFRMDRKTRFIIHGFIDKGEEDWLSNICKNLFKVESVNCICVDWKGGSRTGYTQASQ  120
            TNSNFRMDRKTRFIIHGFIDKGEEDWLSNICKNLFKVESVNCICVDWKGGSRTGYTQASQ
Sbjct  61   TNSNFRMDRKTRFIIHGFIDKGEEDWLSNICKNLFKVESVNCICVDWKGGSRTGYTQASQ  120

Query  121  NIRIVGAEVAYFVEVLKSSLGYSPSNVHVIGHSLGSHAAGEAGRRTNGTIERITGLDPAE  180
            NIRIVGAEVAYFVEVLKSSLGYSPSNVHVIGHSLGSHAAGEAGRRTNGTIERITGLDPAE
Sbjct  121  NIRIVGAEVAYFVEVLKSSLGYSPSNVHVIGHSLGSHAAGEAGRRTNGTIERITGLDPAE  180

Query  181  PCFQGTPELVRLDPSDAKFVDVIHTDAAPIIPNLGFGMSQTVGHLDFFPNGGKQMPGCQK  240
            PCFQGTPELVRLDPSDAKFVDVIHTDAAPIIPNLGFGMSQTVGHLDFFPNGGKQMPGCQK
Sbjct  181  PCFQGTPELVRLDPSDAKFVDVIHTDAAPIIPNLGFGMSQTVGHLDFFPNGGKQMPGCQK  240

Query  241  NILSQIVDIDGIWEGTRDFVACNHLRSYKYYVADSILNPDGFAGFPCDSYNVFTANKCFPC  300
            NILSQIVDIDGIWEGTRDFVACNHLRSYKYYADSILNPDGFAGFPCDSYNVFTANKCFPC
Sbjct  241  NILSQIVDIDGIWEGTRDFVACNHLRSYKYYADSILNPDGFAGFPCDSYNVFTANKCFPC  300

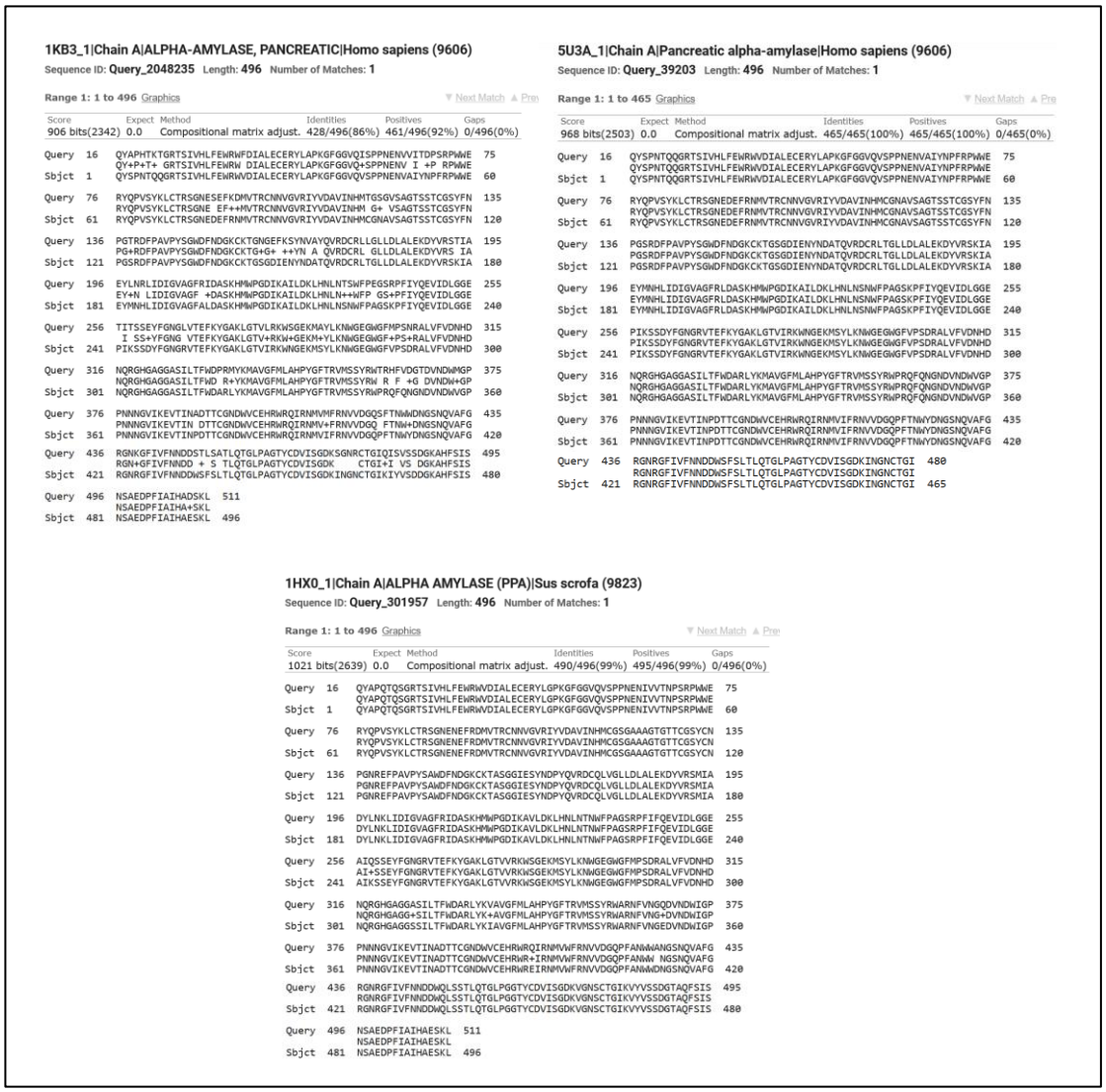
Query  301  PSEGCPQMGHYADRFPGKTNGVSQVFYLNTGDASNFARWRYKVSVTLSGKKVTGHILVSL  360
            PSEGCPQMGHYADRFPGKTNGVSQVFYLNTGDASNFARWRYKVSVTLSGKKVTGHILVSL
Sbjct  301  PSEGCPQMGHYADRFPGKTNGVSQVFYLNTGDASNFARWRYKVSVTLSGKKVTGHILVSL  360

Query  361  FGNEGNSRQYEIYKGTLQPDNTHSDEFDSDVEVGDLQKVKFIWYNNNVINPTLPRVGASK  420
            FGNEGNSRQYEIYKGTLQPDNTHSDEFDSDVEVGDLQKVKFIWY  NVINPTLPRVGASK
Sbjct  361  FGNEGNSRQYEIYKGTLQPDNTHSDEFDSDVEVGDLQKVKFIWY--NVINPTLPRVGASK  418

Query  421  ITVERNDGKVYDFCSQETVREEVLLTLNPC  450
            ITVERNDGKVYDFCSQETVREEVLLTLNPC
Sbjct  419  ITVERNDGKVYDFCSQETVREEVLLTLNPC  448
```

APPENDIX 9

Multiple Sequence Alignment of AMYP



1KB3_1|Chain A|ALPHA-AMYLASE, PANCREATIC|Homo sapiens (9606)

Sequence ID: **Query_2048235** Length: **496** Number of Matches: **1**

Range 1: 1 to 496 Graphics

Score	Expect	Method	Identities	Positives	Gaps
906 bits(2342)	0.0	Compositional matrix adjust.	428/496(86%)	461/496(92%)	0/496(0%)

```
Query  16   QYAPHTKTGRTSIVHLFEWRWFDIALECERYLAPKGFGGVQISPPNENVVITDPSRPWWE  75
            QY+P+T+ GRTSIVHLFEWRW DIALECERYLAPKGFGGVQ+SPPNENV I +P RPWWE
Sbjct  1    QYSPNTQQGRTSIVHLFEWRWVDIALECERYLAPKGFGGVQVSPPNENVAIYNPFRPWWE  60

Query  76   RYQPVSYKLCTRSGNESEFKDMVTRCNNVGVRIYVDAVINHMTGSGVSAGTSSTCGSYFN  135
            RYQPVSYKLCTRSGNE EF++MVTRCNNVGVRIYVDAVINHM G+ VSAGTSSTCGSYFN
Sbjct  61   RYQPVSYKLCTRSGNEDEFRNMVTRCNNVGVRIYVDAVINHMCGNAVSAGTSSTCGSYFN  120

Query  136  PGTRDFPAVPYSGWDFNDGKCKTGNGEFKSYNVAYQVRDCRLLGLLDLALEKDYVRSTIA  195
            PG+RDFPAVPYSGWDFNDGKCKTG+G+ ++YN A QVRDCRL GLLDLALEKDYVRS IA
Sbjct  121  PGSRDFPAVPYSGWDFNDGKCKTGSGDIENYNDATQVRDCRLTGLLDLALEKDYVRSKIA  180

Query  196  EYLNRLIDIGVAGFRIDASKHMWPGDIKAILDKLHNLNTSWFPEGSRPFIYQEVIDLGGE  255
            EY+N LIDIGVAGF +DASKHMWPGDIKAILDKLHNLN++WFP GS+PFIYQEVIDLGGE
Sbjct  181  EYMNHLIDIGVAGFALDASKHMWPGDIKAILDKLHNLNSWFPAGSKPFIYQEVIDLGGE  240

Query  256  TITSSEYFGNGLVTEFKYGAKLGTVLRKWSGEKMAYLKNWGEGWGFMPSNRALVFVDNHD  315
             I SS+YFGNG VTEFKYGAKLGTV+RKW+GEKM+YLKNWGEGWGF+PS+RALVFVDNHD
Sbjct  241  PIKSSDYFGNGRVTEFKYGAKLGTVIRKWNGEKMSYLKNWGEGWGFVPSDRALVFVDNHD  300

Query  316  NQRGHGAGGASILTFWDPRMYKMAVGFMLAHPYGFTRVMSSYRWTRHFVDGTDVNDWMGP  375
            NQRGHGAGGASILTFWD R+YKMAVGFMLAHPYGFTRVMSSYRWPRQFQNGNDVNDWVGP
Sbjct  301  NQRGHGAGGASILTFWDARLYKMAVGFMLAHPYGFTRVMSSYRWPRQFQNGNDVNDWVGP  360

Query  376  PNNNGVIKEVTINADTTCGNDWVCEHRWRQIRNMVMFRNVVDGQSFTNWWDNGSNQVAFG  435
            PNNNGVIKEVTIN DTTCGNDWVCEHRWRQIRNMV+FRNVVDGQ FTNW+DNGSNQVAFG
Sbjct  361  PNNNGVIKEVTINPDTTCGNDWVCEHRWRQIRNMVIFRNVVDGQPFTNWYDNGSNQVAFG  420

Query  436  RGNKGFIVFNNDDSTLSATLQTGLPAGTYCDVISGDKSGNRCTGIQISVSSDGKAHFSIS  495
            RGN+GFIVFNNDD + S TLQTGLPAGTYCDVISGDK    CTGI+I VS DGKAHFSIS
Sbjct  421  RGNRGFIVFNNDDWSFSLTLQTGLPAGTYCDVISGDKINGNCTGIKIYVSDDGKAHFSIS  480

Query  496  NSAEDPFIAIHADSKL  511
            NSAEDPFIAIHA+SKL
Sbjct  481  NSAEDPFIAIHAESKL  496
```

5U3A_1|Chain A|Pancreatic alpha-amylase|Homo sapiens (9606)

Sequence ID: **Query_39203** Length: **496** Number of Matches: **1**

Range 1: 1 to 465 Graphics

Score	Expect	Method	Identities	Positives	Gaps
968 bits(2503)	0.0	Compositional matrix adjust.	465/465(100%)	465/465(100%)	0/465(0%)

```
Query  16   QYSPNTQQGRTSIVHLFEWRWVDIALECERVLAPKGFGGVQVSPPNENVAIYNPFRPWWE  75
            QYSPNTQQGRTSIVHLFEWRWVDIALECERYLAPKGFGGVQVSPPNENVAIYNPFRPWWE
Sbjct  1    QYSPNTQQGRTSIVHLFEWRWVDIALECERYLAPKGFGGVQVSPPNENVAIYNPFRPWWE  60

Query  76   RYQPVSYKLCTRSGNEDEFRNMVTRCNNVGVRIYVDAVINHMCGNAVSAGTSSTCGSYFN  135
            RYQPVSYKLCTRSGNEDEFRNMVTRCNNVGVRIYVDAVINHMCGNAVSAGTSSTCGSYFN
Sbjct  61   RYQPVSYKLCTRSGNEDEFRNMVTRCNNVGVRIYVDAVINHMCGNAVSAGTSSTCGSYFN  120

Query  136  PGSRDFPAVPYSGWDFNDGKCKTGSGDIENYNDATQVRDCRLTGLLDLALEKDYVRSKIA  195
            PGSRDFPAVPYSGWDFNDGKCKTGSGDIENYNDATQVRDCRLTGLLDLALEKDYVRSKIA
Sbjct  121  PGSRDFPAVPYSGWDFNDGKCKTGSGDIENYNDATQVRDCRLTGLLDLALEKDYVRSKIA  180

Query  196  EYMNHLIDIGVAGFRLDASKHMWPGDIKAILDKLHNLNSNWFPAGSKPFIYQEVIDLGGE  255
            EYMNHLIDIGVAGFRLDASKHMWPGDIKAILDKLHNLNSNWFPAGSKPFIYQEVIDLGGE
Sbjct  181  EYMNHLIDIGVAGFRLDASKHMWPGDIKAILDKLHNLNSNWFPAGSKPFIYQEVIDLGGE  240

Query  256  PIKSSDYFGNGRVTEFKYGAKLGTVIRKWNGEKMSYLKNWGEGWGFVPSDRALVFVDNHD  315
            PIKSSDYFGNGRVTEFKYGAKLGTVIRKWNGEKMSYLKNWGEGWGFVPSDRALVFVDNHD
Sbjct  241  PIKSSDYFGNGRVTEFKYGAKLGTVIRKWNGEKMSYLKNWGEGWGFVPSDRALVFVDNHD  300

Query  316  NQRGHGAGGASILTFWDARLYKMAVGFMLAHPYGFTRVMSSYRWPRQFQNGNDVNDWVGP  375
            NQRGHGAGGASILTFWDARLYKMAVGFMLAHPYGFTRVMSSYRWPRQFQNGNDVNDWVGP
Sbjct  301  NQRGHGAGGASILTFWDARLYKMAVGFMLAHPYGFTRVMSSYRWPRQFQNGNDVNDWVGP  360

Query  376  PNNNGVIKEVTINPDTTCGNDWVCEHRWRQIRNMVIFRNVVDGQPFTNWYDNGSNQVAFG  435
            PNNNGVIKEVTINPDTTCGNDWVCEHRWRQIRNMVIFRNVVDGQPFTNWYDNGSNQVAFG
Sbjct  361  PNNNGVIKEVTINPDTTCGNDWVCEHRWRQIRNMVIFRNVVDGQPFTNWYDNGSNQVAFG  420

Query  436  RGNRGFIVFNNDDWSFSLTLQTGLPAGTYCDVISGDKINGNCTGI  480
            RGNRGFIVFNNDDWSFSLTLQTGLPAGTYCDVISGDKINGNCTGI
Sbjct  421  RGNRGFIVFNNDDWSFSLTLQTGLPAGTYCDVISGDKINGNCTGI  465
```

1HX0_1|Chain A|ALPHA AMYLASE (PPA)|Sus scrofa (9823)

Sequence ID: **Query_301957** Length: **496** Number of Matches: **1**

Range 1: 1 to 496 Graphics

Score	Expect	Method	Identities	Positives	Gaps
1021 bits(2639)	0.0	Compositional matrix adjust.	490/496(99%)	495/496(99%)	0/496(0%)

```
Query  16   QYAPQTQSGRTSIVHLFEWRWVDIALECERYLGPKGFGGVQVSPPNENIVVTNPSRPWWE  75
            QYAPQTQSGRTSIVHLFEWRWVDIALECERYLGPKGFGGVQVSPPNENIVVTNPSRPWWE
Sbjct  1    QYAPQTQSGRTSIVHLFEWRWVDIALECERYLGPKGFGGVQVSPPNENIVVTNPSRPWWE  60

Query  76   RYQPVSYKLCTRSGNENEFRDMVTRCNNVGVRIYVDAVINHMCGSGAAAGTGTTCGSYCN  135
            RYQPVSYKLCTRSGNENEFRDMVTRCNNVGVRIYVDAVINHMCGSGAAAGTGTTCGSYCN
Sbjct  61   RYQPVSYKLCTRSGNENEFRDMVTRCNNVGVRIYVDAVINHMCGSGAAAGTGTTCGSYCN  120

Query  136  PGNREFPAVPYSAWDFNDGKCKTASGGIESYNDPYQVRDCQLVGLLDLALEKDYVRSMIA  195
            PGNREFPAVPYSAWDFNDGKCKTASGGIESYNDPYQVRDCQLVGLLDLALEKDYVRSMIA
Sbjct  121  PGNREFPAVPYSAWDFNDGKCKTASGGIESYNDPYQVRDCQLVGLLDLALEKDYVRSMIA  180

Query  196  DYLNKLIDIGVAGFRIDASKHMWPGDIKAVLDKLHNLNTNWFPAGSRPFIFQEVIDLGGE  255
            DYLNKLIDIGVAGFRIDASKHMWPGDIKAVLDKLHNLNTNWFPAGSRPFIFQEVIDLGGE
Sbjct  181  DYLNKLIDIGVAGFRIDASKHMWPGDIKAVLDKLHNLNTNWFPAGSRPFIFQEVIDLGGE  240

Query  256  AIQSSEYFGNGRVTEFKYGAKLGTVVRKWSGEKMSYLKNWGEGWGFMPSDRALVFVDNHD  315
            AI+SSEYFGNGRVTEFKYGAKLGTVVRKWSGEKMSYLKNWGEGWGFMPSDRALVFVDNHD
Sbjct  241  AIKSSEYFGNGRVTEFKYGAKLGTVVRKWSGEKMSYLKNWGEGWGFMPSDRALVFVDNHD  300

Query  316  NQRGHGAGGASILTFWDARLYKVAVGFMLAHPYGFTRVMSSYRWARNFVNGQDVNDWIGP  375
            NQRGHGAGG+SILTFWDARLYK+AVGFMLAHPYGFTRVMSSYRWARNFVNG+DVNDWIGP
Sbjct  301  NQRGHGAGGSSILTFWDARLYKIAVGFMLAHPYGFTRVMSSYRWARNFVNGEDVNDWIGP  360

Query  376  PNNNGVIKEVTINADTTCGNDWVCEHRWRQIRNMVWFRNVVDGQPFANWWANGSNQVAFG  435
            PNNNGVIKEVTINADTTCGNDWVCEHRWR+IRNMVWFRNVVDGQPFANWW NGSNQVAFG
Sbjct  361  PNNNGVIKEVTINADTTCGNDWVCEHRWREIRNMVWFRNVVDGQPFANWWDNGSNQVAFG  420

Query  436  RGNRGFIVFNNDDWQLSSTLQTGLPGGTYCDVISGDKVGNSCTGIKVYVSSDGTAQFSIS  495
            RGNRGFIVFNNDDWQLSSTLQTGLPGGTYCDVISGDKVGNSCTGIKVYVSSDGTAQFSIS
Sbjct  421  RGNRGFIVFNNDDWQLSSTLQTGLPGGTYCDVISGDKVGNSCTGIKVYVSSDGTAQFSIS  480

Query  496  NSAEDPFIAIHAESKL  511
            NSAEDPFIAIHAESKL
Sbjct  481  NSAEDPFIAIHAESKL  496
```

APPENDIX 10

Summary of Pancreatic Enzymes Purification, Enzyme Identification and Confirmation, Enzyme Activity and Glycosylation Analysis

Enzyme	Purification		Enzyme Identification and Confirmation		Enzyme Activity	Glycosylation	
	Anion Exchange (Fraction – mL)	**Gel Filtration (Fraction – mL)**	**1D – SDS Page (Molecular Weight kDa)**	**LC– MS/MS (Protein Coverage | Peptide Identification)**	**Proteolytic (U/mg) Lipolytic (U/mg) Amylolytic (diameter of clear zone, mm)**	***In–silico Analysis***	**Enrichment 1D – SDS Page (Molecular Weight kDa)**
Bovine CBPA1	17 (25.5mL)	26 (26.0mL)	47.05	82.81% 30 peptides	Anion exchange 32–fold (64778.34 U/mg) > positive control (2030.08 U/mg)	NLG>OLG	Crude extract ~ 46.00
Sheep CBPA1	15 (22.5mL)	27 (27.0mL)	46.87	82.53% 20 peptides	Anion exchange 55–fold (111894.06 U/mg) > positive control (2030.08 U/mg)	NLG>OLG	Crude extract ~ 47.00
Bovine BSAL	17 (25.5mL)	–	65.12	30.9% 10 peptides	Anion exchange (0.222 U/mg) ≈ positive control (0.0223 U/mg)	NLG>OLG	–
Sheep TL	15 (22.5mL)	–	51.4	66.09% 17 peptides	Crude extract (0.640 U/mg) ≈ positive control (0.0223 U/mg)	NLG>OLG	–
Bovine AMYP	–	–	–	–	Crude extract (26.7mm) ≈ positive control (27.6mm)	NLG>OLG	–
Sheep Amyp	–	–	–	–	Crude extract (27.0mm) ≈ positive control (28.3mm)	NLG>OLG	–

Note: NLG – N–linked glycosylation and OLG – O–linked glycosylation.

AUTHOR'S PROFILE



Nur Hidayah binti Reshidan completed her Master's in Medical Sciences (Anatomy) (2019) at the Faculty of Medicine, Universiti Teknologi MARA (UiTM) Sungai Buloh. She obtained her Bachelor of Science Degree with Honours in Molecular Biology (2016) at the Faculty of Applied Sciences, Universiti Teknologi MARA (UiTM) Shah Alam. She has finished her Diploma in Microbiology (2014) at the Faculty of Applied Sciences, Universiti Teknologi MARA (UiTM) Kuala Pilah. She has undergone a six–month internship under the Pathology Department at Hospital Tuanku Ampuan Najihah (HTAN), Kuala Pilah. She has had some experience doing cell culture work while she was working as a Research Assistant under the project of Neuroprotective Effects of *Centella Asiatica* on Methamphetamine Induced Neurotoxicity and Micro–RNA Analysis. Her Master's thesis involved the investigation of a natural product known as *Pandanus amaryllifolius* as a supplement to attenuate metabolic syndrome risk factors using animal models induced by fructose drinking water. She was also an active member of the UiTM Postgraduate Society (UiPS). She currently holds the position of Research Officer / Scientist under Program of Advanced & Reproductive Technology at Livestock Research Centre in Malaysian Agricultural Research and Development Institute (MARDI).

LIST OF PUBLICATIONS:

1. Abd Ghapor, A. A., Abdul Nasir, N. A., Sadikan, M. Z., Razali, N., & **Reshidan, N. H.** (2025). Modulation of Sirtuin–1 by Resveratrol as a Potential Therapy in Alleviating Metabolic Syndrome. In Cell Biochemistry and Biophysics, 1–12.
2. **Reshidan, N. H.,** Affendy, N. B., Jonet, M. A., Lamasuddin, D. U., Ariffin, Z. Z., Mat Zain, M., & Abd Hamid, U. M. (2025). Purification and characterisation of Bile–salt activated lipase (BSAL) enzyme from bovine (Bos taurus) pancreas. Asia Pacific Journal of Molecular Biology and Biotechnology, 33 (December 2024), 108–118.
3. Sadikan, M. Z., Lambuk, L., **Reshidan, N. H.**, Abdul Ghani, N. A., Ahmad, A. I., Ahmad Kamal, M. S., Lazaldin, M. A. M., Ahmad Hairi, H., Mohamud, R., & Abdul Nasir, N. A. (2025). Age–Related Macular Degeneration Pathophysiology and Therapeutic Potential of Tocotrienols: An Update. Journal of Ocular Pharmacology and Therapeutics, February.
4. Sadikan, M. Z., Lambuk, L., **Reshidan, N.H**., Ahmad Hairi, H., Abd Ghapor, A. A., Mohamud, R., & Abdul Nasir, N. A. (2025). Molecular Mechanisms of Vitamin E in Ocular Neurodegenerative Disorders: An Update on the Emerging Evidence and Therapeutic Implications. Journal of Ocular Pharmacology and Therapeutics, 00 (00), 1–12.
5. **Reshidan, N. H.**, Jonet, M. A., Zainal Ariffin, Z., & Abd Hamid, U. M. (2024). Purification and Characterization of Pancreatic Carboxypeptidase A1 (CBPA1) of bovine (Bos taurus) and sheep (Ovis aries) for Potential Application as Halal Enzymes. Journal of Pancreatology, 1.
6. Sadikan, M. Z., Hairi, H. A., **Reshidan, N. H.**, & Jusoh, R. R. (2024). Innovations in Gene Therapy for Rare Diseases : Overcoming Delivery Challenges and Paving the Way for Future Treatments. In Compilation of Research Papers on Stem 2024 (Science, Technology, Engineering & Mathematics) (June 2024, Issue July, pp. 54–58). MNNF Publisher.
7. Sadikan, M. Z., Abdul Nasir, N. A., Lambuk, L., Mohamud, R., **Reshidan, N. H.**, Low, E., Singar, S. A., Mohmad Sabere, A. S., Iezhitsa, I., & Agarwal, R. (2023). Diabetic retinopathy: a comprehensive update on in vivo, in vitro and ex vivo experimental models. BMC Ophthalmology, 23 (1), 1–14.

8. Sadikan, M. Z., **Reshidan, N. H.**, & Kamal, M. S. A. (2022). Possible Therapeutic Effects of Ficus Deltoidea (Mas Cotek) Against Diabetic Retinopathy. In Compilation of Research Papers 2022: Science, Technology, Engineering & Mathematics (STEM) (2022nd ed., pp. 1–7). MNNF Publisher.
9. Shamsuddin, N., Noorden, M. S. A., Adenan, M. I., **Reshidan, N. H.**, & Zain, M. M. (2021). The Effects of Centella asiatica Extract (CAE) on Methamphetamine–Induced Neurotoxicity via Human Neuroblastoma Cell Line. ASM Science Journal, 16, 1–9.
10. **Reshidan, N. H.**, Muid, S. A., & Mamikutty, N. (2019). The effects of Pandanus amaryllifolius (Roxb.) leaf water extracts on fructose–induced metabolic syndrome rat model. BMC Complementary Medicine and Therapies, 19 (232), 1–13.

LIST OF CONFERENCES:

1. May 18th – 23th, 2025. – Oral Presentation
   "Identification and characterization of Carboxypeptidase A1 (CBPA1) from bovine (*Bos taurus*) pancreas"
   31st Federation of Asian and Oceanian Biochemists and Molecular Biologists (FAOBMB) Conference & 2025 KSBMB International Conference
2. August 7th – 8th, 2023. – Poster Presentation
   "Potential Pharmacotherapy of Tocotrienol Rich Fraction against Age–related Macular Degeneration: A Mechanism of Action"
   36th Malaysian Society of Pharmacology and Physiology Annual Scientific Meeting 2023.
3. September 28th – 29th, 2022. – Online Oral Presentation
   "*In–silico* Glycosylation Assessment Study of Lipase–Related Protein 2 (LRP2)."
   4th International Symposium & Workshop on Functional Genomics and Structural Biology 2022 (FGSB2022).
4. December 14th – 15th, 2022. – Online Oral Presentation
   "Porcine Enzymes in Industrial Applications: Current State and the Future of Halal"
   The 9th International Conference on Science and Social Research 2022 (CSSR2022).
5. April 18th – 21st, 2019. – Poster Presentation
   "The Effects of *Pandanus amaryllifolius* (Roxb.) Leaf Water Extracts on Metabolic Syndrome Rat Model."
   The 7th Seoul International Congress of Endocrinology and Metabolism in Conjunction with the 38th Annual Scientific Meeting of the Korean Society.
6. April 16th – 17th, 2018 – Poster Presentation
   "*Pandanus amaryllifolius* Roxb. (PA) Leaf Extract Attenuates Obesity in Fructose Induced Metabolic Syndrome Rat Model."
   International Conference of Molecular Medicine in Nutrition, Health and Disease.
7. April 16th – 17th, 2018. – Poster Presentation
   "The Effects of *Pandanus amaryllifolius* Roxb. (PA) Leaf Water Extraction on Hypertension in Fructose Induced Metabolic Syndrome Rat Model."
   International Conference of Molecular Medicine in Nutrition, Health and Disease.

LIST OF AWARDS:

1. Silver Award

   "Bovine Enzymes as Potential Halal Pancreatic Enzyme Replacement Therapy"

   Kelantan Ecohealth Innovation Fair (KEIF) 2024

2. Travel Grant

   "The Effects of *Pandanus amaryllifolius* (Roxb.) Leaf Water Extracts on Metabolic Syndrome Rat Model."

   The 7th Seoul International Congress of Endocrinology and Metabolism (SICEM) in Conjunction with the 38th Annual Scientific Meeting of the Korean Society.